


December 2012

Part 1. Design and Synthesis of Cysteine/Cystine Prodrugs and Bioisosteres Including Symmetrical and Unsymmetrical Disulfides Designed to Increase Cystine Levels in the CNS in Order to Drive the Cystine/Glutamate Antiporter: A Novel Treatment for Schizophrenia and Drug Addiction.
Part 2. Design and Synthesis of Subtype Selective Ester Bioisosteres of BZR Ligands for Gabaa/Benzodiazepine Receptors to Enhance Metabolic Stability

Edward Merle Johnson II
University of Wisconsin-Milwaukee

Follow this and additional works at: <https://dc.uwm.edu/etd>

 Part of the [Biochemistry Commons](#), and the [Organic Chemistry Commons](#)

Recommended Citation

Johnson II, Edward Merle, "Part 1. Design and Synthesis of Cysteine/Cystine Prodrugs and Bioisosteres Including Symmetrical and Unsymmetrical Disulfides Designed to Increase Cystine Levels in the CNS in Order to Drive the Cystine/Glutamate Antiporter: A Novel Treatment for Schizophrenia and Drug Addiction. Part 2. Design and Synthesis of Subtype Selective Ester Bioisosteres of BZR Ligands for Gabaa/Benzodiazepine Receptors to Enhance Metabolic Stability" (2012). *Theses and Dissertations*. 610.
<https://dc.uwm.edu/etd/610>

PART 1. DESIGN AND SYNTHESIS OF CYSTEINE / CYSTINE PRODRUGS AND
BIOISOSTERES INCLUDING SYMMETRICAL AND UNSYMMETRICAL
DISULFIDES DESIGNED TO INCREASE CYSTINE LEVELS IN THE CNS IN
ORDER TO DRIVE THE CYSTINE / GLUTAMATE ANTIporter: A NOVEL
TREATMENT FOR SCHIZOPHRENIA AND DRUG ADDICTION

PART 2. DESIGN AND SYNTHESIS OF SUBTYPE SELECTIVE ESTER
BIOISOSTERES OF BZR LIGANDS FOR GABA_A / BENZODIAZEPINE
RECEPTORS TO ENHANCE METABOLIC STABILITY

by

Edward Merle Johnson II

A Dissertation Submitted in
Partial Fulfillment of the
Requirements for the Degree of
Doctor of Philosophy
In Chemistry

at

The University of Wisconsin – Milwaukee

December, 2012

ABSTRACT

PART 1. DESIGN AND SYNTHESIS OF CYSTEINE / CYSTINE PRODRUGS AND BIOISOSTERES INCLUDING SYMMETRICAL AND UNSYMMETRICAL DISULFIDES DESIGNED TO INCREASE CYSTINE LEVELS IN THE CNS IN ORDER TO DRIVE THE CYSTINE / GLUTAMATE ANTIPORTER: A NOVEL TREATMENT FOR SCHIZOPHRENIA AND DRUG ADDICTION

by

Edward Merle Johnson II

The University of Wisconsin-Milwaukee, 2012
Under the Supervision of Professor James M Cook

Schizophrenia is a debilitating disorder that affects almost 1% of the world's population; pharmacotherapy expenditures for this disorder exceed \$10 billion dollars even though existing medications exhibit a poor safety/efficacy profile. It is estimated that 75% of patients discontinue drug treatment, in part due to poor safety/efficacy. The current data set demonstrates that cysteine prodrug NAC reverse the behavioral and neurochemical effects of PCP used to model schizophrenia.

As a result cysteine prodrugs represent a highly novel approach to treating schizophrenia; indeed, these compounds may ultimately be more effective than existing medications because these drugs target the pathology underlying schizophrenia and reverse behaviors used to model negative symptoms and diminished cognition produced by PCP, which are behaviors and symptoms that are not treated with current first line medications. Specifically, therapeutic endpoints produced by cysteine prodrugs include increasing stimulation of group II metabotropic glutamate receptors and restoring levels of glutathione. The latter effect has the potential to reverse several specific abnormalities that have been observed in schizophrenia including increased oxidative stress, decreased

NMDA receptor function, altered gene expression, and abnormal cell proliferation / synaptic connectivity.

Throughout this study, multiple series of compounds have been presented and explored, specifically 2 series of cysteine/cystine prodrugs, 2 series of cysteine/cystine bioisosteres and 1 series involving the coupling of two different series of compounds, namely, unsymmetrical disulfides (mixed dimers). Also in this study, it will be shown through the use of *in vivo* and *in vitro* screening methods, diketopiperazine cystine prodrug monomers and dialkylated versions show high promise as novel antipsychotic agents. Furthermore, the diketopiperazine cystine prodrug dimers and dialkylated dimers also have shown promise in becoming novel antipsychotic agents by overcoming the detrimental effects of PCP-induced deficits in sensorimotor gating by restoring pre-pulse inhibition in multiple screenings.

Bioisosteres of cysteine and cystine have shown vast improvements over N-Acetylcysteine by competing with C¹⁴ uptake and increasing glutamate levels by driving the cystine/glutamate antiporter. It has also been shown that simple modifications to the cysteine/cystine moiety also improve outcomes far greater than N-Acetylcysteine alone. Once the most effective compounds are determined by screening methods, the research strategy benefits by combining the two such compounds as an unsymmetrical disulfide in order to enhance their effects and help eliminate their disadvantages. As an early example to this approach two mixed dimers were synthesized and have shown extremely positive results in screening methods described here.

ABSTRACT
PART 2. DESIGN AND SYNTHESIS OF SUBTYPE SELECTIVE ESTER
BIOISOSTERES OF BZR LIGANDS FOR GABA_A/ BENZODIAZEPINE
RECEPTORS TO ENHANCE METABOLIC STABILITY

by

Edward Merle Johnson II

The University of Wisconsin-Milwaukee, 2012
Under the Supervision of Professor James M Cook

A series of 1,4-benzodiazepines and imidazobenzodiazepines including bioisosteric ligands was synthesized in search of subtype selective ligands for GABA_A/benzodiazepine receptor subtypes. In this study, it was clear that the improved method for synthesizing benzodiazepines was successful. This is based on the number and quantities of numerous compounds synthesized utilizing the improved method. Although the efficacy of XHe-II-053 (**4**) was decreased in Phase I because of the metabolism of the C-3 ester to the acid, the bioisostere EMJ-I-026 (**5**) has been shown to exhibit non-sedating anxiolytic activity in mice as well as a binding/oocyte profile in vitro consistent with a non-sedating anxiolytic. Seven bioisosteric analogues were designed in order to circumvent any potential metabolic liability in humans of the previously described ligand. In fact, the bioisosteric analogues were much more stable in human liver microsomes than XHe-II-053 (**4**) again indicating these bioisosteres are potential nonsedating anxiolytics as well as useful for treatment of anxiety disorders in human populations. These ligands were also stable on human blood, brain and kidney.

Gratifyingly, ligand **5** was clearly an $\alpha 3$ Bz/GABAergic receptor subtype selective ligand at pharmacologically relevant doses (approximately 100 to 200 nM) and, presumably, provides an agent to study physiologically processes mediated by $\alpha 3$ subtypes including anxiety and, in addition, was much more stable on human liver microsomes. In this regard $\alpha 3$ subtype selective ligand, oxadiazole **5** (EMJ-I-026), has been evaluated in the light dark paradigm and clearly is a nonsedating anxiolytic, wherein this ligand was anxiolytic with no sedative properties, *in vivo*, as compared to diazepam. This study indicated that the ester function in these molecules can be replaced with a metabolically more stable ester bioisostere and still retain anxiolytic activity. The indepth study of these ligands in animal models and other receptor systems are underway by collaborators.

Table of Contents – Part 1.

PART 1. DESIGN AND SYNTHESIS OF CYSTEINE / CYSTINE PRODRUGS AND BIOISOSTERES INCLUDING SYMMETRICAL AND UNSYMMETRICAL DISULFIDES DESIGNED TO INCREASE CYSTINE LEVELS IN THE CNS IN ORDER TO DRIVE THE CYSTINE / GLUTAMATE ANTIPORTER: A NOVEL TREATMENT FOR SCHIZOPHRENIA AND DRUG ADDICTION

Part 1. Title Page.....	1
I. Background and Introduction.....	2
1. General Background to Schizophrenia, Drug Addiction and Current Treatments.....	2
2. Release of Extracellular Glutamate: Identification of a Novel Source.....	9
3. Cystine-Glutamate Antiporter.....	11
4. Glutathione and Cystine-Glutamate Antiporter Activity.....	12
5. Cystine-Glutamate Antiporters and Schizophrenia.	13
6. Clinical Applications of N-Acetylcysteine and Pharmacokinetics.	14
7. Possible Approaches to Increase CNS Cysteine/Cystine Levels.....	15
8. Approach to be Studied: Cysteine/Cystine Analogues.	20
9. Potential Pitfalls in Novel Approaches to Treat CNS Disorders	25
II. Design and Synthesis of Cysteine and Cystine Prodrugs.....	31
1. Initial Approach to the Synthesis of Cysteine and Cystine Prodrugs	31
2. Improved Synthesis of Cysteine and Cystine Prodrugs.....	35
2.1. Preparation of 4-Methylbenzenesulfonyl Chloride.....	53
2.2. Representative Procedure for Synthesis of Bis-Dipiperazinedione (Symmetrical Dimers): Bis-[2,5-Piperazinedione 3-(mercaptomethyl)-] (1).	53
2.3. Synthesis of (R)-2-Amino-3-(phenyldisulfanyl)propanoic acid (9b)	54

2.4. Synthesis of 2-Amino-3-tritylsulfanyl-propionic acid (S-Trityl-L-cysteine) (9c).....	55
2.5. Synthesis of (R)-4-((Phenyldisulfanyl)methyl)oxazolidine- 2,5-dione (10b).	55
2.6. Synthesis of 4-Tritylsulfanylmethyl-oxazolidine-2,5-dione (10c)	56
2.7. Representative Procedure for Synthesis of Diketopiperazine Targets.....	57
2.8. Synthesis of 3-(Mercaptomethyl)-2,5-Piperazinedione (12a) and (R)-3- ((Phenyldisulfanyl)methyl)piperazine-2,5-dione (11b).....	57
2.9. Synthesis of 3-Tritylsulfanylmethyl-piperazine-2,5-dione (27)	59
2.10. Representative Procedure for Synthesis of Dialkylated Diketopiperazine: Preparation of Triethyloxonium tetrafluoroborate	59
2.11. Synthesis of (3,6-Diethoxy-2,5-dihydro-,pyrazin-2-yl)- methanethiol (44).....	61
2.12. Synthesis of Bis-[(3,6-Diethoxy-2,5-dihydro-pyrazin-2-yl)- methanethiol] (46).....	62
2.13. Synthesis of (3R,6R)-6-Benzyl-5-ethoxy-3-(ethylthiomethyl)-1,6- dihydropyrazin-2(3H)-one (49)	63
III. Synthesis of Cysteine and Cystine Bioisosteres.	64
1. Rationale, Design and Synthesis of Cysteine and Cystine Bioisosteres.....	64
2.1. Synthesis of (R)-2-(<i>tert</i> -Butoxycarbonylamino)-3-(tritylthio) propanoic acid (54c)	79
2.2. Synthesis of N,N' –Bis(<i>tert</i> -Butoxy)carbonylcystine (93).	80
2.3. Synthesis of (R)- <i>tert</i> -Butyl 1-(3-isopropyl-1,2,4-oxadiazol-5-yl)-2- (tritylthio) ethylcarbamate (94).....	81
2.4. General Procedure for Cleaving Disulfide Bonds on Bioisosteres	82
2.5. Synthesis of <i>tert</i> -Butyl (1R,1'R)-2,2'-disulfanediyldis(1-(3-isopropyl- 1,2,4-oxadiazol-5-yl)ethane-2,1-diyl)dicarbamate (104).....	83
2.6. Synthesis of (1R,1'R)-2,2'-Disulfanediyldis(1-(3-methyl-1,2,4- oxadiazol-5-yl)ethanamine) (106a , 106b)	84

IV. Synthesis of Protected Cysteine and Cystine Analogues with Various Groups to Alter the Partition Coefficients	85
1. Rationale, Design and Synthesis of Protected Cysteine and Cystine Analogues	85
2.1. Representative Procedure for Synthesis of Dimer 113e	93
2.2. Synthesis of Phenyl acetyl-S-trityl-L-cysteine (108g).....	93
2.3. Synthesis of N-Carbobenzoxy-S-trityl-L-cysteinyglycine ethyl ester (112e)	94
2.4. Synthesis of Bis-[(R)-ethyl 2-(3-mercapto-2-(2-phenylacetamido)propanamido)acetate] (113e)	94
2.5. Synthesis of N,S-Dibenzoyl-L-cysteine Ethyl Ester (115)	95
V. Synthesis of Unsymmetrical Disulfide – Heterodimers.....	96
1. Rationale, Design and Synthesis of Unsymmetrical Disulfides	96
2.1. General Procedure for Preparation of Mixed Dimer of Diketopiperazine and Bioisosteres: Synthesis of <i>tert</i> -Butyl-(R)-2-(2R,5R)-5-benzyl-3,6-dioxopiperazin-2-yl-methyl-disulfanyl-1-(3-isopropyl-1,2,4-oxadiazol-5-yl)ethylcarbamate (118) and <i>tert</i> -Butyl (R)-1-(3-isopropyl-1,2,4-oxadiazol-5-yl)-2-((((2R,5R)-5-isopropyl-3,6-dioxopiperazin-2-yl)methyl)disulfanyl)ethylcarbamate (119)	101
2.2. General Procedure for the Preparation of Unsymmetrical Bis-Dipiperazinedione (Unsymmetrical Dimers)	103
2.2.1. Synthesis of (3S,6S)-3-Benzyl-6-(R)-3,6-dioxopiperazin-2-yl-methyl disulfanyl-methyl-piperazine-2,5-dione (132)	103
2.2.2. Synthesis of <i>tert</i> -Butyl (R)-2-(2R,5R)-5-benzyl-3,6-dioxopiperazin-2-yl-methyl-disulfanyl-1-(3-isopropyl-1,2,4-oxadiazol-5-yl)ethylcarbamate (133)	104
2.3. General Procedure for the Dealkylation of the Boc Group by Chlorotrimethylsilane/Sodium Iodide: Synthesis of (3R,6S)-3-(R)-2-Amino-2-(3-isopropyl-1,2,4-oxadiazol-5-yl)-ethyl-disulfanyl-methyl-6-isopropylpiperazine-2,5-dione (134).....	105
2.4. General Procedure for the Synthesis of Mixed Dimers Using the Benzotriazole Method: [<i>tert</i> -Butyl 1-mercapto-2-(5-phenyl-1H-1,2,4-triazol-3-yl)propan-2-ylcarbamate]-[(R)- <i>tert</i> -butyl 2-mercapto-1-(5-methyl-1H-1,2,4-triazol-3-yl)ethylcarbamate]-disulfide (135).....	106

2.5. General Procedure for Deprotection of the BOC group and Formation of HCl salt of Mixed-Dimers: Synthesis of (R)-2-(((R)-2-Amino-2-(5-methyl-1H-1,2,4-triazol-3-yl)ethyl)disulfanyl)-1-(5-phenyl-1H-1,2,4-triazol-3-yl)ethanamine dihydrochloride (136).....	107
VI. Methods, Results and Discussion	108
1. <i>In Vivo</i> and <i>In Vitro</i> Screening of Novel Compounds	108
1.1. Glutamate Sampling and C ¹⁴ -Cystine Uptake	108
1.2. HPLC Analysis of Glutamate	109
1.3. Preclinical Assessment of Therapeutic Potential.....	110
1.4. Elevated Plus Maze.....	110
1.5. Pre-pulse Inhibition.....	111
2.1. N-Acetylcysteine & PCP-Induced Deficits in Pre-pulse Inhibition	112
2.2. PCP Dose-Dependently Alters Pre-pulse Inhibition and Impact of N-Acetylcysteine on Sensorimotor Gating Deficits Produced by PCP	116
2.3. Efficacy of Compounds from Scheme 3 , Relative to N-Acetylcysteine, in Reversing PCP-Induced Deficits in Sensorimotor Gating in Rats	118
2.4. Efficacy of Compounds 44 and 46 (see Scheme 3 earlier) as Novel Antipsychotic Agents.....	120
2.5. Diketopiperazide Bivalent Ligand 1 (see Scheme 3 earlier, dimer) Produced a Larger Increase in Glutamate in the Prefrontal Cortex Relative to NAC	124
2.6. Efficacy of Diketopiperazide Dimer 1 (see Scheme 3 earlier) as a Novel Antipsychotic Agent.	125
2.7. Efficacy (PO) of Monomers and Dimers from Scheme 4 , Relative to N-Acetylcysteine in Reversing PCP-Induced Deficits in Sensorimotor Gating in Rats.	127
2.8. Efficacy (PO) of Ligands Synthesized and Illustrated in Scheme 25 Relative to N-Acetylcysteine, in Reversing PCP-Induced Deficits in Sensorimotor Gating in Rats.....	129
2.9. Efficacy (PO) of Cystine Prodrug 112e from Scheme 26 Relative to N-Acetylcysteine in Reversing PCP-Induced Deficits in Sensorimotor Gating in Rats	131

2.10. Efficacy (PO) of Mixed Bivalent Ligands that were Prepared and Illustrated in Scheme 29 Relative to N-Acetylcysteine in Reversing PCP-Induced Deficits in Sensorimotor Gating in Rats.....	133
VII. Biological Data for Synthesized Compounds	135
VIII. Conclusion	228
IX. Experimental Section.....	237
Preparation of 4-Methylbenzenesulfonyl Chloride.....	238
Representative Procedure for the Synthesis of the Bis-Dipiperazinedione (Symmetrical Dimers): Bis-[2,5-Piperazinedione, 3-(mercaptomethyl)-] (1).....	238
(R)-2-Amino-3-(phenyldisulfanyl)propanoic acid (9b).....	239
2-Amino-3-tritylsulfanyl-propionic acid (S-Trityl-L-cysteine) (9c)	240
(R)-4-((Phenyldisulfanyl)methyl)oxazolidine-2,5-dione (10b).....	240
4-Tritylsulfanylmethyl-oxazolidine-2,5-dione (10c)	241
Representative Procedure for Synthesis of Diketopiperazine Targets: 3-(Mercaptomethyl)-2,5-Piperazinedione (12a)	242
(R)-3-((Phenyldisulfanyl)methyl)piperazine-2,5-dione (11b).....	243
(3R,6R)-3-Benzyl-6-(mercaptomethyl)piperazine-2,5-dione (12c).....	243
(6R)-3-Isopropyl-6-(mercaptomethyl)piperazine-2,5-dione (12e)	244
(3R,8aR)-3-((Phenyldisulfanyl)methyl)hexahydropyrrolo[1,2-a]pyrazine-1,4-dione (25).....	244
3-Tritylsulfanylmethyl-piperazine-2,5-dione (27).....	245
(6R)-3-(<i>tert</i> -Butylthiomethyl)-6-(mercaptomethyl)piperazine-2,5-dione (32).....	245
(3S,6S)-3-Benzyl-6-(2R,5R)-5-benzyl-3,6-dioxopiperazin-2-yl-methyl-disulfanyl-methyl-piperazine-2,5-dione (36).....	246

(3R,6S)-3-(<i>tert</i> -Butylthiomethyl)-6-(2R,5S)-5-(<i>tert</i> -Butylthiomethyl)-3,6-dioxo-piperazin-2-yl-methyl-disulfanyl-methyl-piperazine-2,5-dione (37)	246
(3R,3'R,6R,6'R)-6,6'-Disulfanediylbis(methylene)bis(3-isopropylpiperazine-2,5-dione) (38)	247
Representative Procedure for Synthesis of Dialkylated Diketopiperazine: Preparation of Triethyloxonium tetrafluoroborate.....	248
(3,6-Diethoxy-2,5-dihydropyrazin-2-yl)-methanethiol (44).....	249
Bis[(3,6-Diethoxy-2,5-dihydropyrazin-2-yl)-methanethiol] (46).....	249
1,2-Bis(2R,5R)-3,6-diethoxy-5-isopropyl-2,5-dihydropyrazin-2-yl-methyl-disulfane (47)	250
1,2-Bis(2R,5R)-5-benzyl-3,6-diethoxy-2,5-dihydropyrazin-2-yl-methyl-disulfane (48)	251
(3R,6R)-6-Benzyl-5-ethoxy-3-(ethylthiomethyl)-1,6-dihydropyrazin-2(3H)-one (49)	251
(R)-2-(<i>tert</i> -Butoxycarbonylamino)-3-(tritylthio)propanoic acid (54c).....	252
N, N'–Bis(<i>tert</i> -Butoxy)carbonylcystine (93).....	253
(R)- <i>tert</i> -Butyl-1-(3-isopropyl-1,2,4-oxadiazol-5-yl)-2-(tritylthio)ethylcarbamate (94)	253
General Procedure for the Cleavage of Disulfide Bonds on Bioisosteres: Used for the Synthesis of Ligands 96 , 98 , 100 and 102	254
(R)- <i>tert</i> -Butyl-2-mercapto-1-(5-methyl-1H-1,2,4-triazol-3-yl) ethylcarbamate [R = CH ₃] (96)	255
(R)- <i>tert</i> -Butyl-1-(5-ethyl-1H-1,2,4-triazol-3-yl)-2-mercapto ethylcarbamate [R = CH ₂ CH ₃] (98)	255
(R)- <i>tert</i> -Butyl-2-mercapto-1-(5-phenyl-1H-1,2,4-triazol-3-yl)ethylcarbamate [R = Ph] (100).....	256
(R)- <i>tert</i> -Butyl-1-(5-isopropyl-1H-1,2,4-triazol-3-yl)-2-mercaptoethylcarbamate [R = CH(CH ₃) ₂] (102).....	256
<i>tert</i> -Butyl (1R,1'R)-2,2'-disulfanediylbis(1-(3-isopropyl-1,2,4-oxadiazol-5-yl)ethane-2,1-diyl)dicarbamate (104)	257
<i>tert</i> -Butyl (1R,1'R)-2,2'-disulfanediylbis(1-(3-methyl-1,2,4-oxadiazol-5-yl)ethane-2,1-diyl)dicarbamate (105).....	258

(1R,1'R)-2,2'-Disulfanediylbis(1-(3-methyl-1,2,4-oxadiazol-5-yl)ethanamine) (106a)	258
(1R,1'R)-2,2'-Disulfanediylbis(1-(3-isopropyl-1,2,4-oxadiazol-5-yl)ethanamine) (106b)	259
Representative Procedure for Synthesis of Compound 113e: Phenyl Acetyl-S-trityl-L-cysteine (108g)	259
N-Carbobenzoxy-S-trityl-L-cysteinylglycine ethyl ester (112e)	260
Bis-[(R)-ethyl 2-(3-mercapto-2-(2-phenylacetamido) propanamido)acetate] (113e)	261
N,S-Dibenzoyl-L-cysteine Ethyl Ester (115)	261
Alternative Route for Synthesis of Unsymmetric Bis-Dipiperazinedione (Unsymmetrical Dimers): (3S,6S)-3-benzyl-6-(R)-3,6-dioxopiperazin-2-yl-methyl-disulfanyl-methylpiperazine-2,5-dione (132)	262
<i>tert</i> -Butyl (R)-2-(2R,5R)-5-benzyl-3,6-dioxopiperazin-2-yl-methyl-disulfanyl-1-(3-isopropyl-1,2,4-oxadiazol-5-yl)ethylcarbamate (133)	263
General Procedure for the Dealkylation of the Boc Group by Chlorotrimethylsilane/Sodium Iodide: (3R,6S)-3-(R)-2-Amino-2-(3-isopropyl-1,2,4-oxadiazol-5-yl-ethyl-disulfanyl-methyl)-6-isopropyl-piperazine-2,5-dione (134)	264
General Procedure for the Synthesis of Mixed Dimers Using the Benzotriazole Method: [<i>tert</i> -Butyl 1-mercapto-2-(5-phenyl-1H-1,2,4-triazol-3-yl)propan-2-ylcarbamate]-[(R)- <i>tert</i> -Butyl 2-mercapto-1-(5-methyl-1H-1,2,4-triazol-3-yl)ethylcarbamate]-disulfide (135)	265
General Procedure for Deprotection of the Boc group and Formation of HCl salt of Mixed-Dimers: (R)-2-(R)-2-Amino-2-(5-methyl-1H-1,2,4-triazol-3-yl)ethyl-disulfanyl-1-(5-phenyl-1H-1,2,4-triazol-3-yl)ethanamine dihydrochloride (136)	266
<i>tert</i> -Butyl (R)-1-(3-isopropyl-1,2,4-oxadiazol-5-yl)-2-(2R,5R)-5-isopropyl-3,6-dioxopiperazin-2-yl-methyl-disulfanyl-ethylcarbamate (137)	266
X. References	268

List of Schemes – Part 1.

Scheme 1. Initial Synthetic Route to Diketopiperazine Targets	32
Scheme 2	33
Scheme 3. General Synthesis of Diketopiperazine Targets	38
Scheme 4. General Coupling of Monomers to Form Symmetrical Disulfides	40
Scheme 5	53
Scheme 6	54
Scheme 7	55
Scheme 8	55
Scheme 9	56
Scheme 10	57
Scheme 11	59
Scheme 12	61
Scheme 13	62
Scheme 14	63
Scheme 15. General Synthesis of Carboxylic Acid Bioisosteres	67
Scheme 16. General Synthesis of Carboxylic Acid Bioisosteres - Continued	68
Scheme 17. General Synthesis of Amide Bioisosteres	69
Scheme 18. General Synthesis of Amide Bioisosteres - Continued	70
Scheme 19	79
Scheme 20	80
Scheme 21	81
Scheme 22	82
Scheme 23	83
Scheme 24	84

Scheme 25. General Synthesis of Protected Analogues with Various Groups to Alter the Partition Coefficients	87
Scheme 26. General Synthesis of Protected Analogues with Glycine and Various Groups to Alter the Partition Coefficients	88
Scheme 27	93
Scheme 28	95
Scheme 29. General Synthesis of Unsymmetrical Disulfides	98
Scheme 30	101
Scheme 31	101
Scheme 32	103
Scheme 33	104
Scheme 34	105
Scheme 35	106
Scheme 36	107

List of Figures – Part 1.

Figure 1. Regulation of Glutamate Signaling by Cystine-Glutamate Antiporters.....	10
Figure 2. Schematic Illustrating the Uptake and Recycling of Cystine.....	12
Figure 3. Lead Compound (1).....	25
Figure 4. Preliminary Studies in Rats using Oral N-Acetyl cysteine (NAC) and Compound 1 (NCE).....	26
Figure 5. List of Relevant Hydrolytic Enzymes Found in the CNS.....	30
Figure 6. Diketopiperazine Targets Using Various Natural D- and L-Amino Acids ..	39
Figure 7. Oral N-Acetylcysteine.....	114
Figure 8. IP N-Acetylcysteine.....	114
Figure 9. Intra-PFC N-Acetylcysteine.....	115
Figure 10. Pre-pulse Inhibition after PCP.....	117
Figure 11. Pre-pulse Inhibition Recovery from PCP after NAC via PO or Intra-PFC.....	117
Figure 12. Pre-pulse Inhibition Recovery with Compounds from Scheme 3	119
Figure 13. Impact of Oral Compound 44 on PCP-Evoked Deficits in Pre-pulse Inhibition.....	122
Figure 14. Impact of Oral Compound 46 on PCP-Evoked Deficits in Pre-pulse Inhibition.....	123
Figure 15. EC-Glutamate Levels after NAC and NCE (1).....	125
Figure 16. Pre-pulse Inhibition Recovery from PCP with NAC and NCE (1).....	126
Figure 17. Pre-pulse Inhibition Recovery with Monomers and Dimers Prepared and Illustrated in Scheme 4	128
Figure 18. Pre-pulse Inhibition Recovery with Monomers and Dimers Prepared and Illustrated in Scheme 25	130
Figure 19. Pre-pulse Inhibition Recovery with Cystine Dimer 112e Prepared and Illustrated in Scheme 26	132

Figure 20. Pre-pulse Inhibition Recovery with Cystine Mixed Dimers Prepared and Illustrated in Scheme 29	134
Figure 21. Targets of Interest Based on Pre-Pulse Inhibition Screening Results	229
Figure 22. Targets of Interest Based on C ¹⁴ Uptake and Glutamate Percent Change Screening Results	230
Figure 23. Targets of Interest that are Closely related to Cysteine/Cystine	232
Figure 24. Dialkylated Diketopiperazine Targets of Interest.....	233
Figure 25. Highly Lipophilic Substituted Targets of Interest.....	234
Figure 26. Highly Lipophilic Substituted Targets with Low Activity.....	235
Figure 27. Bioisostere Targets of Interest.....	236

List of Tables – Part 1.

Table 1. Cysteine and Cystine Prodrugs from Scheme 3 and Scheme 4	41
Table 2. Carboxylic Acid Bioisosteres from Scheme 15 and Scheme 16	71
Table 3. Amide Bioisosteres from Scheme 17 and Scheme 18	72
Table 4. Protected Analogues with Various Groups to Alter the Partition Coefficients from Scheme 25 and Scheme 26	89
Table 5. Unsymmetrical Disulfide Dimers from Scheme 29	99
Table 6. Biological Data for Target Compounds.....	136

Table of Contents – Part 2.

PART 2. DESIGN AND SYNTHESIS OF SUBTYPE SELECTIVE ESTER BIOISOSTERES OF BZR LIGANDS FOR GABA_A/ BENZODIAZEPINE RECEPTORS TO ENHANCE METABOLIC STABILITY

Part 2. Title Page.....	276
I. Introduction	276
1. General Background and Information	276
2. Molecular Modeling.....	287
3. Objectives of this Research.....	292
II. Results and Discussion.....	294
1.1. An Improved Process for the Synthesis of 4H-Imidazo-[1,5-a]- [1,4]-Benzodiazepines	294
1.2. Scope and Limitations.....	296
2. Synthesis of the Bioisosteric Imidazobenzodiazepine EMJ-I-026 (5) and Analogues for Lead Compounds	301
2.1. <i>In Vitro</i> Electrophysiological Studies on EMJ-I-026 (5) for Efficacy at BzR/GABAergic Subtypes	303
2.2. The Light/Dark and Locomotor Activity Test on EMJ-I-026 (5).....	307
2.3. Acid/Base Stability Studies on EMJ-II-026 (5).....	311
2.4. <i>In Vitro</i> Metabolic Stability of XHe-II-053 (4) and EMJ-I-026 (5)	312
2.5. Synthesis of YT-III-40 (9)	314
2.6. Synthesis of YT-III-41(10)	316
2.7. Synthesis of YT-III-42 (14)	317
2.8. Synthesis of YT-III-44 (16)	320

III. Conclusion.....	323
IV. Screening Methods	324
1. Computer Modeling Methods.....	324
2. Competition Binding Assays (With Dr. Majumder and Dr. Roth).....	325
3. Preparation of Cloned mRNA (with Dr. R. Furtmüller, Dr. J. Ramerstorfer and Dr. W. Sieghart).....	325
4. Functional Expression of GABA _A Receptors (with Dr. R. Furtmüller, Dr. J. Ramerstorfer and Dr. W. Sieghart).....	326
5. Electrophysiological Experiments (with Dr. R. Furtmüller, Dr. J. Ramerstorfer and Dr. W. Sieghart).....	327
V. Experimental Section.....	329
7-Chloro-4-Methyl-3,4-Dihydro-1H-Benzo-[e]-[1,4]-Diazepine-2,5-Dione (1h).....	330
General Procedure for the Synthesis of Imidazo-[1,5-a]-[1,4]- Benzodiazepines	330
Large Scale Procedure for the Synthesis of Imidazo-[1,5-a]-[1,4]- Benzodiazepines (3j)	331
Ethyl-8-Chloro-6-Phenyl-4 <i>H</i> -Imidazo-[1,5-a]-[1,4]-Benzodiazepine-3- Carboxylate (3a)	332
Ethyl-8-Bromo-6-Phenyl-4 <i>H</i> -Imidazo-[1,5-a]-[1,4]-Benzodiazepine-3- Carboxylate (3b)	332
(<i>R</i>)-Ethyl-8-Bromo-4-Methyl-6-(2'-Fluorophenyl)-4 <i>H</i> -Imidazo-[1,5-a]-[1,4]- Benzodiazepine-3-Carboxylate (3c)	333
(<i>R</i>)-Ethyl-8-Bromo-4-Ethyl-6-(2'-Fluorophenyl)-4 <i>H</i> -Imidazo-[1,5-a]-[1,4]- Benzodiazepine-3-Carboxylate (3d).....	333
(<i>S</i>)-Ethyl-8-Bromo-4-Ethyl-6-(2'-Fluorophenyl)-4 <i>H</i> -Imidazo-[1,5-a]-[1,4]- Benzodiazepine-3-Carboxylate (3e)	334
Ethyl-8-Bromo-6-Phenyl-4 <i>H</i> -Imidazo-[1,5-a]-Thieno-[2,3-f]-[1,4]- Diazepine-3-Carboxylate (3f).....	334

Ethyl-8-Fluoro-5,6-Dihydro-5-Methyl-6-Oxo-4 <i>H</i> -Imidazo-[1,5- <i>a</i>]-[1,4]-Benzodiazepine-3-Carboxylate (3g)	335
Ethyl-8-Chloro-5,6-Dihydro-5-Methyl-6-Oxo-4 <i>H</i> -Imidazo-[1,5- α]-[1,4]-Benzodiazepine-3-Carboxylate (3h)	335
(<i>S</i>)-Ethyl-7-Bromo-11,12,13,13a-Tetrahydro-9-Oxo-9 <i>H</i> -Imidazo-[1,5- <i>a</i>]-Pyrrolo-[2,1- <i>d</i>]-[1,4]-Benzodiazepine-1-Carboxylate (3i)	336
Ethyl-8-Bromo-5,6-Dihydro-5-Methyl-6-Oxo-4 <i>H</i> -Imidazo-[1,5- <i>a</i>]-[1,4]-Benzodiazepine-3-Carboxylate (3j)	337
<i>tert</i> -Butyl-8-Bromo-5,6-Dihydro-5-Methyl-6-Oxo-4 <i>H</i> -Imidazo-[1,5- <i>a</i>]-[1,4]-Benzodiazepine-3-Carboxylate (3k)	337
5-(8-Ethynyl-6-Phenyl-4 <i>H</i> -Benzo-[<i>f</i>]-Imidazo-[1,5- <i>a</i>]-[1,4]-Diazepine)-3-Isopropyl-1,2,4-Oxadiazole (5 , EMJ-I-026)	338
5-(8-Ethynyl-6-(2-Fluorophenyl)-4 <i>H</i> -Benzo-[<i>f</i>]-Imidazo-[1,5- <i>a</i>]-[1,4]-Diazepine-3-yl)-3-Isopropyl-1,2,4-Oxadiazole (9 , YT-III-40)	339
5-(8-Cyclopropyl-6-Phenyl-4 <i>H</i> -Benzo-[<i>f</i>]-Imidazo-[1,5- <i>a</i>]-[1,4]-Diazepine-3-yl)-3-Isopropyl-1,2,4-Oxadiazole (10 , YT-III-41)	340
8-Cyclopropyl-3-(3-Isopropyl-1,2,4-Oxadiazole-5-yl)-5-Methyl-4 <i>H</i> -Benzo-[<i>f</i>]-Imidazo-[1,5- <i>a</i>]-[1,4]-Diazepine-6(5 <i>H</i>)-one (14 , YT-III-42)	341
(<i>S</i>)-5-(8-Ethynyl-6-(2-Fluorophenyl)-4-Methyl-4 <i>H</i> -Benzo-[<i>f</i>]-Imidazo-[1,5- <i>a</i>]-[1,4]-Diazepine-3-yl)-3-Isopropyl-1,2,4-Oxadiazole (16 , YT-III-44)	342
VI. References	343
Curriculum Vita	358

List of Schemes – Part 2.

Scheme 1	297
Scheme 2 with Binding Data	302
Scheme 3 with Binding Data	315
Scheme 4 with Binding Data	316
Scheme 5 with Binding Data	319
Scheme 6 with Binding Data	322

List of Figures – Part 2.

Figure 1. Proposed Topology of a GABA _A Receptor Subunit	278
Figure 2. Longitudinal (A) and Cross-Sectional (B) Schematic Representations of a Ligand-Gated Ion Channel.....	279
Figure 3. Absolute Subunit Arrangement of the $\alpha 1\beta 2\gamma 2$ GABA _A Receptor when Viewed from the Synaptic Cleft	280
Figure 4. Relative Locations of the Descriptors and Regions of the Unified Pharmacophore/ Receptor Model	289
Figure 5. Orthogonal Views of the Overlap of the Included Volumes of the Pharmacophore / Receptor Models for $\alpha 1\beta 3\gamma 2$ and the Other Five Receptor Subtypes ($\alpha 2\beta 3\gamma 2$, $\alpha 3\beta 3\gamma 2$, $\alpha 4\beta 3\gamma 2$, $\alpha 5\beta 3\gamma 2$, and $\alpha 6\beta 3\gamma 2$, Respectively).....	291
Figure 6. Oocyte Efficacy and <i>In Vitro</i> Receptor Binding Data on EMJ-I-026 (5)...	305
Figure 7. The Light / Dark Test and Locomotor Activity Test on EMJ-I-026 (5). ...	309
Figure 8. Binding Affinity at $\alpha x\beta 3\gamma 2$ GABA _A /BzR Subtypes (Values are Reported in nM) for YT-III-231 (8)	310
Figure 9. Carboxylic Acid of XHe-II-053	313
Figure 10. Binding Affinity at $\alpha x\beta 3\gamma 2$ GABA _A /BzR Subtypes (Values are Reported in nM) for YT-II-76 (13).....	318

List of Tables – Part 2.

Table 1. Action of Benzodiazepines at GABA _A $\alpha(1-6)\beta3\gamma2$ Receptor Subtypes.	284
Table 2. Examples of Imidazo[1,5-a][1,4]benzodiazepines Obtained using the New One Pot Procedure.....	299
Table 3. Acid / Base Stability Studies of XHe-II-053 (4) and EMJ-I-026 (5).....	311
Table 4. <i>In vitro</i> Metabolic Stability of Compounds 4 , 5 and 11 using Human Liver Microsomes by SRI International	313

PART 1. DESIGN AND SYNTHESIS OF CYSTEINE / CYSTINE PRODRUGS AND
BIOISOSTERES INCLUDING SYMMETRICAL AND UNSYMMETRICAL
DISULFIDES DESIGNED TO INCREASE CYSTINE LEVELS IN THE CNS IN
ORDER TO DRIVE THE CYSTINE / GLUTAMATE ANTIporter: A NOVEL
TREATMENT FOR SCHIZOPHRENIA AND DRUG ADDICTION

by

Edward Merle Johnson II

I. Background and Introduction

1. General Background to Schizophrenia, Drug Addiction and Current Treatments.

Schizophrenia is a debilitating disorder afflicting 1% of the world's population. The development of effective medications to treat schizophrenia is reliant on advances in characterizing the underlying pathophysiology. Chlorpromazine and other phenothiazines are considered first generation antipsychotics (termed "typical antipsychotics") useful in the treatment of schizophrenia.^{1,2} However, the antipsychotic efficacy of phenothiazines was, in fact, serendipitously discovered. These drugs were initially used for their antihistaminergic properties and later for their potential anesthetic effects during surgery.¹ Hamon and colleagues extended the use of phenothiazines to psychiatric patients and quickly uncovered the antipsychotic properties of these compounds; shortly thereafter, the pharmacologic characteristics of dopamine receptor blockade were linked to the antipsychotic action of chlorpromazine (Thorazine).¹ This led to the development of additional dopamine receptor antagonists, including haloperidol (Haldol). For nearly fifty years dopamine antagonists were the standard treatment for schizophrenia even though these drugs induce severe side effects ranging from Parkinson's disease-like motor impairments to sexual dysfunction and are only effective in treating the positive symptoms of schizophrenia.²

In the 1970's, clozapine became the first atypical or 2nd generation antipsychotic agent introduced.² Clinical trials have shown that clozapine produces fewer motor side

effects and exhibits improved efficacy against positive and negative symptoms relative to 1st generation compounds.^{2,3} However, clozapine was briefly withdrawn from the market because of the potential to produce severe agranulocytosis, a potentially fatal side effect requiring patients to undergo routine costly hematological monitoring. As a result, clozapine is only approved for treatment-resistant schizophrenia; this did not occur in the U.S. until 1990. Although also a dopamine receptor antagonist, the therapeutic site of action for clozapine is thought to involve blockade of serotonin receptors. This led to the generation of other serotonin receptor antagonists in the 1990's with the goal of improving the safety profile of clozapine.

The growth potential for novel antipsychotics was revealed following the introduction of risperidone in 1994; within two years risperidone overtook haloperidol in the number of prescriptions written by physicians. While it was generally assumed that the newer 2nd generation antipsychotics also exhibited the favorable efficacy profile produced by clozapine, the clinical data was ambiguous. As a result, NIH recently funded the largest (1,493 participants), longest (18 months), most expensive (\$42.6 million), and most thorough (1 typical and 4 atypical drugs were included) clinical trial to examine this assumption. The results of the Clinical Antipsychotic Trials of Intervention Effectiveness (CATIE), released in September 2005 indicated there was no benefit to the newer 2nd generation compounds (clozapine was not tested); specifically 1st and 2nd generation drugs did not differ in the incidence of severe motor side-effects nor were 2nd generation agents found to be more effective than 1st generation antipsychotics.⁴

In the CATIE trial, 74% of the patients discontinued treatment prior to completing the 18 month trial in part due to a lack of efficacy and intolerability of the treatment regimen. As a result, current expenditures on antipsychotic agents may underestimate the full market potential. Regardless, atypicals currently have over 90% of the \$10 billion antipsychotic market. Collectively, these data indicate there is a pressing need for novel antipsychotic agents. It is important to note that the efficacy of the prototypical 1st and 2nd generation (chlorpromazine, clozapine) antipsychotics were serendipitously discovered; the development of effective antipsychotic agents will be facilitated by understanding and targeting the pathophysiology underlying schizophrenia, as mentioned above.

Evidence indicates that the pathophysiology of schizophrenia involves a dysregulation in cortical functioning. Altered cortical functioning in schizophrenia involves, in part, altered glutamate signaling NMDA Receptor antagonists, including phencyclidine (PCP), produce a broad range of schizophrenia-like symptoms in healthy individuals^{5,6,7,8} and exacerbate symptoms in schizophrenic patients.^{9,10} PCP or the related compound ketamine also produces parallel cognitive and behavioral alterations in rodents that are used as a preclinical model of schizophrenia, including pronounced deficits in working memory and social withdrawal.^{11,12,13} Altered cortical functioning in schizophrenia has also been attributed to diminished glutathione which can account for a number of specific abnormalities associated with schizophrenia including increased oxidative stress, altered gene expression, and abnormal cell proliferation and connectivity.^{14,15} Cystine-glutamate antiporters, which exchange extracellular cystine for

intracellular glutamate may underlie cortical dysfunction in schizophrenia. Recent laboratory data illustrates that glutamate released from these antiporters provides endogenous tonic stimulation to group II mGluRs and thereby regulates synaptic glutamate and dopamine release.^{16,17} Thus, altered glutamate signaling could arise as a consequence of decreased cystine-glutamate exchange.

Furthermore, cystine transport via cystine-glutamate exchange is the rate-limiting step in the synthesis of glutathione; therefore, the depletion of glutathione in schizophrenics indicates diminished cystine-glutamate exchange. Drs. J. Meador-Woodruff and V. Haroutunian at the University of Michigan and Mount Sinai School of Medicine, respectively, have recently discovered that the expression of cystine-glutamate antiporters is reduced in post mortem tissue obtained from schizophrenics.¹⁷ Collectively, these data indicate that altered cystine-glutamate exchange may contribute to the pathology of schizophrenia. Increasing the activity of cystine-glutamate exchange reverses the behavioral and neurochemical effects of PCP that are used to model schizophrenia. Specifically, it has been recently determined that the cysteine prodrug N-Acetylcysteine (NAC), used to increase the activity of cystine-glutamate antiporters, reverses the PCP-induced alterations in glutamate signaling in the prefrontal cortex, as well as PCP-induced deficits in cognitive function and social withdrawal. Accordingly, the main goal of the present research is to determine the antipsychotic properties of cysteine/cystine prodrugs.

Addiction to psychomotor stimulants is marked by a transition in drug consumption from a casual, recreational style of use to a more compulsive, excessive pattern.^{18,19,20} Acute cocaine use is associated with numerous effects, including feelings of euphoria and increased energy, which likely contribute to repeated recreational consumption. Chronic use results in plasticity that is thought to underlie the emergence of persistent craving and paranoia that contributes to compulsive drug seeking behavior.^{21,22,23} Unfortunately, cocaine addiction still is lacking an effective pharmacotherapy, which will likely require compounds targeting plasticity pathogenesis for the transition in use patterns.

Uncontrolled drug use and heightened susceptibility to relapse are defining features of addiction that contribute to the transition in drug consumption from a recreational to a compulsive pattern.^{18,19} Identification of drug-induced neuroplasticity underlying this transition should facilitate the development of effective pharmacotherapies. Long-term plasticity which results in augmented excitatory neurotransmission within corticostriatal pathways has been implicated in addiction. Human cocaine abusers exposed to craving-inducing stimuli exhibit increased activation of excitatory circuits originating in cortical regions, including orbital and prefrontal cortex and projecting to the ventral striatum.^{24,25} Preclinical data also indicate the existence of drug-induced plasticity leading to activation of corticostriatal pathways. Activation of these circuits results in heightened extracellular glutamate in the nucleus accumbens^{26,27} and stimulation of ionotropic glutamate receptors, both of which are necessary for cocaine primed reinstatement.^{28,29} Furthermore, the dorsomedial prefrontal

cortex has been shown to be necessary for reinstatement produced by exposure to drug-paired cues using the contextual reinstatement paradigm and in response to electrical foot shock.³⁰ As a result, identification of cellular mechanisms capable of regulating synaptic glutamate may represent targets in the treatment of addiction.³¹

Recent data illustrates that glutamate released from these cystine-glutamate antiporters provides endogenous tonic stimulation to group II metabotropic glutamate receptors (mGluRs) and thereby regulate synaptic glutamate and dopamine release.³² Thus, altered glutamate signaling could arise as a consequence of decreased cystine-glutamate exchange. Repeated cocaine administration has been shown to blunt the activity of cystine-glutamate exchange³², which likely contributes to a sequence of events including diminished group II mGluR autoregulation³³ and increased excitatory neurotransmission in the nucleus accumbens. Cysteine prodrugs, such as N-Acetylcysteine (NAC), are used to drive cystine-glutamate exchange by elevating extracellular cystine levels, thereby creating a steep cystine concentration gradient.

Preclinical studies have shown N-Acetylcysteine is effective in blocking compulsive drug-seeking in rodents. Further, extant clinical data also show a reduction in cocaine use and craving in cocaine abusers receiving NAC. Unfortunately, the full clinical efficacy of targeting cystine-glutamate exchange may be unrealized when utilizing NAC due to extensive first-pass metabolism and limited passive transport of this drug across the blood-brain barrier. **As a result, here we propose to synthesize novel cysteine or cystine prodrugs. Note, cysteine is the reduced form of cystine and is**

readily oxidized *in vivo* to cystine thus elevating either cysteine or cystine levels would increase cystine-glutamate exchange. We will then utilize *in vitro* and *in vivo* screens to select the most promising novel compounds. Potential for therapeutic efficacy of the novel compounds will be determined in animal models involving drug-seeking behavior produced by stress, drug-paired cues, and a cocaine priming injection.

Addiction to cocaine and other illicit drugs is estimated to cost our society \$181 billion which equates to \$603 per U.S. citizen. The cost of addiction can be dramatically lowered through the use of treatments; unfortunately, many drugs of abuse, including cocaine, lack a single approved pharmacotherapy. Addiction to psychomotor stimulants, such as cocaine, is marked by a transition in drug consumption from a casual, recreational style of use to a more compulsive, excessive pattern that arises as a result of drug-induced changes in brain functioning. In order to develop effective treatments, it will likely be necessary to identify and target the altered brain functioning underlying addiction. Towards this end, drug-induced changes in glutamate release from cystine-glutamate antiporters have been linked to pathological alterations in neural transmission and normalizing cystine-glutamate function blocks compulsive drug-seeking in preclinical models. Furthermore, small-scale clinical studies using N-Acetylcysteine to target cystine-glutamate exchange have shown modest efficacy including reduced drug craving and cocaine use. The efficacy of N-Acetylcysteine is limited due to extensive metabolism in the liver and poor passive transport into the brain. Large doses are required for efficacy which can result in liver toxicity.^{18,19,22}

As a result in the present research one seeks to develop novel ligands that are more potent and effective in targeting cystine-glutamate exchange in the brain. They necessarily need to be of longer duration *in vivo* than N-Acetylcysteine and more readily pass through the blood brain barrier. This will involve the design of compounds and the synthesis of the most promising ones in order to utilize them *in vitro* and *in vivo* screening techniques to determine which compounds are most effective and potent in targeting cystine-glutamate exchange. Specifically, mixed cortical cell cultures will be employed to compare the capacity of brain cells to utilize the novel ligands to target cystine-glutamate antiporters.

Later the potency and efficacy of these novel compounds in blocking cocaine-primed, stress-primed and cocaine-paired use primed reinstatement in preclinical models of compulsive drug seeking will be assessed. Collectively, this research has the potential to identify cystine-glutamate antiporters as a novel target in the treatment of addiction and to generate a series of compounds that may ultimately be effective in treating cocaine addiction as well as schizophrenia.^{17,20,29}

2. Release of extracellular glutamate: Identification of a novel source.

Unlike traditional neurotransmitters, glutamate release is from both vesicular and nonvesicular stores. While synaptically released vesicular glutamate has been studied in great detail, basal extracellular glutamate sampled *in vivo* is present in micromolar concentrations in the extracellular space outside of the synaptic cleft. This pool of

glutamate is primarily maintained by nonvesicular release since levels are relatively insensitive to blockade of voltage-dependent Na^+ and Ca^{++} channels.^{34,35,36} Nonvesicular glutamate release has also been detected in hippocampal and prefrontal cortical tissue slices³⁷ indicating that nonvesicular release is not unique to the nucleus accumbens nor is it an artifact of microdialysis. The origin of nonvesicular glutamate has recently been demonstrated to arise, in part, from cystine-glutamate exchange.³² Data indicate that unlike Na^+ or Ca^{++} channels, blockade of cystine-glutamate antiporters produces a >50% decrease in extracellular glutamate levels in the nucleus accumbens.³² As stated above, this pool of glutamate contributes to synaptic neurotransmission by supplying endogenous tone to extrasynaptic group II mGluRs. Therefore, cystine-glutamate antiporters represent a novel cellular mechanism capable of modulating synaptic glutamate release into the nucleus accumbens following activation of corticostriatal pathways. In light of the importance of glutamate signaling for brain functioning in the normal and diseased states, it is important to characterize the role of cystine-glutamate antiporters to schizophrenia.

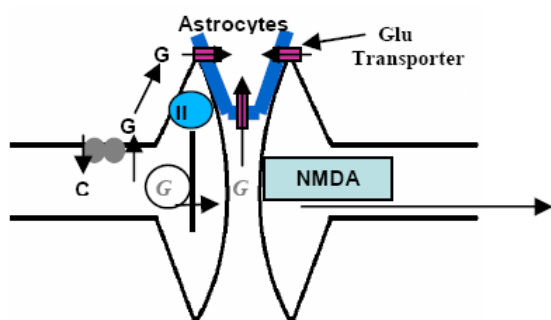


Figure 1. Regulation of glutamate signaling by cystine-glutamate antiporters. Nonvesicular release of glutamate (G) stimulates group II metabotropic glutamate receptors (mGluRs). Stimulation of these receptors decreases the release of vesicular glutamate (G) into the synapse, decreasing glutamate receptor signaling. C, cystine; G, glutamate; II, group II mGluRs.

3. Cystine-Glutamate Antiporter.

Cystine-glutamate antiporters function by transporting extracellular cystine (oxidized form of cysteine) into cells coupled with the export of intracellular glutamate.^{38,39} The antiporter exists as two separate proteins, the light chain xCT unique to cystine-glutamate antiporters and the heavy chain 4F2 that is common to many amino acid transporters.^{40,41} The antiporter is ubiquitously distributed throughout the body and brain.^{39,42,43} The regulation of cystine-glutamate antiporter activity is poorly understood, however, previous studies have indicated that extracellular cystine concentration and intracellular glutathione levels⁴⁴ can regulate the activity of these antiporters.

Cysteine prodrugs, including N-Acetylcysteine, are commonly used to elevate extracellular levels of cystine or cysteine, as well as intracellular glutathione levels, because these compounds are safer, more stable, and more likely to penetrate the blood brain barrier.^{45,46,47} In essence, cysteine prodrugs appear to penetrate the blood brain barrier, are rapidly degraded first into cysteine. Cysteine is subsequently oxidized into cystine because of the oxygen rich milieu of the extracellular space. The elevation in cystine increases the substrate concentration gradient, thereby increasing the activity of cystine-glutamate antiporters. The net effect is an increase in glutamate release and an increase in the synthesis of glutathione.

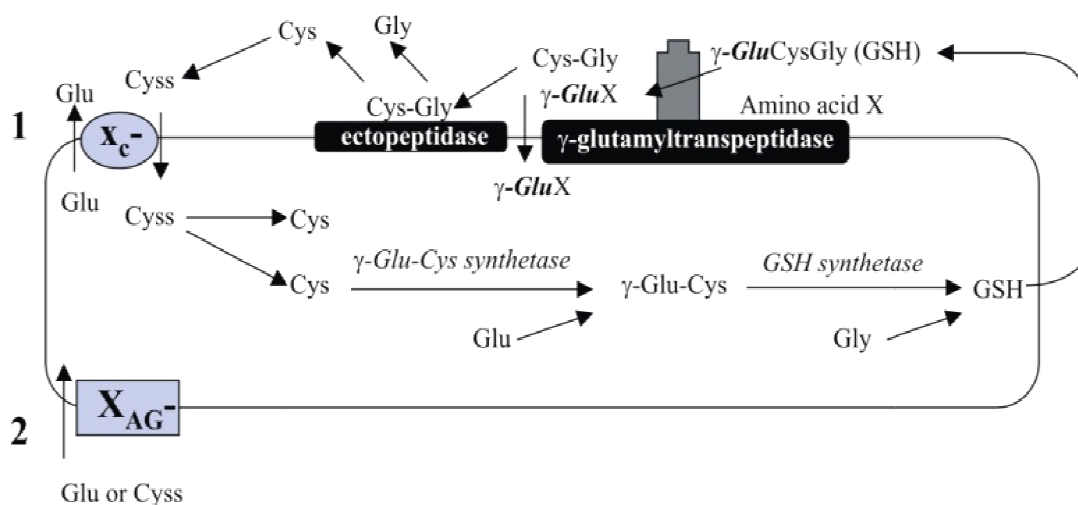
Figure 2

Figure 2. Schematic illustrating the uptake and recycling of cystine. Schematic of three uptake mechanisms for cyst(e)ine, including cystine-glutamate antiporters (x_c^- ; 1), Na^+ -dependent glutamate transporters (X_{AG}^- ; 2), and γ -glutamyltranspeptidase (3), which only occurs if cystine serves as the acceptor for the γ -Glu moiety (e.g., amino acid x). Glu (glutamate), Cyss (cystine), Cys (cysteine), γ -Glu-Cys (γ -glutamylcysteine), Gly (glycine), GSH, glutathione.

4. Glutathione and Cystine-Glutamate Antiporter Activity.

Once transported into the cell, cystine is rapidly reduced to cysteine.^{48,49}

Intracellular cysteine represents the rate-limiting step in the synthesis of the antioxidant glutathione.³⁷ Excess glutathione is released into the extracellular space, where it is degraded by γ -glutamyltranspeptidase into cysteine. Cysteine is subsequently oxidized into cystine because of the oxygen rich milieu of the extracellular space. This cycle appears to be the major source of extracellular cystine in the brain.⁴⁹ Alterations in glutathione levels can impact the activity of cystine-glutamate exchange. Specifically, a decrease in glutathione following oxidative stress results in an increase in the expression

of xCT, the active subunit of cystine-glutamate exchange. This will serve to increase cystine-glutamate exchange assuming that the substrates (e.g., extracellular cystine) are available.

5. Cystine-Glutamate Antiporters and Schizophrenia.

Extant data indicate that diminished cystine-glutamate exchange may contribute to the pathophysiology of schizophrenia. First, schizophrenia is associated with a profound reduction in prefrontal cortical glutathione levels.⁵⁰ A reduction in glutathione indicates decreased cystine-glutamate exchange because a) cystine-glutamate exchange is the rate-limiting step in glutathione synthesis; b) metabolism of glutathione is the primary source of extracellular cystine needed to maintain the activity of cystine-glutamate antiporters. Secondly, diminished cystine-glutamate exchange may also contribute to a decrease in the levels of xCT, the active subunit for cystine-glutamate exchange, which has recently been observed. This would be an expected compensatory change following diminished cystine uptake in an attempt to maintain glutathione levels. Thirdly, a recent study indicates an increase in the levels of group II mGluRs in post mortem tissue from schizophrenics.⁵¹ This would be an expected compensatory change following a reduction in the stimulation of this receptor. These studies are consistent with the hypothesis that diminished activity of cystine-glutamate antiporters contributes to the pathophysiology of schizophrenia.

As a result, cysteine prodrugs may be effective antipsychotic agents, in part, by directly targeting the pathology underlying schizophrenia. Moreover, cysteine prodrugs will likely achieve a number of therapeutic endpoints including: a) increased group II mGluR stimulation; b) decreased synaptic glutamate; c) increased NMDA receptor stimulation; and d) increase glutathione levels.

6. Clinical Applications of N-Acetylcysteine and Pharmacokinetics.

N-Acetylcysteine (NAC) is the only cysteine prodrug used clinically; for these purposes it has been proposed as a mechanism to restore glutathione, which is or has been proposed as a therapeutic endpoint for a number of conditions including respiratory disorders⁵², acetaminophen-induced hepatotoxicity^{53,54,55}, HIV^{56,57,58,59}, influenza⁶⁰, malaria⁶¹, cancer^{62,63,64}, Alzheimer's⁶⁵, and heart disease.^{66,67,68} There are a number of advantages to NAC, including a favorable safety profile even following long-term administration of high doses (e.g., 1-4 g/day); a dose range that has IRB approval to administer to cocaine addicts.^{18,19} However, pro-oxidant effects of NAC in this dose range have been observed in healthy individuals.⁶⁹ High doses are needed because of the poor oral bioavailability of NAC, which has been estimated at four and ten percent.^{70,71,72} Disulfide linking to proteins and deacetylation of NAC in the intestinal mucosa and lumen are probably the greatest factors in this apparent low oral bioavailability of NAC.

Brain tissue levels are considerably lower and have been estimated to be in the range of 0.4% of plasma levels (or ~ 0.016-0.04% of orally administered NAC). This is

due, in part, to poor passive penetration of the blood brain barrier, which is not surprising given a partition coefficient of -0.99 as opposed to 2-4 generally associated with reasonable passive diffusion.^{70,72} **As a result, these studies indicate a need to generate novel cysteine prodrugs that exhibit less first pass metabolism and a higher partition coefficient. If developed, these compounds could result in increased potency and efficacy as well as a diminished pro-oxidant effects associated with high dose NAC administration.** It is important to note that NAC administration in cocaine abusers is well tolerated, but the longest period monitored was 28 weeks in a small patient population.⁷³ It is possible that pro-oxidant effects of high dose NAC administration may produce toxicity when administered in larger populations for a longer period of time. Furthermore, higher doses of NAC may yield even greater efficacy than what is being tested.

7. Possible Approaches to increase CNS Cysteine/Cystine Levels.

As previously stated above, the overall goal of the research is to increase cysteine/cystine levels in the central nervous system (CNS). Even though the main pathway to accomplish this goal is to synthesize various analogues of cysteine/cystine in order to bypass metabolism, penetrate the blood brain barrier and deliver cysteine/cystine to the CNS, other pathways were considered and explored. The first of such other pathways included pharmaceutical formulation techniques. Currently, cystine/cysteine and analogues (NAC) are either commercially available as an oral solution or an immediate release tablet/capsule formulation. This, of course, causes the compound to be

quickly released and either absorbed by the body or eliminated due to GI overload; bioavailability is around 5-6%. This immediate release type of formulation also must be taken multiple times a day at high quantities to maintain desired serum concentrations. The idea is to design either a slow release (sustained release) formulation that will slowly release a large amount of the desired compound (cystine/cysteine) over 8 to 12, or 12 to 24 hrs.

This, of course, could be done by a number of methods: a) using time released micro-encapsulated pellets compressed into a tablet or loaded into a capsule; b) partition tablet design that would allow for the immediate release of some drug, followed by the slow release of the remaining drug in either 1 to 4 slow dissolving partitions; c) osmotic pump type capsule that will slowly release a steady stream of the desired compound into the GI system; d) matrix type tablets which will slowly erode and release the desired compound. All methods described above have been and are currently used in the pharmaceutical field to provide a vehicle for once or twice a day dosing.

Of course, this formulation approach is not novel, except for the case of it here for cystine/cysteine and analogues (NAC). This approach does have a few drawbacks associated with it, as found in other drugs on the market that employs a similar approach such as a) dose dumping (where all of the drug is prematurely released); b) time and resources in order to design and formulation of the release vehicle and product (should be able to incorporate current technology to assist with this method).

Some possible advantages include a) once or twice daily dosing of the drug; b) provide a constant stream of drug to the GI system which may result in greater absorption, which in turn would outpace the metabolism of the drug, permitting for higher serum levels and higher CNS levels; c) be a relatively quick and easy method in addressing cystine/cysteine rapid metabolism and poor bioavailability; d) relatively cheaper and faster than designing and synthesizing many series of new cystine/cysteine analogues.

Another idea for formulation is to design and implement an oil/water type vehicle in which the desired compound, cystine/cysteine or analogues, is encapsulated in many micro lipid bilayer cells and stored in a gel capsule. This method could be accomplished by a study and discovery of the correct commercially available lipid used in micro bilayer creation. Once the appropriate lipid is found, the size of the micro lipid bilayer cells would have to be addressed. Currently, micro lipid bilayers are created by rapidly stirring the mixture of water, drug and lipid then pressing it through a predefined pore size filter. The pore size will determine the micro lipid bilayer cell size. This cell size would have to be studied and experimented with to obtain the desired outcome in the body. The cells cannot be too large because they will not be absorbed correctly and may even be digested by the GI system before absorption. Too small of a cell size will not carry enough of the desired drug and my end up tied up and carried by the plasma proteins and other transporter systems in the blood.

Some disadvantages may include: a) the time and potential cost in developing the correct vehicle; however, using current literature and other resources may help reduce this problem; b) The potential biological effect of overloading the body with lipids (weight gain, fatty liver, high triglycerides, ect.); c) the need for multiple daily doses to maintain levels; d) digestion of the micro lipid bilayer cells and dose dumping.

Some possible advantages would include: a) a method to get cystine/cysteine or analogues (NAC) rapidly absorbed and past the liver in first pass metabolism; b) potential slower metabolism of the drug due to the drug being hidden in the micro cells; c) constant stream of free drug into the blood, as the micro lipid bilayer cells slowly breakdown, they will release the drug into the blood similar to a slow release formulation; d) potential higher CNS levels due to the ability of the micro lipid bilayer cells to move readily and passively transverse the Blood, Brain Barrier (BBB).

The second, and more chemistry chemically-based approach to increase the cysteine/cystine levels in the CNS in order to drive the cystine/glutamate antiporter would be to make series of cysteine/cystine analogues. This was the method that was studied here and will be described from this point on. The thought was to drive the cystine/glutamate antiporter by providing cysteine/cystine at high enough concentrations in the CNS to facilitate the antiporter action. However, this method was different from current pharma perspectives because this study focused only on one desired outcome (product), cystine. All compounds currently designed or studied here should have no biological activity in their original form but require conversion into cystine/cysteine, *in*

in vivo. This approach limits the testing of such compounds because in order for the compounds to show activity, they must be metabolized or transformed into the active compound (cystine/cysteine). For the many different series, all compounds were designed to be given orally in order to be converted into cystine/cysteine. Any method of testing that bypasses metabolism will result in a possible negative result.

The ideal approach would be to design better ligands to drive the cystine/glutamate antiporter that can be given either orally or tested *in vitro* and have similar outcomes. The process would involve analyzing cystine and determining the key structures that are responsible for receptor binding and activation of the antiporter (Structure Activity Relationships). After which, one could start designing new ligands that should bind to the receptor and activate the antiporter. In the process of design, certain issues will be addressed and incorporated into the ligands.

Metabolism is a major issue to be addressed. When new ligands are designed, care will be taken to ensure that the final ligands will not be sensitive to rapid metabolism by the body. This will be accomplished by incorporation of certain functional groups and likewise, elimination of certain functional groups. Along with metabolism, solubility is also a key issue to address. As with metabolism, great care will be taken to ensure the final ligands possess the appropriate solubility profile by including certain functional groups. Solubility is better expressed as the LogP of a compound. This is an important issue to address because a ligand must have the ability to cross the BBB and enter the CNS. Once again, in the design of the final ligands, care will be taken to ensure the

appropriate LogP (between 2-5), although some ligands may be outside of this range for practical reasons or as negative controls.

This approach does have certain drawbacks that must be realized which include: a) since the antiporter will be driven by ligands and not cystine, the ligand will enter the nerve cell and won't be converted into glutathione, which has been shown to be beneficial further down the line; b) the potential amount of time and cost associated with the design and synthesis of a new series of ligands that may or may not even bind to the receptor and activate the antiporter, which is, of course, a usual problem associated with medicinal chemistry.

Some advantages of the ligand approach include: a) the use of high throughput screening techniques. Since the ligands will be designed and synthesized in the active form, *in vitro* testing will be easier and more reliable; b) the lack of the metabolism requirement to convert the ligand into the active compound; c) all of which would lead to shorter down time in the design of future ligands and improving outcomes.

8. Approach to be studied: cysteine/cystine analogues.

This research relates generally to the treatment of schizophrenia and drug addiction by increasing cysteine/cystine levels in the CNS. More particularly, the present research is directed to the design and synthesis of cysteine and cystine prodrugs designed to be metabolized into cysteine and cystine, therefore, increasing

cysteine and cystine levels in the CNS. This research also involves the design and synthesis of cysteine and cystine mimics known as bioisosteres, used to drive the cystine-glutamate antiporter. Together, all of these analogues will be studied for their usefulness as antipsychotic medications in the treatment of schizophrenia. As well, the respective compounds are applicable for the potential reduction of drug cravings in drug addicted individuals. This approach will also be useful in determining some structure active relationships of the cystine/glutamate antiporter.

The cystine-glutamate antiporter is a highly novel cellular process that likely contributes to the pathology underlying schizophrenia and drug addiction. Unlike existing medications, cysteine prodrugs appear to exert antipsychotic properties, in part, by reversing pathology underlying the disease. While no one theory or mechanism of pharmacological effect is adopted herein, cysteine prodrugs appear to restore diminished signaling to glutamate receptors and diminished glutathione levels observed in schizophrenics. A depleted glutathione level can lead to a number of effects which are observed in schizophrenia such as: increased oxidative stress, and impaired cystine-glutamate antiporter activity, glutamate neurotransmission, synaptic connection, and gene expression.

Increased excitatory neurotransmission in the nucleus accumbens may arise, in part, by diminished activity of cystine-glutamate antiporters. The recent data collected in the present research illustrates that glutamate released from these antiporters provides endogenous tonic stimulation to group II or 2/3 metabotropic glutamate receptors

(mGluRs) and thereby regulates synaptic glutamate and dopamine release. Thus, altered glutamate signaling could arise as a consequence of decreased cystine-glutamate exchange. Repeated cocaine administration has been shown to blunt the activity of cystine-glutamate exchange, as mentioned, which likely contributes to a sequence of events including diminished group II mGluR autoregulation and increased excitatory neurotransmission in the nucleus accumbens.

Impaired cystine-glutamate antiporter activity and faulty glutamate neurotransmission bear on the issue of uncontrolled drug use, i.e., drug addiction, as described above. Cysteine prodrugs, such as N-Acetylcysteine (NAC), are used to drive cystine-glutamate exchange by apparently elevating extracellular cystine levels, thereby creating a steep cystine concentration gradient. Preclinical studies have shown N-Acetylcysteine to be effective in blocking compulsive drug-seeking in rodents. Furthermore, extant clinical data also shows a reduction in cocaine use and craving in cocaine abusers receiving NAC. Unfortunately, the full clinical efficacy of targeting cystine-glutamate exchange may be unrealized when utilizing NAC due to extensive first-pass metabolism and limited passive transport of this drug across the blood-brain barrier. The prodrugs described in this research should not significantly be eliminated by liver metabolism and should readily pass through the blood-brain barrier. Cysteine is the reduced form of cystine and is readily oxidized *in vivo* to cystine; therefore, elevating either cysteine or cystine is believed to increase cystine-glutamate exchange, as described earlier.

The cysteine prodrug NAC has been previously shown to have a favorable safety/tolerability profile in human subjects.^{70,71} In fact, NAC has been used for decades in humans for other indications (e.g., as a mucolytic, acetaminophen toxicity)^{53,54,55,63} and as an experimental treatment (HIV, cancer)^{56,57,58,59,62,63,64} without producing severe adverse effects.^{70,72} However, NAC undergoes extensive first pass metabolism requiring the usage of high doses that limit the utility of the drug and, potentially, increase the chances of side effects due to the buildup of metabolized by-products, as discussed.^{70,72} The prodrugs presently described in this research are designed to substantially avoid the problem of first pass metabolism and poor blood brain barrier permeability, and therefore exhibit increased efficacy as compared to prior cysteine prodrugs as illustrated by improved potency and/or efficacy.

Repeated cocaine alters glutamate neurotransmission even following protracted withdrawal and this likely contributes to addiction since abnormal activation of corticostriatal pathways correlates with craving in humans and is necessary for cocaine seeking in rodents. Revealing cellular mechanisms underlying altered corticostriatal activation should advance our understanding of the neurobiological basis of addiction and identify novel therapeutic targets.

Models of pathological glutamate signaling proposed to underlie addiction need to account for the existence of multiple pools of extracellular glutamate. Aside from synaptic glutamate maintained by vesicular release, extrasynaptic glutamate is sustained primarily by nonvesicular release. In support, basal extrasynaptic glutamate sampled by

microdialysis is largely independent of vesicular glutamate. Glutamate transporters may partition the two pools by limiting glutamate overflow from the synapse into extrasynaptic compartments, and restricting entry of nonvesicular glutamate into synapses. Although confined to the extrasynaptic compartment, nonvesicular glutamate regulates neurotransmission by stimulating group II metabotropic glutamate receptors (mGluRs) which are extrasynaptic receptors capable of inhibiting vesicular release. Therefore, extrasynaptic receptors permit crosstalk between the two pools and indicate that altered nonvesicular glutamate release may contribute to pathological glutamate signaling linked to addiction.

Cystine-glutamate exchange via the cystine/glutamate transporter system may be critical in the capacity of extrasynaptic glutamate to regulate corticostriatal signaling in the normal and pathological states. First, nonvesicular release from cystine-glutamate exchange maintains basal extracellular glutamate in the nucleus accumbens, and thereby regulates the extent of endogenous group II mGluR stimulation. Repeated cocaine blunts transporter activity which leads to reduced basal and increased cocaine-evoked glutamate in the nucleus accumbens that persists for at least three weeks after the last cocaine treatment.^{27,28} These changes are relevant for drug seeking since N-Acetylcysteine, a cysteine prodrug used to drive the transporter system, blocks cocaine-evoked glutamate in the nucleus accumbens and subsequent cocaine-induced reinstatement.^{27,28}

9. Potential Pitfalls in Novel Approaches to Treat CNS Disorders.

Since the approach here relies heavily on the design and synthesis of cyclic peptide analogues of cysteine and cystine, the concerns in regard to novel medicinal chemistry follow here. There is no guarantee that these cyclic peptides will be efficiently hydrolyzed by amidases or metabolized to liberate cystine, although many amidases and nonselective peptidase hydrolyases exist in the brain tissue.^{70,72} Substitutions on these cyclic diketopiperazine rings can potentially further complicate the liberation of cystine since hydrolysis of amides can be hindered due to steric crowding. Hence, without any direct evidence of whether such hydrolysis will take place, different types of analogues will be prepared.

Based primarily on data from the first lead compound (**1**), as shown in **Figure 3** and **Figure 4**, this approach definitely shows promise. According to what is known about the mechanism of the transporter and the mechanism of cystine in the transporter, the first lead compound (**1**) most likely remained intact longer in the blood and passed through the blood brain barrier after which it was hydrolyzed by enzymes or decomposed into the desired product, cystine.

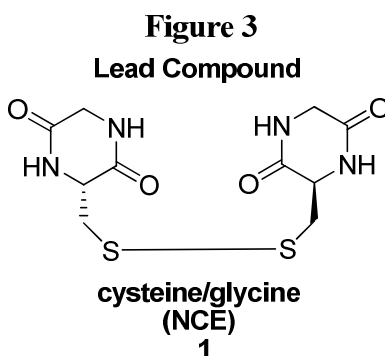
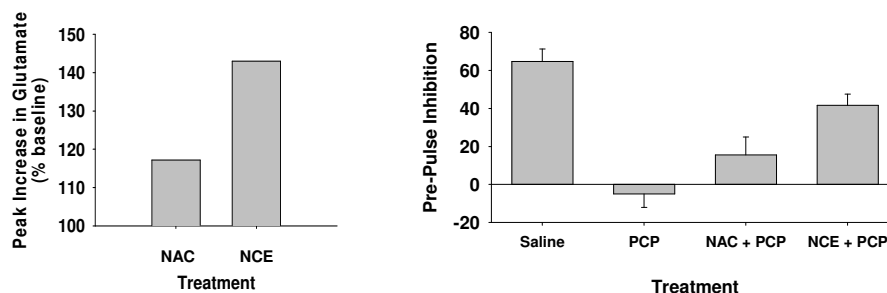


Figure 4

Preliminary studies in rats using oral N-acetyl cysteine (NAC) and compound 1 (NCE) in the PCP model.



Sensorimotor gating, a process compromised in schizophrenic patients, is often measured using pre-pulse inhibition whereby a mild auditory stimulus (pre-pulse, 2-15 db above background) precedes (100 ms) a startle-eliciting auditory stimulus (50 dB above background). Intact sensorimotor gating will result in suppression of the startle reflex when preceded by the pre-pulse. Since improvement in pre-pulse inhibition tracks improvement in symptoms that are largely insensitive to current treatments, this paradigm has become one of the most commonly used screening paradigms. **Figure 4** illustrates the capacity of PCP to disrupt pre-pulse inhibition, rendering the pre-pulse ineffective in suppressing the startle reflex. PCP is commonly used to disrupt pre-pulse inhibition because this abnormality, in addition to negative and cognitive symptoms, is insensitive to 1st generation antipsychotics, thereby providing predictive validity. Also illustrated in **Figure 4** is the impact of N-Acetylcysteine (NAC) and NCE on sensorimotor gating deficits produced by phencyclidine administered orally (right). * indicates a significant difference from rats receiving PCP only (e.g., 0 N-Acetylcysteine or NCE), Fisher LSD, $p < 0.05$.

One concern early on in the design plan was that substitutions on diketopiperazine rings can potentially further complicate the liberation of cystine for hydrolysis of amides can be further retarded due to steric crowding. Fortunately, it was shown very early by Abderhalden,⁷⁴ in 1932, that “cleavage experiments in which the action of 0.1 N NaOH, 5 N HCl, trypsin-kinase and erepsin on amino-acid-(2,5-diketopiperazine)s was determined and showed that the substitution of an amino acid radically greatly diminished the stability of the diketopiperazine ring which readily opened up to form the tripeptide.”⁷⁴

Furthermore, it was also shown earlier by Kawai,⁷⁵ in 1928, that “glycine-DL-phenylalanine as well as II (the diketopiperazine) was hydrolyzed asymmetrically by crepsin and the digestion mixture showed distinct L-rotation after a certain time.”⁷⁵ However, it was also shown by the same author that “III (another diketopiperazine) was not hydrolyzed by erepsin, trypsin, ect..”⁷⁵ which indicates one can manipulate stability by substituent patterns.

Other authors later reported that certain diketopiperazines were not hydrolyzed by enzymes. In 1936, Greenstein⁷⁶ reported “the diketopiperazine, anhydro-l-lysyl-glutamic amide, was completely resistant to pepsin, trypsin and papain-HCN.”⁷⁶ The author does caution the reader that “while these results are not sufficient in themselves to discredit the diketopiperazine hypothesis, they do imply that considerable caution should be exercised in applying the anhydride structure to proteins.”⁷⁶

After further studies by Abderhalden⁷⁷, it was reported in 1940 that based on another author's work (Sibata) "pepsin should be able to split basic peptide anhydrides while the splitting of the acid anhydrides by trypsin, papain and cathepsin should also be possible."⁷⁷ Abderhalden used numerous enzymes in his studies including dipeptidases, polypeptidases, trypsinokinases, and pepsin. "Although the experimental conditions varied widely, negative (non-hydrolysis) results were obtained with all substrates and all enzymes."⁷⁷ However, the author continues to report "upon repeating some of the experiments, it was found that glycyl-L-glutamic acid anhydride was split up by trypsinokinases."⁷⁷

Based on these authors, it was apparent that the debate on whether diketopiperazines were readily metabolized by enzymes was a complicated matter. While it was possible to find cases where diketopiperazines were metabolized, it is also just as easy to find cases where they were not. It is important to note, that based on a majority of the cases, the more sterically hindered diketopiperazine was either more rapidly metabolized or decomposed to the hydrolysis product which would be hydrolyzed readily in the CNS by amidases, peptidases and non-specific hydrolyases.^{74,76,77}

Due to these discrepancies, further reading and research into the subject was required. Martins and Carvalho published a mini-review in 2007 in regard to the use of diketopiperazines as drugs, their biological activity and synthesis.⁷⁸ As pointed out in the article, "their peculiar heterocyclic system (diketopiperazine) found in several natural products constitutes a rich source of new biologically active compounds."⁷⁸ The authors

established their importance by providing a list of the most common biological uses for diketopiperazines. “Some of the most important biological activities of diketopiperazines are related to the inhibition of plasminogen activator inhibitor-1 (PAI-1) and alteration of cardiovascular and blood clotting functions. They also express activity as antitumour, antiviral, antifungal, antibacterial, and antihyperglycaemic agents as well as affinity for calcium channels and opioid receptors, GABAergic receptors, serotonergic 5-HT₁ and oxytocin receptors”⁷⁸. “Diketopiperazines are privileged structures for the discovery of new lead compounds by combinatorial chemistry and are considered ideal for the rational development of new therapeutic agents” as described by Martins.⁷⁸ The metabolism of diketopiperazines is referenced as “diketopiperazines are considered as constrained amino acid and protein β -turn mimetics. An additional example of the recognition and metabolism of cyclic dipetides by enzymes was demonstrated with tyrosine hydroxylase, which catalyses the limiting step in catecholamine biosynthesis.”⁷⁸

As one concluded, the issue concerning the fate of diketopiperazines in the mammalian body is complex and multifaceted. However, it is certain that diketopiperazines hold a very important part in the drug discovery process as is demonstrated by the current drugs in clinical trials and the ones being marketed.⁷⁸ Listed below in **Figure 5** are a list of relevant hydrolytic enzymes found in the CNS. These enzymes should play a major role in the metabolism of the cysteine/cystine prodrugs, bioisosteres and analogues synthesized in order to release the desired compound cysteine/cystine.

Figure 5: List of Relevant Hydrolytic Enzymes Found in the CNS

- 1) Peptidases – hydrolyzes amide (peptide) bonds into an amine and a carboxylic acid
 - a. General Peptidases – nonspecifically hydrolyzes amide bonds on a wide range of compounds
 - b. Aminopeptidases – specific to protein metabolism and amino acid peptide bonds
 - c. Cysteinylglycinase – hydrolyzes the peptide bond between cysteine and glycine
 - d. Cysteine proteases – specific to peptide bonds that contain the amino acid cysteine
 - e. Serine proteases – specific to peptide bonds that contain the amino acid serine
- 2) Esterases – hydrolyzes esters into an acid and an alcohol
 - a. General Esterases – nonspecifically hydrolyzes ester bonds on a wide range of compounds
 - b. Acylesterases – hydrolyzes off acetyl groups (acetic acid)
 - c. Thioesterases – hydrolyzes thioesters to form thiols and carboxylic acid
- 3) **Hydrolases – nonspecifically catalyzes the hydrolysis of chemical bonds**
 - a. **Hydrolyzes the following bonds: amide bonds, esters bonds, anhydride bonds, sulfur-sulfur bonds, carbon-sulfur bonds, carbon-carbon bonds, ether bonds, along with a wide range of other functional groups**

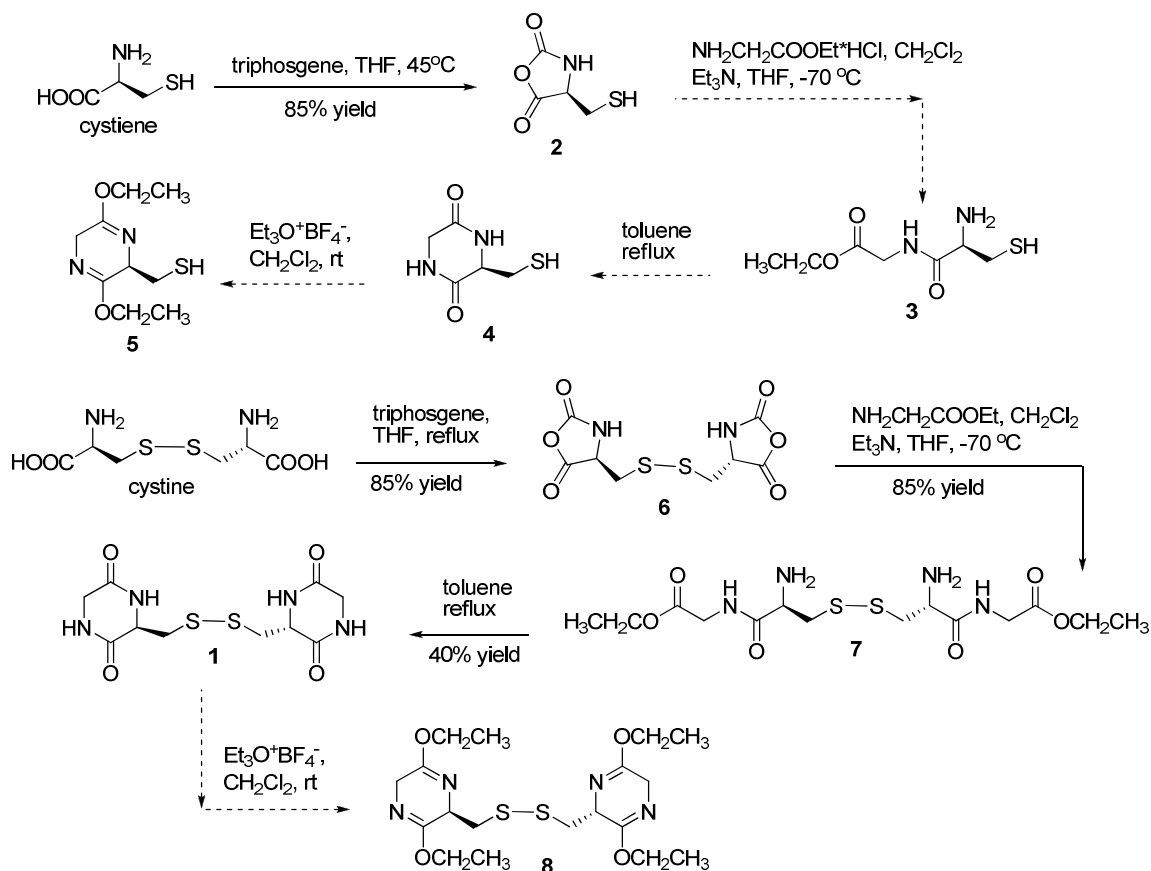
II. Design and Synthesis of Cysteine and Cystine Prodrugs

1. Initial Approach to the Synthesis of Cysteine and Cystine Prodrugs

The initial approach was to design cysteine and cystine prodrugs that will be either metabolized or chemical converted, *in vivo*, into the desired product, cystine. Since cysteine is known to be oxidized into cystine in the extracellular region of the brain, either end-point was desirable. Using chemistry previously described by Schölkopf⁷⁹ and scaled up in our laboratory, a synthetic route was outlined that followed the classic Schölkopf chiral auxiliary pathway, **Scheme 1**.⁷⁹ Cysteine or the dimer cystine were suspended (individually) in THF and treated with triphosgene and heated to 45°C. The unstable anhydride intermediates, **2** and **6** respectively, which resulted were treated with glycine ethyl ester HCl salt under basic conditions at -70 °C. This should have resulted in the more stable esters **3** and **7**, respectively. Heating esters **3** and **7** (individually) to reflux in toluene would normally promote intramolecular cyclization to form the first diketopiperazine targets, **4** and **1**, respectively, after which, the final desired diketopiperazines could be obtained through simple alkylation (see **5** and **8**).

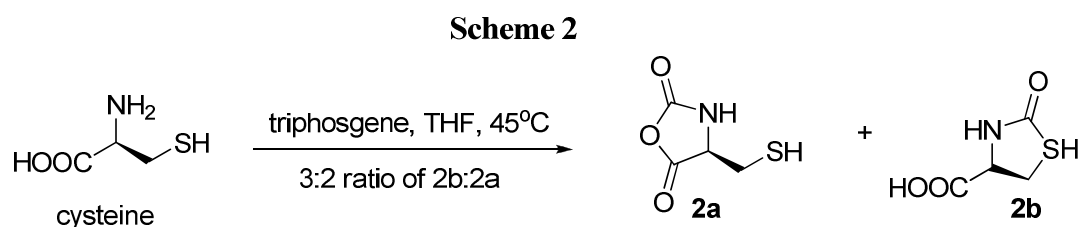
Scheme 1

Initial Synthetic Route to Diketopiperazine Targets



Certain problems became apparent during the large scale synthesis of the desired diketopiperazine targets **5** and **8**. Cysteine, unlike many other amino acids used in the past,⁷⁹ has a reactive side chain and free thiol, which can undergo addition cyclization reactions when treated with triphosgene, as shown in **Scheme 2**. Although this problem was discussed and ways to overcome this problem were previously devised, such as protecting the thiol group, it was decided to proceed with the original synthetic pathway. The secondary product turned out to be more difficult to remove and made up a significant amount of the yield (~65%) compared to the initial estimates. Continuation of this synthetic route proved to cause additional problems with solubility and unidentifiable

byproducts, which was thought to be formed by the polymerization of the cysteine with itself or glycine. Because of these problems and the need to synthesize analogues quickly for in vitro and in vivo testing, the cysteine pathway was temporarily held to pursue the cysteine pathway.



Since cystine is the disulfide of cysteine, there was no free thiol group to react and cyclize during the anhydride formation or the intramolecular cyclization reaction. However, there was another problem not confronted when the monomer of the amino acid had been employed. Since, cystine was a dimer, there are twice as many amino acid functional groups that must be considered when carrying out reactions. Also, these functional groups are in close proximity to each other and may undergo intramolecular reactions or intermolecular reactions to form polymers. In order to prevent intermolecular reactions, all reactions were carried out under conditions of high dilution; 4-5 times that of normal. Also, each reaction was cooled and heated only when needed to prevent any unintentional intramolecular reactions from taking place.

Although certain precautions were taken to prevent side reactions and prevent problems, it became apparent in the beginning that the disulfide amino acid cystine will be difficult to work with as a starting material. The solubility of the disulfide was much

lower than the monomer, which was to be expected, but to the extent that the reactions took 3-4 times longer, even after adjusting the equivalents and concentrations of the other reagents to closely match past procedures due to the larger volume of solvent required for solubility and to prevent intermolecular reactions with the disulfide amino acids.

Confirmation that each reaction went to completion was also difficult due to the solubility of the starting material and product along with the presences of multiple functional groups in a symmetric compound. After each reaction was complete, workup (filtering and washing) and recrystallization of the product from water/methanol resulted in very low yields (~15-25% of **1**) compared to the initial parent compounds and pathways previously executed in this laboratory (90-98%), in other work.⁷⁹

In the initial synthetic route to the diketopiperazine targets, the cysteine pathway did not work in a practical sense and will need to be revised for future exploration. Although the cystine pathway did offer some benefits to the cysteine pathway, it also had some problems and will also be revised for future exploration. Of the initial compounds proposed, only compound **1** was synthesized in any measurable quantity (30 grams) and has been tested *in vivo* on rats to determine if this line of compounds will be advantageous to pursue. In the preliminary studies shown before, it is clear that compared to the current standard, N-acetyl cysteine, diketopiperazine **1** (NCE) was more active (see **Figure 4**) and analogues pursued further.

2. Improved Synthesis of Cysteine and Cystine Prodrugs.

Based on the knowledge from the previous chemistry and the problems confronted, the synthesis of the diketopiperazine targets was revised to provide an improved pathway which would result in fewer side products and yet provide an opportunity for drug development. As shown in **Scheme 3**, the lead diketopiperazine targets **12** and **13** are outlined.^{79,80,81,82} The chemistry employed is analogous to the Schölkopf chiral auxiliary currently being used in Milwaukee for alkaloid total synthesis and was scaled up to kilogram scale.⁷⁹ Protection of the thiol (-SH group) in cysteine using tert-butyl alcohol in the presence of hydrochloric acid or phenylsulfenyl chloride or triphenyl methyl chloride was required to insure the formation of the Schölkopf chiral auxiliary and prevent other cyclization reactions, as previously depicted above in **Scheme 2**. The S-protected-cysteines (**9a-9c**) were treated with triphosgene (individually) to form the unstable anhydride intermediates (**10a-10c**). This step was followed by condensation with any number of the desired amino acid ethyl or methyl esters, followed by heating to reflux in toluene to effect the intramolecular cyclization to targets (**11a-11c**), respectively.

Outlined in **Figure 6** are the possible compounds that can be made from using naturally occurring amino acids. However, unnatural amino acids and designer amino acids can also be prepared and will be incorporated into the list of test compounds. The initial choices for monomer and dimers are boldfaced and underlined in **Figure 6**. Diketopiperazine compounds containing amino acids cysteine, glycine, phenylalanine,

proline, and valine (**12a**, **12b**, **12c**, **12d**, **12e**) were considered the most important target compounds. These compounds were chosen for reasons of either partition coefficients (valine, proline), active transport (phenylalanine, proline), or the breakdown products are important for glutamate/cystine antiporter function (cysteine, glycine).

Thiol deprotection of diketopiperazine **11** using the appropriate reagents will lead to the free thiol targets (see **12**). Alkylation of amide **12** will produce another desired prodrug diimide **13**. During the design of this synthetic route, it was discovered that simple hydrolysis of diimide **13** with trace amounts of hydrochloric acid and water resulted in the production of monoimides **14** and **15**, which are patented. Upon further treatment with acidic water, monoimides **14** and **15** were completely converted back into the dealkylated diketopiperazine (see **12**), which would occur in the stomach, as planned.

The treatment of target compounds (**11b-11c**, **12**) with either a) 2-mercaptoethanol, b) iodine and pyridine in dichloromethane, or c) catalytic amounts of iodine in ethanol, produced the symmetrical disulfide dimer **16**, as shown in **Scheme 4**.

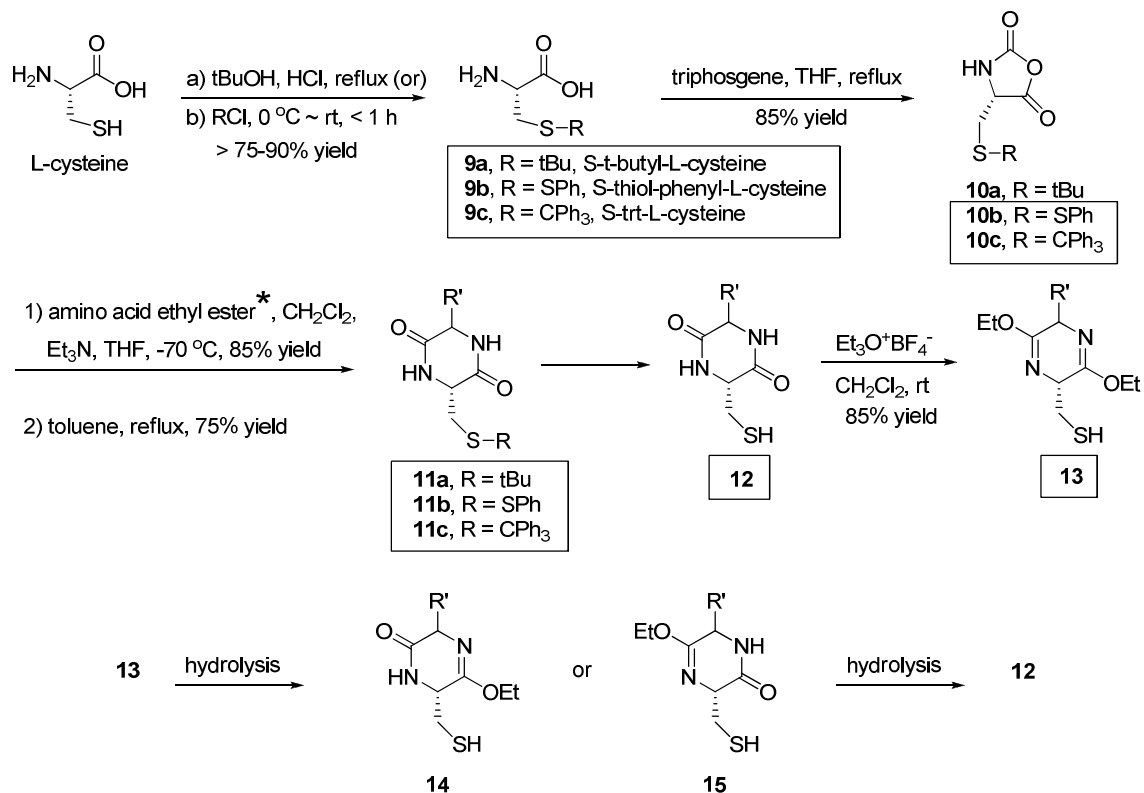
This revised synthetic route, **Scheme 3**, had many advantages over the initial route outlined above in **Scheme 1**. a) To date this is the only practical synthetic route that leads to both monomers and dimers (cysteine and cystine prodrugs), b) protection of the thiol group prevents side cyclization reactions and facilitates chromatographic purification, c) initial monomer synthesis eliminates the problems of multiple functional

groups reacting with reagents or each other simultaneously, d) the occurrence of undesired intramolecular and intermolecular side reactions is decreased, e) this work can be easily expanded to incorporate additional amino acid reagents.

Listed in **Table 1** is a list of compounds prepared following **Scheme 3** and **Scheme 4** by members of the Cook group, under the direction of myself and/or synthesized by myself, the primary project researcher. Compounds that are “boxed” in each general scheme were actually synthesized as shown in the general scheme. After which is a detailed listing of some key reactions and target prodrugs. **The complete experimental details are located in Chapter IX – Experimental Section, and includes weights, molar quantities, volumes, temperatures, and spectral data.**

The rationale of the prodrug approach is that upon oral administration in a subject, chemical entities are readily converted *in vivo* to the pharmaceutically active compounds in either the stomach (pH=2) or the gut (pH=10). According to the previous literature⁷⁸ and preliminary studies, the diketopiperazine targets should pass largely intact through first pass metabolism and then should be hydrolyzed (cleaved) into the corresponding amino acids by peptidases or hydrolyases in cells contained within the CNS depicted before in **Figure 5**.

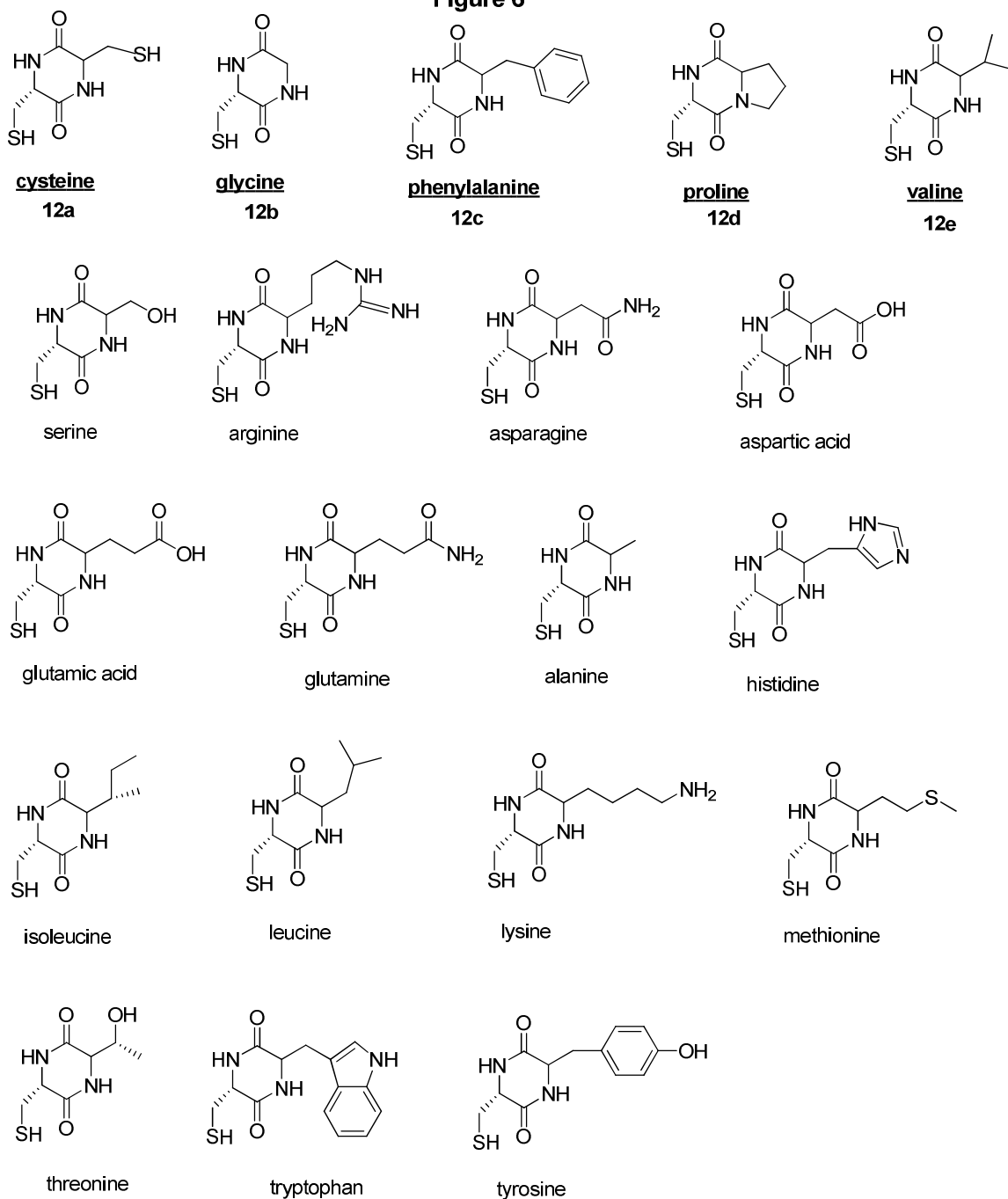
General Synthesis of Diketopiperazine Targets Scheme 3



* All natural and selected unnatural amino acids can be used.

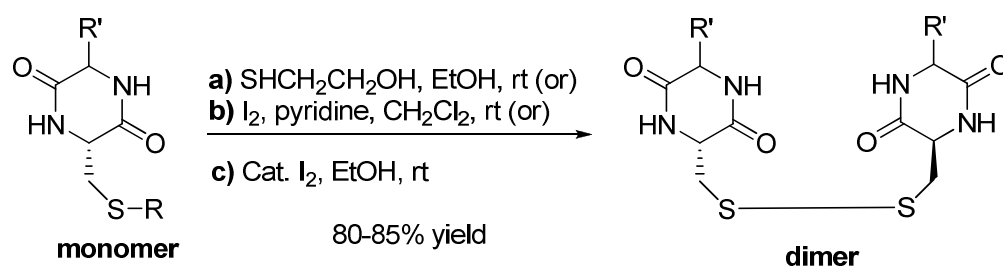
**Diketopiperazine Targets Using Various
Natural D- and L-Amino Acids**

Figure 6*



* First targets in series are underlined above.

**General Coupling of Monomers to
Form Symmetrical Disulfides
Scheme 4**



11b, R = SPh
11c, R = CPh₃
12, R = H

16

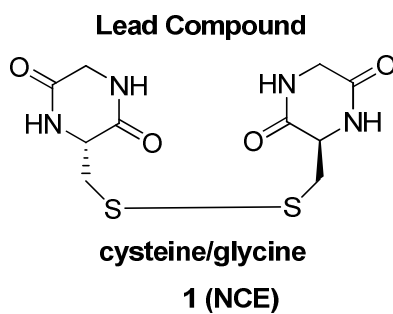
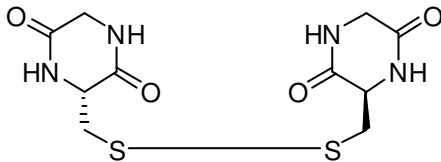
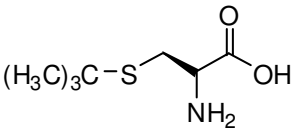
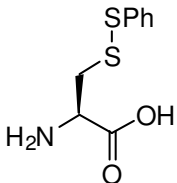
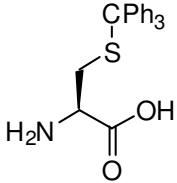
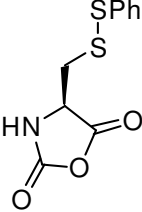
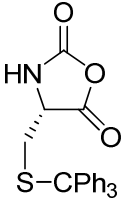
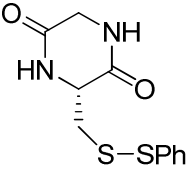
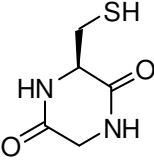
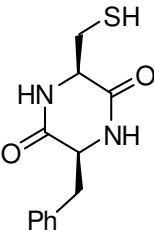
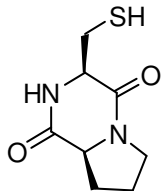
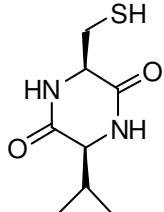
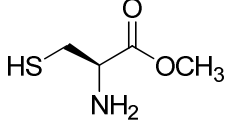
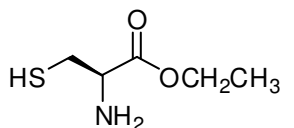
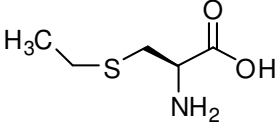
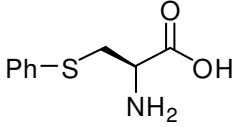
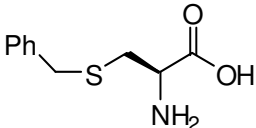
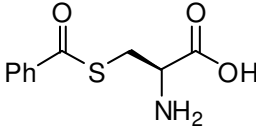


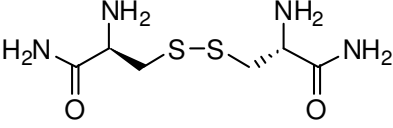
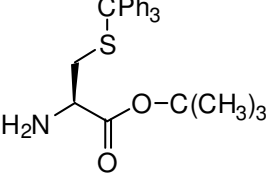
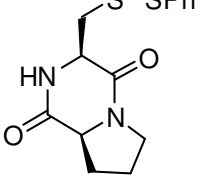
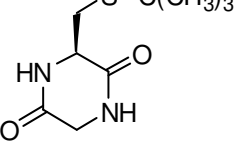
Table 1. Cysteine and Cystine Prodrugs from Scheme 3 and Scheme 4

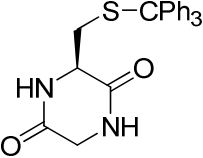
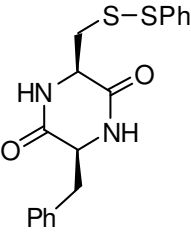
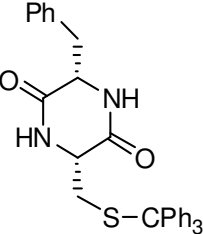
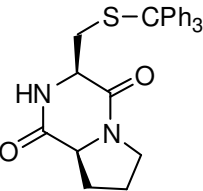
<p>Compound Number: 1 Cook Code: WYME-ST-GG Promentis Code: Pro-052 Chemical Formula: C₁₀H₁₄N₄O₄S₂ Molecular Weight: 318.37 Log P: -3.2 Prodrug/Bioisostere: Prodrug Monomer/Dimer: Dimer</p>	
<p>Compound Number: 9a Cook Code: ME-StBu Promentis Code: Pro-048 Chemical Formula: C₇H₁₅NO₂S Molecular Weight: 177.26 Log P: 0.21 Prodrug/Bioisostere: Prodrug Monomer/Dimer: Monomer</p>	
<p>Compound Number: 9b Cook Code: WYME-SSPh Promentis Code: Pro-044 Chemical Formula: C₉H₁₁NO₂S₂ Molecular Weight: 229.32 Log P: 1.76 Prodrug/Bioisostere: Prodrug Monomer/Dimer: Monomer</p>	
<p>Compound Number: 9c Cook Code: WYME-STrt Promentis Code: Pro-058 Chemical Formula: C₂₂H₂₁NO₂S Molecular Weight: 363.47 Log P: 4.39 Prodrug/Bioisostere: Prodrug Monomer/Dimer: Monomer</p>	

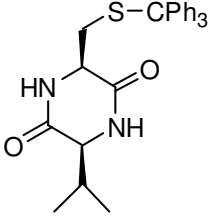
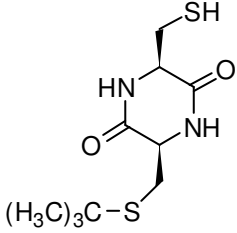
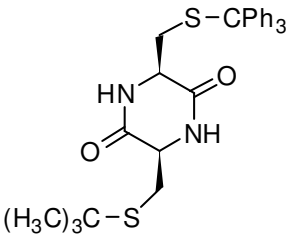
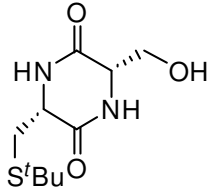
<p>Compound Number: 10b Cook Code: WYME-SSPh-5 Promentis Code: Pro-045 Chemical Formula: C₁₀H₉NO₃S₂ Molecular Weight: 255.31 Log P: 2.29 Prodrug/Bioisostere: Prodrug Monomer/Dimer: Monomer</p>	
<p>Compound Number: 10c Cook Code: N/A Promentis Code: N/A Chemical Formula: C₂₃H₁₉NO₃S Molecular Weight: 389.47 Log P: 4.93 Prodrug/Bioisostere: Prodrug Monomer/Dimer: Monomer</p>	
<p>Compound Number: 11b Cook Code: N/A Promentis Code: N/A Chemical Formula: C₁₁H₁₂N₂O₂S₂ Molecular Weight: 268.36 Log P: 0.85 Prodrug/Bioisostere: Prodrug Monomer/Dimer: Monomer</p>	
<p>Compound Number: 12a Cook Code: WYME-SBGH Promentis Code: Pro-013 Chemical Formula: C₅H₈N₂O₂S Molecular Weight: 160.19 Log P: -1.83 Prodrug/Bioisostere: Prodrug Monomer/Dimer: Monomer</p>	
<p>Compound Number: 12c Cook Code: WYME-SBPh Promentis Code: Pro-015 Chemical Formula: C₁₂H₁₄N₂O₂S Molecular Weight: 250.32 Log P: 0.34 Prodrug/Bioisostere: Prodrug Monomer/Dimer: Monomer</p>	

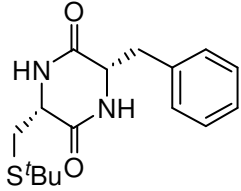
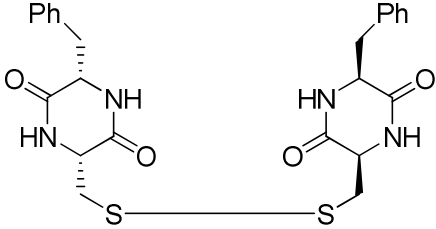
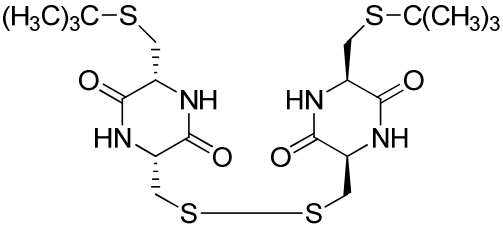
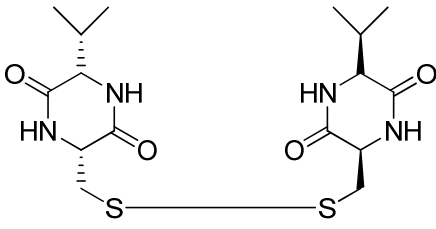
<p>Compound Number: 12d Cook Code: WYME-SBPr Promentis Code: Pro-068 Chemical Formula: C₈H₁₂N₂O₂S Molecular Weight: 200.26 Log P: -1.13 Prodrug/Bioisostere: Prodrug Monomer/Dimer: Monomer</p>	
<p>Compound Number: 12e Cook Code: WYME-SBVa Promentis Code: Pro-018 Chemical Formula: C₈H₁₄N₂O₂S Molecular Weight: 202.27 Log P: -0.45 Prodrug/Bioisostere: Prodrug Monomer/Dimer: Monomer</p>	
<p>Compound Number: 17 Cook Code: WYME-051407-SM Promentis Code: Pro-024 Chemical Formula: C₄H₉NO₂S Molecular Weight: 135.18 Log P: -0.66 Prodrug/Bioisostere: Prodrug Monomer/Dimer: Monomer</p>	
<p>Compound Number: 18 Cook Code: WYME-051707-SE Promentis Code: Pro-021 Chemical Formula: C₅H₁₁NO₂S Molecular Weight: 149.21 Log P: -0.32 Prodrug/Bioisostere: Prodrug Monomer/Dimer: Monomer</p>	

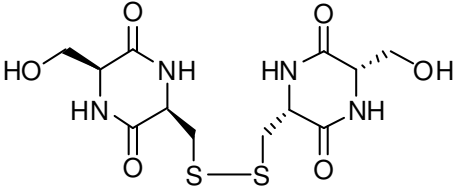
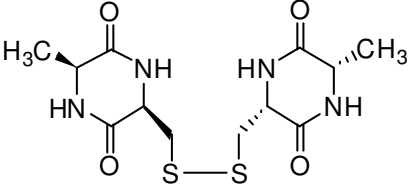
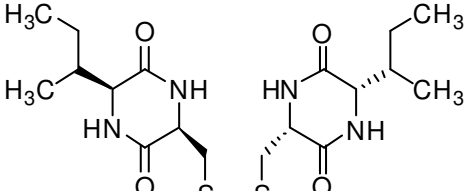
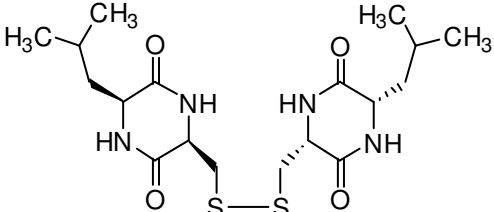
<p>Compound Number: 19 Cook Code: ME-SEt Promentis Code: Pro-023 Chemical Formula: C₅H₁₁NO₂S Molecular Weight: 149.21 Log P: -0.33 Prodrug/Bioisostere: Prodrug Monomer/Dimer: Monomer</p>	
<p>Compound Number: 20 Cook Code: ME-SPh Promentis Code: Pro-027 Chemical Formula: C₉H₁₁NO₂S Molecular Weight: 197.25 Log P: 1.0 Prodrug/Bioisostere: Prodrug Monomer/Dimer: Monomer</p>	
<p>Compound Number: 21 Cook Code: ME-SBZY Promentis Code: Pro-020 Chemical Formula: C₁₀H₁₃NO₂S Molecular Weight: 211.28 Log P: 1.07 Prodrug/Bioisostere: Prodrug Monomer/Dimer: Monomer</p>	
<p>Compound Number: 22 Cook Code: WYME-SPhCO Promentis Code: Pro-029 Chemical Formula: Molecular Weight: 225.26 Log P: 0.94 Prodrug/Bioisostere: Prodrug Monomer/Dimer: Monomer</p>	

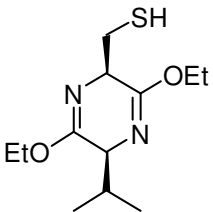
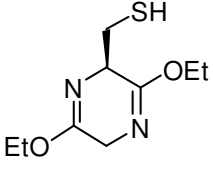
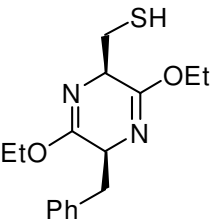
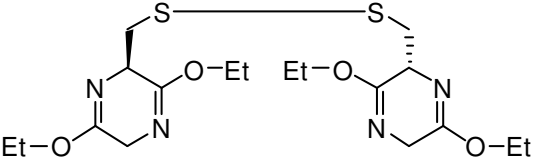
<p>Compound Number: 23 Cook Code: WYME-SS-am Promentis Code: Pro-032 Chemical Formula: $C_6H_{14}N_4O_2S_2$ Molecular Weight: 238.33 Log P: -2.69 Prodrug/Bioisostere: Prodrug Monomer/Dimer: Dimer</p>	
<p>Compound Number: 24 Cook Code: WYME-ST-tBu Promentis Code: Pro-061 Chemical Formula: $C_{26}H_{29}NO_2S$ Molecular Weight: 419.58 Log P: 5.53 Prodrug/Bioisostere: Prodrug Monomer/Dimer: Monomer</p>	
<p>Compound Number: 25 Cook Code: WYME-SBPr6 Promentis Code: Pro-016 Chemical Formula: $C_{14}H_{16}N_2O_2S_2$ Molecular Weight: 308.42 Log P: 1.55 Prodrug/Bioisostere: Prodrug Monomer/Dimer: Monomer</p>	
<p>Compound Number: 26 Cook Code: ME-StBu-6 Promentis Code: Pro-049 Chemical Formula: $C_9H_{16}N_2O_2S$ Molecular Weight: 216.3 Log P: -0.7 Prodrug/Bioisostere: Prodrug Monomer/Dimer: Monomer</p>	

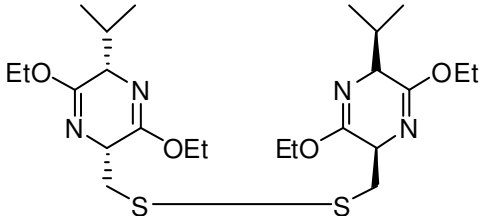
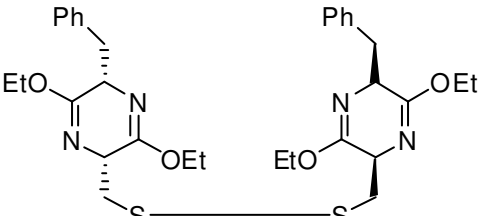
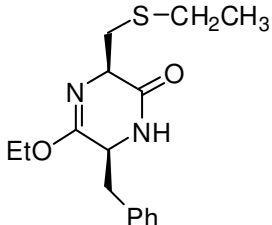
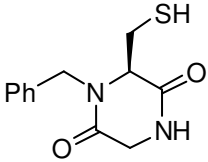
<p>Compound Number: 27 Cook Code: WYME-ST-G6 Promentis Code: Pro-051 Chemical Formula: $C_{24}H_{22}N_2O_2S$ Molecular Weight: 402.51 Log P: 3.48 Prodrug/Bioisostere: Prodrug Monomer/Dimer: Monomer</p>	 <chem>CSC1CN(C(=O)N1)CC2=CC=CC=C2</chem>
<p>Compound Number: 28 Cook Code: WyME-SB-P6 Promentis Code: Pro-014 Chemical Formula: $C_{18}H_{18}N_2O_2S_2$ Molecular Weight: 358.48 Log P: 3.01 Prodrug/Bioisostere: Prodrug Monomer/Dimer: Monomer</p>	 <chem>CSC1CN(C(=O)N1)CC2=CC=CC=C2C3=CC=CC=C3</chem>
<p>Compound Number: 29 Cook Code: WyME-ST-P6 Promentis Code: Pro-055 Chemical Formula: $C_{31}H_{28}N_2O_2S$ Molecular Weight: 492.63 Log P: 5.65 Prodrug/Bioisostere: Prodrug Monomer/Dimer: Monomer</p>	 <chem>CSC1CN(C(=O)N1)C2=CC=CC=C2C3=CC=CC=C3</chem>
<p>Compound Number: 30 Cook Code: WYME-ST-Pr Promentis Code: Pro-057 Chemical Formula: $C_{27}H_{26}N_2O_2S$ Molecular Weight: 442.57 Log P: 4.19 Prodrug/Bioisostere: Prodrug Monomer/Dimer: Monomer</p>	 <chem>CSC1CN(C(=O)N1)C2CCCN2</chem>

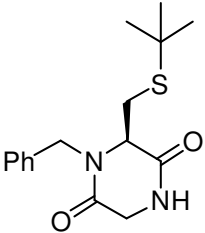
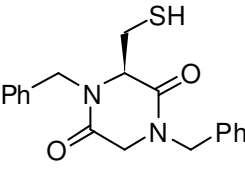
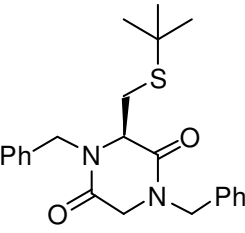
<p>Compound Number: 31 Cook Code: WYME-ST-V6 Promentis Code: Pro-062 Chemical Formula: $C_{27}H_{28}N_2O_2S$ Molecular Weight: 444.59 Log P: 4.86 Prodrug/Bioisostere: Prodrug Monomer/Dimer: Monomer</p>	
<p>Compound Number: 32 Cook Code: WYME-SBSS Promentis Code: Pro-017 Chemical Formula: $C_{10}H_{18}N_2O_2S_2$ Molecular Weight: 262.39 Log P: -0.24 Prodrug/Bioisostere: Prodrug Monomer/Dimer: Monomer</p>	
<p>Compound Number: 33 Cook Code: WYME-ST-S6 Promentis Code: Pro-059 Chemical Formula: $C_{29}H_{32}N_2O_2S_2$ Molecular Weight: 504.71 Log P: 5.08 Prodrug/Bioisostere: Prodrug Monomer/Dimer: Monomer</p>	
<p>Compound Number: 34 Cook Code: N/A Promentis Code: Pro-1036 Chemical Formula: $C_{10}H_{18}N_2O_3S$ Molecular Weight: 246.33 Log P: -1.07 Prodrug/Bioisostere: Prodrug Monomer/Dimer: Monomer</p>	

<p>Compound Number: 35 Cook Code: N/A Promentis Code: Pro-1038 Chemical Formula: $C_{16}H_{22}N_2O_2S$ Molecular Weight: 306.42 Log P: 1.46 Prodrug/Bioisostere: Prodrug Monomer/Dimer: Monomer</p>	
<p>Compound Number: 36 Cook Code: WyME-ST-PP Promentis Code: Pro-056 Chemical Formula: $C_{24}H_{26}N_4O_4S_2$ Molecular Weight: 498.62 Log P: 1.13 Prodrug/Bioisostere: Prodrug Monomer/Dimer: Dimer</p>	
<p>Compound Number: 37 Cook Code: WYME-ST-SS Promentis Code: Pro-060 Chemical Formula: $C_{20}H_{34}N_4O_4S_4$ Molecular Weight: 522.77 Log P: -0.01 Prodrug/Bioisostere: Prodrug Monomer/Dimer: Dimer</p>	
<p>Compound Number: 38 Cook Code: WYME-ST-VV Promentis Code: Pro-064 Chemical Formula: $C_{16}H_{26}N_4O_4S_2$ Molecular Weight: 402.53 Log P: -0.45 Prodrug/Bioisostere: Prodrug Monomer/Dimer: Dimer</p>	

<p>Compound Number: 39 Cook Code: N/A Promentis Code: Pro-1016 Chemical Formula: $C_{12}H_{18}N_4O_6S_2$ Molecular Weight: 378.42 Log P: -3.93 Prodrug/Bioisostere: Prodrug Monomer/Dimer: Dimer</p>	
<p>Compound Number: 40 Cook Code: N/A Promentis Code: Pro-1022 Chemical Formula: $C_{12}H_{18}N_4O_4S_2$ Molecular Weight: 346.43 Log P: -2.22 Prodrug/Bioisostere: Prodrug Monomer/Dimer: Dimer</p>	
<p>Compound Number: 41 Cook Code: N/A Promentis Code: Pro-1024 Chemical Formula: $C_{18}H_{30}N_4O_4S_2$ Molecular Weight: 430.59 Log P: 0.39 Prodrug/Bioisostere: Prodrug Monomer/Dimer: Dimer</p>	
<p>Compound Number: 42 Cook Code: N/A Promentis Code: Pro-1025 Chemical Formula: $C_{18}H_{30}N_4O_4S_2$ Molecular Weight: 430.59 Log P: 0.25 Prodrug/Bioisostere: Prodrug Monomer/Dimer: Dimer</p>	

<p>Compound Number: 43 Cook Code: WYME-BFVa Promentis Code: Pro-005 Chemical Formula: $C_{12}H_{13}N_2O_2S$ Molecular Weight: 258.38 Log P: 2.49 Prodrug/Bioisostere: Prodrug Monomer/Dimer: Monomer</p>	
<p>Compound Number: 44 Cook Code: WYME-0625-SBBFGE Promentis Code: Pro-011 Chemical Formula: $C_9H_{16}N_2O_2S$ Molecular Weight: 216.3 Log P: 1.12 Prodrug/Bioisostere: Prodrug Monomer/Dimer: Monomer</p>	
<p>Compound Number: 45 Cook Code: WYME-BFPh Promentis Code: Pro-004 Chemical Formula: $C_{16}H_{22}N_2O_2S$ Molecular Weight: 306.42 Log P: 3.28 Prodrug/Bioisostere: Prodrug Monomer/Dimer: Monomer</p>	
<p>Compound Number: 46 Cook Code: WYME-SBB-FGL Promentis Code: Pro-012 Chemical Formula: $C_{18}H_{30}N_4O_4S_2$ Molecular Weight: 430.59 Log P: 2.69 Prodrug/Bioisostere: Prodrug Monomer/Dimer: Dimer</p>	

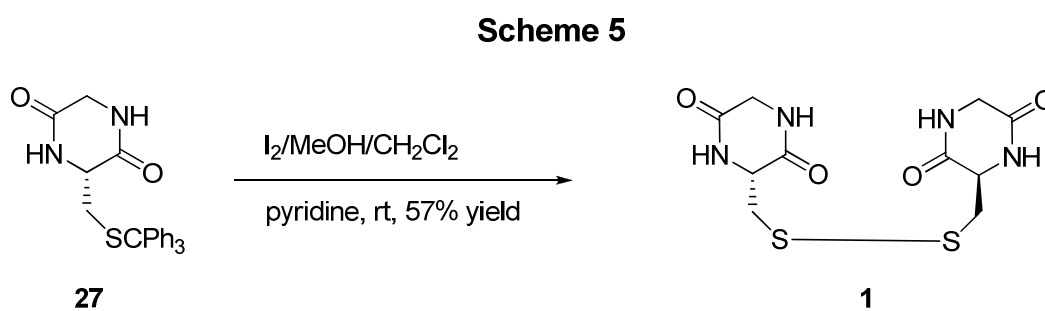
<p>Compound Number: 47 Cook Code: WYME-SSB-FVV Promentis Code: Pro-065 Chemical Formula: $C_{24}H_{42}N_4O_4S_2$ Molecular Weight: 514.74 Log P: 5.44 Prodrug/Bioisostere: Prodrug Monomer/Dimer: Dimer</p>	
<p>Compound Number: 48 Cook Code: WYME-SSB-FPP Promentis Code: Pro-066 Chemical Formula: $C_{32}H_{42}N_4O_4S_2$ Molecular Weight: 610.83 Log P: 7.02 Prodrug/Bioisostere: Prodrug Monomer/Dimer: Dimer</p>	
<p>Compound Number: 49 Cook Code: WYME-STBF-PhM Promentis Code: Pro-047 Chemical Formula: $C_{16}H_{22}N_2O_2S$ Molecular Weight: 306.42 Log P: 2.4 Prodrug/Bioisostere: Prodrug Monomer/Dimer: Monomer</p>	
<p>Compound Number: 50 Cook Code: WYME-SH-NPh6 Promentis Code: Pro-080 Chemical Formula: $C_{12}H_{14}N_2O_2S$ Molecular Weight: 250.32 Log P: 0.14 Prodrug/Bioisostere: Prodrug Monomer/Dimer: Monomer</p>	

<p>Compound Number: 51 Cook Code: WYME-ST-N6 Promentis Code: Pro-071 Chemical Formula: C₁₆H₂₂N₂O₂S Molecular Weight:306.4 Log P: 1.27 Prodrug/Bioisostere: Prodrug Monomer/Dimer: Monomer</p>	
<p>Compound Number: 52 Cook Code: WYME-SB-GH6NPh Promentis Code: Pro-084 Chemical Formula: C₁₉H₂₀N₂O₂S Molecular Weight: 340.4 Log P: 2.11 Prodrug/Bioisostere: Prodrug Monomer/Dimer: Monomer</p>	
<p>Compound Number: 53 Cook Code: WYME-ST-N2Ph Promentis Code: Pro-092 Chemical Formula: C₂₃H₂₈N₂O₂S Molecular Weight: 396.5 Log P: 3.23 Prodrug/Bioisostere: Prodrug Monomer/Dimer: Monomer</p>	

2.1. Preparation of 4-Methylbenzenesulfonyl Chloride.⁷⁸

4-Methylbenzenesulfonyl chloride is not commercially available and, therefore, must be synthesized. Under a nitrogen atmosphere, N-chlorosuccinimide was slurried in methylene chloride. While stirring at rt, 4-methylbenzenethiol was added to the mixture. The clear solution which resulted was then allowed to stir at rt. A small amount of precipitate which formed was removed by filtration. The filtrate, assumed to contain the theoretical quantity of 4-methylbenzenesulfonyl chloride was used immediately and directly in many of the following synthetic transformations.

2.2. Representative Procedure for Synthesis of Bis-Dipiperazinedione (Symmetrical Dimers): Bis-[2,5-Piperazinedione, 3-(mercaptomethyl)-] (1).

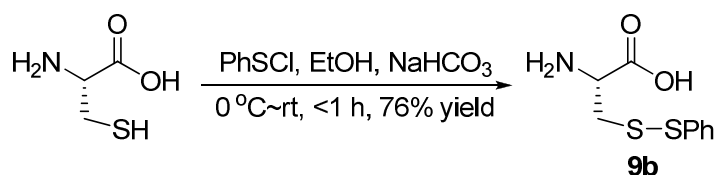


As shown in **Scheme 5**, the trityl protected diketo-piperazine **27** was dissolved in a solution of methylene chloride and methanol with stirring. Pyridine was then added to the mixture which resulted, followed by a solution of iodine in methanol. The mixture was allowed to stir at rt. The reaction progress was followed by TLC until all the starting

material was consumed. The solution was stirred for a total of 26 h and the precipitate was filtered off. The solid was washed with cold methanol and then decolorized by shaking with 10% aqueous sodium bisulfate. The precipitate was filtered and dried to yield dimer **1** as white solid.

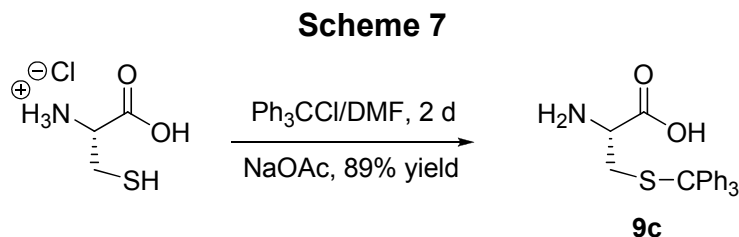
2.3. Synthesis of (R)-2-Amino-3-(phenyldisulfanyl)propanoic acid (**9b**).

Scheme 6



As shown in **Scheme 6**, powdered sodium bicarbonate was added to a solution of L-cysteine hydrochloride mono-hydrate in absolute ethanol at 0 °C in one portion. Phenylsulfenyl chloride was then added dropwise with stirring to the mixture. After the complete addition of the reagent, the reaction mixture was allowed to stand at rt and the sodium chloride, which was produced during the reaction, was removed by filtration. After bringing the pH of the solution to alkaline by the addition of pyridine into the filtrate, the fine precipitate which formed, was allowed to stand for a couple of hours, after which it was filtrated and washed well with ethanol. It was dried to provide the crude acid as a white solid. After recrystallization from aq HCl (1.0 N), the final product S-thiol-phenyl-L-cysteine (**9b**) was obtained as colorless plates.

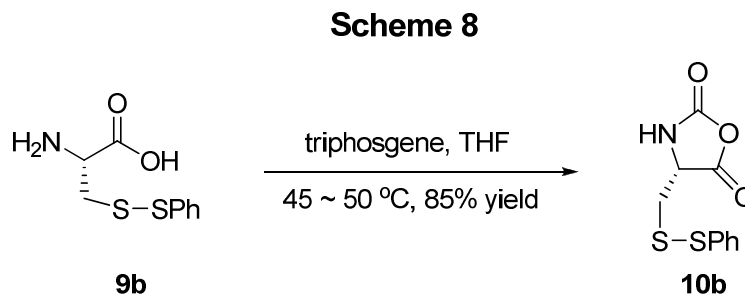
2.4. Synthesis of 2-Amino-3-tritylsulfanyl-propionic acid (*S*-trityl-L-cysteine) (**9c**).



As shown in **Scheme 7**, L-Cysteine hydrochloride and trityl chloride were stirred in DMF for 2 days at rt. A 10% sodium acetate solution was then added dropwise and the white precipitate (**9c**) which formed was filtered and washed with distilled water.

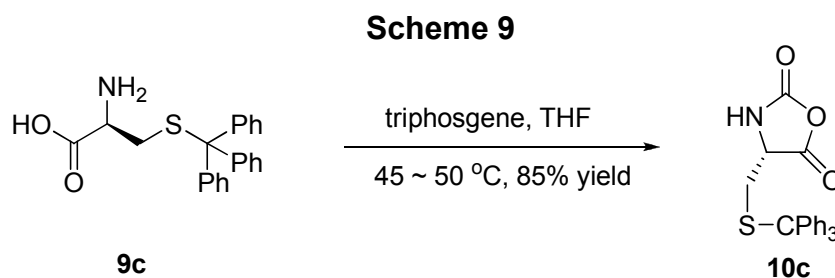
Afterward, the residue was stirred in acetone at 50 °C for 30 min, after which it was cooled to 0 °C and filtered. The precipitate (**9c**) was washed with a little acetone and diethyl ether and dried in vacuo. *S*-Trityl-L-cysteine **9c** was obtained as a white powder.

2.5. Synthesis of (*R*)-4-((Phenyldisulfanyl)methyl)oxazolidine-2,5-dione (**10b**).



As shown in **Scheme 8**, to a rapidly stirred suspension of S-thiol-phenyl-L-cysteine (**9b**) in THF was added solid triphosgene in one portion at 45-50 °C. The mixture was stirred until the solution becomes homogeneous. The solution was then purged with argon overnight into a NaOH bubbler to remove any residual phosgene. The solvent was evaporated *in vacuo* and this provided anhydride **10b**. Due to the unstable nature of this anhydride, it was stored in the refrigerator under an atmosphere of argon and used immediately in a later step without further purification.

2.6. Synthesis of 4-tritylsulfanylmethyl-oxazolidine-2,5-dione (**10c**).

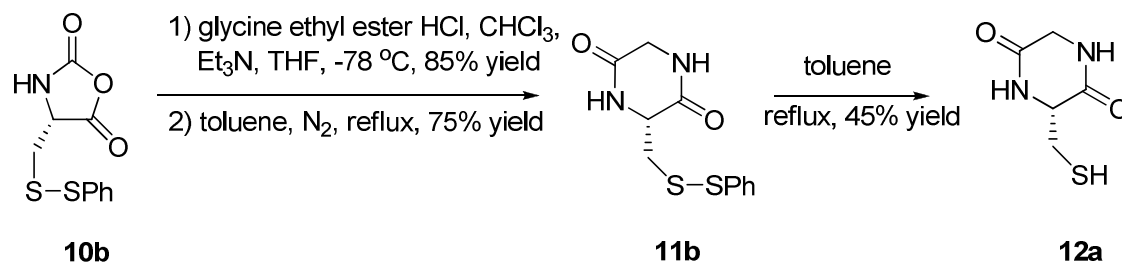


As shown in **Scheme 9**, to a rapidly stirred suspension of S-trityl-L-cysteine (**9c**) in THF was added solid triphosgene in one portion at 45-50 °C. The mixture was stirred until the solution becomes homogeneous. The solution was purged with argon overnight into a NaOH bubbler to remove any residual phosgene. The solvent was evaporated *in vacuo* and this provided anhydride **10c**. Due to the unstable nature of this anhydride, it was stored in the refrigerator under an atmosphere of argon and used immediately in a later step without further purification.

2.7. Representative Procedure for Synthesis of Diketopiperazine

Targets.

Scheme 10



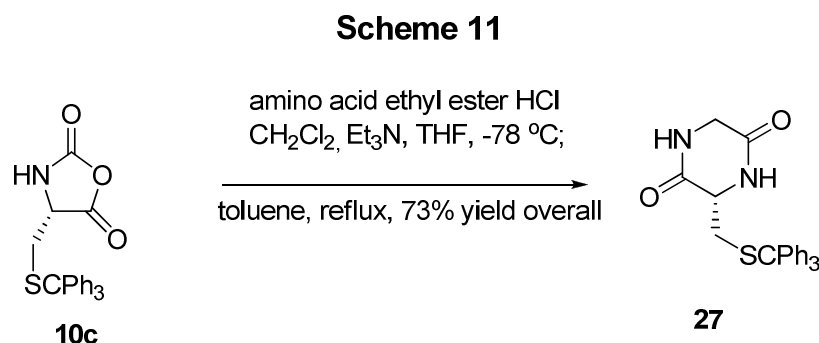
2.8. Synthesis of 3-(Mercaptomethyl)-2,5-Piperazinedione (12a) and (R)-3-((Phenyldisulfanyl)methyl)piperazine-2,5-dione (11b).

As shown in **Scheme 10**, a) a solution of the *N*-carboxy-anhydride **10b** in THF was added dropwise to a vigorously stirred mixture of glycine ethyl ester hydrochloride, freshly distilled triethylamine and dry chloroform at $-78\text{ }^{\circ}\text{C}$ in a three-neck flask. The reaction mixture was allowed to warm to $0\text{ }^{\circ}\text{C}$ over 8 h, and then was allowed to stir at rt for 12 h, after which the reaction solution was filtered to remove the triethylamine hydrochloride which precipitated. The filtrate was then concentrated under reduced pressure ($< 40\text{ }^{\circ}\text{C}$) and the crude dipeptide ester was used for the preparation of the diketopiperazine **12a**, directly in the next step.

b) The crude dipeptide ester **11b** was heated in refluxing toluene for 12 h and then cooled down to rt and kept at 0 °C for 16 h. The bislactam **12a** which precipitated was isolated by vacuum filtration, washed with ether and dried under vacuum at 100 °C to provide pure diketopiperazine **12a**. The filtrate, which resulted, produced from washing the desired diketopiperazine was evaporated under vacuum and toluene was added to the residue. The toluene solution was heated at reflux for another 40 h (under argon) and then the above steps were repeated to collect additional grams of diketopiperazine **12a**.

c) The solution which resulted from step b above was cooled to 0 °C and kept at 0 °C for 12 h in the refrigerator. The precipitate, which resulted, was filtered and provided phenyl-thiol analog **11b**.

2.9. Synthesis of 3-Tritylsulfanylmethyl-piperazine-2,5-dione (27).



Was prepared following the procedure for the preparation of **12a**. It is important to note that the trityl protected thiol group was not cleaved during reflux in toluene as in the case of the S-thiol phenyl group, as shown in **Scheme 11**.

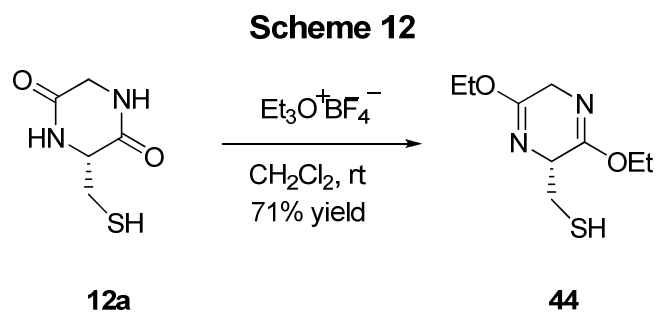
2.10. Representative Procedure for Synthesis of Dialkylated

Diketopiperazine: Preparation of Triethyloxonium Tetrafluoroborate.⁷⁹

Note: Triethyloxonium tetra-fluoroborate is an expensive reagent; however, it is relatively easy to prepare even on large scale. A three-neck flask, pressure equilibrating dropping funnel and a condenser were dried in an oven at $150\text{ }^\circ\text{C}$ and assembled while hot under an atmosphere of argon. When the equipment had cooled to rt, ether which had been previously dried over sodium benzophenone ketyl and boron trifluoride diethyletherate were combined [Note: On this scale the colorless BF_3 etherate was obtained from a freshly opened new bottle. If the reagent was slightly yellow or if the

reaction was scaled down, the BF_3 etherate needed to be vacuum distilled first]. The ethereal solution which resulted was heated to a gentle reflux after which dry epichlorohydrin was added dropwise over 1 h. The mixture was heated at reflux for an additional 1 h and allowed to stand at rt (under argon) overnight. The ether was removed by applying a positive pressure of argon in one neck of the flask while forcing the ether out through a filter stick (fritted glass tube) inserted into another neck of the flask and into a collection flask. The slightly yellow solid which remained in the flask was rinsed twice in the same manner with anhydrous ether to provide a crystalline white solid. The solid was not weighed but directly used in the next steps

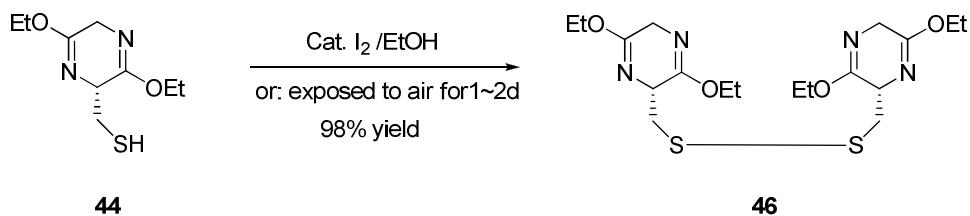
2.11. Synthesis of (3,6-Diethoxy-2,5-dihydro-,pyrazin-2-yl)-methanethiol (44**).**



As shown in **Scheme 12**, dry CH_2Cl_2 was added to the flask which contained the freshly prepared triethyloxonium tetrafluoroborate from the previous reaction (under argon). To this solution was added the diketopiperazine **12a** in portions with stirring. After 2 h the reaction mixture became homogenous. The solution was stirred at rt under argon for 72 h, after which the mixture was added *via* a cannula to an aq solution of NH_4OH mixed with ice. The organic layer was washed with a saturated aq solution of NaHCO_3 and brine after which it was dried (K_2CO_3). After filtration the solvent was removed under reduced pressure to provide the bis-ethoxy lactim ether **44** as a clear yellow liquid that was further purified by flash chromatography.

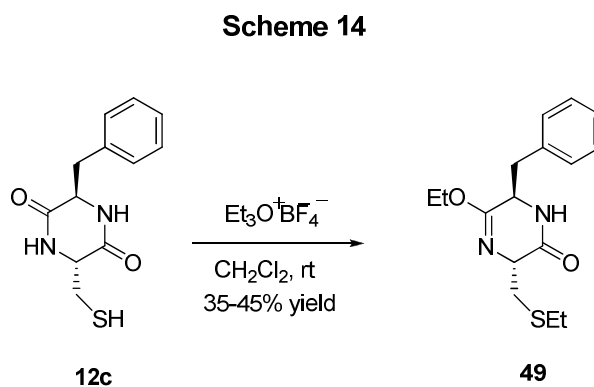
2.12. Synthesis of bis-[(3,6-Diethoxy-2,5-dihydro-pyrazin-2-yl)-methanethiol] (46**).**

Scheme 13



As shown in **Scheme 13**, to the bis-ethoxy lactim ether **44** in dry EtOH was added a catalytic amount of I₂ at rt. The mixture was stirred for 6~ 12 h under air until the analysis (TLC, silica gel) indicated the reaction was complete. The organic solvent was evaporated under reduced pressure. The mixture which resulted was dissolved into EtOAc, washed with an aq solution of saturated sodium thiosulfate and dried (Na₂SO₄). The solvent was then removed under reduced pressure which provided the cystine prodrug dimer **46**.

2.13. Synthesis of (3R,6R)-6-Benzyl-5-ethoxy-3-(ethylthiomethyl)-1,6-dihydropyrazin-2(3H)-one (49).



As shown in **Scheme 14**, compound **49** was prepared following the procedure for preparation of **44** using only 1 equivalent of triethyloxonium tetrafluoroborate added to a solution of diketopiperazine **12c**.

III. Synthesis of Cysteine and Cystine Bioisosteres.

1. Rationale, Design and Synthesis of Cysteine and Cystine Bioisosteres.

A second strategy that was studied is outlined in **Scheme 15, Scheme 16, Scheme 17, and Scheme 18**. The rationale was to make bioisosteres of the desired amino acids, L-cysteine and L-cystine with improved partition coefficients in order to facilitate passive delivery through the blood brain barrier and eliminate the need for intra- and extra-cellular peptidases to liberate the desired amino acids. As stated before, the bioisostere targets are unlikely to be metabolized or cleaved to produce cysteine or cystine; however, they will be used to drive the cystine-glutamate antiporter, releasing glutamate into a subject's extra-cellular (extra-synaptic) space without increased production of glutathione.

The term "bioisostere" refers to a compound which results from the exchange of an atom or of a group of atoms with another, broadly similar, atom or group of atoms. Such an exchange is termed a "bioisosteric replacement" and is useful to create a new compound with similar biological properties to the parent compound. The bioisosteric replacement may be physicochemically or topologically based. Bioisosteric replacement generally enhances desired biological or physical properties of a compound without making significant changes in chemical structure. For example, the replacement of a hydrogen atom with a fluorine atom at a site of metabolic oxidation in a drug candidate may prevent such metabolism from taking place. Because the fluorine atom is similar in size to the hydrogen atom the overall topology of the molecule is not significantly

affected, leaving the desired biological activity unaffected. However, with a blocked pathway for metabolism, the drug candidate may have a longer half-life. Another example is aromatic rings, a phenyl -C₆H₅ ring can often be replaced by a different aromatic ring such as thiophene or naphthalene which may improve efficacy or change binding specificity of a respective bioisostere.

Outlined in **Scheme 15** and **Scheme 16** is the conversion of L-cysteine to bioisosteres of carboxylic acid groups, while outlined in **Scheme 17** and **Scheme 18** is a pathway to amide bioisosteres. Cysteine will be protected as previously described above to prevent side reactions and converted into the corresponding bioisostere.

In **Scheme 15**, carboxylic acid bioisosteres, the desired tetrazole intermediates **56a-56c** will be formed (individually) following the intermolecular cyclization of the ethylcyanide amides **55a-55c** with sodium azide.^{80,83} Finally, the preferred tetrazole bioisosteres (**57a-57c**) will be obtained after a simple dealkylation of tetrazoles **56a-56c**, respectively.^{80,83} Once the bioisostere is formed, the other functional groups can be either protected or modified as shown in the rest of **Scheme 15** and continued in **Scheme 16**.

In **Scheme 17** the 1,2,4-oxadiazole bioisosteres, **67a-67d** can be directly synthesized from the corresponding protected amino acids using literature procedures.^{80,84,85,86} The 1,2,4-triazole bioisosteres (**69a-69e**), and the 1,3,4-oxadiazole bioisosteres (**70a-70e**) can be synthesized through a hydrazine intermediate (**68**) as

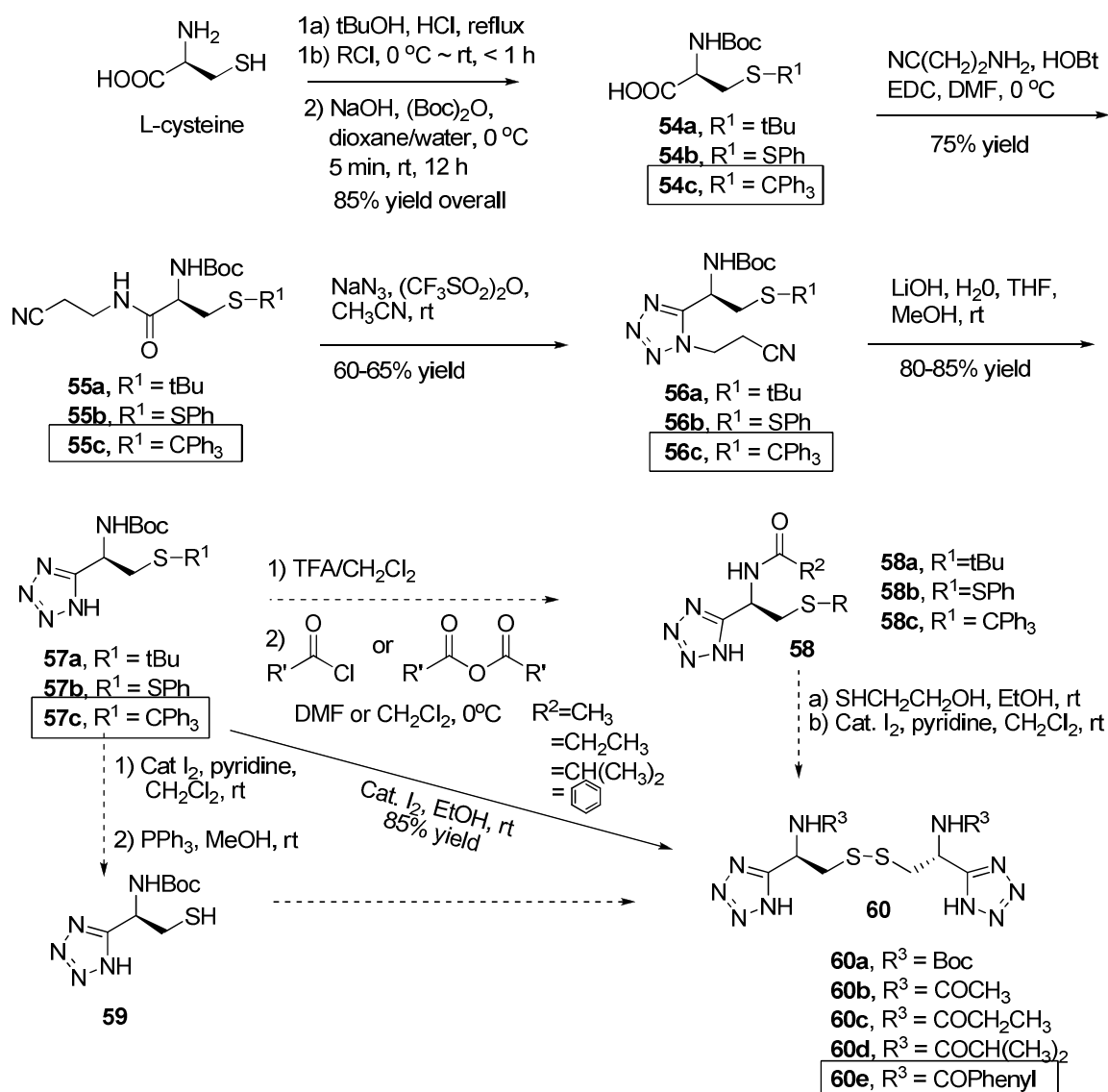
discussed in the literature.^{84,85,86} After each bioisostere is synthesized, these compounds can be tested for biological activity with the alkylated thiol group intact or reacted with either a) catalytic amounts of iodine and pyridine in dichloromethane or b) triphenylphosphine in methanol to remove the thiol protecting group, as shown in **Scheme 18**, to produce the free thiol target monomers (**72a-72e**).⁸⁰ Once again, these target monomers (**72a-72e**) can be used for biological testing as free thiols or further reacted with catalytic amounts of iodine in ethanol to form symmetrical dimers (**73a-73e**).⁸⁰ They may also be reacted with various amino ethyl esters (methyl ester may also be used) to produce target compounds (**74**), which can be prepared as either free thiols (**76**) or symmetrical dimers (**75**).

The present method to synthesize bioisosteres has many advantages over previous routes including, but not limited to: a) same synthetic route leads to both monomers and dimers (cysteine and cystine bioisosteres); b) protection of functional groups prevents side reactions (e.g., cyclization); c) the initial monomer synthesis eliminates problems associated with multiple functional groups; and d) the described route can be easily expanded to incorporate minor chemical modifications.

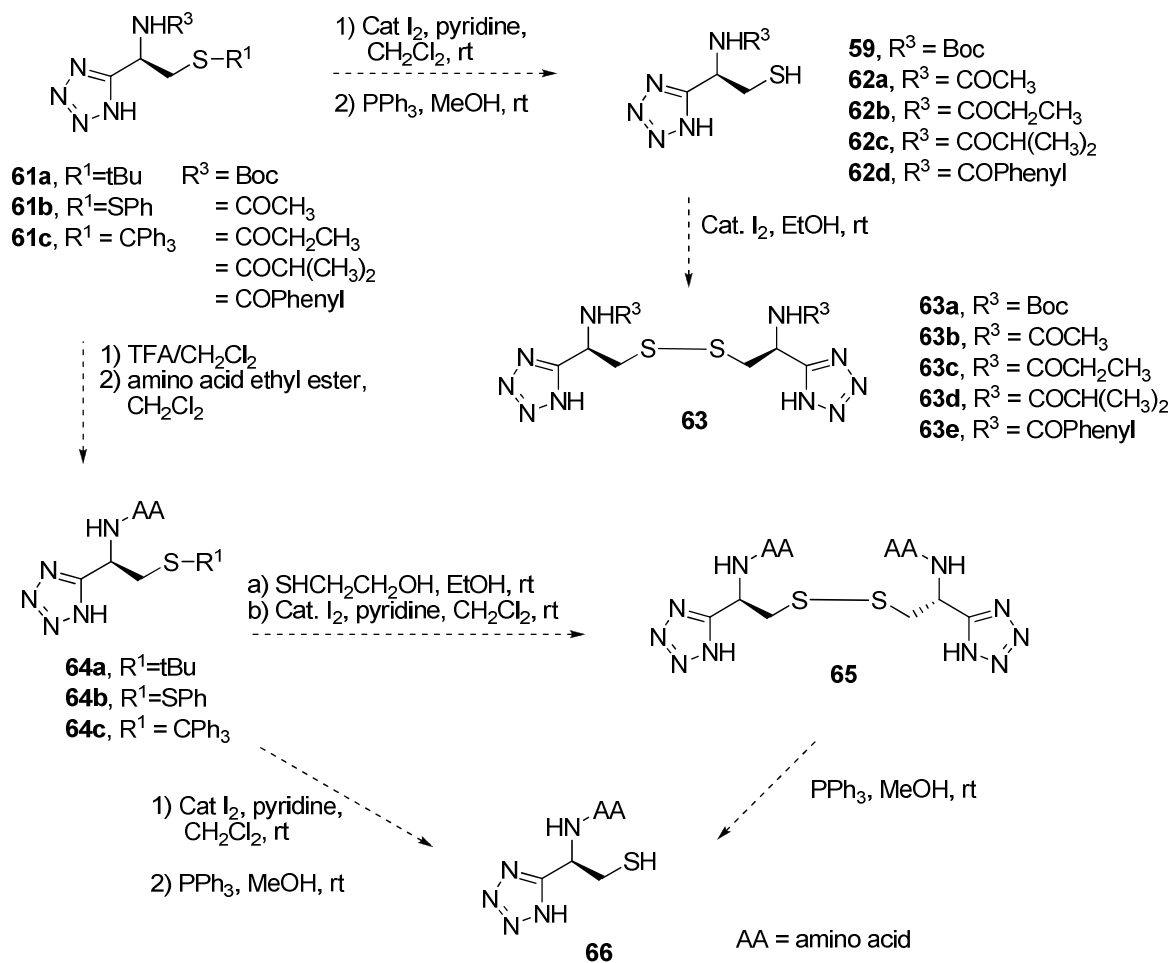
Listed in **Table 2** and **Table 3** is a list of compounds prepared following **Scheme 15** and **Scheme 16**, and **Scheme 17** and **Scheme 18**, respectively, by members of the Cook group, under the direction of myself and/or synthesized by myself, the primary project researcher. Compounds that are “boxed” in each general scheme were actually synthesized as shown in the general scheme. After which is a detailed listing of some key

reactions and target prodrugs. After which is a detailed listing of some key reactions and target compounds. **The complete experimental details are located in Chapter IX – Experimental Section, and includes weights, molar quantities, volumes, temperatures, and spectral data.**

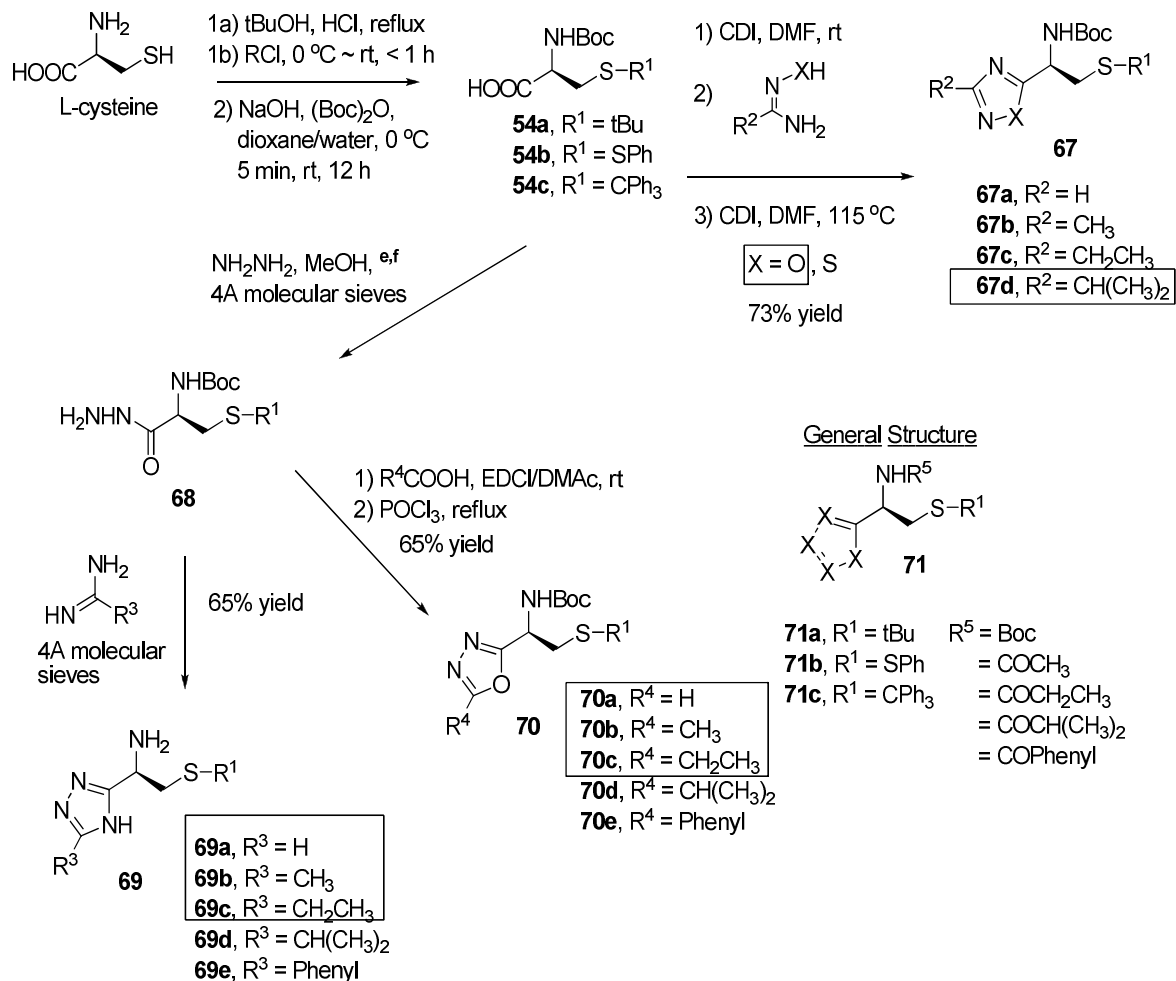
General Synthesis of Carboxylic Acid Bioisosteres Scheme 15



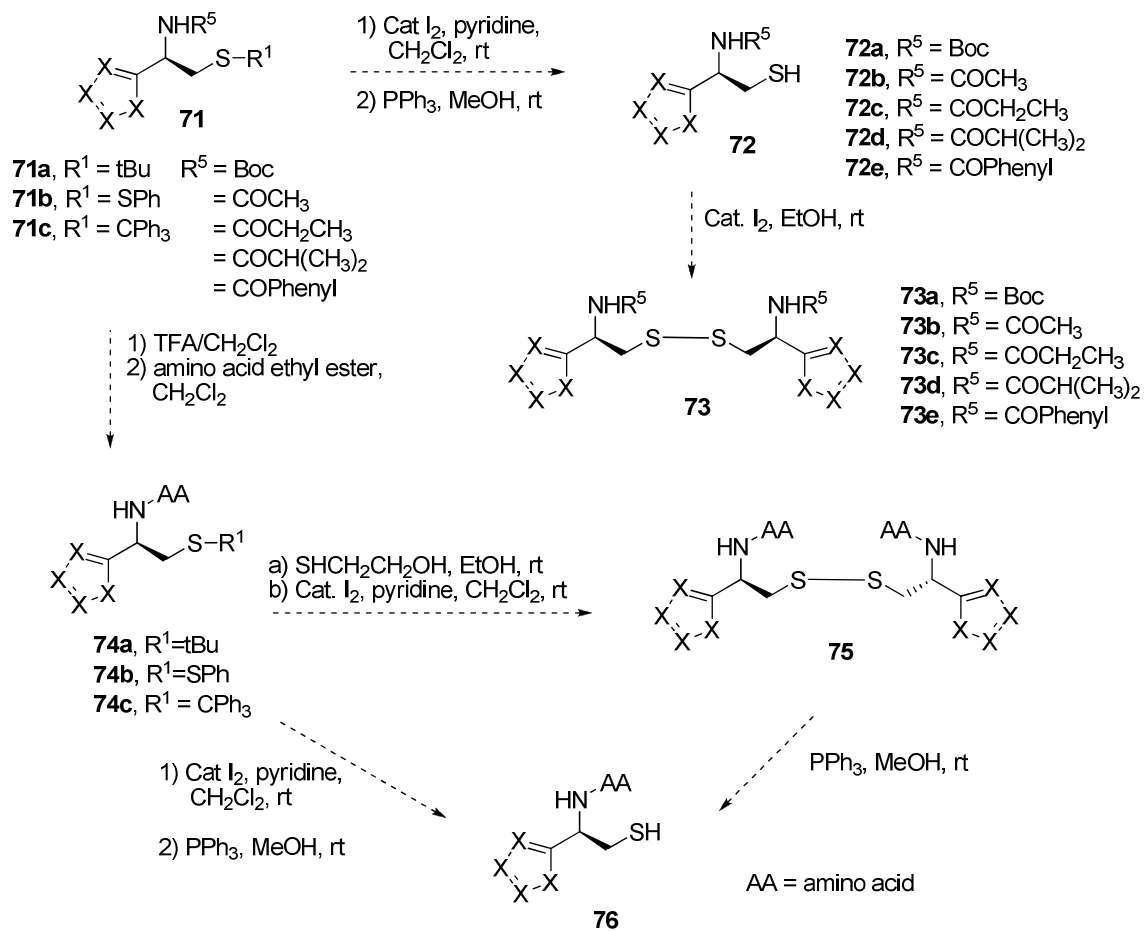
**General Synthesis of Carboxylic Acid Bioisosteres
Continued
Scheme 16**



General Synthesis of Amide Bioisosteres Scheme 17



**Synthesis of Amide Bioisosteres
Continued
Scheme 18**



General Structure from Scheme 7

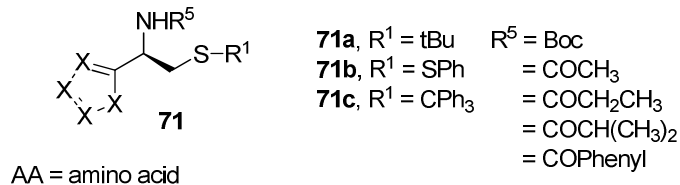
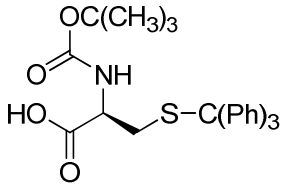
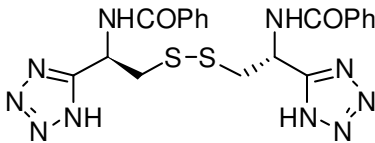
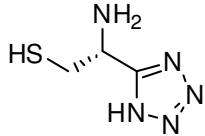
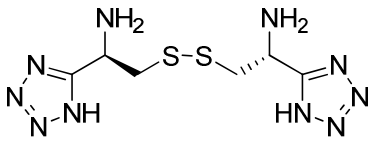


Table 2. Carboxylic Acid Bioisosteres from Scheme 15 and Scheme 16

<p>Compound Number: 54c Cook Code: N/A Promentis Code: N/A Chemical Formula: C₂₇H₂₉NO₄S Molecular Weight: 463.59 Log P: 5.78 Prodrug/Bioisostere: Prodrug Monomer/Dimer: Monomer</p>	
<p>Compound Number: 60e Cook Code: WYME-SS-NPh4N Promentis Code: Pro-079 Chemical Formula: C₂₀H₂₀N₁₀O₂S₂ Molecular Weight: 496.57 Log P: 3.09 Prodrug/Bioisostere: Bioisostere Monomer/Dimer: Dimer</p>	
<p>Compound Number: 76 Cook Code: WYME-ST-4NTMS Promentis Code: Pro-069 Chemical Formula: C₃H₇N₅S Molecular Weight: 145.0 Log P: -0.52 Prodrug/Bioisostere: Bioisostere Monomer/Dimer: Monomer</p>	
<p>Compound Number: 77 Cook Code: WY-SS-4NTMS Promentis Code: Pro-070 Chemical Formula: C₆H₁₂N₁₀S₂ Molecular Weight: 288.0 Log P: -0.57 Prodrug/Bioisostere: Bioisostere Monomer/Dimer: Dimer</p>	

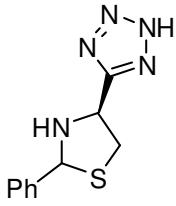
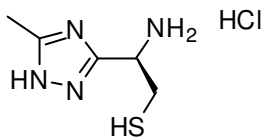
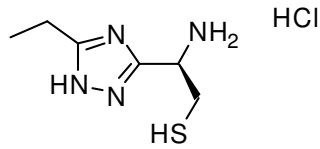
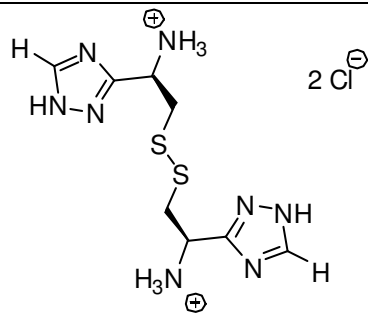
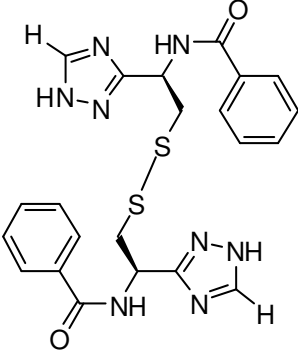
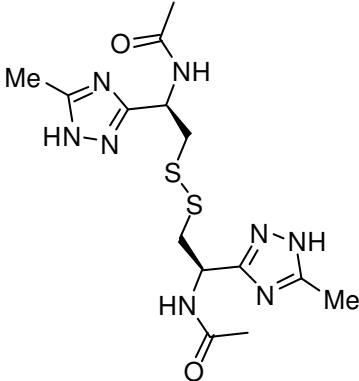
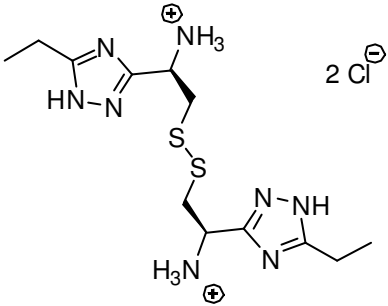
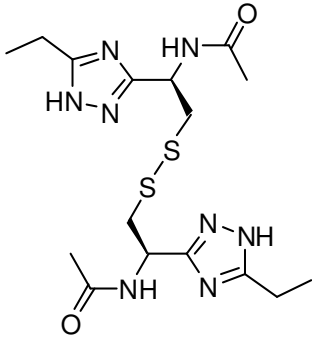
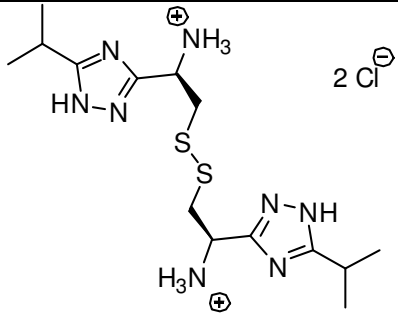
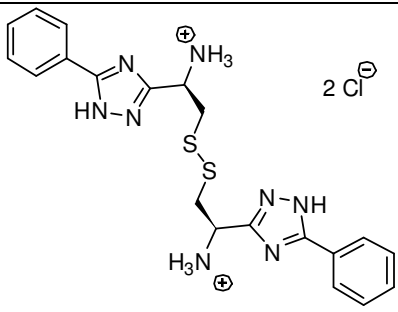
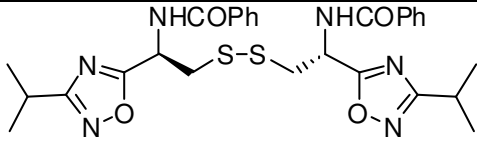
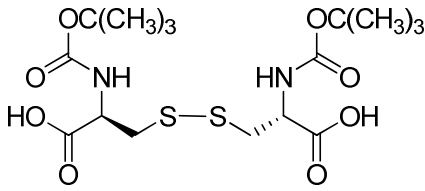
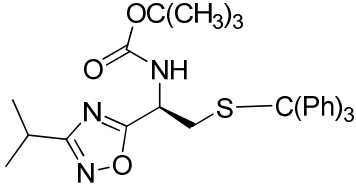
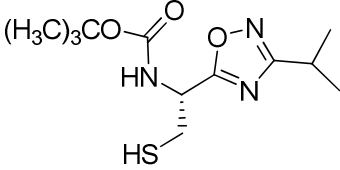
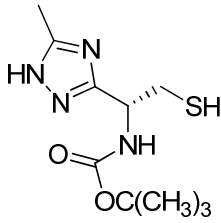
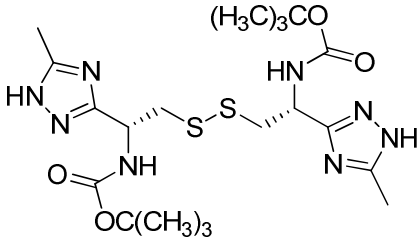
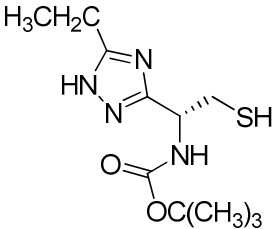
<p>Compound Number: 78 Cook Code: WYME-NS-5PhN4 Promentis Code: Pro-083 Chemical Formula: C₁₀H₁₁N₅S Molecular Weight: 233.0 Log P: 2.2 Prodrug/Bioisostere: Bioisostere Monomer/Dimer: Monomer</p>	
---	---

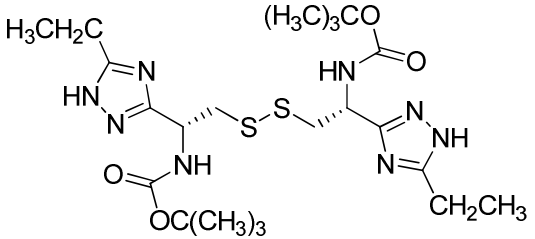
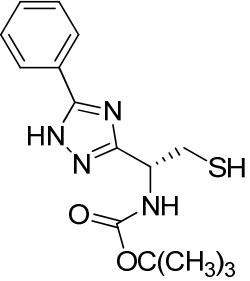
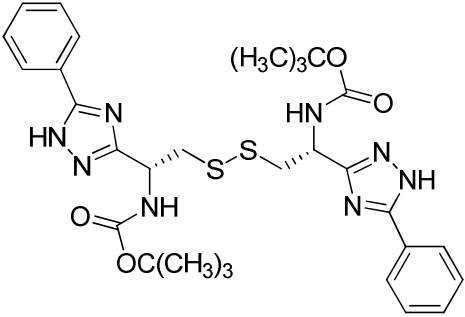
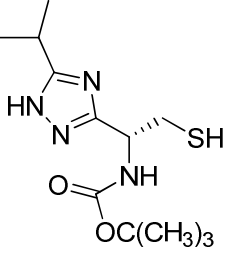
Table 3. Amide Bioisosteres from Scheme 17 and Scheme 18	
<p>Compound Number: 79 Cook Code: MWL-273 Promentis Code: Pro-088 Chemical Formula: C₅H₁₁ClN₄ Molecular Weight: 194.69 Log P: 0.59 Prodrug/Bioisostere: Bioisostere Monomer/Dimer: Monomer</p>	
<p>Compound Number: 80 Cook Code: MWL-283 Promentis Code: Pro-090 Chemical Formula: C₆H₁₃ClN₄S Molecular Weight: 208.71 Log P: 1.16 Prodrug/Bioisostere: Bioisostere Monomer/Dimer: Monomer</p>	
<p>Compound Number: 81 Cook Code: MWL-249 Promentis Code: Pro-078 Chemical Formula: C₈H₁₆C₁₂N₈S₂ Molecular Weight: 359.3 Log P: -1.32 Prodrug/Bioisostere: Bioisostere Monomer/Dimer: Dimer</p>	

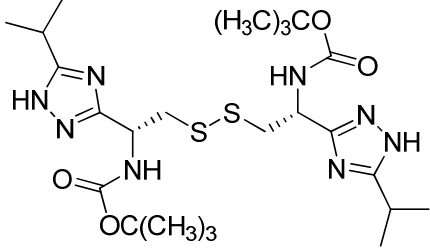
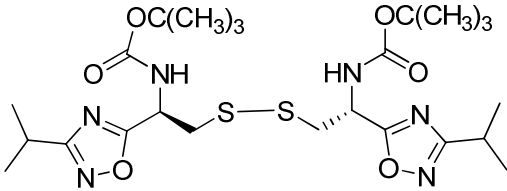
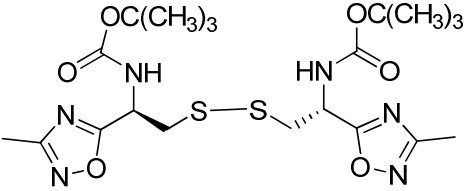
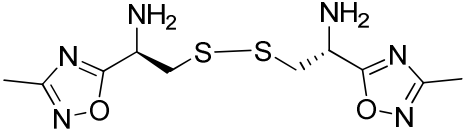
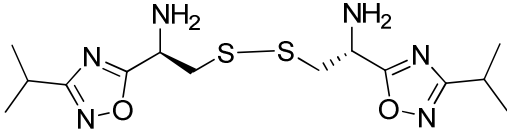
<p>Compound Number: 82 Cook Code: MWL-299 Promentis Code: Pro-081 Chemical Formula: $C_{22}H_{22}N_8O_2S_2$ Molecular Weight: 494.59 Log P: 3.95 Prodrug/Bioisostere: Bioisostere Monomer/Dimer: Dimer</p>	
<p>Compound Number: 83 Cook Code: MWL-258 Promentis Code: Pro-077 Chemical Formula: $C_{14}H_{22}N_8O_2S_2$ Molecular Weight: 398.51 Log P: 1.49 Prodrug/Bioisostere: Bioisostere Monomer/Dimer: Dimer</p>	
<p>Compound Number: 84 Cook Code: MWL-235 Promentis Code: Pro-076 Chemical Formula: $C_{12}H_{24}Cl_2N_8S_2$ Molecular Weight: 415.41 Log P: -2.21 Prodrug/Bioisostere: Bioisostere Monomer/Dimer: Dimer</p>	
<p>Compound Number: 85 Cook Code: MWL-309 Promentis Code: Pro-085 Chemical Formula: $C_{16}H_{26}N_8O_2S_2$ Molecular Weight: 426.56 Log P: 2.64 Prodrug/Bioisostere: Bioisostere Monomer/Dimer: Dimer</p>	

<p>Compound Number: 86 Cook Code: MWL-284 Promentis Code: Pro-082 Chemical Formula: $C_{26}H_{30}N_8O_2S_2$ Molecular Weight: 550.7 Log P: 6.44 Prodrug/Bioisostere: Bioisostere Monomer/Dimer: Dimer</p>	
<p>Compound Number: 87 Cook Code: WYME-SSI-AB Promentis Code: Pro-038 Chemical Formula: $C_{20}H_{32}N_6O_6S_2$ Molecular Weight: 516.63 Log P: 4.56 Prodrug/Bioisostere: Bioisostere Monomer/Dimer: Dimer</p>	
<p>Compound Number: 88 Cook Code: WYME-SSI-P Promentis Code: Pro-039 Chemical Formula: $C_{14}H_{26}C_{12}N_6O_2S_2$ Molecular Weight: 445.43 Log P: 3.89 Prodrug/Bioisostere: Bioisostere Monomer/Dimer: Dimer</p>	
<p>Compound Number: 89 Cook Code: MWL-224 Promentis Code: Pro-073 Chemical Formula: $C_{10}H_{20}Cl_2N_8S$ Molecular Weight: 387.36 Log P: -3.12 Prodrug/Bioisostere: Bioisostere Monomer/Dimer: Dimer</p>	

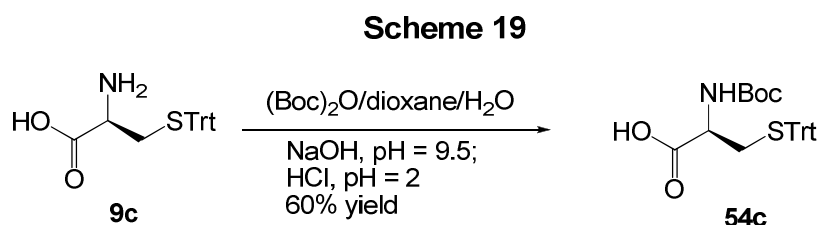
<p>Compound Number: 90 Cook Code: MWL-236 Promentis Code: Pro-074 Chemical Formula: $C_{14}H_{28}Cl_2N_8S_2$ Molecular Weight: 443.46 Log P: -1.8 Prodrug/Bioisostere: Bioisostere Monomer/Dimer: Dimer</p>	
<p>Compound Number: 91 Cook Code: MWL-220 Promentis Code: Pro-072 Chemical Formula: $C_{20}H_{24}Cl_2N_8S_2$ Molecular Weight: 511.49 Log P: -1.09 Prodrug/Bioisostere: Bioisostere Monomer/Dimer: Dimer</p>	
<p>Compound Number: 92 Cook Code: WYME-SS-iPNPh Promentis Code: Pro-075 Chemical Formula: $C_{28}H_{32}N_6O_4S_2$ Molecular Weight: 580.72 Log P: 7.55 Prodrug/Bioisostere: Bioisostere Monomer/Dimer: Dimer</p>	
<p>Compound Number: 93 Cook Code: N/A Promentis Code: N/A Chemical Formula: $C_{16}H_{28}N_2O_8S_2$ Molecular Weight: 440.53 Log P: 1.4 Prodrug/Bioisostere: Prodrug Monomer/Dimer: Dimer</p>	

<p>Compound Number: 94 Cook Code: N/A Promentis Code: N/A Chemical Formula: $C_{31}H_{35}N_3O_3S$ Molecular Weight: 529.69 Log P: 8.42 Prodrug/Bioisostere: Bioisostere Monomer/Dimer: Monomer</p>	
<p>Compound Number: 95 Cook Code: N/A Promentis Code: N/A Chemical Formula: $C_{12}H_{21}N_3O_3S$ Molecular Weight: 287.38 Log P: 3.11 Prodrug/Bioisostere: Bioisostere Monomer/Dimer: Monomer</p>	
<p>Compound Number: 96 Cook Code: N/A Promentis Code: N/A Chemical Formula: $C_{10}H_{18}N_4O_2S$ Molecular Weight: 258.34 Log P: 1.98 Prodrug/Bioisostere: Bioisostere Monomer/Dimer: Monomer</p>	
<p>Compound Number: 97 Cook Code: N/A Promentis Code: N/A Chemical Formula: $C_{20}H_{34}N_8O_4S_2$ Molecular Weight: 514.21 Log P: 4.41 Prodrug/Bioisostere: Bioisostere Monomer/Dimer: Dimer</p>	
<p>Compound Number: 98 Cook Code: N/A Promentis Code: N/A Chemical Formula: $C_{11}H_{20}N_4O_2S$ Molecular Weight: 272.37 Log P: 2.55 Prodrug/Bioisostere: Bioisostere Monomer/Dimer: Monomer</p>	

<p>Compound Number: 99 Cook Code: N/A Promentis Code: N/A Chemical Formula: $C_{22}H_{38}N_8O_4S_2$ Molecular Weight: 542.25 Log P: 5.56 Prodrug/Bioisostere: Bioisostere Monomer/Dimer: Dimer</p>	
<p>Compound Number: 100 Cook Code: N/A Promentis Code: N/A Chemical Formula: $C_{15}H_{20}N_4O_2S$ Molecular Weight: 320.41 Log P: 3.36 Prodrug/Bioisostere: Bioisostere Monomer/Dimer: Monomer</p>	
<p>Compound Number: 101 Cook Code: N/A Promentis Code: N/A Chemical Formula: $C_{30}H_{38}N_8O_4S_2$ Molecular Weight: 638.25 Log P: 7.18 Prodrug/Bioisostere: Bioisostere Monomer/Dimer: Dimer</p>	
<p>Compound Number: 102 Cook Code: N/A Promentis Code: N/A Chemical Formula: $C_{12}H_{22}N_4O_2S$ Molecular Weight: 286.39 Log P: 3.04 Prodrug/Bioisostere: Bioisostere Monomer/Dimer: Monomer</p>	

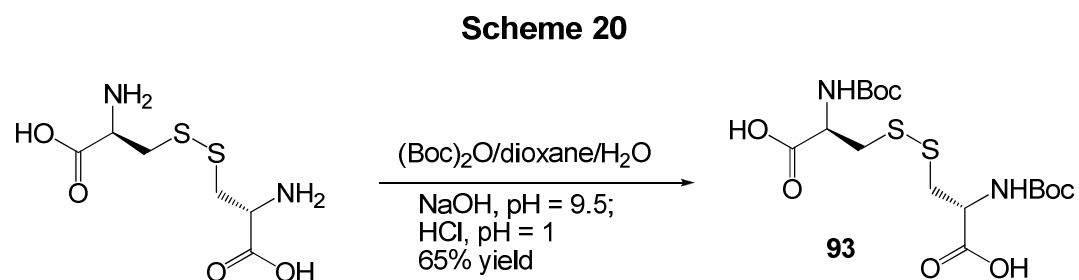
<p>Compound Number: 103 Cook Code: N/A Promentis Code: N/A Chemical Formula: $C_{24}H_{42}N_8O_4S_2$ Molecular Weight: 570.77 Log P: 6.53 Prodrug/Bioisostere: Bioisostere Monomer/Dimer: Dimer</p>	
<p>Compound Number: 104 Cook Code: N/A Promentis Code: N/A Chemical Formula: $C_{24}H_{40}N_6O_6S_2$ Molecular Weight: 572.74 Log P: 6.68 Prodrug/Bioisostere: Bioisostere Monomer/Dimer: Dimer</p>	
<p>Compound Number: 105 Cook Code: N/A Promentis Code: N/A Chemical Formula: $C_{20}H_{32}N_6O_6S_2$ Molecular Weight: 516.63 Log P: 4.56 Prodrug/Bioisostere: Bioisostere Monomer/Dimer: Dimer</p>	
<p>Compound Number: 106a Cook Code: N/A Promentis Code: N/A Chemical Formula: $C_{10}H_{16}N_6O_2S_2$ Molecular Weight: 316.40 Log P: 1.77 Prodrug/Bioisostere: Bioisostere Monomer/Dimer: Dimer</p>	
<p>Compound Number: 106b Cook Code: N/A Promentis Code: N/A Chemical Formula: $C_{14}H_{24}N_6O_2S_2$ Molecular Weight: 372.51 Log P: 3.89 Prodrug/Bioisostere: Bioisostere Monomer/Dimer: Dimer</p>	

2.1. Synthesis of (R)-2-(*tert*-Butoxycarbonylamino)-3-(tritylthio)propanoic acid (**54c**).



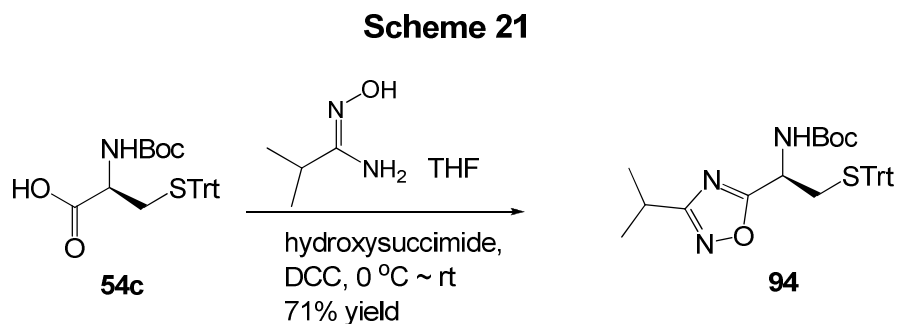
As shown in **Scheme 19**, to a solution of Trt-Cys-OH, **9c**, in dioxane (60 mL) and water was added di-*tert*-butyldicarbonate at 45 °C, and the solution was adjusted with NaOH(4M) until pH = 9.5, and then stirred at the same temperature overnight. Once the reaction was done via analysis by TLC (silica gel), water and dioxane were removed under reduced pressure. The residue was dissolved into water and extracted with ethyl acetate. The aq layer was adjusted to pH = 2 with dilute HCl while in an ice bath, and then the aq layer was extracted with ethyl acetate. The combined ethyl acetate layers were washed with water and dried over anhydrous magnesium sulfate. Removal of the solvent under reduced pressure yielded a yellow oil. The residue was then dissolved into ethyl ether and carefully a 1:1 mixture of ethyl ether and hexane was added with stirring to precipitate out the white solid, **54c**.

2.2. Synthesis of N,N'-Bis(tert-Butoxy)carbonylcystine (**93**).



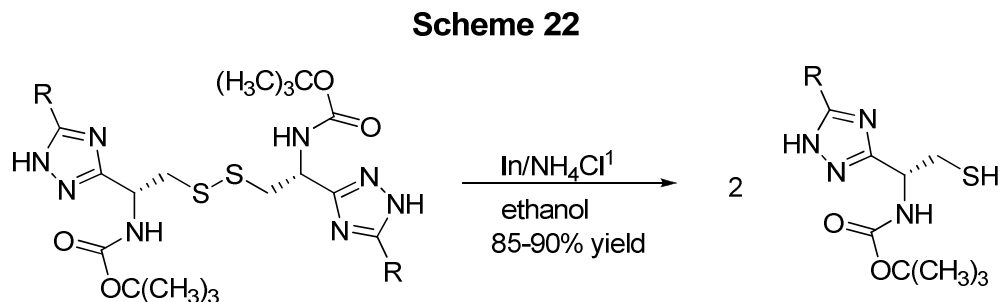
As shown in **Scheme 20**, to a solution of commercial L-cystine in aq NaOH, a solution of di-*tert*-butyldi-carbonate in dioxane was added at 0 °C. The reaction mixture was stirred at 0 °C for 5 min and then allowed to stir at rt for 12 h. Fifty percent of the volume of dioxane was removed under reduced pressure and the mixture was extracted with ethyl acetate. The combined aq phases were acidified (pH = 1) with aq HCl (1 M) and extracted with ethyl acetate. The combined organic layers were washed with brine, dried (Na_2SO_4), filtered and concentrated under reduced pressure to afford protected cystine **93** as white solid.

2.3. Synthesis of (R)-tert-Butyl 1-(3-isopropyl-1,2,4-oxadiazol-5-yl)-2-(tritylthio) ethylcarbamate (94).



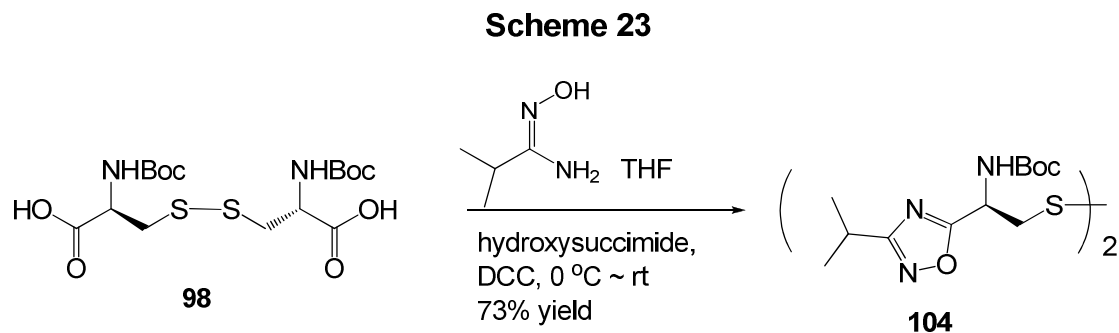
As shown in **Scheme 21**, to a solution of trityl protected Boc-L-cysteine **54c**, isobutyl-imidoxine and hydroxysuccinimide in THF was added at 0 °C over 15 min to a solution of DCC in THF. The mixture was allowed to stir for 16 h while the temperature was allowed to warm to rt. The mixture was then cooled to 0 °C and the precipitate which formed was removed by filtration. The filtrate was concentrated under vacuum and then dissolved into ethyl acetate. A small amount of precipitate formed and was filtered out. The organic layer was washed with a dilute aq sodium bicarbonate solution, brine, dried (Na₂SO₄) and was then removed under reduced pressure to give trityl protected Boc-L-cysteine acetamidoxime ester as white crystals. This material was taken up in toluene and the mixture was heated at reflux for 3 h and the water which formed was removed via a Dean-Stark trap. The solvent was removed under vacuum and the residue was purified by flash chromatography to form the white crystals of bioisostere monomer **94**.

2.4. General Procedure for Cleaving Disulfide Bonds on Bioisosteres.



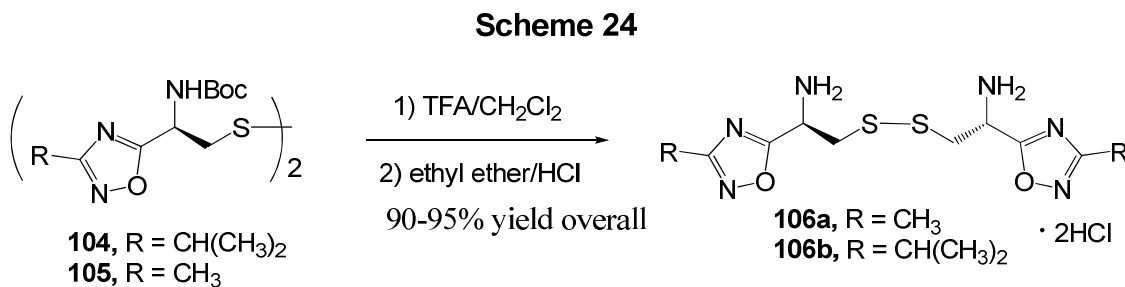
As shown in **Scheme 22**, the bioisostere disulfide (1 mmol) was dissolved in ethanol and indium (1.1 mmol) was added in one portion while stirring. Then anhydrous NH_4Cl (2.2 mmol) was added to the suspension while stirring. The mixture was heated to reflux under argon for 4-6 hrs. After full conversion of the starting material was achieved via analysis by TLC, the solids were removed by filtration over a bed of celite. The solvent was removed under reduced pressure until dryness. The residue was washed well with water to dissolve the inorganic salts. The mixture was filtered and dried to yield the product. The monomer can be purified by crystallization from dichloromethane (DCM) or ethanol. This procedure was used to make bioisostere monomers **96** ($\text{R} = \text{CH}_3$), **98** ($\text{R} = \text{CH}_2\text{CH}_3$), **100** ($\text{R} = \text{Ph}$) and **102** ($\text{R} = \text{CH}(\text{CH}_3)_2$) from their corresponding bisbioisosteric dimers **97**, **99**, **101** and **103**.

2.5. Synthesis of *tert*-Butyl (1*R*,1'*R*)-2,2'-disulfaneylbis(1-(3-isopropyl-1,2,4-oxadiazol-5-yl)ethane-2,1-diyl)dicarbamate (104**).**



As shown in **Scheme 23**, to a solution of Boc-L-cystine **98** isobutyl-imidoxime and hydroxysuccinimide in THF was added at 0 °C over 15 min to a solution of DCC in THF. The mixture was allowed to stir for 16 h while the temperature was allowed to warm to 20 °C. The mixture was cooled to 0 °C and the precipitate which formed was removed by filtration. The filtrate was concentrated under vacuum and then dissolved into ethyl acetate. The small amount of precipitate which formed was filtered off. The organic layer was washed with dilute aq sodium bicarbonate solution, brine, dried (anhydrous Na₂SO₄) and removed under reduced pressure to give Boc-L-cystine bis(acetamidoxime) ester as white crystals. This material was taken up in toluene and the mixture was heated at reflux for 3 h and the water which formed was removed via a Dean-Stark trap. The solvent was removed under vacuum and the residue was purified by flash chromatography to provide white crystals of bioisostere dimer **104**.

2.6. Synthesis of (1R,1'R)-2,2'-Disulfanediylbis(1-(3-methyl-1,2,4-oxadiazol-5-yl)ethanamine) (106a, 106b).



As shown in **Scheme 24**, to a solution of **104** (or **105**) in DCM, cooled to 0 °C, was slowly added TFA. The solution was gradually warmed up to rt and allowed to stir for 2 h until analysis by TLC indicated the starting material had disappeared. The solvent was removed under reduced pressure and the residue was dissolved into ethyl acetate. The solution was washed with saturated aq sodium bicarbonate solution, brine and dried (anhydrous Na₂SO₄). The solvent was removed under reduced pressure and ethyl ether was added to the form an oil. Ethyl ether saturated with HCl gas was added at 0 °C until a white solid precipitated out. The solid was then collected by filtration and yielded the hydrochloride salt of **106b** (or **106a**).

IV. Synthesis of Protected Cysteine and Cystine Analogues with Various Groups to Alter the Partition Coefficients.

1. Rationale, Design and Synthesis of Protected Cysteine and Cystine Analogues.

In an unrelated approach (**Scheme 25** and **Scheme 26**) to the two synthetic pathways (prodrugs and bioisosteres) described previously, L-cysteine and L-cystine were protected as acyl analogues with alkyl esters. They were synthesized to improve their partition coefficient (Log P) and circulatory half life in the blood to determine if passive delivery into the brain through the blood brain barrier was feasible.⁸⁷ Various alkyl amides or alkyl esters were incorporated into the target compounds (see **107** and **112**) in **Scheme 25** and **Scheme 26**, respectively. Symmetrical cystine dimer target compounds (see **109** and **113**) were synthesized from the corresponding cysteine analogues (see **107**, **108** and **112**) by the addition of a catalytic amount of iodine as shown in **Scheme 25** and **Scheme 26**. The target molecules depicted in **Scheme 25** and **Scheme 26** should result in more exposure and increased brain levels, as compared to previous unprotected cysteine and cystine analogues.

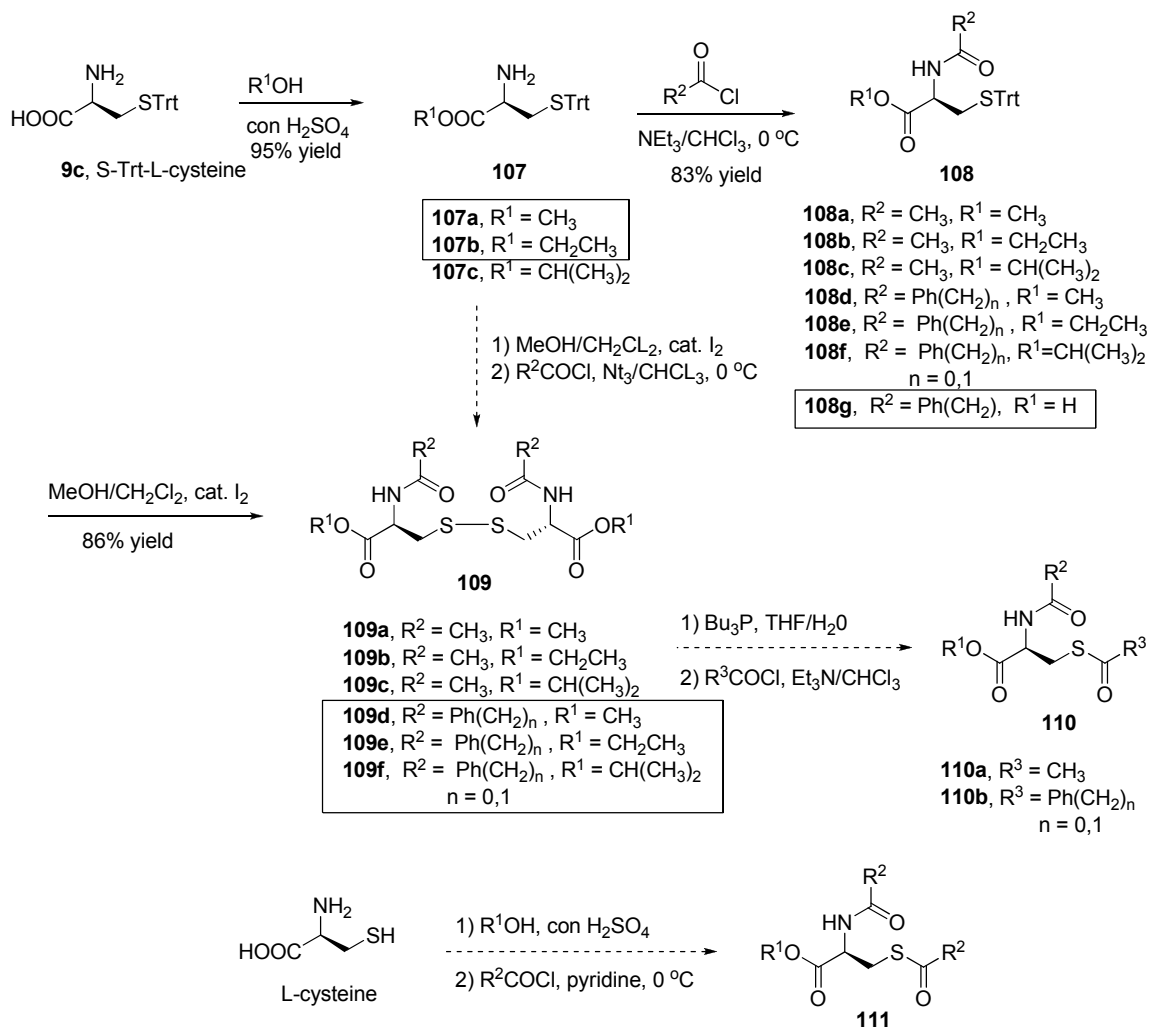
It is noteworthy that this approach altered the partition coefficient by completely protecting the cysteine/cystine moiety. Synthetic challenges, such as solubility and stability of intermediates which resulted and the target compounds, have previously prevented others in the field from obtaining protected analogues in significant quantities,

even for research studies.⁸⁷ Glycine was incorporated into some of these prodrugs, **Scheme 26**, to provide a more efficient method of delivery of both amino acids, cysteine and glycine to the cystine-glutamate antiporter in the CNS. Again, all prodrugs would be expected to be hydrolyzed (cleaved) into the corresponding amino acid, cysteine and glycine *in vivo*, by peptidases, esterases and hydrolyases in the brain which were outlined earlier in **Figure 5**.⁸⁷

Although this method was not intellectually challenging, the concept was based on sound principles of medicinal chemistry and should increase the area under the curve (AUC) for the corresponding amino acids, cysteine and cystine, which would result in more exposure and possibly increased brain levels⁸⁷.

Listed in **Table 4** is a list of compounds prepared following **Scheme 25** and **Scheme 26**, by members of the Cook group, under the direction of myself and/or synthesized by myself, the primary project researcher. Compounds that are “boxed” in each general scheme were actually synthesized as shown in the general scheme. After which is a detailed listing of some key reactions and target prodrugs. **The complete experimental details are located in Chapter IX – Experimental Section, and includes weights, molar quantities, volumes, temperatures, and spectral data.**

**General Synthesis of Protected Analogues with Various Groups to Alter the Partition Coefficients
Scheme 25**



**General Synthesis of Protected Analogues with
Glycine and Various Groups to Alter the Partition
Coefficients
Scheme 26**

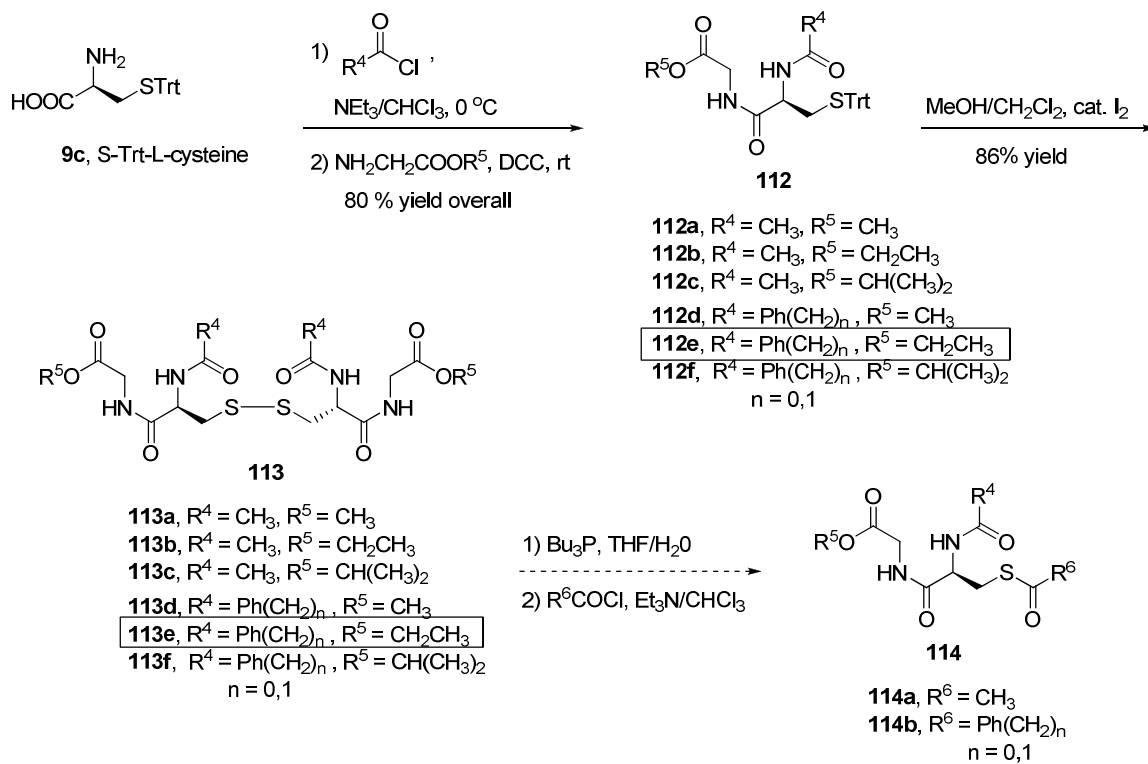
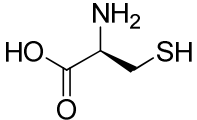
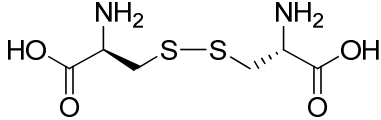
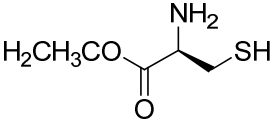
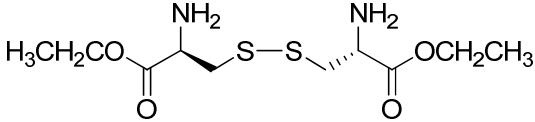
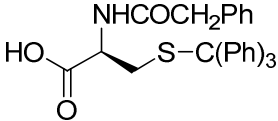
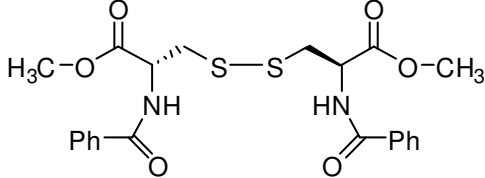
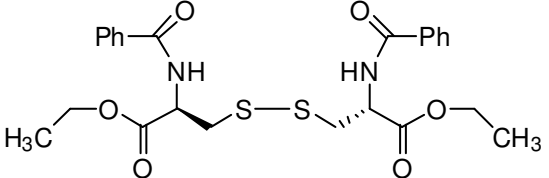
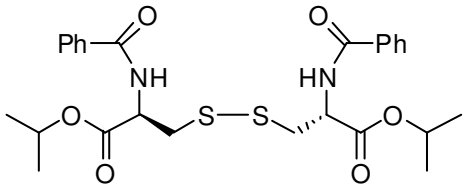
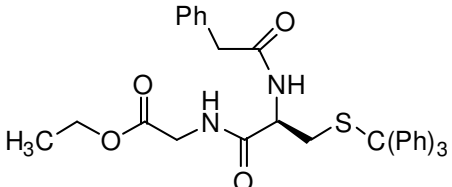
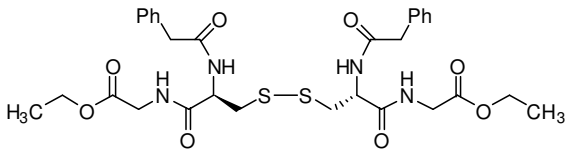
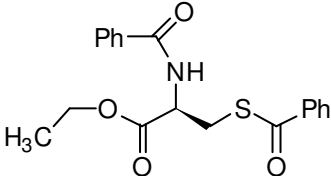
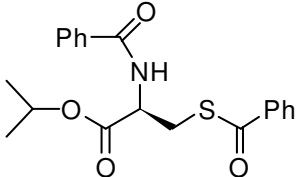
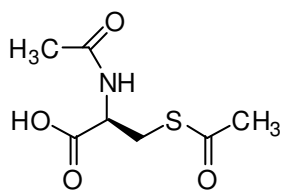
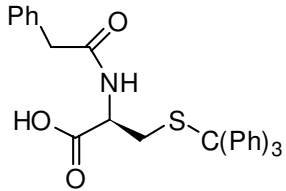
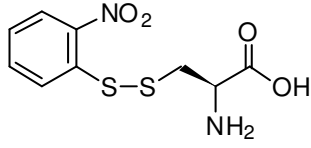
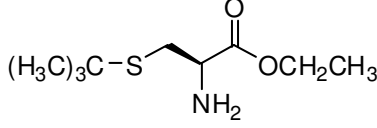
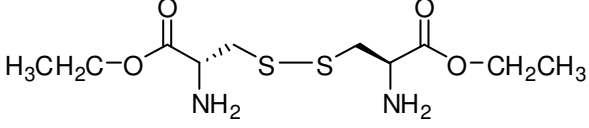
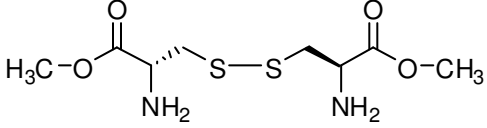
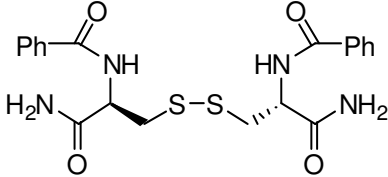
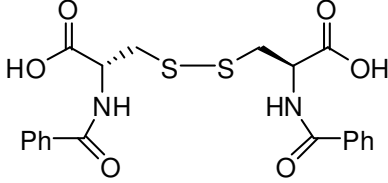
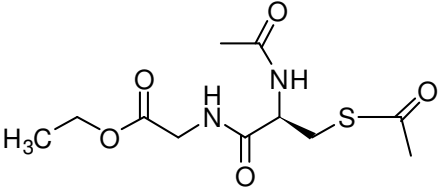


Table 4. Protected Analogues with Various Groups to Alter the Partition Coefficients From Scheme 25 and Scheme 26

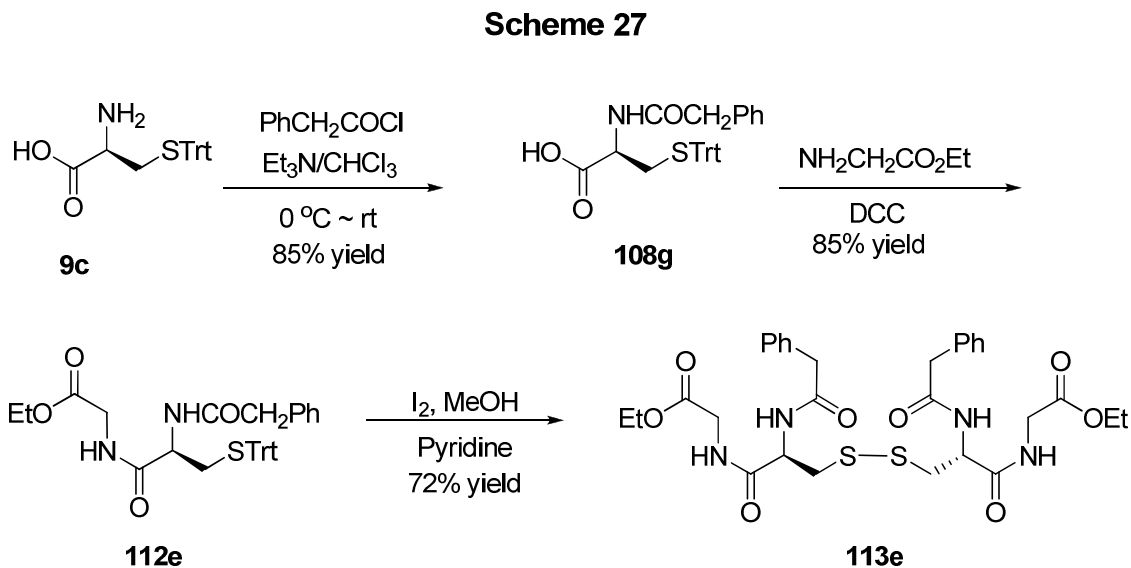
 <p>Cysteine Log P: -0.92</p>	 <p>Cystine Log P: -1.38</p>
 <p>Cysteine Ethyl Ester Log P: -0.32</p>	 <p>Cystine Ethyl Ester Log P: -0.18</p>
<p>Compound Number: 108g Cook Code: N/A Promentis Code: N/A Chemical Formula: C₃₀H₂₇NO₃S Molecular Weight: 481.61 Log P: 6.17 Prodrug/Bioisostere: Prodrug Monomer/Dimer: Monomer</p>	
<p>Compound Number: 109d Cook Code: WYME-SS-BM Promentis Code: Pro-034 Chemical Formula: C₂₂H₂₄N₂O₆S₂ Molecular Weight: 476.57 Log P: 2.8 Prodrug/Bioisostere: Prodrug Monomer/Dimer: Dimer</p>	
<p>Compound Number: 109e Cook Code: WYME-SS-BE Promentis Code: Pro-033 Chemical Formula: C₂₄H₂₈N₂O₆S₂ Molecular Weight: 504.62 Log P: 3.48 Prodrug/Bioisostere: Prodrug Monomer/Dimer: Dimer</p>	

<p>Compound Number: 109f Cook Code: WYME-SS-NPiPr Promentis Code: Pro-091 Chemical Formula: $C_{26}H_{32}N_2O_6S_2$ Molecular Weight: 532.67 Log P: 4.11 Prodrug/Bioisostere: Prodrug Monomer/Dimer: Monomer</p>	
<p>Compound Number: 112e Cook Code: WYME-ST-C9 Promentis Code: Pro-050 Chemical Formula: $C_{34}H_{34}N_2O_4S$ Molecular Weight: 566.71 Log P: 5.62 Prodrug/Bioisostere: Prodrug Monomer/Dimer: Monomer</p>	
<p>Compound Number: 113e Cook Code: WYME-11g Promentis Code: Pro-003 Chemical Formula: $C_{30}H_{38}N_4O_8S_2$ Molecular Weight: 646.77 Log P: 1.07 Prodrug/Bioisostere: Prodrug Monomer/Dimer: Monomer</p>	
<p>Compound Number: 115 Cook Code: WYME-10e Promentis Code: Pro-001 Chemical Formula: $C_{19}H_{19}NO_4S$ Molecular Weight: 357.42 Log P: 3.37 Prodrug/Bioisostere: Prodrug Monomer/Dimer: Monomer</p>	
<p>Compound Number: 116 Cook Code: WYME-10f Promentis Code: Pro-002 Chemical Formula: $C_{20}H_{21}NO_4S$ Molecular Weight: 371.45 Log P: 3.69 Prodrug/Bioisostere: Prodrug Monomer/Dimer: Monomer</p>	

<p>Compound Number: 117 Cook Code: WYME-diA Promentis Code: Pro-008 Chemical Formula: C₇H₁₁NO₄S Molecular Weight: 205.23 Log P: -1.02 Prodrug/Bioisostere: Prodrug Monomer/Dimer: Monomer</p>	
<p>Compound Number: 118 Cook Code: WYME-SPh-CCO Promentis Code: Pro-028 Chemical Formula: C₃₀H₂₇NO₃S Molecular Weight: 481.61 Log P: 6.17 Prodrug/Bioisostere: Prodrug Monomer/Dimer: Monomer</p>	
<p>Compound Number: 119 Cook Code: WYME-SNPS Promentis Code: Pro-026 Chemical Formula: C₉H₁₀N₂O₄S₂ Molecular Weight: 274.32 Log P: -1.03 Prodrug/Bioisostere: Prodrug Monomer/Dimer: Monomer</p>	
<p>Compound Number: 120 Cook Code: WYME-SM-tBu Promentis Code: Pro-025 Chemical Formula: Molecular Weight: 205.32 Log P: 0.81 Prodrug/Bioisostere: Prodrug Monomer/Dimer: Monomer</p>	
<p>Compound Number: 121 Cook Code: WYME-051707-SSE Promentis Code: Pro-036 Chemical Formula: C₁₀H₂₀N₂O₄S₂ Molecular Weight: 296.41 Log P: -0.18 Prodrug/Bioisostere: Prodrug Monomer/Dimer: Dimer</p>	

<p>Compound Number: 122 Cook Code: WYME-060307-SSM Promentis Code: Pro-037 Chemical Formula: $C_8H_{16}N_2O_4S_2$ Molecular Weight: 268.35 Log P: -0.86 Prodrug/Bioisostere: Prodrug Monomer/Dimer: Dimer</p>	
<p>Compound Number: 123 Cook Code: WYME-SSNBam Promentis Code: Pro-040 Chemical Formula: $C_{20}H_{22}N_4O_4S_2$ Molecular Weight: 446.55 Log P: 0.97 Prodrug/Bioisostere: Prodrug Monomer/Dimer: Dimer</p>	
<p>Compound Number: 124 Cook Code: ME-SBZ Promentis Code: Pro-019 Chemical Formula: $C_{20}H_{20}N_2O_6S_2$ Molecular Weight: 448.51 Log P: 2.28 Prodrug/Bioisostere: Prodrug Monomer/Dimer: Dimer</p>	
<p>Compound Number: 125 Cook Code: WYME-diAcGly Promentis Code: Pro-087 Chemical Formula: $C_{11}H_{18}N_2O_5S$ Molecular Weight: 290.3 Log P: -1.57 Prodrug/Bioisostere: Prodrug Monomer/Dimer: Monomer</p>	

2.1. Representative Procedure for the Synthesis of Dimer 113e.



2.2. Synthesis of Phenyl acetyl-S-trityl-L-cysteine (108g).

As shown in **Scheme 27**, a solution of phenylacetyl chloride in chloroform was added to a suspension of S-trityl-L-cysteine **9c** in chloroform containing triethylamine cooled in ice. The mixture was allowed to stir at 0–5 °C for 15 min and at rt for 24 h. Water was added and pH was adjusted to 1.5 with 5 N aq HCl. The aq phase was removed and the organic phase was washed with a saturated aq solution of sodium chloride, dried (anhydrous Na₂SO₄) and concentrated under reduced pressure to give a white crystalline solid of the protected cysteine compound **108g**.

2.3. Synthesis of N-Carbobenzoxy-S-trityl-L-cysteinyglycine ethyl ester (112e).

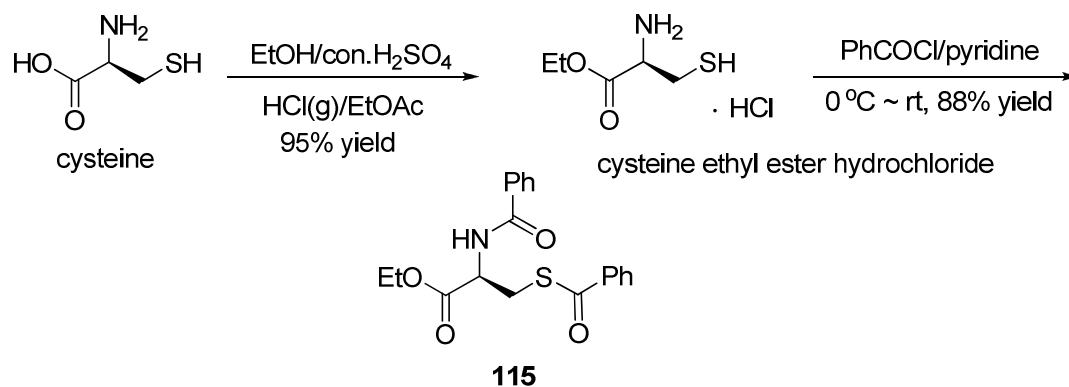
As shown in **Scheme 27**, phenyl acetyl-S-trityl-L-cysteine **108g** and N, N'-dicyclohexycarbodiimide was added to a solution of glycine ethyl ester hydrochloride in chloroform and triethylamine. After the solution was allowed to stir at rt overnight, followed by addition of a few drops of 50% acetic acid, the insoluble precipitate of dicyclohexylurea was removed by filtration; the filtrate was washed successively with dilute hydrochloric acid, potassium hydrogen carbonate and water, dried over sodium sulfate and evaporated to dryness. The residue was treated with ethyl acetate. Some undissolved material (dicyclohexylurea) was filtered off and the filtrate was concentrated *in vacuo* to a small volume. A crystalline solid of the glycine coupled protected cysteine **112e** was separated out.

2.4. Synthesis of Bis-[(R)-ethyl 2-(3-mercapto-2-(2-phenylacetamido)propanamido)acetate] (113e).

As shown in **Scheme 27**, the previously obtained glycine protected cysteine **112e** was dissolved in methanol and a catalytic amount of iodine was added with stirring, after which pyridine was added to the solution with stirring and the final product **113e** was obtained as a white solid.

2.5. Synthesis of N,S-dibenzoyl-L-cysteine ethyl ester (115).

Scheme 28



As shown in **Scheme 28**, benzyol chloride was added to a solution of pure L-cysteine ethyl ester hydrochloride, which was either synthesized as shown above in **Scheme 28** or purchased commercially, in pyridine precooled to 0 °C. The solution was allowed to stir for 1 h at rt, and then the mixture was poured onto ice. The precipitate was collected by filtration and was recrystallized from methanol to provide the dibenzoylated cysteine **115**.

V. Synthesis of Unsymmetrical Disulfide – Heterodimers.

1. Rationale, Design and Synthesis of Unsymmetrical Disulfides.

As previously described, numerous target compounds have been proposed and synthesized. Target compounds consisting of cysteine and cystine diketopiperazine prodrugs, cysteine and cystine bioisosteres, and various cysteine and cystine functionally protected analogues (to alter the partition coefficient), including all monomers and symmetrical disulfide dimers have been prepared. However, one more important series of target compounds have to be described, hetero (unsymmetrical) disulfide dimers. This new series of target compounds could potentially combine the advantages of two different previously described target series in an effort to eliminate or reduce any potential disadvantages of any of the series described above, moreover, to expand the SAR from homodimers to heterodimers. Any disadvantage of the former would only be identified after *in vitro* and *in vivo* biology was obtained. Normally this type of mixing and matching of different target compounds would be reserved until a larger amount of data was obtained for each target series; however, since obtaining preliminary results *in vitro* was key and easier to perform, it was decided to initiate this approach now to determine if such unsymmetrical disulfides could realistically be synthesized on large enough scale for biological testing.

The synthesis of hetero (unsymmetrical) disulfide dimers (**Table 5**) was preferably accomplished by using a one-pot reaction with 1-chlorobenzotriazole, as shown in **Scheme 29**.⁸⁸ The free thiol diketopiperazine (**12**), or theoretically any

previously synthesized free thiol, whether diketopiperazine, bioisostere or functionally protected cysteine/cystine moieties, can be treated with 1-chlorobenzotriazole and benzotriazole in acetonitrile to form sulfenyl chloride intermediate (**126**). Upon addition of benzotriazole, intermediate (**127**) is formed and then treated with thiourea at low temperature to form intermediate (**128**). The addition of thiourea was remove excess 1-chlorobenzotriazole and prevent homodimers formation upon addition of second thiol. Addition of the second desired free thiol will result in the final unsymmetrical disulfide dimer (**129**).

An alternate method would involve using a catalytic amount of iodine in the presence of an equal molar amount of any two triphenyl methane protected thiol cysteine prodrugs (**11**). The desired target compound (**130**) can be separated and purified using simple column chromatography.

Listed in **Table 5** is a list of compounds prepared following **Scheme 29** by members of the Cook group, under the direction of myself and/or synthesized by myself, the primary project researcher. Compounds that are “boxed” in each general scheme were actually synthesized as shown in the general scheme, after which is a detailed listing of some key reactions and target prodrugs. **The complete experimental details are located in Chapter IX – Experimental Section, and includes weights, molar quantities, volumes, temperatures, and spectral data.**

General Synthesis of Unsymmetrical Disulfides⁸⁸
Scheme 29

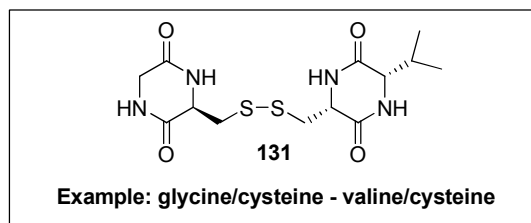
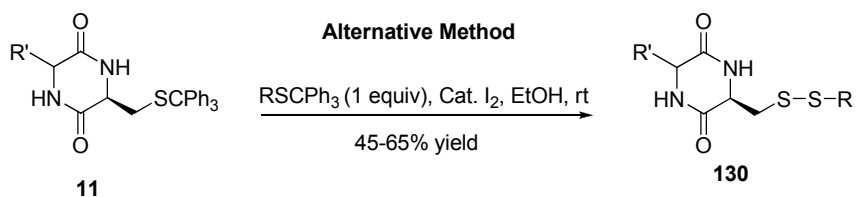
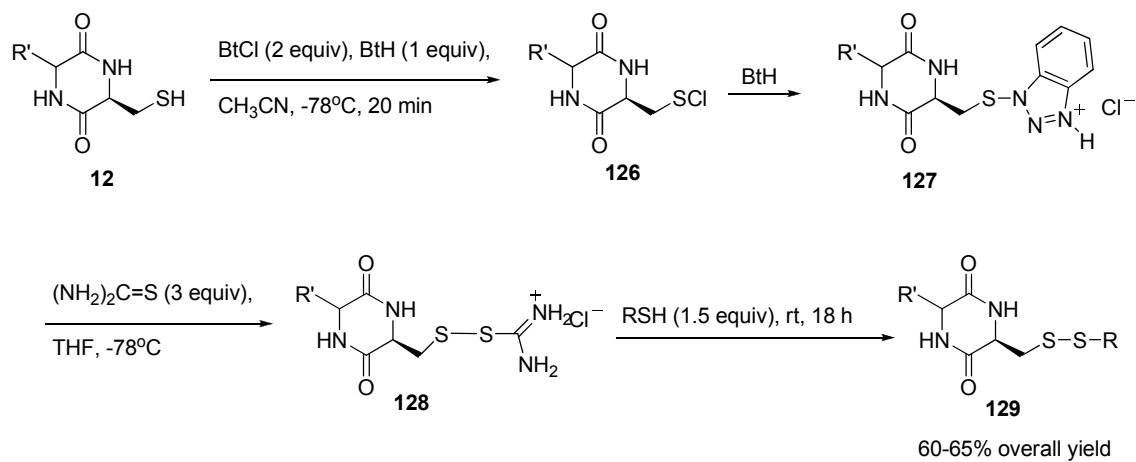
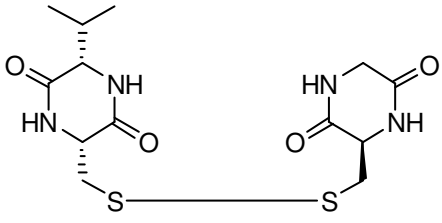
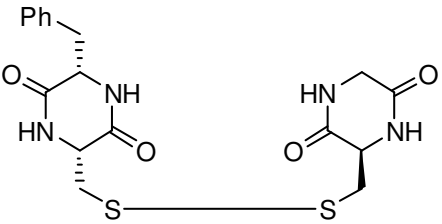
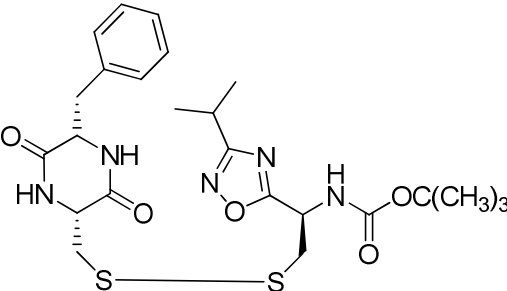
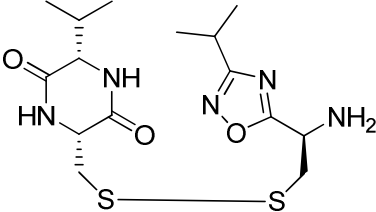


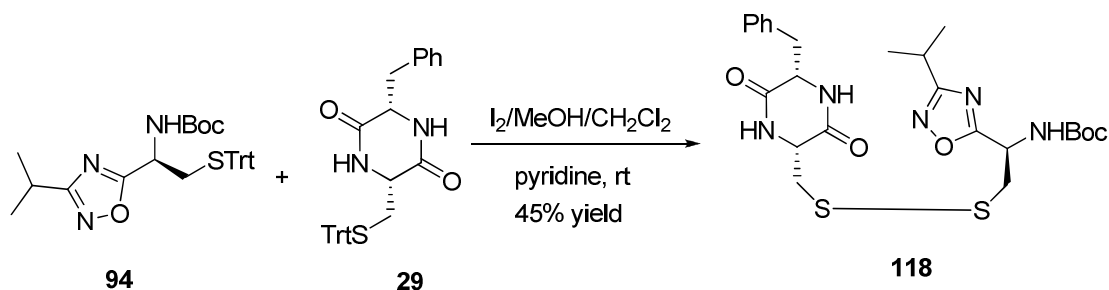
Table 5. Unsymmetrical Disulfide Dimers From Scheme 29

<p>Compound Number: 131 Cook Code: WYME-ST-GV Promentis Code: Pro-054 Chemical Formula: $C_{13}H_{20}N_4O_4S_2$ Molecular Weight: 360.45 Log P: -1.83 Prodrug/Bioisostere: Prodrug Monomer/Dimer: Dimer</p>	
<p>Compound Number: 132 Cook Code: WYME-ST-GP Promentis Code: Pro-053 Chemical Formula: $C_{17}H_{20}N_4O_4S_2$ Molecular Weight: 408.5 Log P: -1.04 Prodrug/Bioisostere: Prodrug Monomer/Dimer: Dimer</p>	
<p>Compound Number: 133 Cook Code: WYME-STPh-iPr Promentis Code: N/A Chemical Formula: $C_{24}H_{33}N_5O_5S_2$ Molecular Weight: 535.68 Log P: 3. Prodrug/Bioisostere: Both Monomer/Dimer: Dimer (Mixed)</p>	
<p>Compound Number: 134 Cook Code: WYME-STVa-iPr-dBOC Promentis Code: N/A Chemical Formula: $C_{15}H_{25}N_5O_3S_2$ Molecular Weight: 387.52 Log P: 1.72 Prodrug/Bioisostere: Both Monomer/Dimer: Dimer (Mixed)</p>	

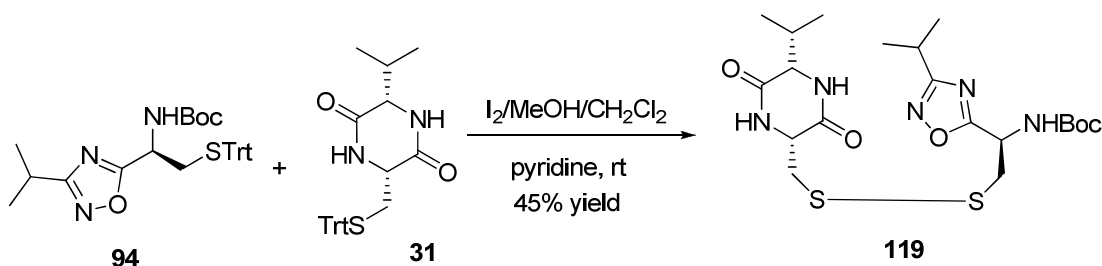
<p>Compound Number: 135 Cook Code: VD-MD-01 Promentis Code: N/A Chemical Formula: $C_{25}H_{36}N_8O_4S_2$ Molecular Weight: 576.73 Log P: 5.8 Prodrug/Bioisostere: Bioisostere Monomer/Dimer: Dimer (Mixed)</p>	
<p>Compound Number: 136 Cook Code: VR-MD-02 Promentis Code: N/A Chemical Formula: $C_{15}H_{22}Cl_2N_8S_2$ Molecular Weight: 448.08 Log P: 3.01 Prodrug/Bioisostere: Bioisostere Monomer/Dimer: Dimer (Mixed)</p>	<p style="text-align: center;">136</p>
<p>Compound Number: 137 Cook Code: WYME-STVa-iPr Promentis Code: N/A Chemical Formula: $C_{20}H_{33}N_5O_5S_2$ Molecular Weight: 487.64 Log P: 3.11 Prodrug/Bioisostere: Bioisostere Monomer/Dimer: Dimer (Mixed)</p>	

2.1. General Procedure for Preparation of Mixed Dimers of Diketopiperazines and Bioisosteres: Synthesis of *tert*-Butyl-(R)-2-(2R,5R)-5-benzyl-3,6-dioxopiperazin-2-yl-methyl-disulfanyl-1-(3-isopropyl-1,2,4-oxadiazol-5-yl)ethylcarbamate (118) and *tert*-Butyl (R)-1-(3-isopropyl-1,2,4-oxadiazol-5-yl)-2-(2R,5R)-5-isopropyl-3,6-dioxopiperazin-2-yl-methyl-disulfanyl ethylcarbamate (119).

Scheme 30



Scheme 31

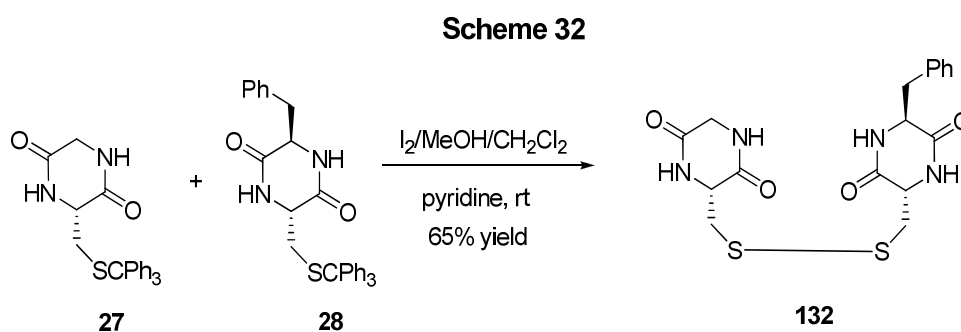


As shown in **Scheme 30** and **Scheme 31** above, the trityl protected diketopiperazine **29** (or **31**), individually, and bioisostere **94** were dissolved in a solution of dichloromethane and methanol with stirring. Pyridine was then added to the mixture which resulted and was followed by a solution of iodine in methanol. The mixture was

allowed to stir for 1 h at rt until analysis by TLC (silica gel) indicated that the reaction was proceeding slowly by the appearance of a new spot under the starting material (UV light). After stirring for 2 h the mixture was concentrated under reduced pressure and a small amount of methanol was added. The solution was allowed to stir an additional 23 hours, and then washed with a saturated aq sodium thiosulfate solution. The solvent was then removed under reduced pressure. The residue which resulted was dissolved in ethyl acetate and the precipitate which resulted was collected by filtration to yield the unsymmetrical dimer **118** (or **119**), individually, as white solids.

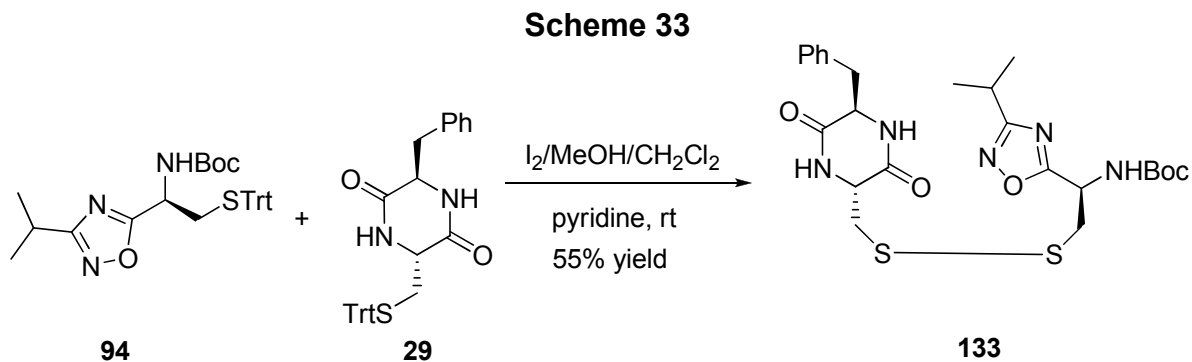
2.2. General Procedure for Preparation of Unsymmetrical Bis-Dipiperazinediones (Unsymmetrical Dimers).

2.2.1. Synthesis of (3*S*,6*S*)-3-Benzyl-6-(*R*)-3,6-dioxopiperazin-2-yl-methyl-disulfanyl-methyl-piperazine-2,5-dione (**132**).



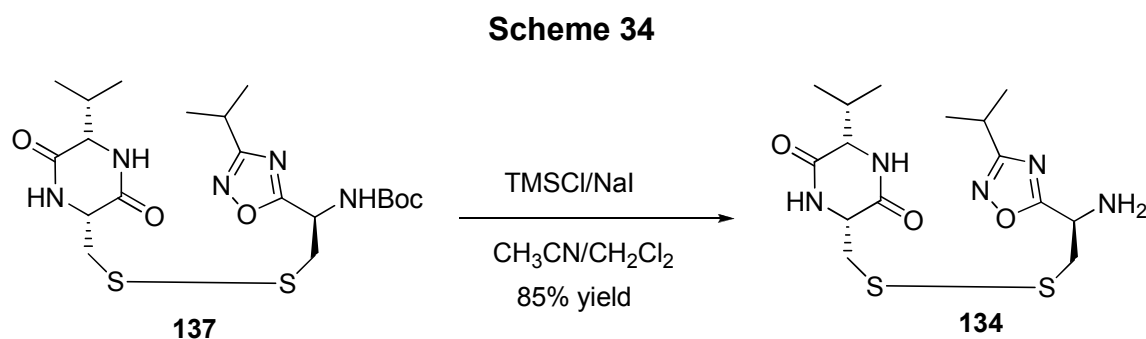
As shown in **Scheme 32**, an equal molar equivalent of the trityl protected diketopiperazines **27** and **28** were dissolved in a solution of methylene chloride and methanol with stirring. Pyridine was then added to the mixture, which resulted, followed by a solution of iodine in methanol. The mixture was allowed to stir for 1 h at rt. No precipitate had formed by this time; however, analysis by TLC indicated that the reaction was proceeding slowly by the appearance of a new spot under the starting material (UV light). A precipitate began to form within 2 h after concentrating the solution and addition of a small amount of methanol. The solution which resulted was allowed to stir an additional 23 h and the precipitate which formed was filtered off. The solid was washed with cold methanol. The precipitate was filtered and dried to yield the unsymmetrical dimer **132** as a yellow solid.

2.2.2. Synthesis of *tert*-Butyl (R)-2- (2R,5R)-5-benzyl-3,6-dioxopiperazin-2-yl-methyl-disulfanyl-1-(3-isopropyl-1,2,4-oxadiazol-5-yl)ethylcarbamate (133).



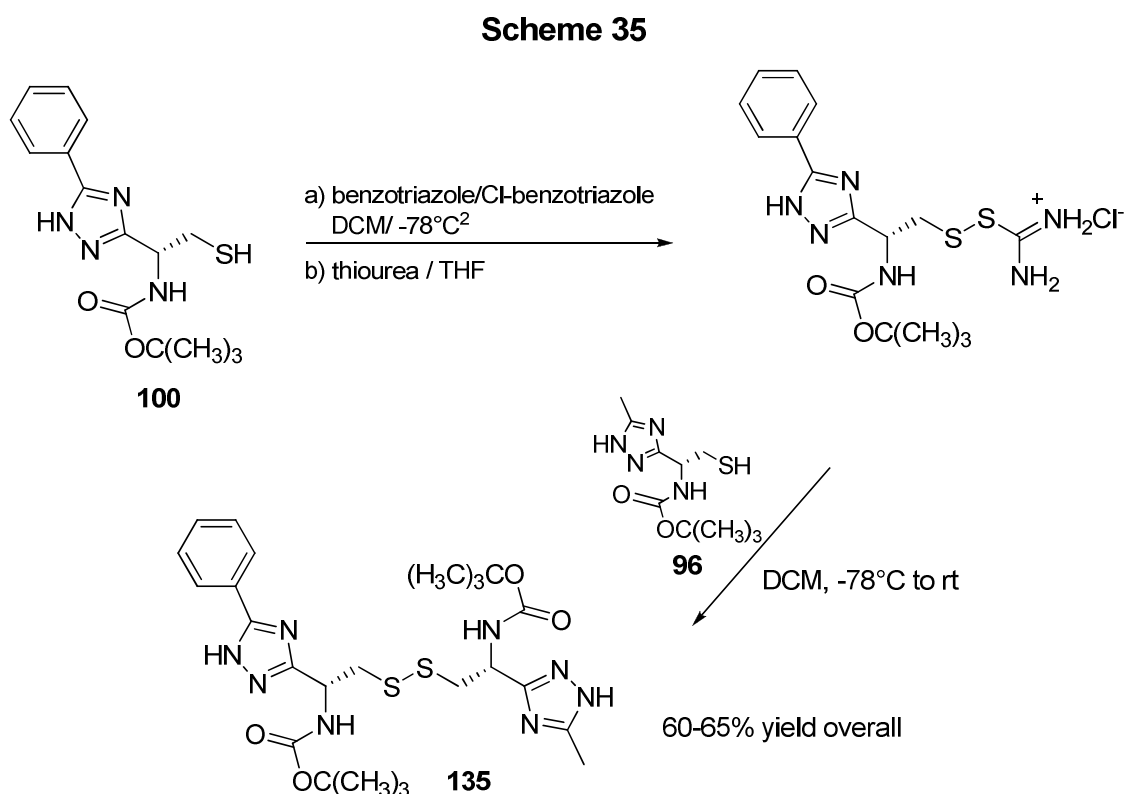
As shown in **Scheme 33**, an equal molar equivalent of the trityl protected diketopiperazine **29** and bioisostere **94** were dissolved in a solution of methylene chloride and methanol with stirring. Pyridine was then added to the mixture, which resulted and this was followed by a solution of iodine in methanol. The mixture was allowed to stir for 1 h at rt until analysis by TLC indicated that the reaction was proceeding slowly by the appearance of a new spot under the starting material (UV light). After stirring for 2 h the mixture was concentrated under reduced pressure and a small amount of methanol was added. The solution was allowed to stir an additional 23 hours, and then washed with a saturated aq sodium thiosulfate solution and the solvent was removed under reduced pressure. The residue which resulted was dissolved in ethyl acetate and the precipitate which resulted was collected by filtration to yield the unsymmetrical dimer **133** as white solid.

2.3. General Procedure for the Dealkylation of the Boc Group by Chlorotrimethylsilane/Sodium Iodide: Synthesis of (3R,6S)-3-(R)-2-Amino-2-(3-isopropyl-1,2,4-oxadiazol-5-yl)ethyl-disulfanyl-methyl-6-isopropylpiperazine-2,5-dione (134).



The reactions were generally carried out on 1 mmol scale in a 10 mL flask and flushed continuously with dry argon. As shown in **Scheme 34**, chlorotrimethylsilane was slowly added with continuous stirring to a solution of the corresponding dimer **137** and sodium iodide in acetonitrile/dichloromethane. The reaction mixture was allowed to stir at rt until the completion of the reaction was indicated on analysis by TLC (silica gel). The solvent was removed under reduced pressure and the residue, which resulted, was dissolved into the mixed solvent (CH_2Cl_2 / methanol = 9:1). The solution was washed with small amount of saturated aq sodium thiosulfate solution, brine and dried over anhydrous Na_2SO_4 . The products were further purified by plate chromatography on silica gel (preparative TLC) to yield pure unsymmetrical dimer **134**.

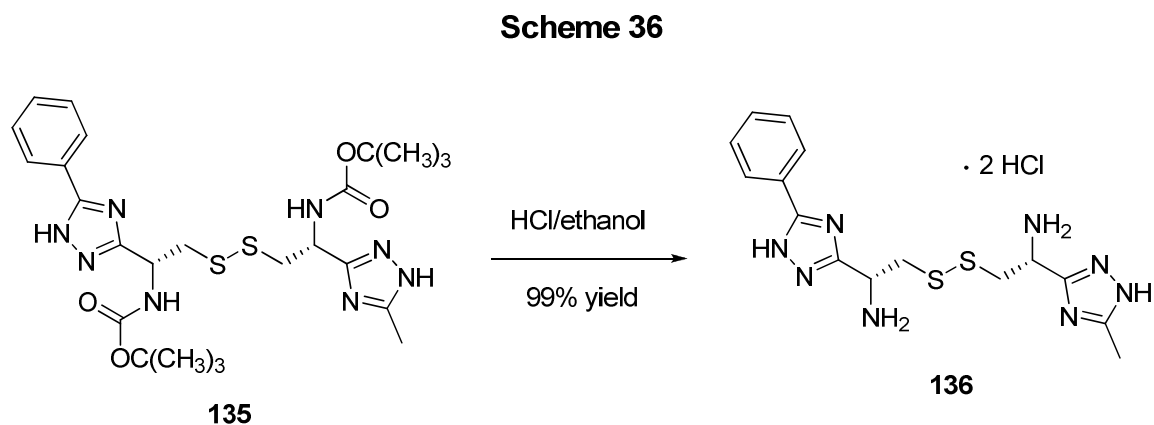
2.4. General Procedure for the Synthesis of Mixed Dimers using the Benzotriazole Method⁸⁸: [tert-Butyl 1-mercapto-2-(5-phenyl-1H-1,2,4-triazol-3-yl)propan-2-ylcarbamate]-[(R)-tert-butyl 2-mercapto-1-(5-methyl-1H-1,2,4-triazol-3-yl)ethylcarbamate]-disulfide (135).



As shown in **Scheme 35**, a solution of triazole monomer **100** was added slowly under an inert atmosphere to a stirred solution of benzotriazole and chloro-benzotriazole in dichloromethane (DCM) at -78°. After 30 min a solution of thiourea in anhydrous THF was added and stirring continued for 30 min. The other triazole monomer **96** in DCM was added while the temperature was maintained at -78°C. The solution was allowed to stir for 18-20 h, while the mixture slowly warmed to rt. The solvent was removed under

reduced pressure and the residue was dissolved in DCM followed by washing with water. The organic layer was dried (anhydrous Na_2SO_4) and the solvent was then removed under reduced pressure and the unsymmetrical dimer **135** was purified by chromatography.

2.5. General Procedure for Deprotection of the BOC group and Formation of HCl Salt of Mixed-dimers: Synthesis of (R)-2-(R)-2-Amino-2-(5-methyl-1H-1,2,4-triazol-3-yl)ethyl-disulfanyl-1-(5-phenyl-1H-1,2,4-triazol-3-yl)ethanamine dihydrochloride (136**).**



As shown in **Scheme 36**, the unsymmetrical dimer **135** was dissolved in EtOH and a saturated solution of anhydrous HCl in EtOH was added. The mixture was stirred for 2 h, after which the solvent was removed under reduced pressure. The oily residue which formed was dissolved in distilled water and washed with DCM to remove organic impurities. The water was then removed under reduced pressure and the gummy residue was finally dried under high vacuum to obtain the solid hydrochloride salt of the unsymmetrical dimer **136**.

VI. Methods, Results and Discussion.

1. *In Vivo* and *In Vitro* screening of target cysteine and cystine analogues (with Dr Baker).

The radio-labeled cystine uptake and glutamate release assays were conducted in order to assess the degree to which the target analogues bind to the cystine/glutamate antiporter driving the desired glutamate release. Provided below are the experimental protocols of five different *in vivo* and *in vitro* screening methods. All *in vivo* and *in vitro* screening was performed by Dr David Baker and his group at Marquette University, Milwaukee, WI.

1.1. Glutamate Sampling and C¹⁴-Cystine Uptake.

The initial screening of compounds was performed using an *in vitro* culture system of human glial cells from brain astrocytoma (1321N1) to determine which compounds have the most promising profile of action for further study. Although a mixed cortical culture was initially proposed for the *in vitro* work, a human glioma cell line was ultimately chosen due to its higher expression of system Xc-cells, which were plated on 24 well plates coated with poly-D-lysine and laminin and grown in a balanced salt solution supplemented with 5% heat inactivated horse serum, 5% fetal bovine serum, 2 mM glutamine and glucose (total 21mM). Cultures were maintained in humidified 5% CO₂ incubators at 37°C for 3-4 days before experiments were performed. At this time the cultures had formed a single confluent layer. For experiments, cultures were washed 3

times into a Na-free HEPES and HCO_3^- -buffered balanced salt solution. After 1 hour, zero time point samples were taken for glutamate analysis by HPLC; at this point test compounds were added. Samples of the media were taken at 1 and 3 hours for glutamate analysis by HPLC. The C^{14} -cystine (0.025 mCi/mL) was then added for 20 minutes. Following the C^{14} -cystine exposure, cultures were washed 3 times with ice cold HEPES buffered saline solution and dissolved in 250 μL sodium dodecyl sulfate (0.1%). An aliquot (200 μL) was removed and added to scintillation fluid for counting. Values were normalized to C^{14} -cystine uptake in untreated controls on the same experimental plate.

1.2. HPLC Analysis of Glutamate.

The concentration of glutamate in the samples was quantified by comparing peak heights from samples and external standards using HPLC coupled to fluorescence detection. Precolumn derivatization of glutamate with o-phthalaldehyde was performed using a Shimadzu LC10AD VP autosampler. The mobile phase consisted of 17% acetonitrile, 100 mM Na_2HPO_4 and 0.1 mM EDTA, pH of 5.90. Glutamate was separated using a reversed-phase column (4 μm ; 150 X 4.6 mm; Phenomenex, Torrance, CA), and detected using a Shimadzu 10RF-AXL fluorescence detector with an excitation and emission wavelength of 320 and 400 nm, respectively.

1.3. Preclinical Assessment of Therapeutic Potential.

Pre-pulse inhibition (PPI) was proposed as the sole behavioral screen; however, by reducing the number of compounds synthesized, we were able to include a second behavioral screen. Thus, behavioral screening of each compound involved a primary screen using elevated plus maze (EPM) and a secondary screen using PPI. EPM was chosen because it is high throughput, requires a compound to penetrate the blood-brain barrier, and is sensitive to increases in cystine-glutamate exchange. For both behaviors, N-Acetylcysteine was run to determine a minimum benchmark for an improved approach. For PPI, clozapine was also run as an optimal mark of efficacy.

1.4. Elevated Plus Maze.

Rats were tested in a standard elevated plus maze; testing occurred in a dimly illuminated room using only two lights mounted over the maze. Animals were allowed to habituate to the room for at least one hour prior to treatment. One hour prior to testing, rats received a pro-drug (0-100 mg/kg, po). For testing, the rat was placed in the elevated plus maze for five minutes, alternating the starting position between facing an open arm and facing a closed arm. The session was recorded and an observer blind to treatment recorded the number of explorations, entries and time spent in the open arm. Explorations were defined as the rat placing two feet into an open arm without fully entering said arm. Entries were defined as the rat placing all four feet in an open arm.

Time of entry in the open arm was recorded from the time the rat placed four feet in the open arm until two of the rats' feet entered the open square.

1.5. Pre-pulse Inhibition.

Rats were placed on a platform in a sound attenuating chamber (10.875"x14"x19.5") that rested on a motion sensing plate. During all sessions the background noise was held constant at 60 dB. A matching session was conducted to determine the magnitude of the average startle response for each rat. This session consisted of a five minute habituation period followed by 20 trials; 17 trials involved the presentation of a single auditory stimulus (pulse stimulus; 50 dB above the background noise) and three trials in which a pre-pulse stimulus (12 db above background) was presented 100 ms before the pulse auditory stimulus. Rats were then assigned into the various treatment groups so that the magnitude of the startle response was equivalent across all groups. Two days later a testing session was conducted to assess sensorimotor gating. One hour prior to testing, rats received a prodrug (0-100 mg/kg, po) and 50 minutes later acute PCP (0-1.5 mg/kg, sc).

The testing session consisted of a five minute habituation period, after which rats received 58 discrete trials; 26 trials during which the pulse stimulus (50 db above background) was presented alone, eight trials each in which the pulse stimulus was preceded by a prepulse stimulus (5, 10, or 15 db above background) and eight background trials with no pulse (No stimulus; background noise only). The first six pulse

alone trials were not included in the average startle stimulus to achieve a relatively stable level of startle reactivity. The percent of pre-pulse inhibition was determined as 100- (average pre-pulse startle response/average startle stimulus alone) x100.

2.1. N-Acetylcysteine & PCP-Induced Deficits in Pre-pulse Inhibition.

The following data set illustrate the present drawbacks associated with N-acetylcysteine, specifically the extensive hepatic metabolism and poor blood brain permeability. Depicted in **Figure 7** is the impact of N-acetylcysteine administered orally (po) on deficits in pre-pulse inhibition produced by phencyclidine. As described below, deficits in pre-pulse inhibition following the administration of phencyclidine represent one of the most common preclinical paradigms used to screen potential antipsychotic agents. Oral administration of N-acetylcysteine (administered 60 min prior to testing; n = 7-10/group), which is subjected to hepatic metabolism, fails to significantly attenuate deficits in pre-pulse inhibition produced by phencyclidine (0 NAC + PCP, control).

The data depicted in the **Figure 8** illustrate the impact of N-acetylcysteine (n = 5-6/group; injected 60 min prior to testing) when administered into the intraperitoneal (ip) cavity in order to circumvent hepatic metabolism. N-Acetylcysteine failed to significantly restore sensorimotor gating at any of the three pre-pulse stimulus intensities, likely a result of poor blood brain permeability.

Depicted in **Figure 9** is the impact of N-acetylcysteine infused directly into the rodent prefrontal cortex, the region thought to underlie sensorimotor gating. Direct infusion of N-acetylcysteine (0-100 microM) circumvents the pharmacokinetic aspects of N-acetylcysteine that mitigate its use as a pharmacotherapy for schizophrenia, including extensive hepatic metabolism and poor blood brain permeability. As indicated in **Figure 9**, infusion of N-acetylcysteine (10 mg/kg, 30 mg/kg, and 100 mg/kg) into the prefrontal cortex significantly restored inhibition of a startle response at each concentration tested (n = 6-8/group; * indicates a significant increase relative to PCP rats receiving no NAC, Fisher LSD, $p < 0.05$). Note, N-Acetylcysteine-induced reversal of the effects of PCP compare favorably in comparison to the effect of clozapine, arguably the most effect antipsychotic on the market.

Figure 7
Oral N-acetylcysteine

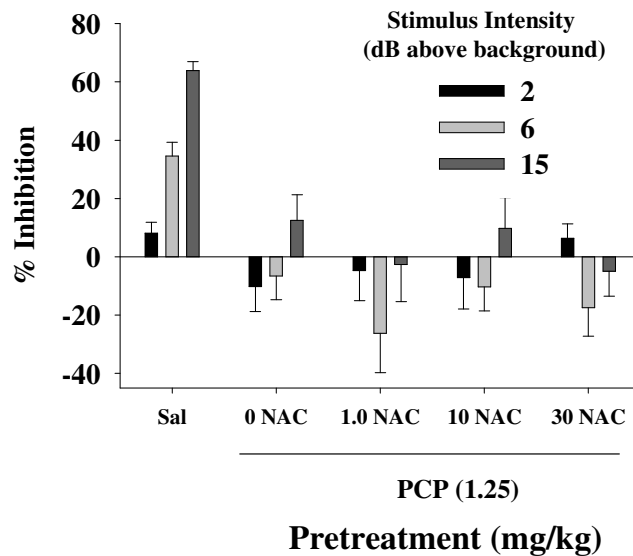


Figure 8
IP N-acetylcysteine

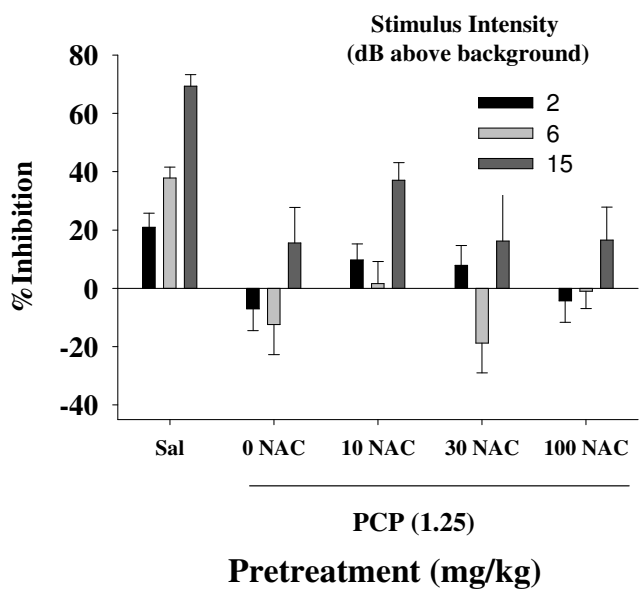
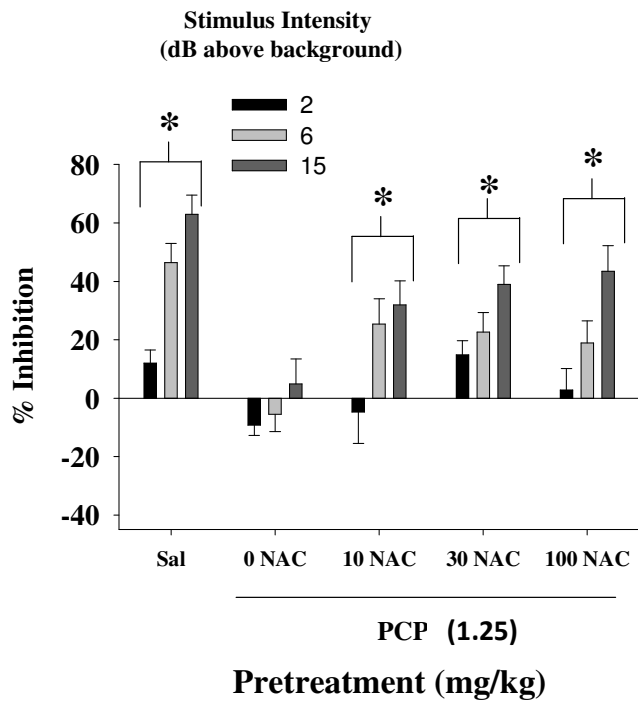


Figure 9
Intra-PFC N-acetylcysteine



2.2. PCP Dose-Dependently Alters Pre-pulse Inhibition and Impact of N-Acetylcysteine on Sensorimotor Gating Deficits Produced by PCP.

Sensorimotor gating, a process compromised in schizophrenic patients, is often measured using pre-pulse inhibition whereby a mild auditory stimulus (pre-pulse, 2-15 db above background) precedes (100 ms) a startle-eliciting auditory stimulus (50 dB above background) as shown above. Intact sensorimotor gating will result in suppression of the startle reflex when preceded by the pre-pulse. Since improvement in pre-pulse inhibition tracks improvement in symptoms that are largely insensitive to current treatments, this paradigm has become one of the most commonly used screening paradigms. Illustrated in **Figure 10** is the capacity of PCP to disrupt pre-pulse inhibition rendering the pre-pulse ineffective in suppressing the startle reflex. PCP is commonly used to disrupt pre-pulse inhibition because this abnormality, in addition to negative and cognitive symptoms, is insensitive to 1st generation antipsychotics thereby providing predictive validity.

Illustrated in **Figure 11** is the impact of N-acetylcysteine on sensorimotor gating deficits produced by phencyclidine administered orally (left) or directly into the prefrontal cortex (right), which is likely the therapeutic site of action for cysteine prodrugs [n= 6-46/group. * indicates a significant difference from rats receiving PCP only (e.g., no N-acetylcysteine), Fisher LSD, $p < 0.05$].

Figure 10

Pre-pulse Inhibition after PCP

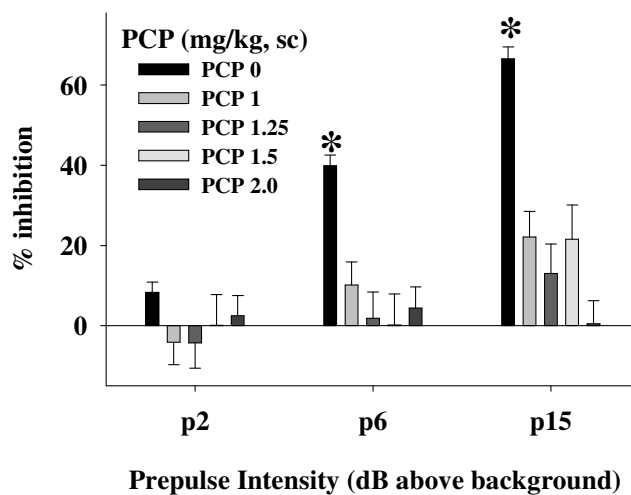
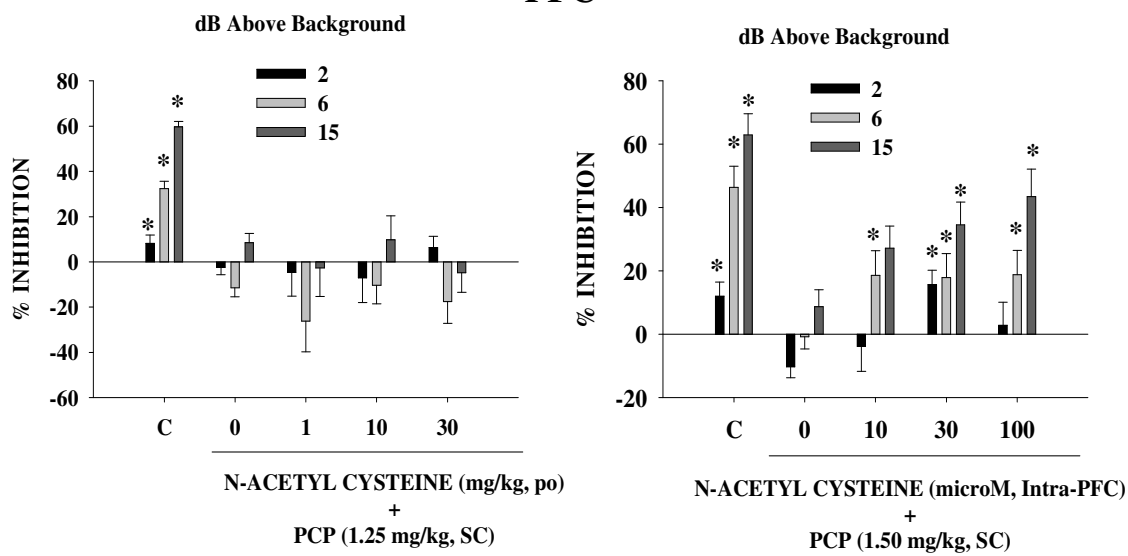


Figure 11

Pre-Pulse Inhibition Recovery from PCP after NAC via PO or Intra-PFC

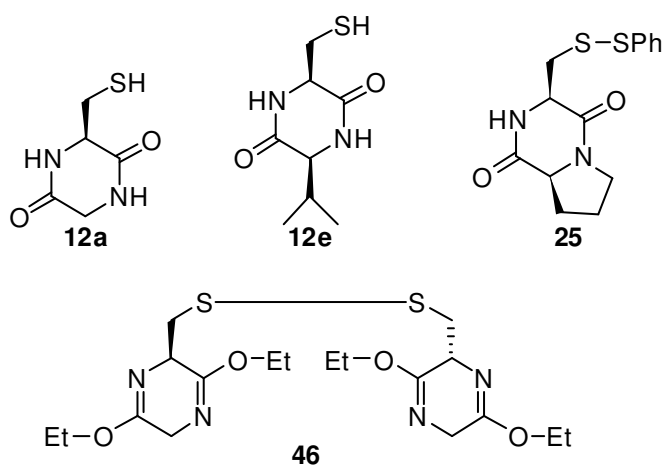
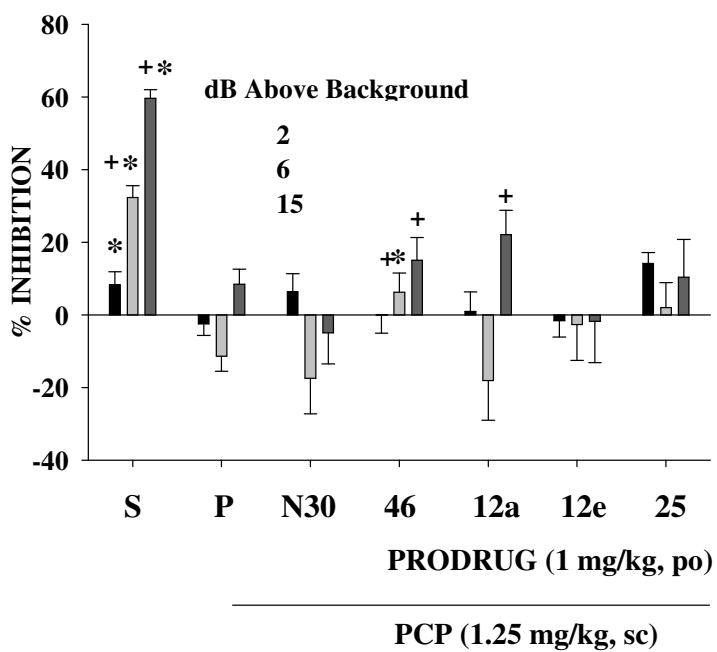


2.3. Efficacy of Compounds from Scheme 3 Relative to N-Acetylcysteine in Reversing PCP-Induced Deficits in Sensorimotor Gating in Rats.

Illustrated in **Figure 12** is a bar graph in which inhibition of a startle response in response to a load stimulus (pulse) when preceded by a pre-pulse stimulus (2-15 db above background) is depicted. Pre-pulse inhibition is a commonly used paradigm to screen antipsychotic agents for use in treatment of schizophrenia. The pre-pulse stimulus presented at 15 dB above background reduced the startle response in saline controls (SC; n = 46) by > 60% relative to the response elicited following exposure to the pulse only. Rats pretreated with phencyclidine only (P; 1,25 mg/kg, SC; n = 42) failed to exhibit a reduction in the response elicited by the pulse even when preceded by the pre-pulse (regardless of stimulus intensity). This reflects sensorimotor gating deficits common to patients afflicted with schizophrenia. Rats pretreated (60 min) with N-acetylcysteine (30 mg/kg, PO) failed to exhibit sensorimotor gating. Note: Direct delivery of N-acetylcysteine into the brain reverses phencyclidine-induced deficits in sensorimotor gating, which is consistent with clinical trials establishing the antipsychotic efficacy of this compound. Rats pretreated (60 min) with the target diketopiperazides synthesized earlier depicted in **Scheme 3** (n = 7-22/group), most notably target compounds **12a** and **46** (cystine prodrugs) exhibited a significant difference relative to either rats receiving PCP alone (P, Fisher LSD, $p < 0.05$) and/or N-acetylcysteine (N 30 = 30 mg/kg; +, Fisher LSD, $p < 0.05$; S = saline). Collectively, these data indicate the efficacy of these compounds and this synthesis Scheme to generate novel antipsychotics that exceed the potential of N-acetylcysteine.

Figure 12

**Pre-pulse Inhibition Recovery
with Compounds from Scheme 3**



2.4. Efficacy of Compounds 44 and 46 (see Scheme 3 earlier) as Novel Antipsychotic Agents.

Startle chambers (Kinder Scientific; 10.875”x14”x19.5”) utilized for all experiments were housed in a sound attenuating chamber and mounted to a motion sensing plate. During all sessions the background noise was held constant at 60 dB by presenting white noise through a speaker mounted above the animal. Rats underwent a 5-minute habituation session prior to all matching and test sessions. Matching sessions were used to determine the magnitude of each rat’s startle response to a loud auditory stimulus (pulse; 50 dB above background; 20 ms), which was assessed following the presentation of seventeen pulse stimuli (50 dB above background) presented alone and three pulse stimuli (50 dB above background) preceded by a mild auditory stimulus (pre-pulse; 12 dB above background; 20 ms). Rats were then assigned to treatment groups such that the magnitude of the startle response was equivalent across all groups. Test sessions consisted of 60 trials, 28 in which the pulse stimulus was presented alone (Pulse), 24 trials in which the pulse stimulus was preceded (100 ms) by a mild auditory stimulus (Pre-pulse; 2, 6, 15 dB above background), and 8 silent trials (No stimulus; background noise only). The percent pre-pulse inhibition was calculated as the magnitude of the startle response when the pulse was preceded by pre-pulse stimuli divided by the magnitude of the startle response when only the pulse stimulus is presented (x 100).

Prior to testing, rats received a cysteine prodrug (0-1 mg/kg, po.; n = 9-15/group) and 50 min later an injection of PCP (0-1.25 mg/kg, sc). Ten minutes later, rats underwent the test session as described above. The novel cysteine prodrug **44**, described in **Scheme 3**, administered orally to rodents 60 min prior to testing at a dose of 1 mg/kg produced a significant increase in sensorimotor gating as assessed by inhibition of a startle response as shown in **Figure 13** (* indicates a significant increase relative to PCP rats receiving no cysteine prodrug, Fisher LSD, $p < 0.05$). Note, these data compare quite favorably to the results obtained with oral administration of N-acetylcysteine.

The data depicted in the **Figure 14** were collected as described above, except bivalent ligand **46**, a cystine prodrug dimer, described in **Scheme 3** was administered 60 minutes prior to testing (n=9-11/group). Analysis of the data demonstrate, oral administration of cystine prodrug dimer **46** significantly restored sensorimotor gating at the highest pre-pulse intensity.

Figure 13

Impact of Oral Monomer 44 on PCP-Evoked
Deficits in Pre-pulse Inhibition

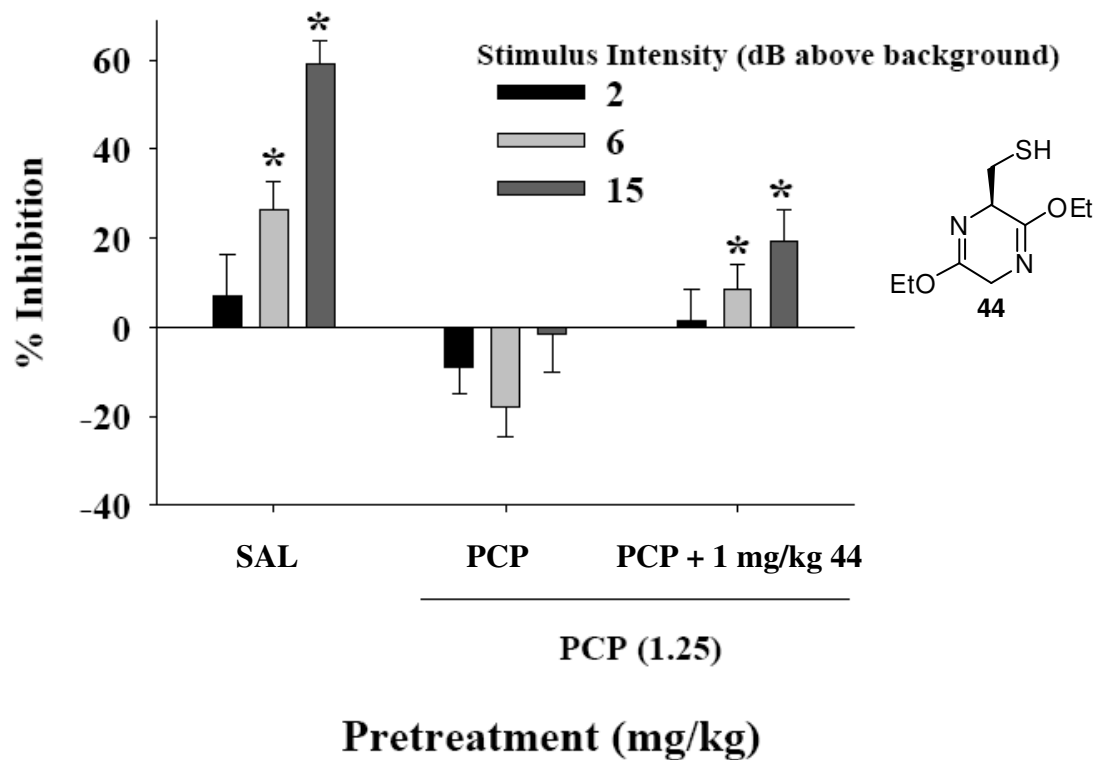
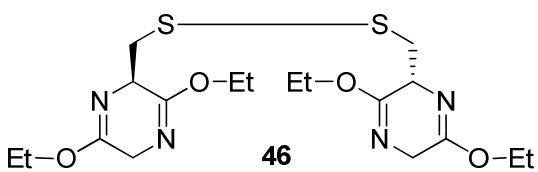
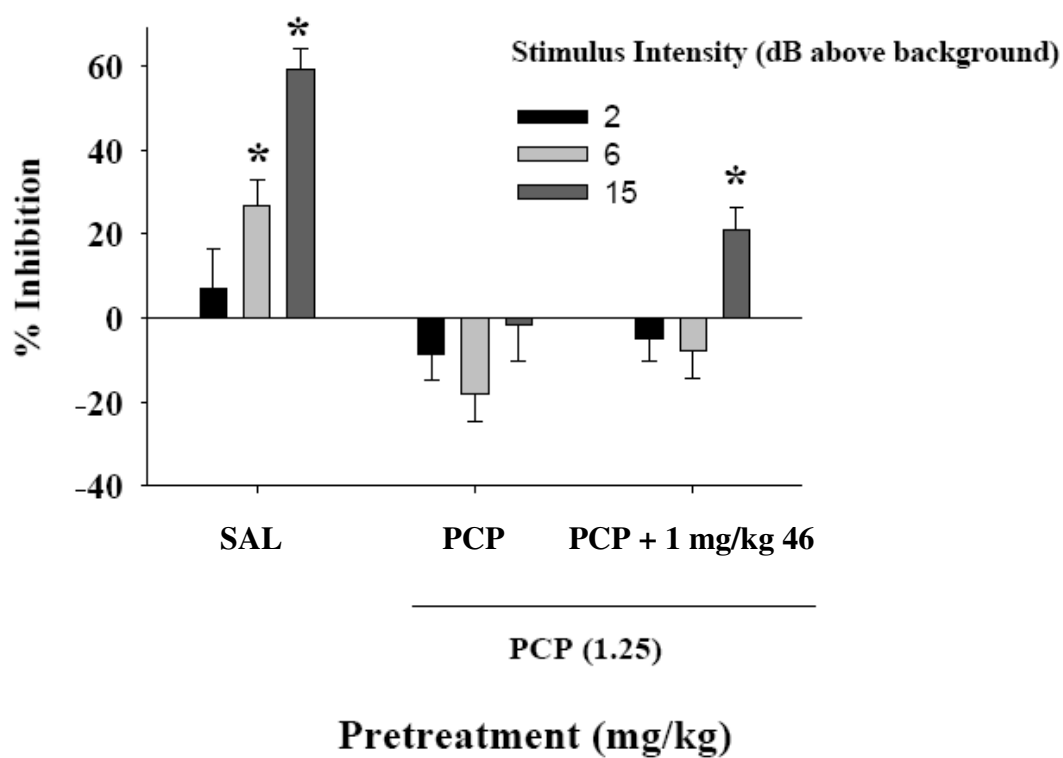


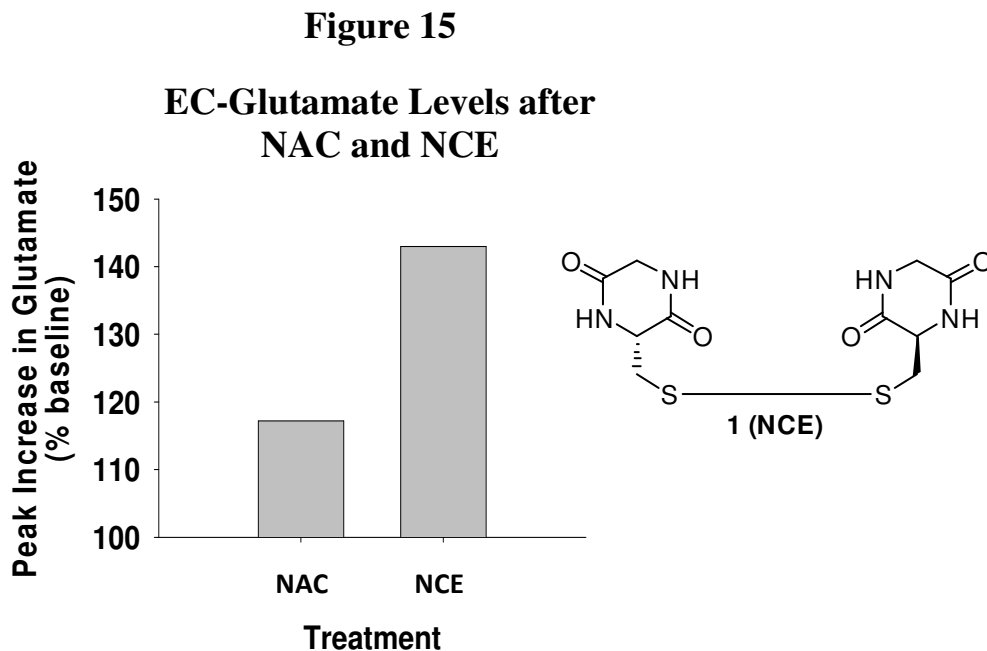
Figure 14

Impact of Oral Dimer 46 on PCP-Evoked
Deficits in Pre-pulse Inhibition



2.5. Diketopiperazide Bivalent Ligand 1 (see Scheme 3 earlier, dimer) Produced a Larger Increase in Glutamate in the Prefrontal Cortex Relative to NAC.

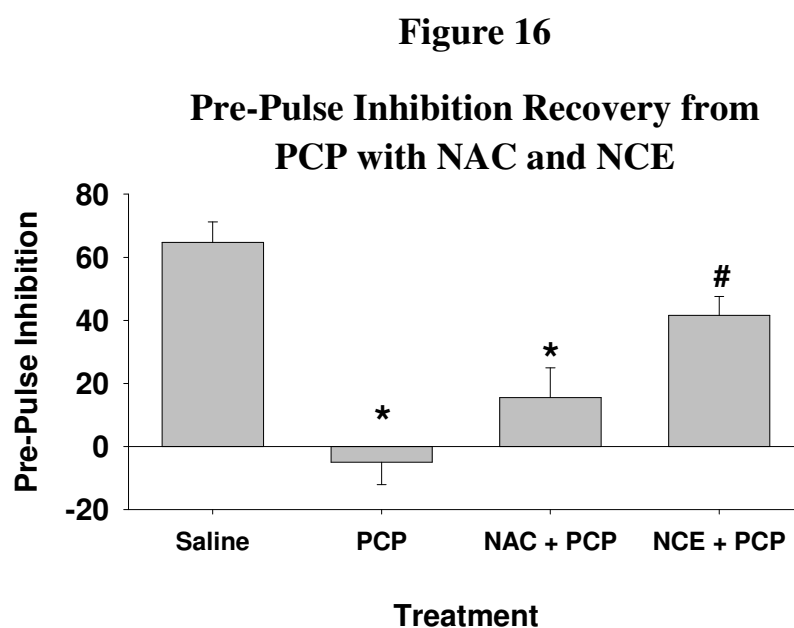
Depicted in **Figure 15** is a bar graph which illustrates extracellular glutamate in the prefrontal cortex (compared to baseline) following administration of cysteine prodrugs N-acetylcysteine (60 mg/kg, ip; n = 4) or target dimer **1**, cystine prodrug dimer, (indicated as NCE in **Figure 15**) (30 mg/kg, po; n = 3) in rats. Analysis of these results indicated a much larger peak increase in glutamate was obtained for cystine prodrug dimer **1** relative to N-acetylcysteine (NAC). Cystine prodrug dimer **1** was given to the animal orally and thereby subjected to potential first-pass metabolism. Conversely, N-acetylcysteine was given ip in order to avoid extensive first pass metabolism that would occur following oral administration. Thus, cystine prodrug dimer **1** produced a larger relative increase in glutamate in rats as compared to NAC even though NAC was given in its preferred route of administration and at twice the concentration. This increased glutamate level indicated that cystine prodrug dimer **1** was successful in elevating extracellular cystine levels and driving cystine-glutamate exchange, a phenomenon understood to be beneficial in overcoming drug addiction.



2.6. Efficacy of Diketopiperazine Dimer 1 (see Scheme 3 earlier) as a Novel Antipsychotic Agent.

Illustrated in **Figure 16** is a bar graph which depicts inhibition of a startle response in response to a load stimulus (pulse) when preceded by a pre-pulse stimulus (15 db above background). As described previously, rats pretreated with N-acetylcysteine (30 mg/kg, po; n = 5) 60 minutes prior to phencyclidine administration exhibited a trend toward improved sensorimotor gating ($p = 0.07$). Rats pretreated with target compound

1, cystine prodrug dimer, (termed NCE in **Figure 16**) (30 mg/kg, po; n = 4) exhibited a significant improvement in sensorimotor gating relative to PCP controls and rats receiving NAC + PCP (* indicates a significant increase relative to PCP rats receiving no cysteine prodrug, Fisher LSD, $p < 0.05$). Collectively, these data indicate the efficacy of cystine prodrug dimer **1** as a novel antipsychotic that exceeds the potential of N-acetylcysteine.

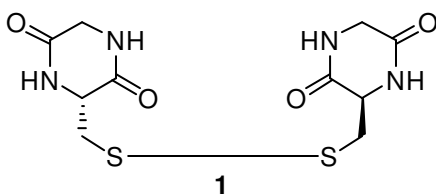
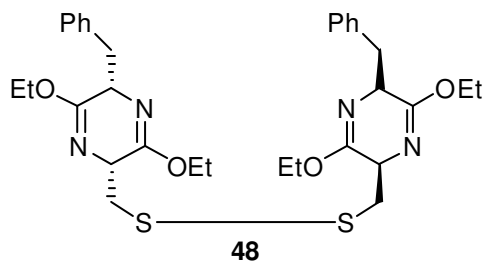
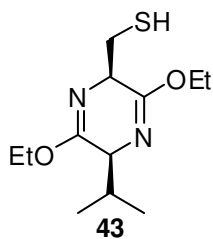
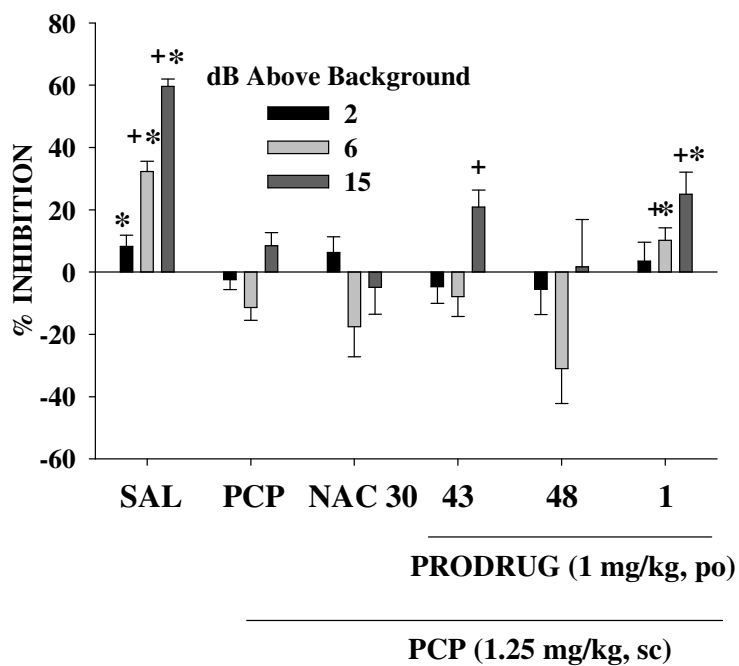


2.7. Efficacy (PO) of Monomers and Dimers from Scheme 4, Relative to N-Acetylcysteine in Reversing PCP-Induced Deficits in Sensorimotor Gating in Rats.

Illustrated in **Figure 17** is a bar graph which depicts the inhibition of a startle response in response to a load stimulus (pulse) when preceded by a pre-pulse stimulus (2-15 db above background). As described previously, rats pretreated (60 minutes) with prodrugs illustrated in **Scheme 4** (n = 7-14/group), notably target analogues **1** and **43**, cystine prodrugs, exhibited a significant difference relative to either rats receiving PCP alone (*, Fisher LSD, p < 0.05) and/or N-acetylcysteine (n = 30; 30 mg/kg; +, Fisher LSD, p < 0.05). Collectively, these data indicated the efficacy of these compounds and the analogues prepared in **Scheme 4** to generate novel antipsychotics that exceed the potential of N-acetylcysteine.

Figure 17

**Pre-pulse Inhibition Recovery with
Monomers and Dimers Prepared and
Illustrated in Scheme 4**

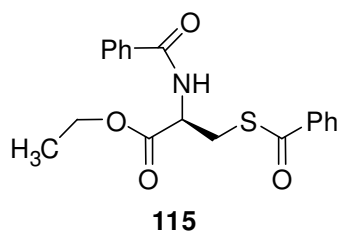
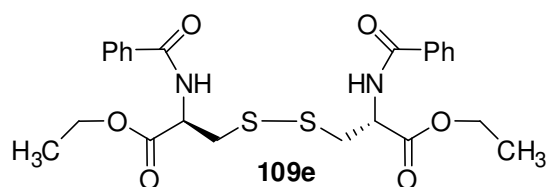
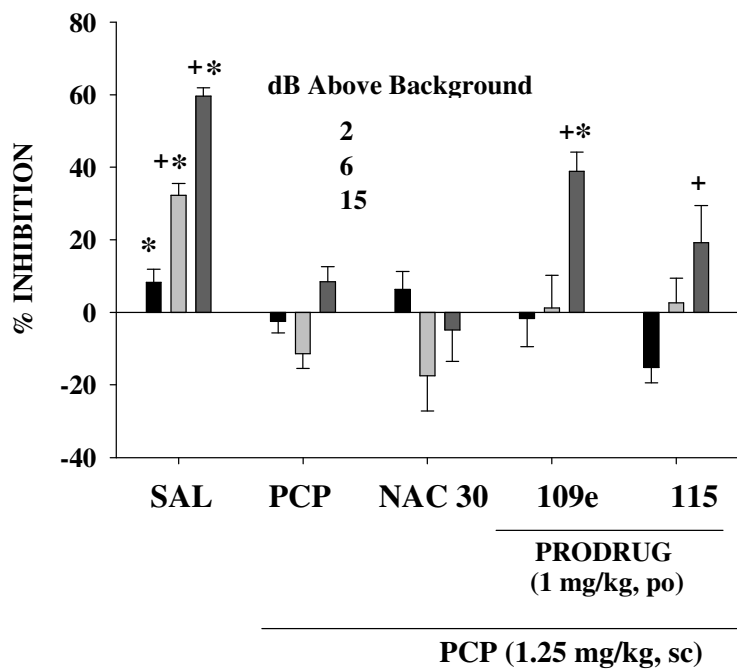


2.8. Efficacy (PO) of Ligands Synthesized and Illustrated in Scheme 25 Relative to N-Acetylcysteine in Reversing PCP-Induced Deficits in Sensorimotor Gating in Rats.

Depicted in **Figure 18** is a bar graph which illustrates the inhibition of a startle response in response to a load stimulus (pulse) when preceded by a pre-pulse stimulus (2-15 db above background). As described previously, rats pretreated (60 minutes) with ligands synthesized and illustrated in **Scheme 25** (n = 7/group), especially target prodrugs **109e** and **115**, cystine prodrugs, exhibited a significant difference relative to either rats receiving PCP alone (*, Fisher LSD, p < 0.05) and/or N-acetylcysteine (n = 30; 30 mg/kg; +, Fisher LSD, p < 0.05). Collectively, these data indicated the efficacy of these prodrugs and the synthetic approach in **Scheme 25** to generate novel antipsychotics that exceeds the potential of N-acetylcysteine. It appears here, based only on the PPI screen, that cystine prodrug **109e** is much more potent than cystine prodrug **115** in the reversal of pre-pulse inhibition of startle affected by PCP.

Figure 18

**Pre-pulse Inhibition Recovery with
Monomers and Dimers Prepared and
Illustrated in Scheme 25**

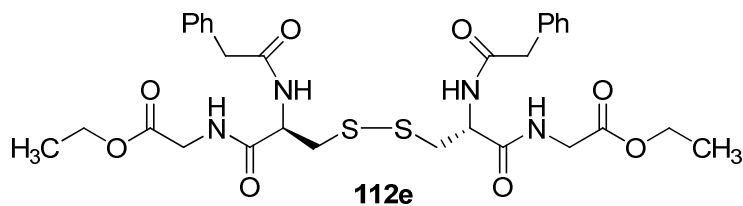
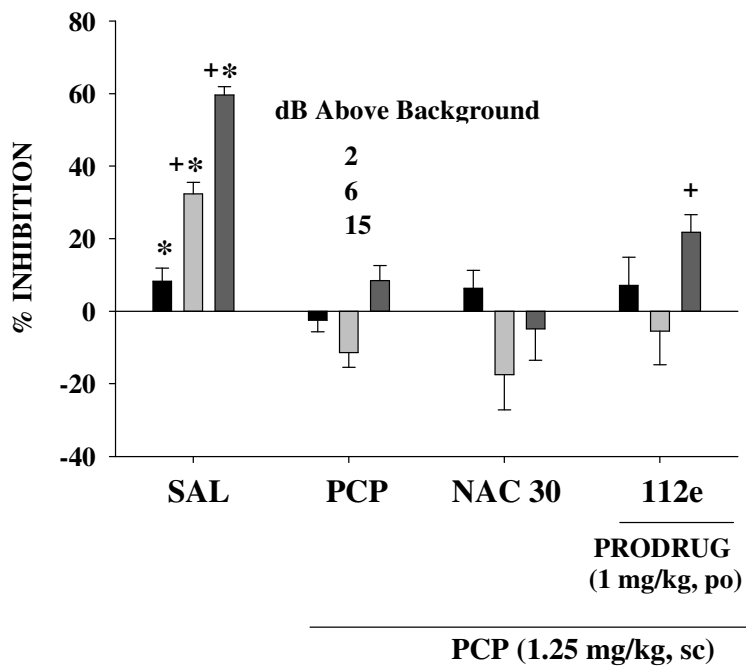


2.9. Efficacy (PO) of Cystine Prodrug 112e from Scheme 26 Relative to N-Acetylcysteine in Reversing PCP-Induced Deficits in Sensorimotor Gating in Rats.

Illustrated in **Figure 19** is a bar graph which depicts the inhibition of a startle response in response to a load stimulus (pulse) when preceded by a pre-pulse stimulus (2-15 db above background) with cystine prodrug **112e**. As described previously, rats pretreated (60 minutes) with the target dimer **112e**, a cystine prodrug, synthesized and illustrated in **Scheme 26** ($n = 7$) exhibited a significant difference (*) relative to rats receiving N-acetylcysteine ($n = 30$; 30 mg/kg; +, Fisher LSD, $p < 0.05$). Collectively, these data indicated the efficacy of this compound and the analogues depicted in **Scheme 26** to generate potential novel antipsychotics that exceed the potential of N-acetylcysteine.

Figure 19

**Pre-pulse Inhibition Recovery with
Cystine Dimer 112e Prepared and
Illustrated in Scheme 26**

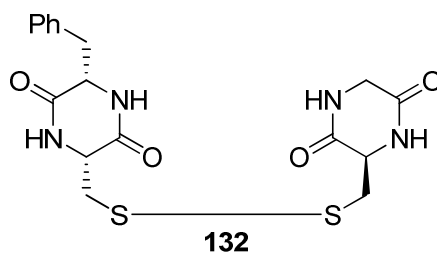
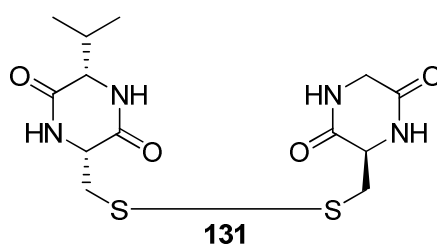
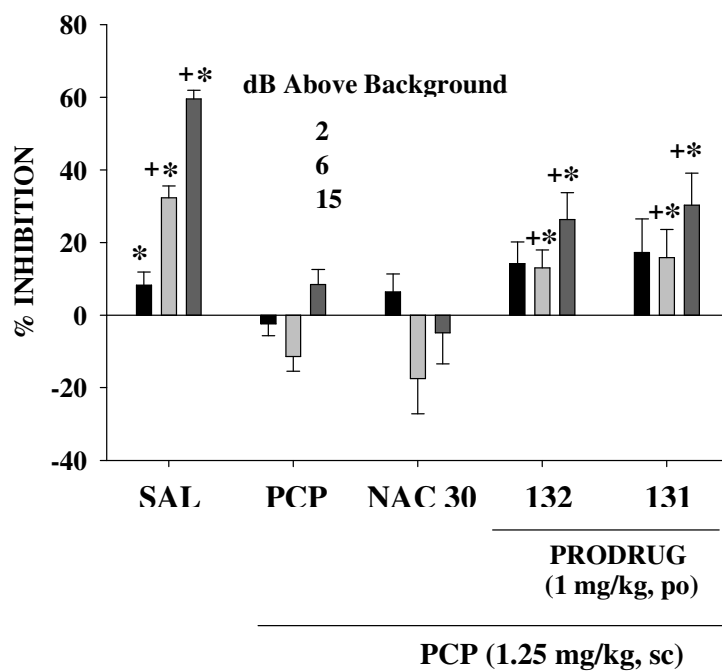


2.10. Efficacy (PO) of Mixed Bivalent Ligands that were Prepared and Illustrated in Scheme 29 Relative to N-Acetylcysteine in Reversing PCP-Induced Deficits in Sensorimotor Gating in Rats.

Outlined in **Figure 20** is a bar graph which illustrates the inhibition of a startle response in response to a loud stimulus (pulse) when preceded by a pre-pulse stimulus (2-15 db above background). As described previously, rats pretreated (60 minutes) with N-acetylcysteine into the brain reverses phencyclidine-induced deficits in sensorimotor gating, which is consistent with clinical trials establishing the antipsychotic efficacy of this compound. Rats pretreated (60 minutes) with compounds synthesized and depicted in **Scheme 29** (n = 7/group), cystine mixed dimers **131** and **132**, cystine prodrug heterodimers, exhibited a significant difference relative to either rats receiving PCP alone (*, Fisher LSD, p < 0.05) and/or N-acetylcysteine (n = 30; 30 mg/kg; +, Fisher LSD, p < 0.05). Collectively, these data indicated the efficacy of these compounds and the synthesis of ligands in **Scheme 29** to generate potential novel antipsychotics that exceeds the potential of N-acetylcysteine.

Figure 20

**Pre-pulse Inhibition Recovery with
Cystine Mixed Dimers Prepared and
Illustrated in Scheme 29**



VII. Biological Data for Target Compounds.

There are two or three sets of *in vitro* and *in vivo* biological data for each of the cystine or cysteine related analogues listed below in **Table 6**. Examination of the C¹⁴ uptake test indicates ability of the analogue to compete with C¹⁴ labeled uptake of cystine into the cell. A decrease in the C¹⁴ labeled cystine uptake indicates that the compound is competing with and/or restricting C¹⁴ labeled cystine uptake into the cell (* indicates a significant difference from the control value, with error bars, $p < 0.05$). This decrease in C¹⁴ labeled cystine uptakes represent a desired effect since the goal is to have the cystine / cysteine related analogues release cystine/cysteine or be active in the antiporter.

Analysis of the glutamate percent change screen indicates the percent change in glutamate after the cell was treated with a solution of the analogue. This change represents the activation and turnover of the cystine-glutamate antiporter. The higher the response in the glutamate percent change, compared to the control, the more effective the compound is at driving the cystine-glutamate antiporter and increasing glutamate levels in the extra-synaptic space which is the desired response. The elevated plus maze is reported in seconds and is the time it takes a rat to complete the plus maze after the target ligand was administered. The elevated plus maze is a study for cognitive deficits or enhancements that may be due to the target analogues. For further information and details about each test refer to the Methods and Results Section.

Table 6. Biological Data for Cysteine and Cystine Analogues**Compound Number: 1**

Cook Code: WYME-ST-GG

Promentis Code: Pro-052

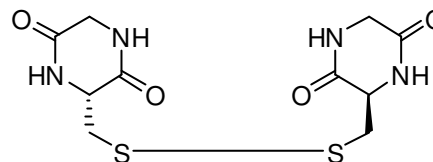
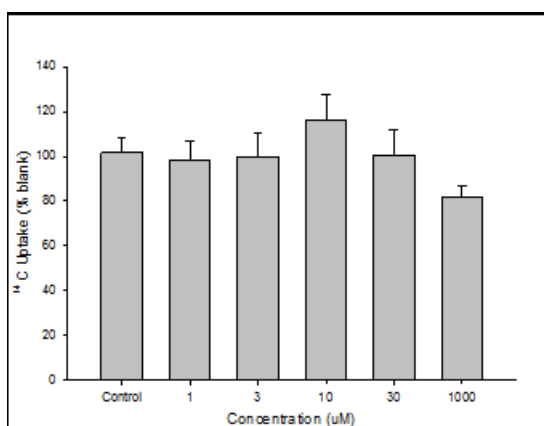
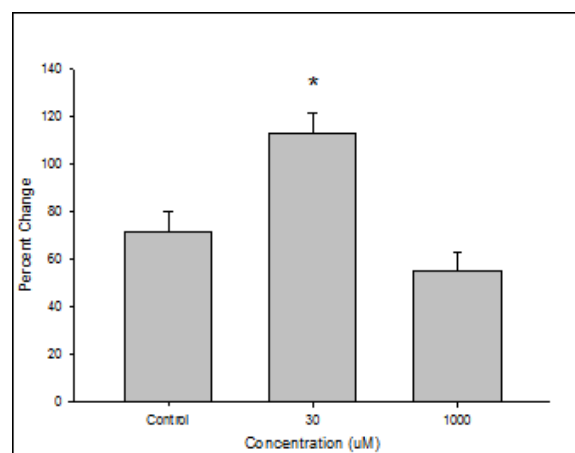
Chemical Formula: $C_{10}H_{14}N_4O_4S_2$

Molecular Weight: 318.37

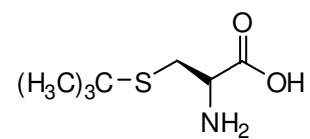
Log P: -3.2

Prodrug/Bioisostere: Prodrug

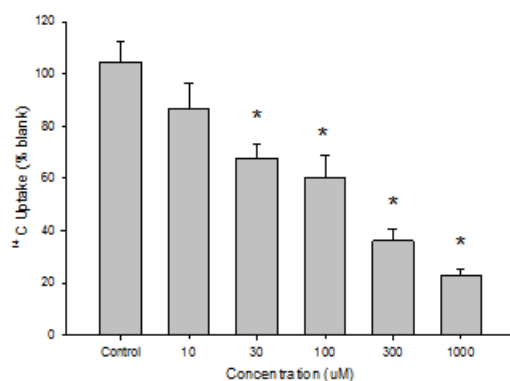
Monomer/Dimer: Dimer

 **C^{14} Uptake****Glutamate Percent Change**

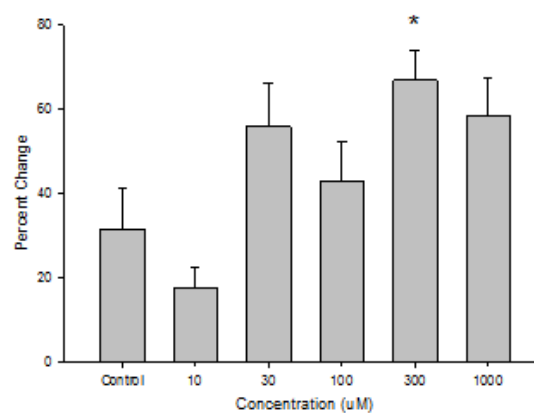
Compound Number: 9a
Cook Code: ME-StBu
Promentis Code: Pro-048
Chemical Formula: $C_7H_{15}NO_2S$
Molecular Weight: 177.26
Log P:0.21
Prodrug/Bioisostere: Prodrug
Monomer/Dimer: Monomer



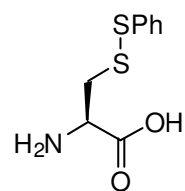
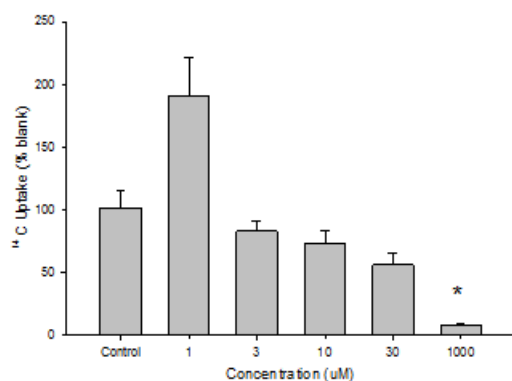
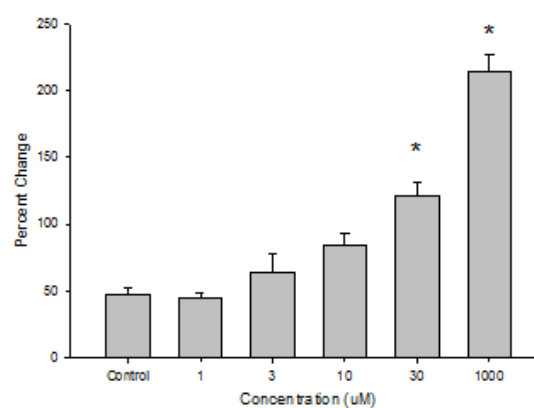
C^{14} Uptake



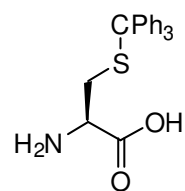
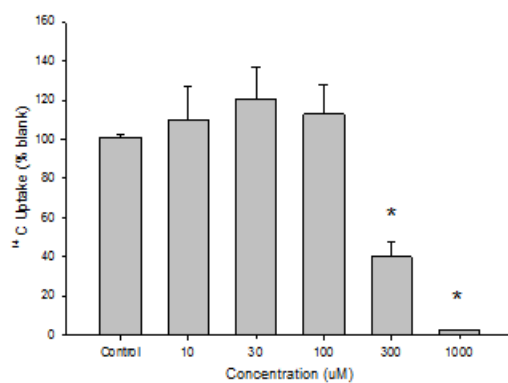
Glutamate Percent Change



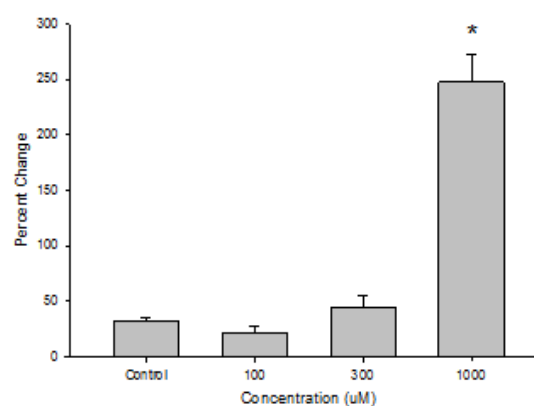
Compound Number: 9b
Cook Code: WYME-SSPh
Promentis Code: Pro-044
Chemical Formula: $C_9H_{11}NO_2S_2$
Molecular Weight: 229.32
Log P: 1.76
Prodrug/Bioisostere: Prodrug
Monomer/Dimer: Monomer

**C¹⁴ Uptake****Glutamate Percent Change**

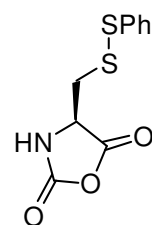
Compound Number: 9c
Cook Code: WYME-STrt
Promentis Code: Pro-058
Chemical Formula: $C_{22}H_{21}NO_2S$
Molecular Weight: 363.47
Log P: 4.39
Prodrug/Bioisostere: Prodrug
Monomer/Dimer: Monomer

 C^{14} Uptake

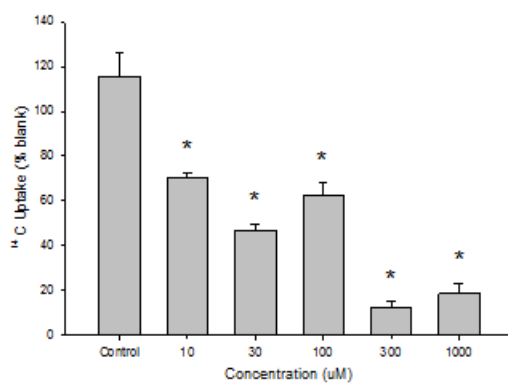
Glutamate Percent Change



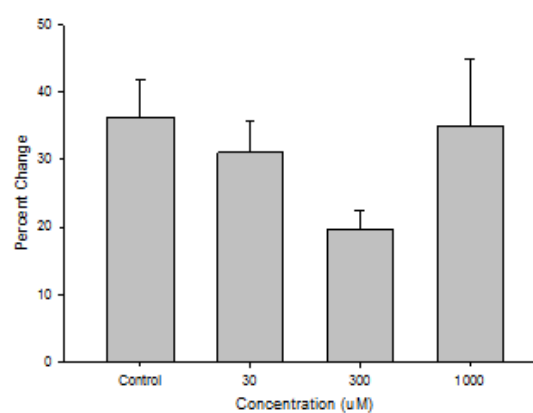
Compound Number: 10b
Cook Code: WYME-SSPh-5
Promentis Code: Pro-045
Chemical Formula: $C_{10}H_9NO_3S_2$
Molecular Weight: 255.31
Log P: 2.29
Prodrug/Bioisostere: Prodrug
Monomer/Dimer: Monomer



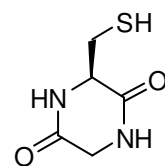
C^{14} Uptake



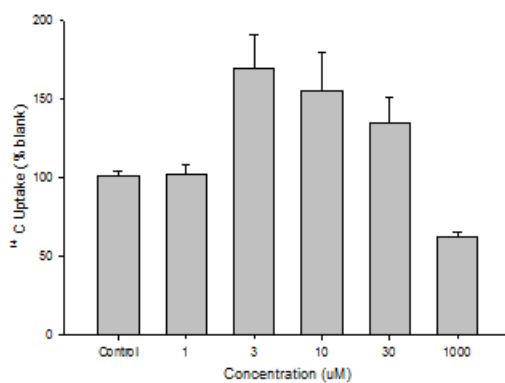
Glutamate Percent Change



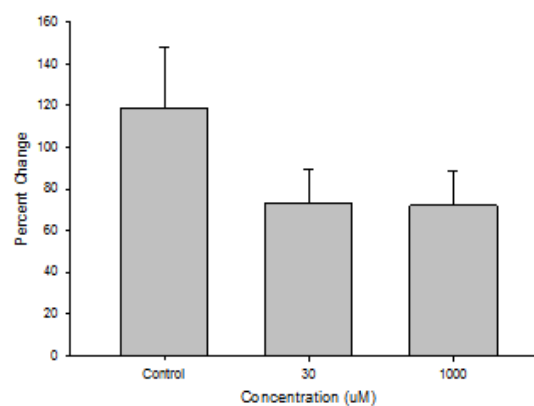
Compound Number: 12a
Cook Code: WYME-SBGH
Promentis Code: Pro-013
Chemical Formula: $C_5H_8N_2O_2S$
Molecular Weight: 160.19
Log P: -1.83
Prodrug/Bioisostere: Prodrug
Monomer/Dimer: Monomer



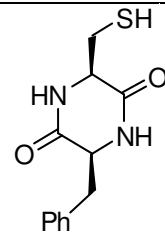
C^{14} Uptake



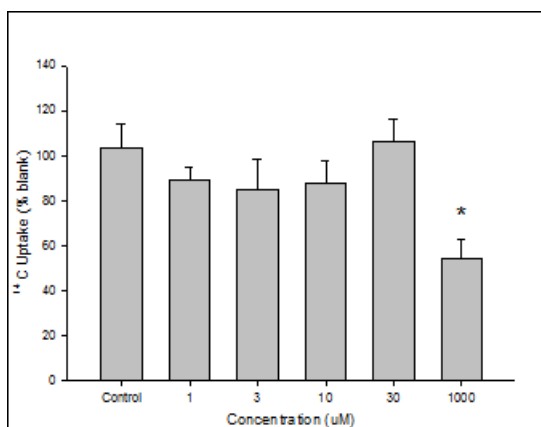
Glutamate Percent Change



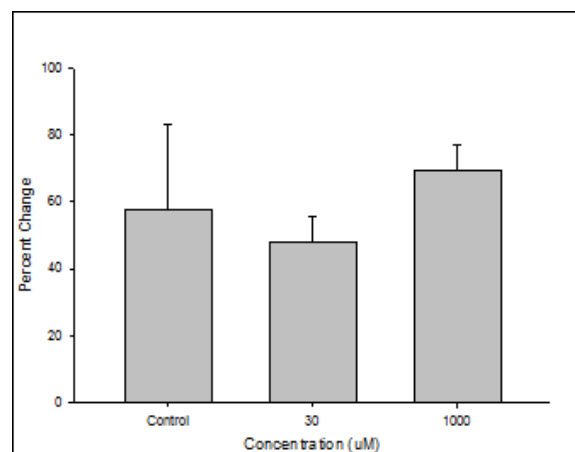
Compound Number: 12c
Cook Code: WYME-SBPh
Promentis Code: Pro-015
Chemical Formula: $C_{12}H_{14}N_2O_2S$
Molecular Weight: 250.32
Log P: 0.34
Prodrug/Bioisostere: Prodrug
Monomer/Dimer: Monomer



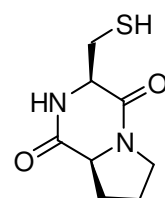
C^{14} Uptake



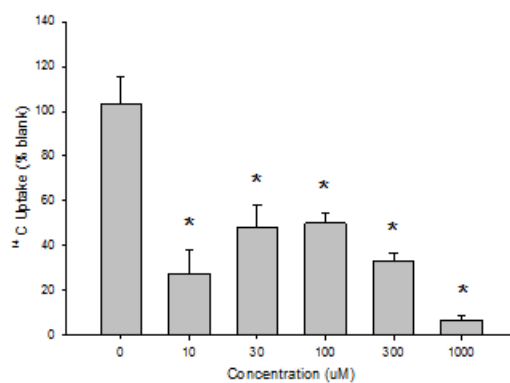
Glutamate Percent Change



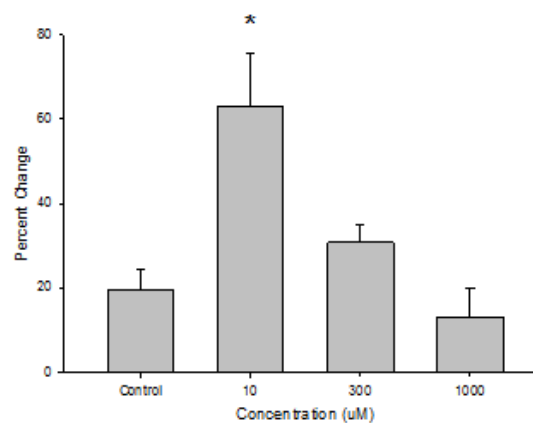
Compound Number: 12d
Cook Code: WYME-SBPr
Promentis Code: Pro-068
Chemical Formula: $C_8H_{12}N_2O_2S$
Molecular Weight: 200.26
Log P: -1.13
Prodrug/Bioisostere: Prodrug
Monomer/Dimer: Monomer



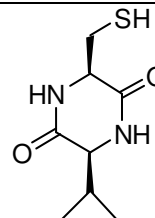
C^{14} Uptake



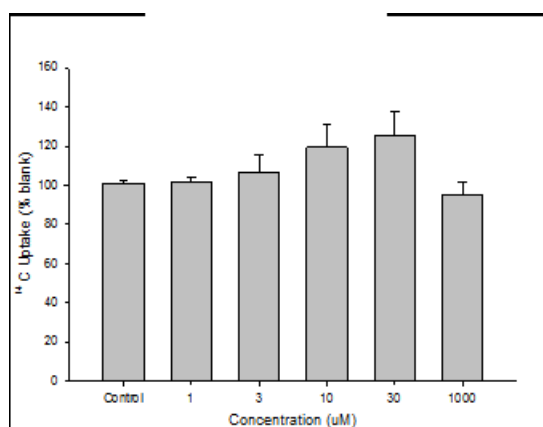
Glutamate Percent Change



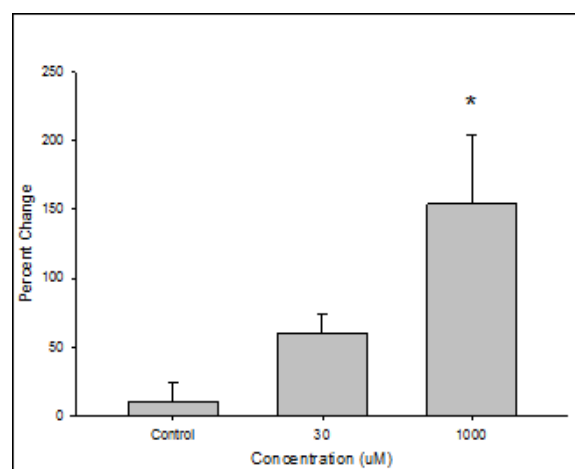
Compound Number: 12e
Cook Code: WYME-SBVa
Promentis Code: Pro-018
Chemical Formula: $C_8H_{14}N_2O_2S$
Molecular Weight: 202.27
Log P: -0.45
Prodrug/Bioisostere: Prodrug
Monomer/Dimer: Monomer



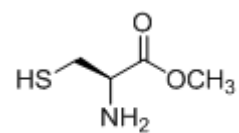
C^{14} Uptake



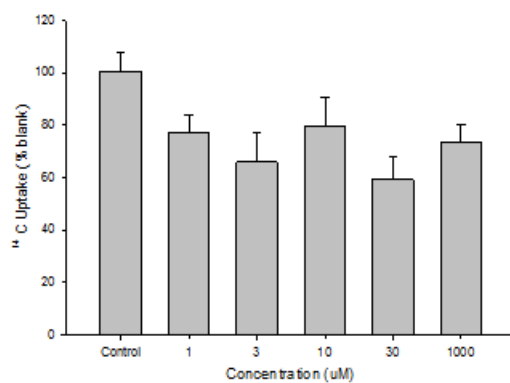
Glutamate Percent Change



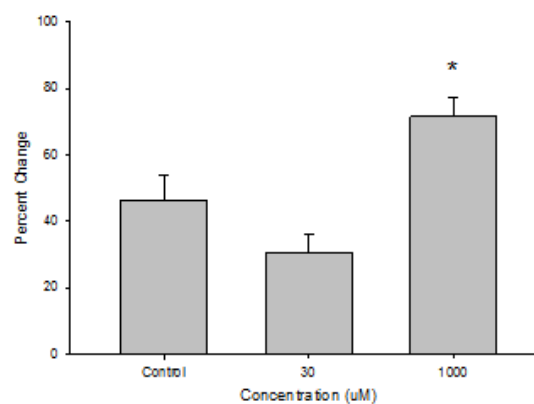
Compound Number: 17
Cook Code: WYME-051407-SM
Promentis Code: Pro-024
Chemical Formula: $C_4H_9NO_2S$
Molecular Weight: 135.18
Log P: -0.66
Prodrug/Bioisostere: Prodrug
Monomer/Dimer: Monomer



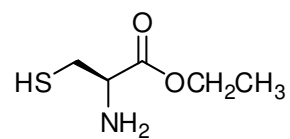
C^{14} Uptake



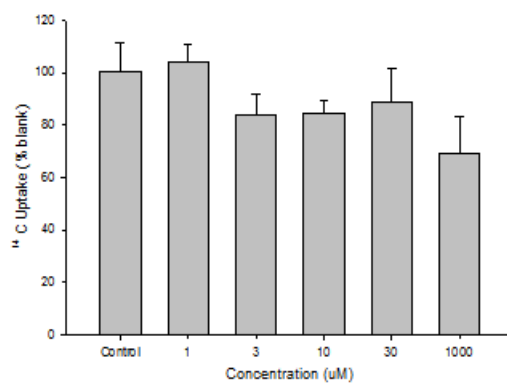
Glutamate Percent Change



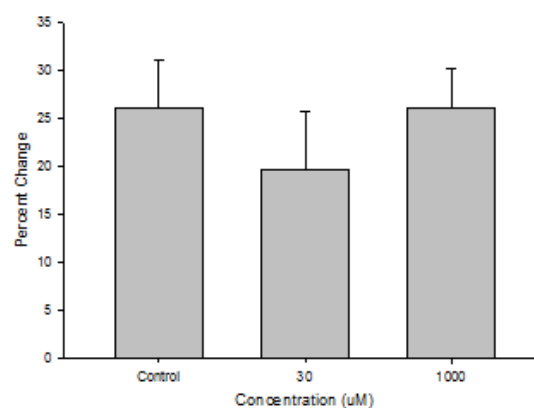
Compound Number: 18
Cook Code: WYME-051707-SE
Promentis Code: Pro-021
Chemical Formula: $C_5H_{11}NO_2S$
Molecular Weight: 149.21
Log P: -0.32
Prodrug/Bioisostere: Prodrug
Monomer/Dimer: Monomer



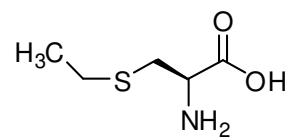
C^{14} Uptake



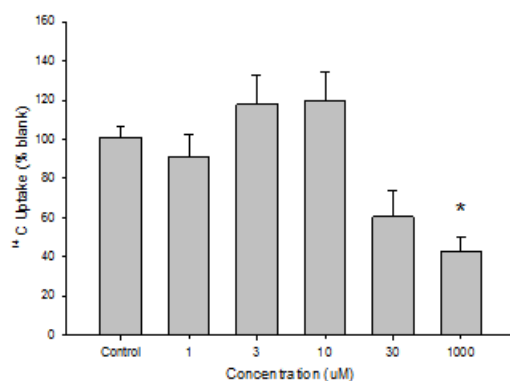
Glutamate Percent Change



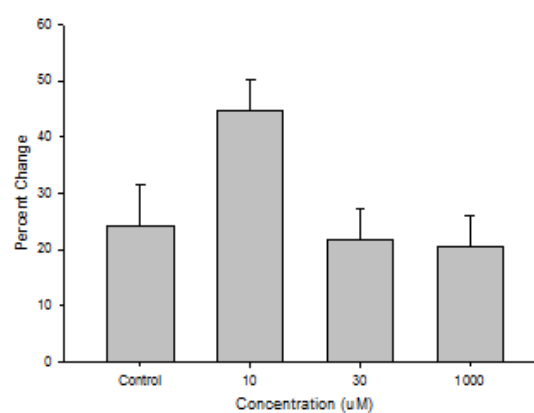
Compound Number: 19
Cook Code: ME-SEt
Promentis Code: Pro-023
Chemical Formula: $C_5H_{11}NO_2S$
Molecular Weight: 149.21
Log P: -0.33
Prodrug/Bioisostere: Prodrug
Monomer/Dimer: Monomer



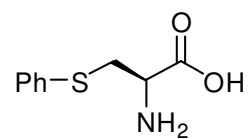
C^{14} Uptake



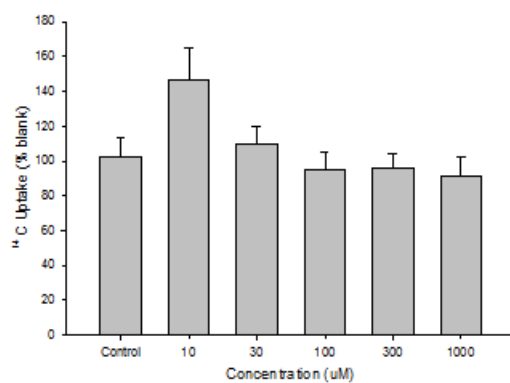
Glutamate Percent Change



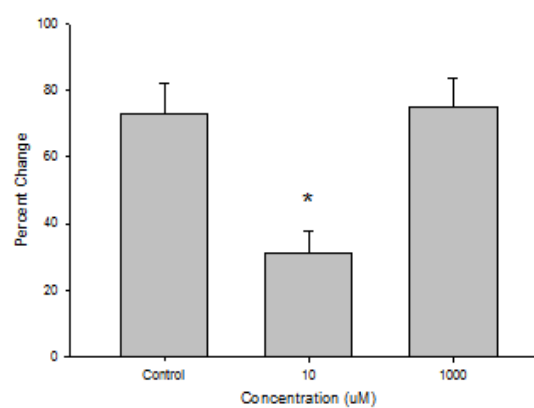
Compound Number: 20
Cook Code: ME-SPh
Promentis Code: Pro-027
Chemical Formula: $C_9H_{11}NO_2S$
Molecular Weight: 197.25
Log P: 1.0
Prodrug/Bioisostere: Prodrug
Monomer/Dimer: Monomer



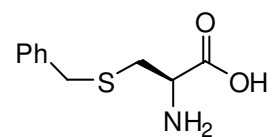
C^{14} Uptake



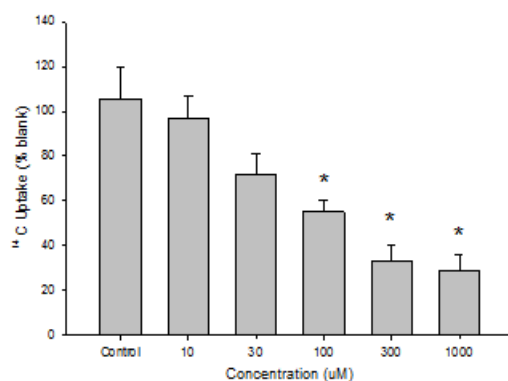
Glutamate Percent Change



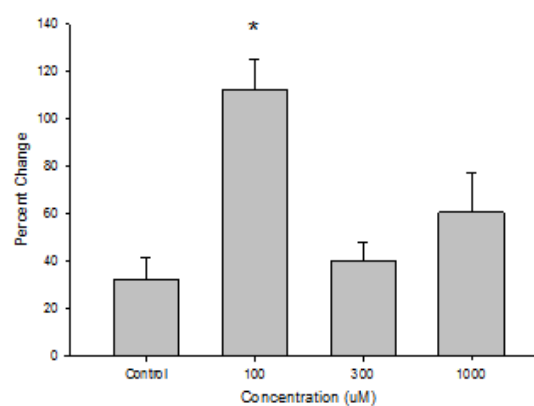
Compound Number: 21
Cook Code: ME-SBZY
Promentis Code: Pro-020
Chemical Formula: $C_{10}H_{13}NO_2S$
Molecular Weight: 211.28
Log P: 1.07
Prodrug/Bioisostere: Prodrug
Monomer/Dimer: Monomer



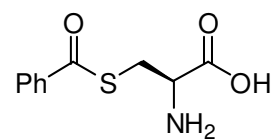
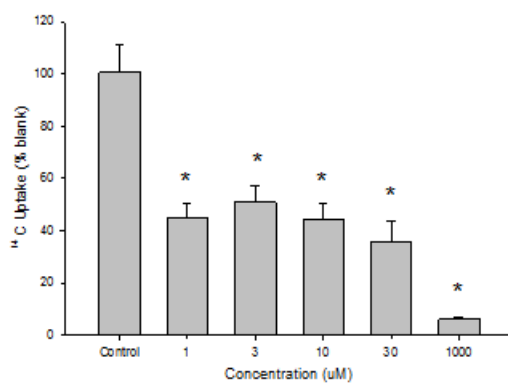
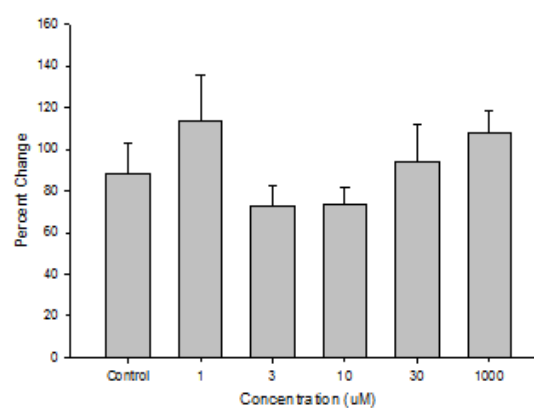
C^{14} Uptake



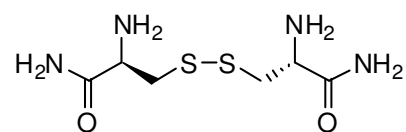
Glutamate Percent Change



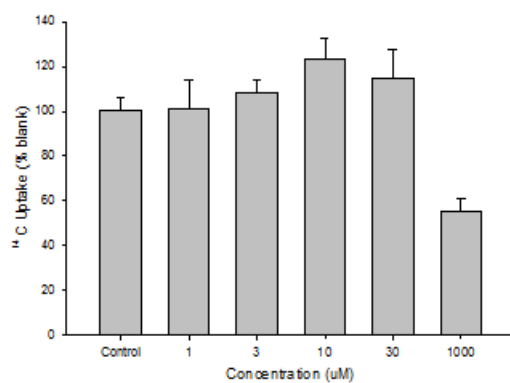
Compound Number: 22
Cook Code: WYME-SPhCO
Promentis Code: Pro-029
Chemical Formula:
Molecular Weight: 225.26
Log P: 0.94
Prodrug/Bioisostere: Prodrug
Monomer/Dimer: Monomer

**C¹⁴ Uptake****Glutamate Percent Change**

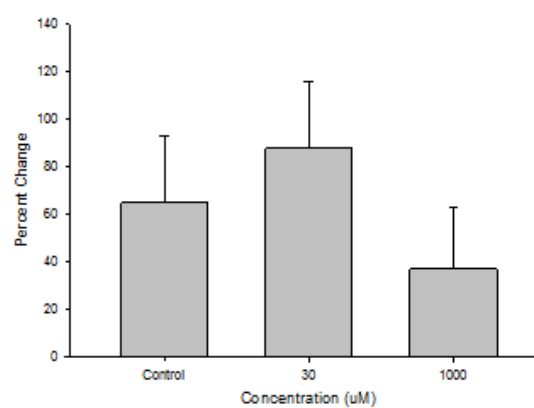
Compound Number: 23
Cook Code: WYME-SS-am
Promentis Code: Pro-032
Chemical Formula: $C_6H_{14}N_4O_2S_2$
Molecular Weight: 238.33
Log P: -2.69
Prodrug/Bioisostere: Prodrug
Monomer/Dimer: Dimer



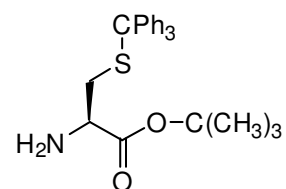
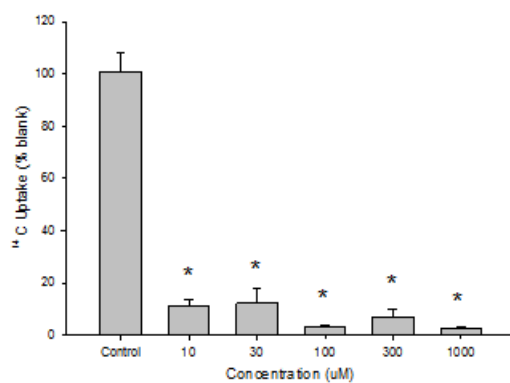
C^{14} Uptake



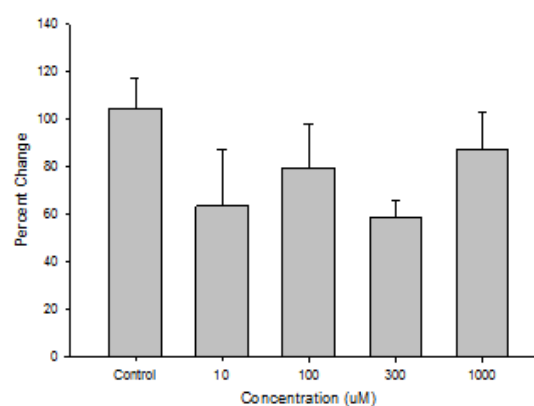
Glutamate Percent Change



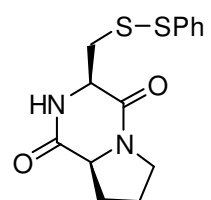
Compound Number: 24
Cook Code: WYME-ST-tBu
Promentis Code: Pro-061
Chemical Formula: $C_{26}H_{29}NO_2S$
Molecular Weight: 419.58
Log P: 5.53
Prodrug/Bioisostere: Prodrug
Monomer/Dimer: Monomer

 C^{14} Uptake

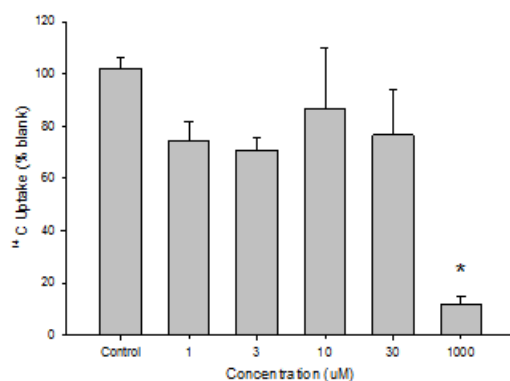
Glutamate Percent Change



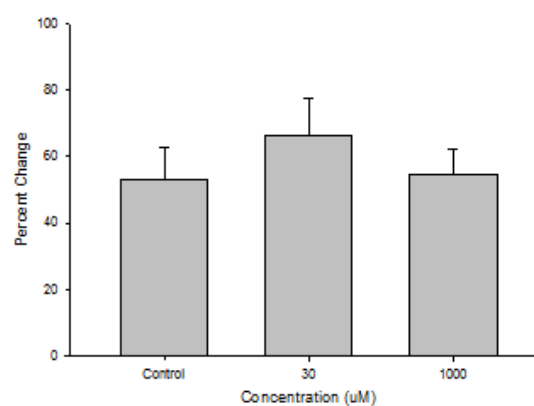
Compound Number: 25
Cook Code: WYME-SBPr6
Promentis Code: Pro-016
Chemical Formula: $C_{14}H_{16}N_2O_2S_2$
Molecular Weight: 308.42
Log P: 1.55
Prodrug/Bioisostere: Prodrug
Monomer/Dimer: Monomer



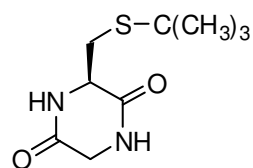
C^{14} Uptake



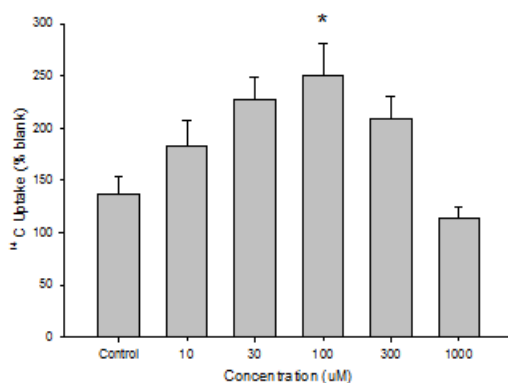
Glutamate Percent Change



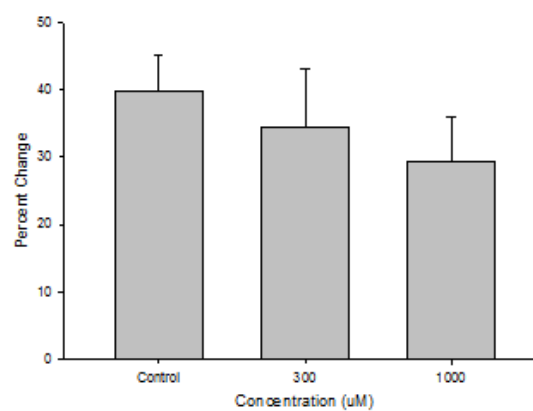
Compound Number: 26
 Cook Code: ME-StBu-6
 Promentis Code: Pro-049
 Chemical Formula: $C_9H_{16}N_2O_2S$
 Molecular Weight: 216.3
 Log P: -0.7
 Prodrug/Bioisostere: Prodrug
 Monomer/Dimer: Monomer



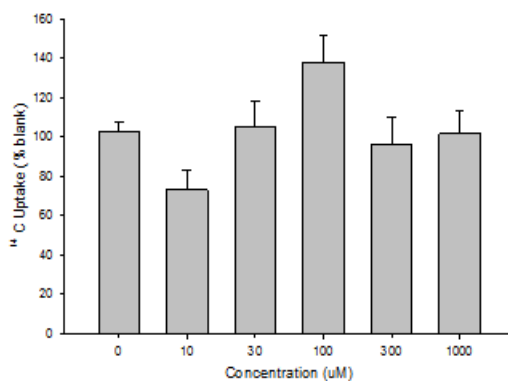
C^{14} Uptake



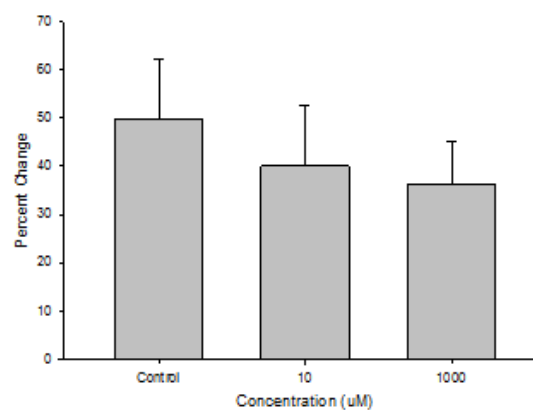
Glutamate Percent Change



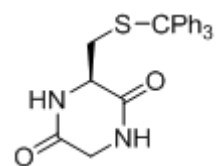
C^{14} Uptake



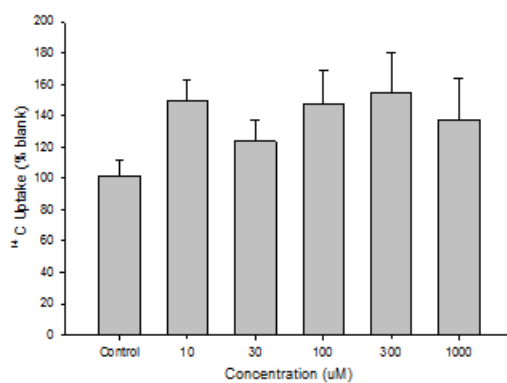
Glutamate Percent Change



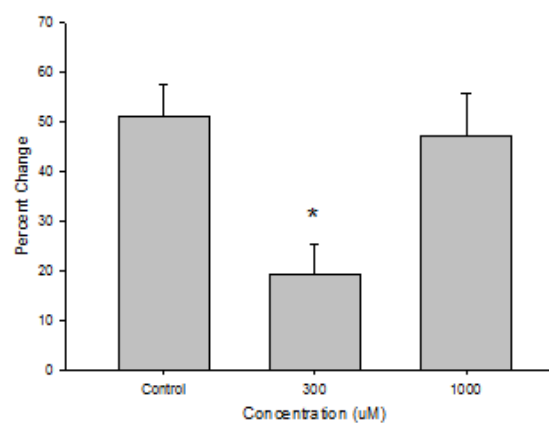
Compound Number: 27
Cook Code: WYME-ST-G6
Promentis Code: Pro-051
Chemical Formula: $C_{24}H_{22}N_2O_2S$
Molecular Weight: 402.51
Log P: 3.48
Prodrug/Bioisostere: Prodrug
Monomer/Dimer: Monomer



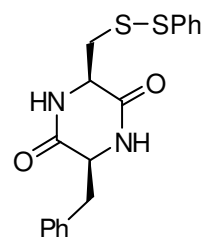
C^{14} Uptake



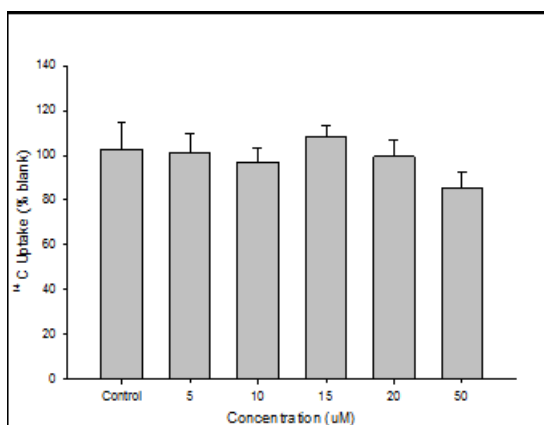
Glutamate Percent Change



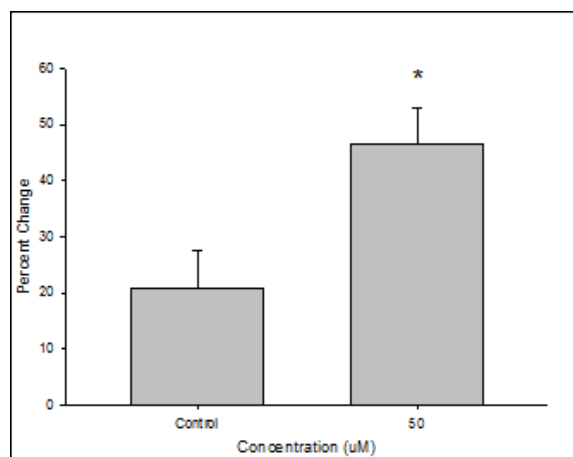
Compound Number: 28
 Cook Code: WyME-SB-P6
 Promentis Code: Pro-014
 Chemical Formula: $C_{18}H_{18}N_2O_2S_2$
 Molecular Weight: 358.48
 Log P: 3.01
 Prodrug/Bioisostere: Prodrug
 Monomer/Dimer: Monomer



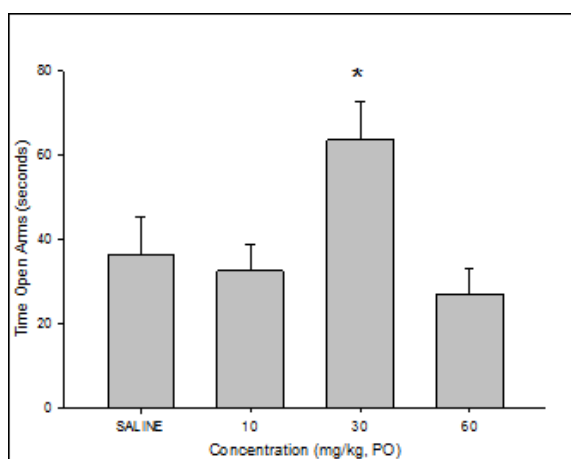
C^{14} Uptake



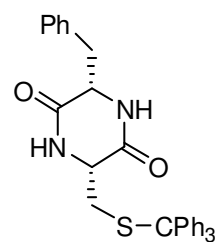
Glutamate Percent Change



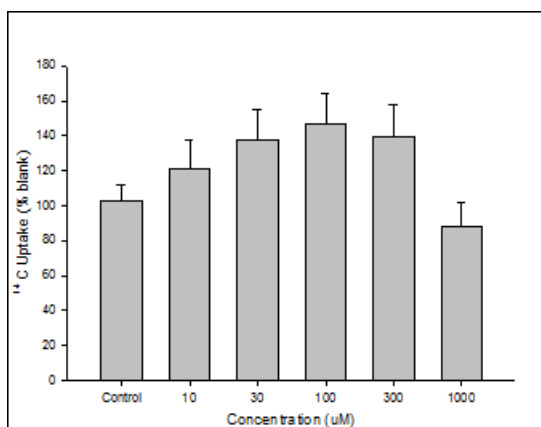
Elevated Plus Maze



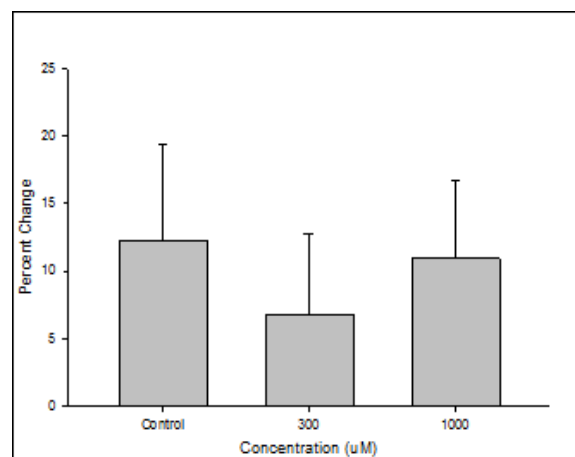
Compound Number: 29
Cook Code: WyME-ST-P6
Promentis Code: Pro-055
Chemical Formula: $C_{31}H_{28}N_2O_2S$
Molecular Weight: 492.63
Log P: 5.65
Prodrug/Bioisostere: Prodrug
Monomer/Dimer: Monomer



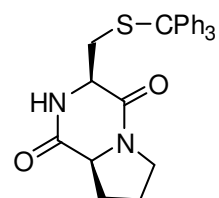
C^{14} Uptake



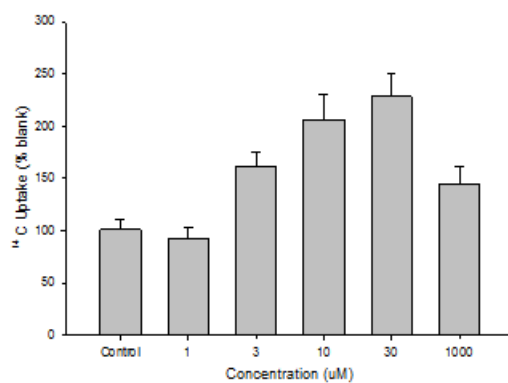
Glutamate Percent Change



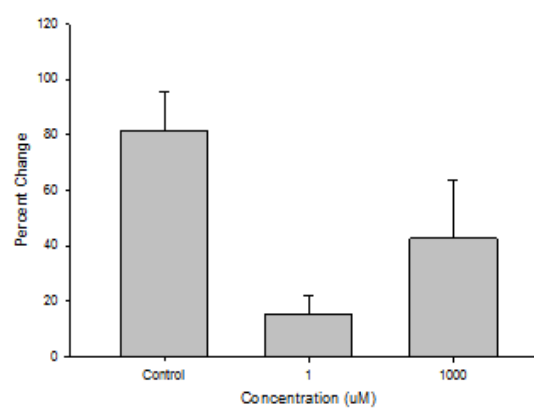
Compound Number: 30
Cook Code: WYME-ST-Pr
Promentis Code: Pro-057
Chemical Formula: $C_{27}H_{26}N_2O_2S$
Molecular Weight: 442.57
Log P: 4.19
Prodrug/Bioisostere: Prodrug
Monomer/Dimer: Monomer



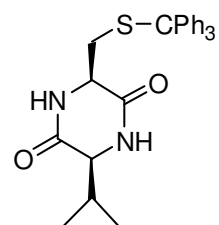
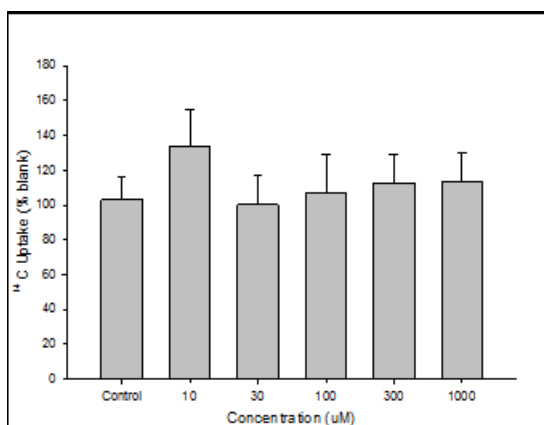
C^{14} Uptake



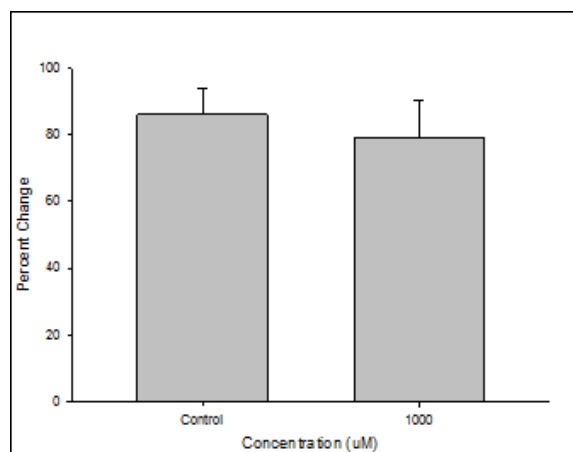
Glutamate Percent Change



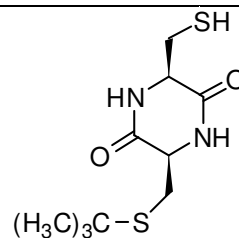
Compound Number: 31
Cook Code: WYME-ST-V6
Promentis Code: Pro-062
Chemical Formula: $C_{27}H_{28}N_2O_2S$
Molecular Weight: 444.59
Log P: 4.86
Prodrug/Bioisostere: Prodrug
Monomer/Dimer: Monomer

 C^{14} Uptake

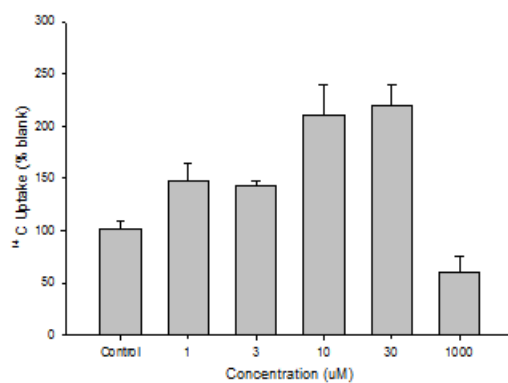
Glutamate Percent Change



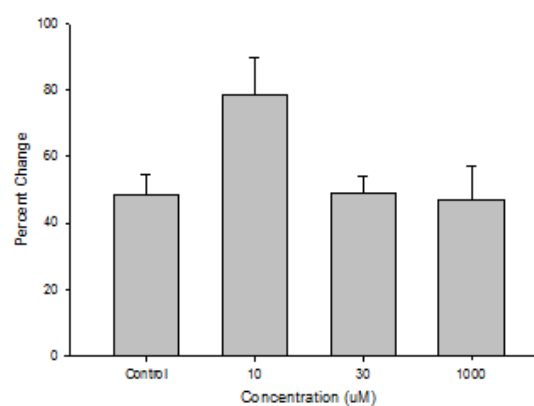
Compound Number: 32
Cook Code: WYME-SBSS
Promentis Code: Pro-017
Chemical Formula: $C_{10}H_{18}N_2O_2S_2$
Molecular Weight: 262.39
Log P: -0.24
Prodrug/Bioisostere: Prodrug
Monomer/Dimer: Monomer



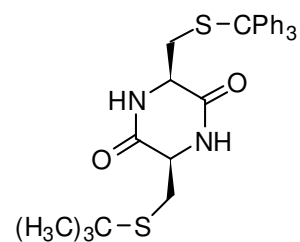
C^{14} Uptake



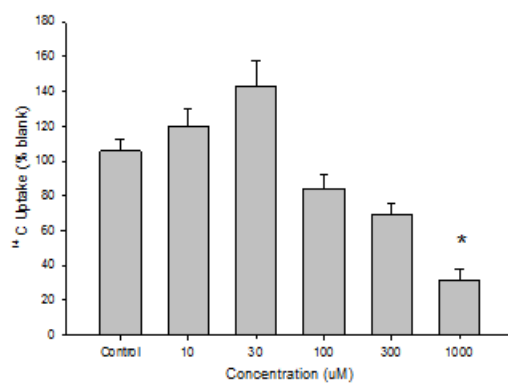
Glutamate Percent Change



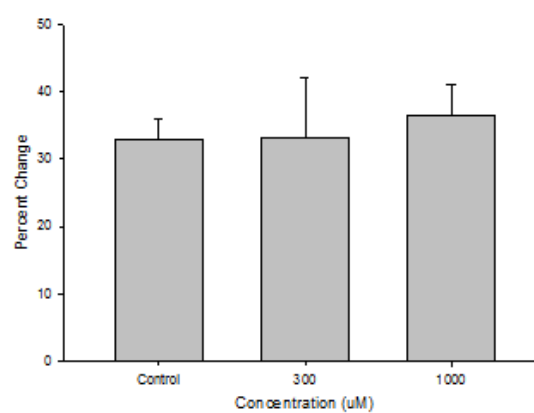
Compound Number: 33
Cook Code: WYME-ST-S6
Promentis Code: Pro-059
Chemical Formula: $C_{29}H_{32}N_2O_2S_2$
Molecular Weight: 504.71
Log P: 5.08
Prodrug/Bioisostere: Prodrug
Monomer/Dimer: Monomer



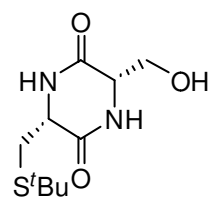
C^{14} Uptake



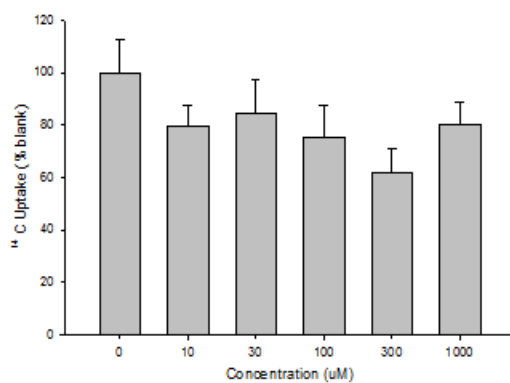
Glutamate Percent Change



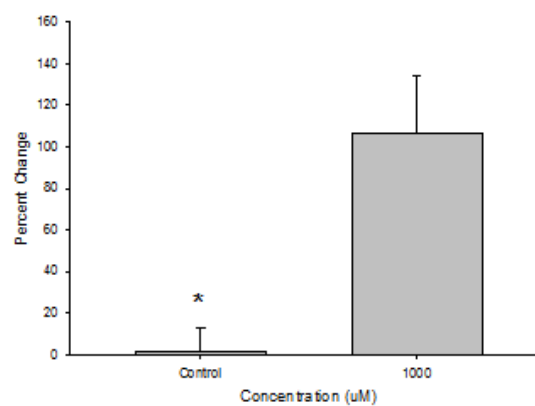
Compound Number: 34
Cook Code: N/A
Promentis Code: Pro-1036
Chemical Formula: $C_{10}H_{18}N_2O_3S$
Molecular Weight: 246.33
Log P: -1.07
Prodrug/Bioisostere: Prodrug
Monomer/Dimer: Monomer



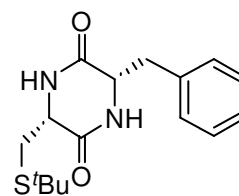
C^{14} Uptake



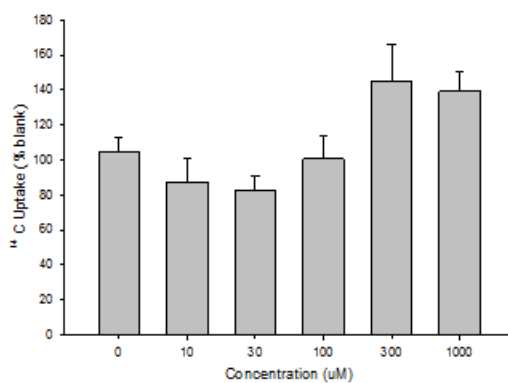
Glutamate Percent Change



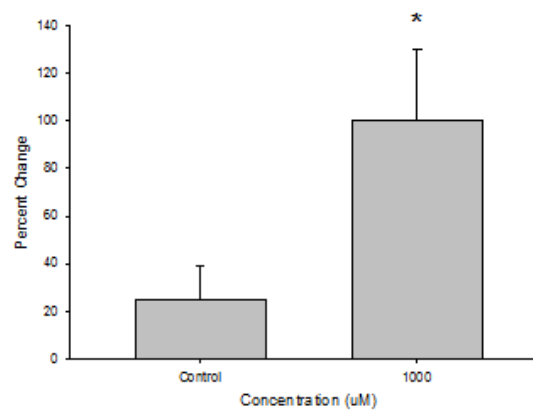
Compound Number: 35
Cook Code: N/A
Promentis Code: Pro-1038
Chemical Formula: $C_{16}H_{22}N_2O_2S$
Molecular Weight: 306.42
Log P: 1.46
Prodrug/Bioisostere: Prodrug
Monomer/Dimer: Monomer



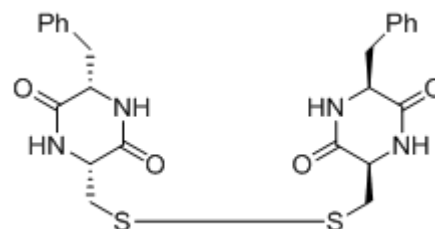
C^{14} Uptake



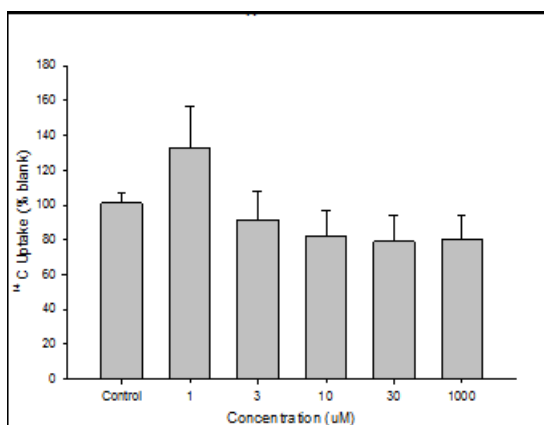
Glutamate Percent Change



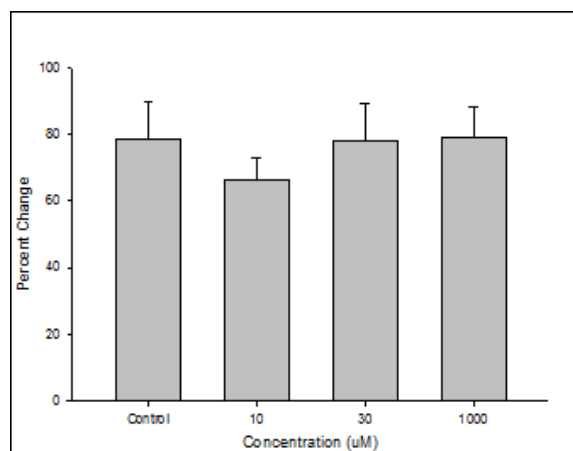
Compound Number: 36
Cook Code: WyME-ST-PP
Promentis Code: Pro-056
Chemical Formula: $C_{24}H_{26}N_4O_4S_2$
Molecular Weight: 498.62
Log P: 1.13
Prodrug/Bioisostere: Prodrug
Monomer/Dimer: Dimer



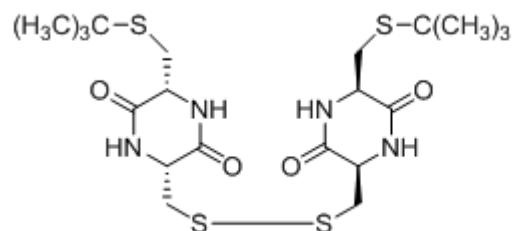
C^{14} Uptake



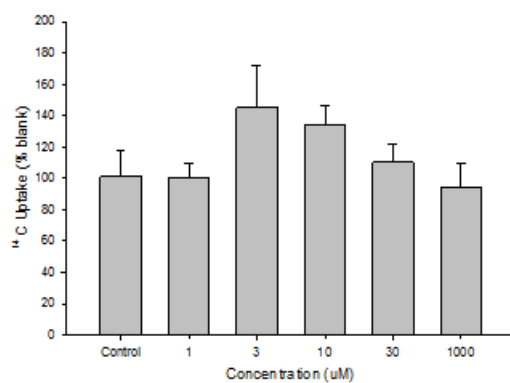
Glutamate Percent Change



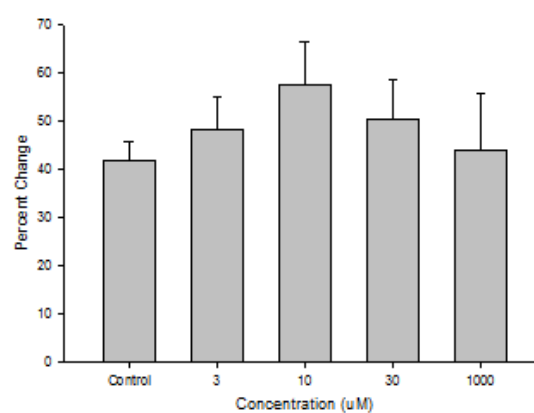
Compound Number: 37
 Cook Code: WYME-ST-SS
 Promentis Code: Pro-060
 Chemical Formula: $C_{20}H_{34}N_4O_4S_4$
 Molecular Weight: 522.77
 Log P: -0.01
 Prodrug/Bioisostere: Prodrug
 Monomer/Dimer: Dimer



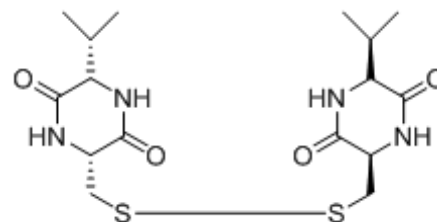
C^{14} Uptake



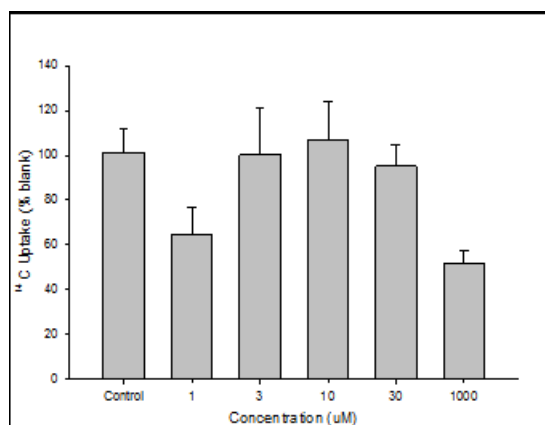
Glutamate Percent Change



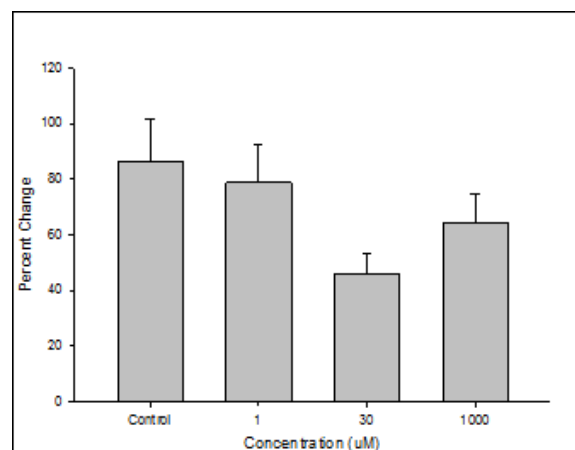
Compound Number: 38
Cook Code: WYME-ST-VV
Promentis Code: Pro-064
Chemical Formula: $C_{16}H_{26}N_4O_4S_2$
Molecular Weight: 402.53
Log P: -0.45
Prodrug/Bioisostere: Prodrug
Monomer/Dimer: Dimer



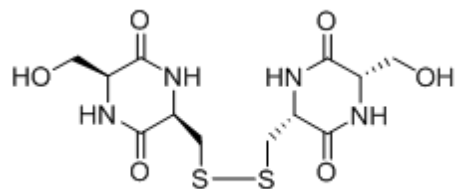
C^{14} Uptake



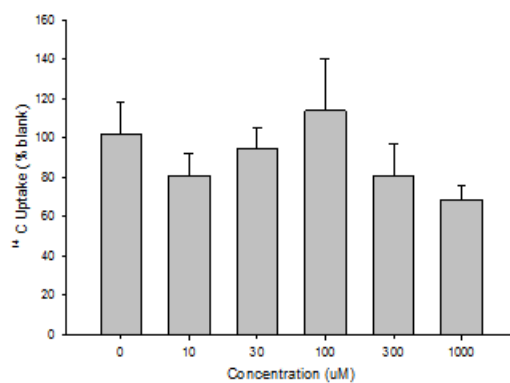
Glutamate Percent Change



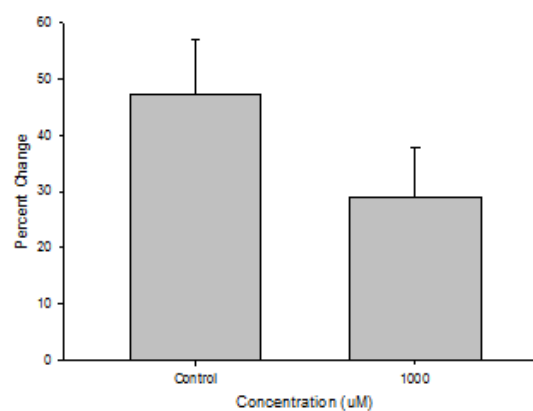
Compound Number: 39
Cook Code: N/A
Promentis Code: Pro-1016
Chemical Formula: $C_{12}H_{18}N_4O_6S_2$
Molecular Weight: 378.42
Log P: -3.93
Prodrug/Bioisostere: Prodrug
Monomer/Dimer: Dimer



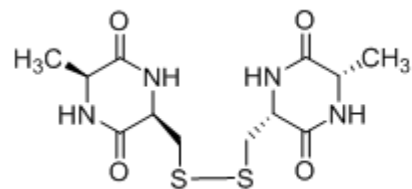
C^{14} Uptake



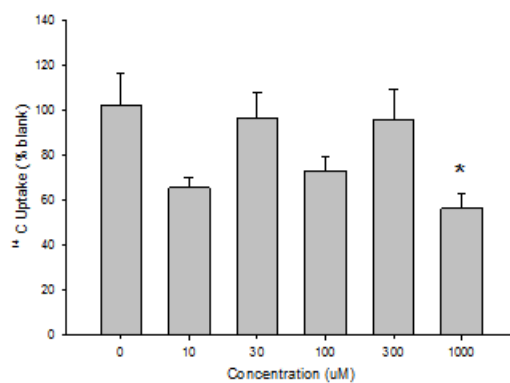
Glutamate Percent Change



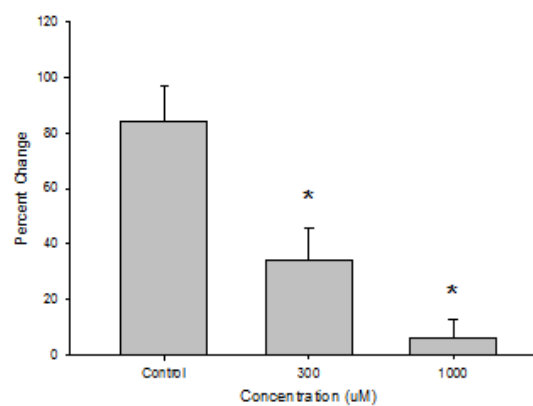
Compound Number: 40
Cook Code: N/A
Promentis Code: Pro-1022
Chemical Formula: $C_{12}H_{18}N_4O_4S_2$
Molecular Weight: 346.43
Log P: -2.22
Prodrug/Bioisostere: Prodrug
Monomer/Dimer: Dimer



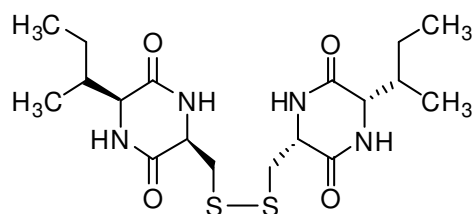
C^{14} Uptake



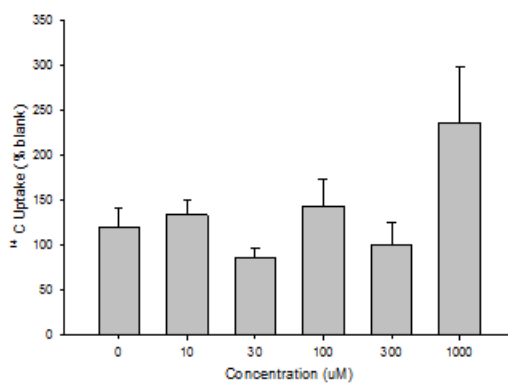
Glutamate Percent Change



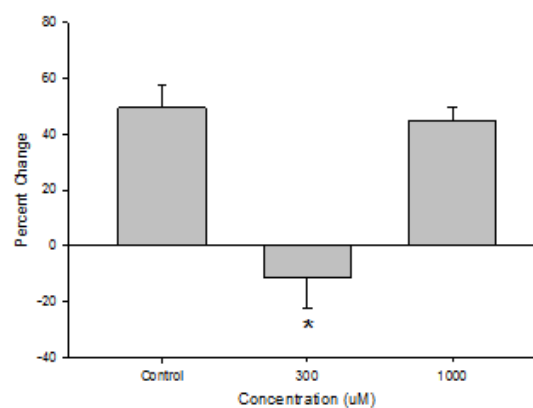
Compound Number: 41
Cook Code: N/A
Promentis Code: Pro-1024
Chemical Formula: $C_{18}H_{30}N_4O_4S_2$
Molecular Weight: 430.59
Log P: 0.39
Prodrug/Bioisostere: Prodrug
Monomer/Dimer: Dimer



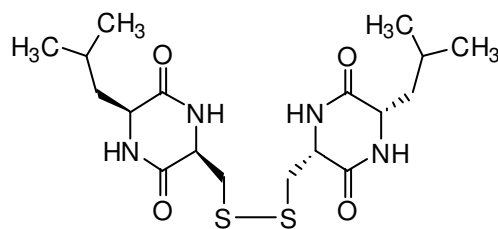
C^{14} Uptake



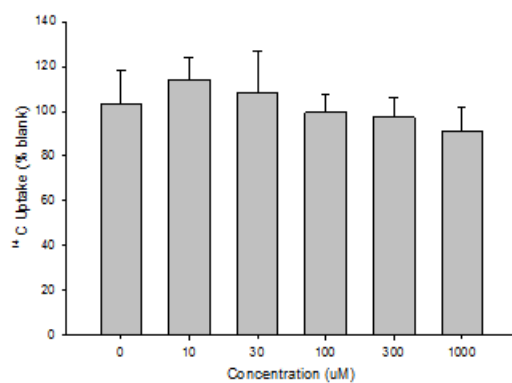
Glutamate Percent Change



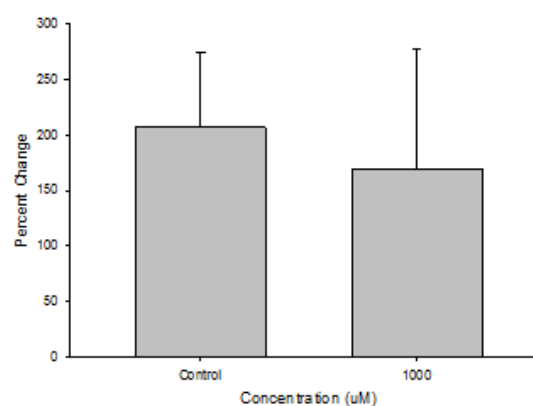
Compound Number: 42
Cook Code: N/A
Promentis Code: Pro-1025
Chemical Formula: $C_{18}H_{30}N_4O_4S_2$
Molecular Weight: 430.59
Log P: 0.25
Prodrug/Bioisostere: Prodrug
Monomer/Dimer: Dimer



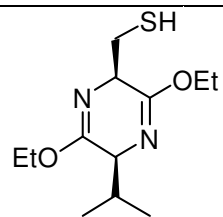
C^{14} Uptake



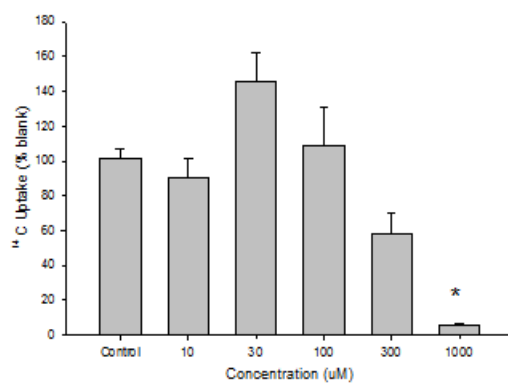
Glutamate Percent Change



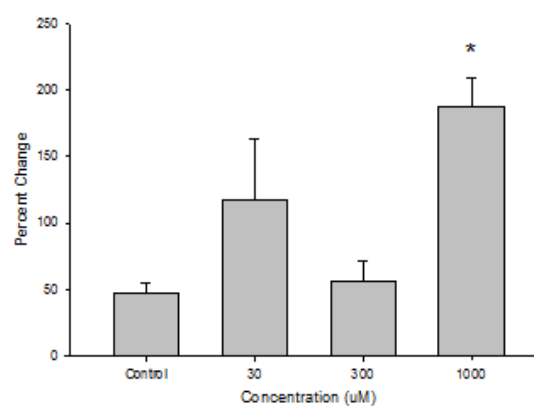
Compound Number: 43
Cook Code: WYME-BFVa
Promentis Code: Pro-005
Chemical Formula: $C_{12}H_{33}N_2O_2S$
Molecular Weight: 258.38
Log P: 2.49
Prodrug/Bioisostere: Prodrug
Monomer/Dimer: Monomer



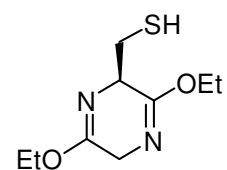
C^{14} Uptake



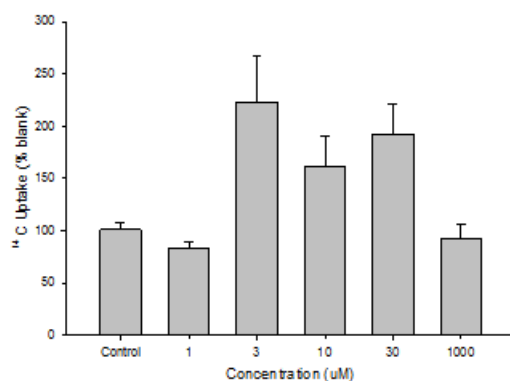
Glutamate Percent Change



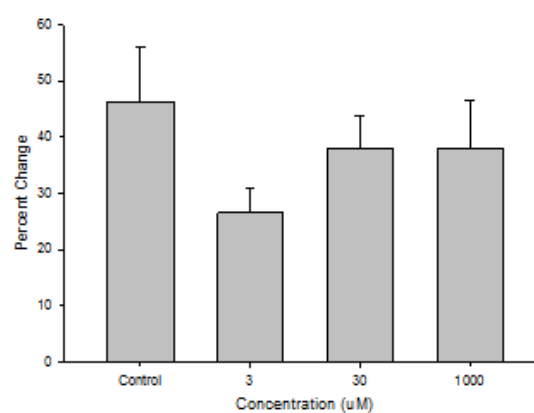
Compound Number: 44
Cook Code: WYME-0625-SBBFGE
Promentis Code: Pro-011
Chemical Formula: $C_9H_{16}N_2O_2S$
Molecular Weight: 216.3
Log P: 1.12
Prodrug/Bioisostere: Prodrug
Monomer/Dimer: Monomer



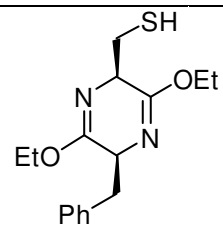
C^{14} Uptake



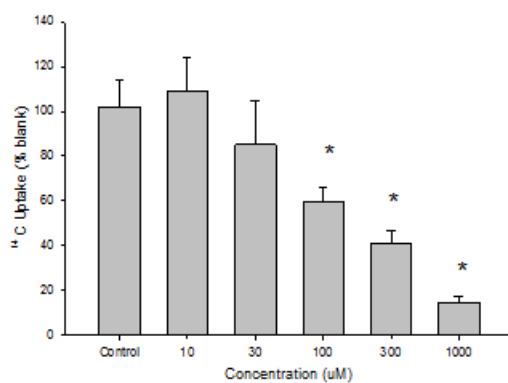
Glutamate Percent Change



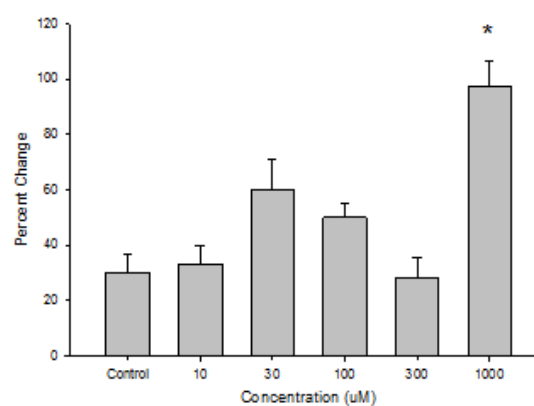
Compound Number: 45
Cook Code: WYME-BFPh
Promentis Code: Pro-004
Chemical Formula: $C_{16}H_{22}N_2O_2S$
Molecular Weight: 306.42
Log P: 3.28
Prodrug/Bioisostere: Prodrug
Monomer/Dimer: Monomer



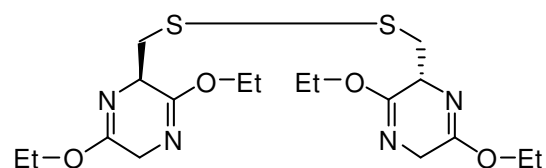
C^{14} Uptake



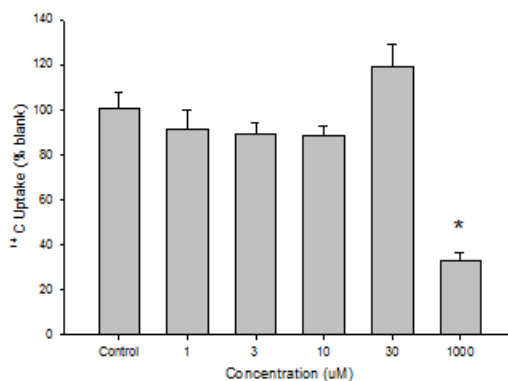
Glutamate Percent Change



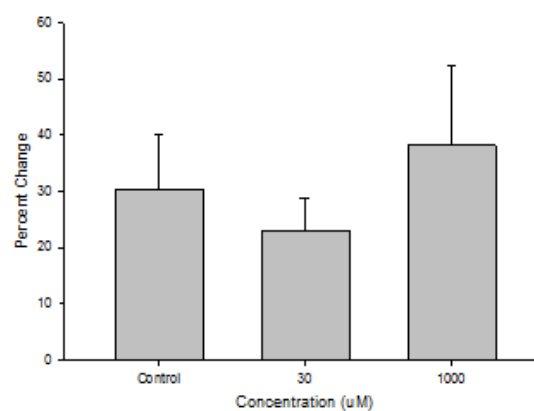
Compound Number: 46
 Cook Code: WYME-SBB-FGL
 Promentis Code: Pro-012
 Chemical Formula: $C_{18}H_{30}N_4O_4S_2$
 Molecular Weight: 430.59
 Log P: 2.69
 Prodrug/Bioisostere: Prodrug
 Monomer/Dimer: Dimer



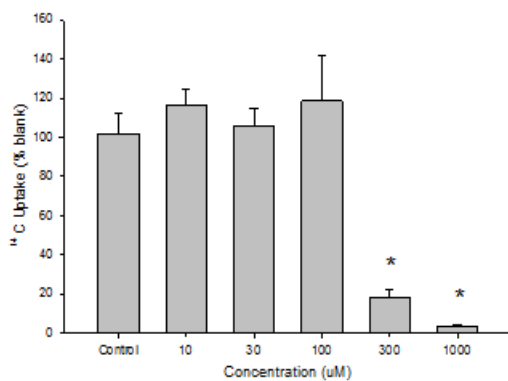
C^{14} Uptake



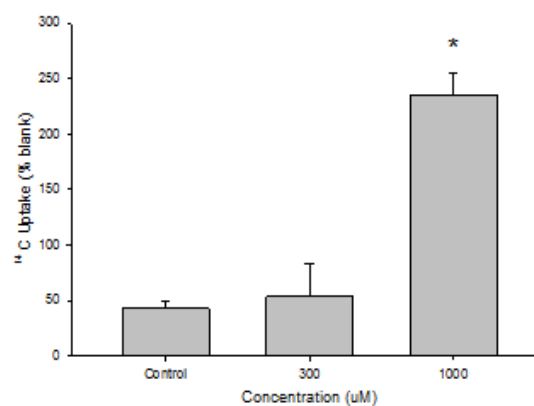
Glutamate Percent Change



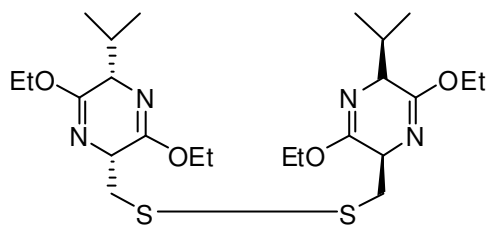
C^{14} Uptake



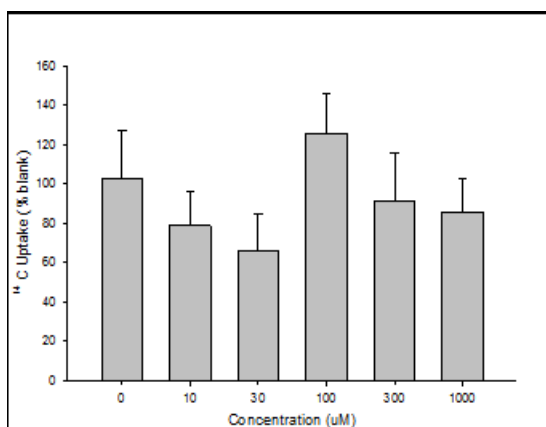
Glutamate Percent Change



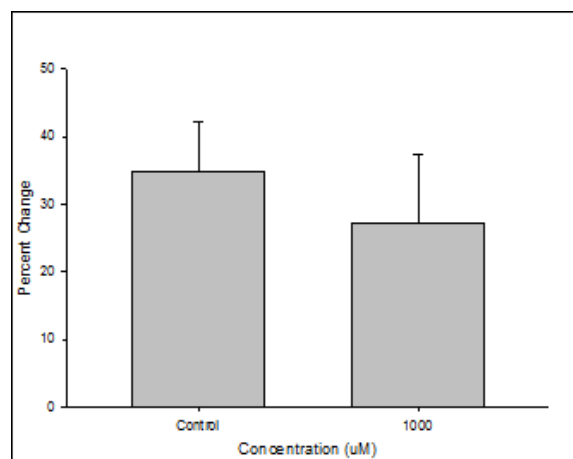
Compound Number: 47
Cook Code: WYME-SSB-FVV
Promentis Code: Pro-065
Chemical Formula: $C_{24}H_{42}N_4O_4S_2$
Molecular Weight: 514.74
Log P: 5.44
Prodrug/Bioisostere: Prodrug
Monomer/Dimer: Dimer



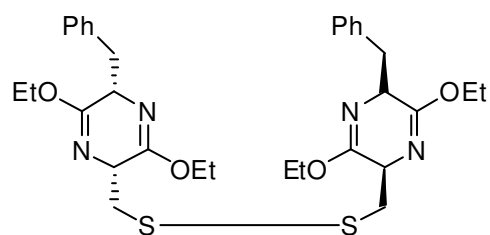
C^{14} Uptake



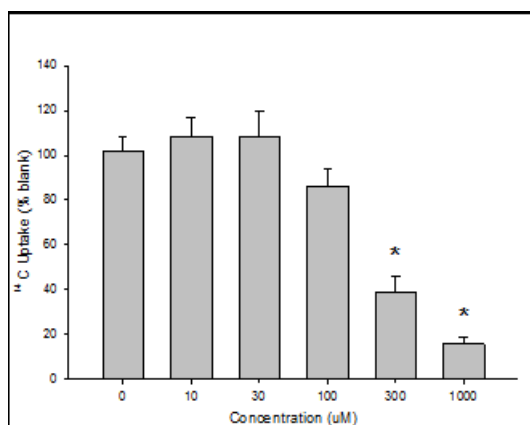
Glutamate Percent Change



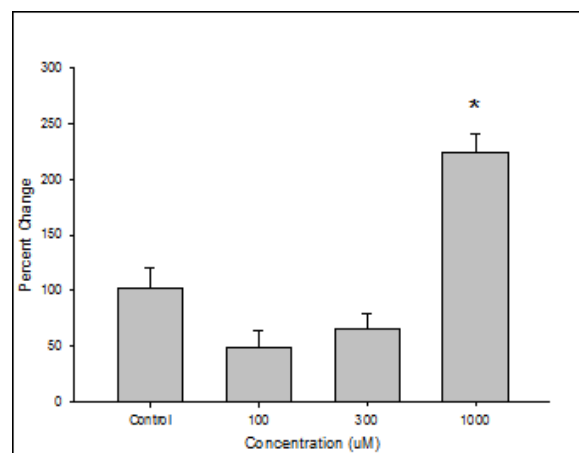
Compound Number: 48
Cook Code: WYME-SSB-FPP
Promentis Code: Pro-066
Chemical Formula: $C_{32}H_{42}N_4O_4S_2$
Molecular Weight: 610.83
Log P: 7.02
Prodrug/Bioisostere: Prodrug
Monomer/Dimer: Dimer



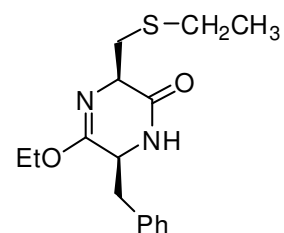
C^{14} Uptake



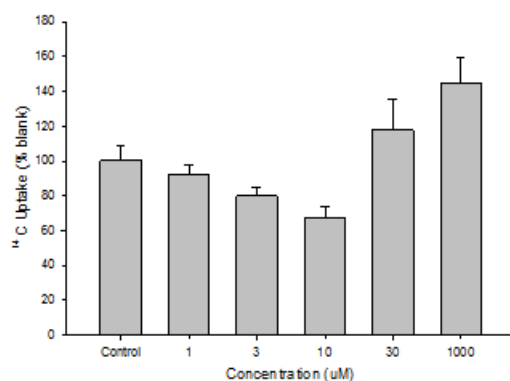
Glutamate Percent Change



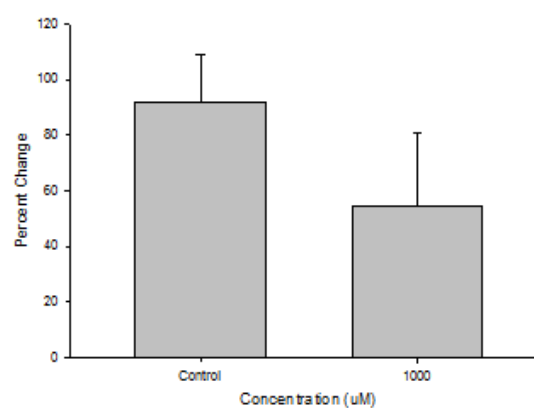
Compound Number: 49
Cook Code: WYME-STBF-PhM
Promentis Code: Pro-047
Chemical Formula: $C_{16}H_{22}N_2O_2S$
Molecular Weight: 306.42
Log P: 2.4
Prodrug/Bioisostere: Prodrug
Monomer/Dimer: Monomer



C^{14} Uptake



Glutamate Percent Change



Compound Number: 50

Cook Code: WYME-SH-NPh6

Promentis Code: Pro-080

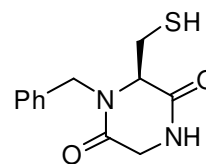
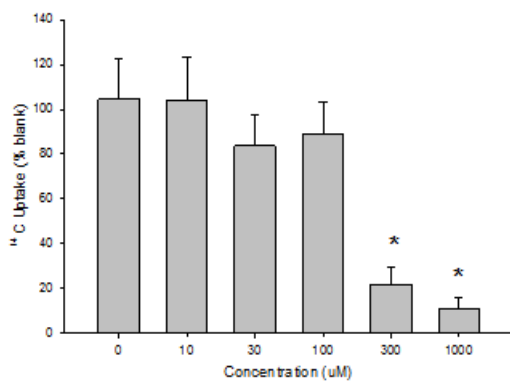
Chemical Formula: $C_{12}H_{14}N_2O_2S$

Molecular Weight: 250.32

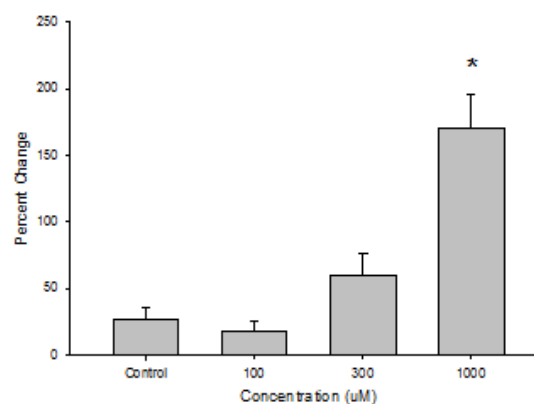
Log P: 0.14

Prodrug/Bioisostere: Prodrug

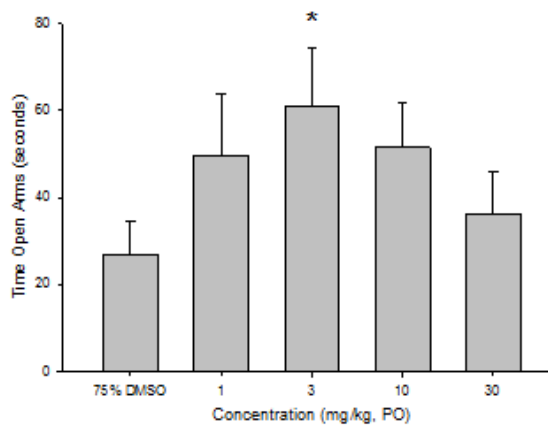
Monomer/Dimer: Monomer

 C^{14} Uptake

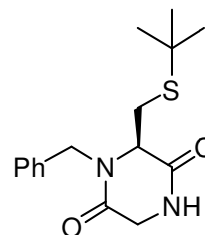
Glutamate Percent Change



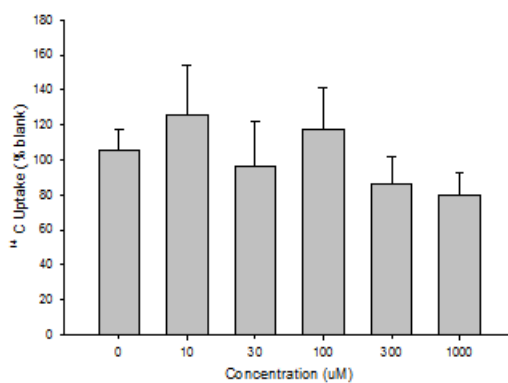
Elevated Plus Maze



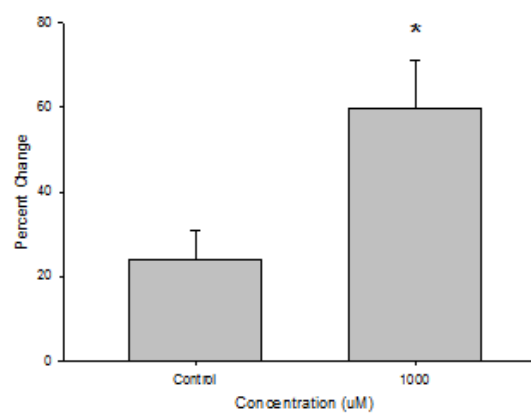
Compound Number: 51
Cook Code: WYME-ST-N6
Promentis Code: Pro-071
Chemical Formula: $C_{16}H_{22}N_2O_2S$
Molecular Weight: 306.4
Log P: 1.27
Prodrug/Bioisostere: Prodrug
Monomer/Dimer: Monomer



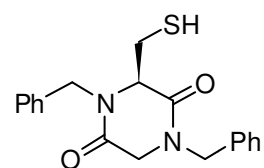
C^{14} Uptake



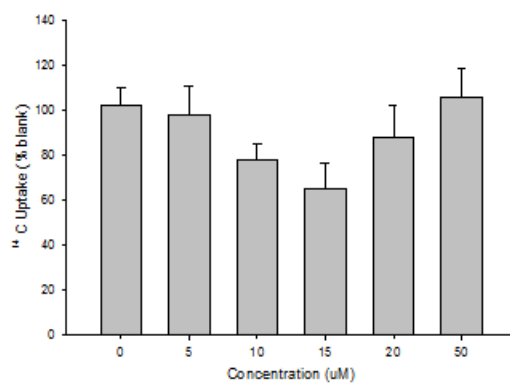
Glutamate Percent Change



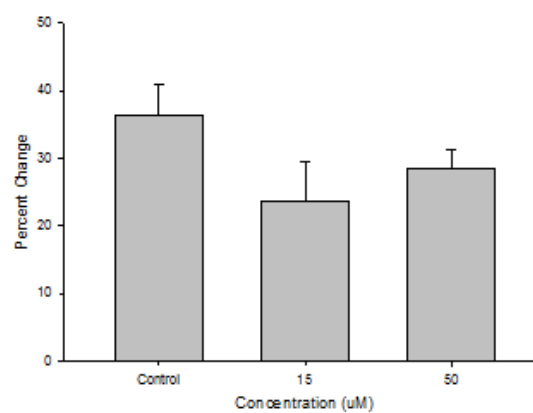
Compound Number: 52
Cook Code: WYME-SB-GH6NPh
Promentis Code: Pro-084
Chemical Formula: $C_{19}H_{20}N_2O_2S$
Molecular Weight: 340.4
Log P: 2.11
Prodrug/Bioisostere: Prodrug
Monomer/Dimer: Monomer



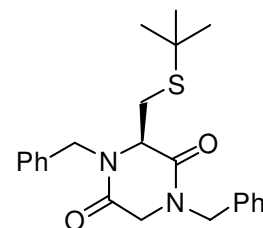
C^{14} Uptake



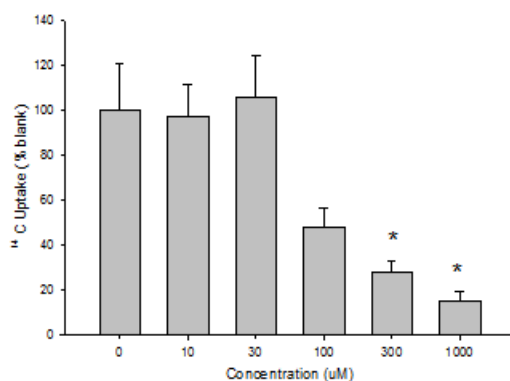
Glutamate Percent Change



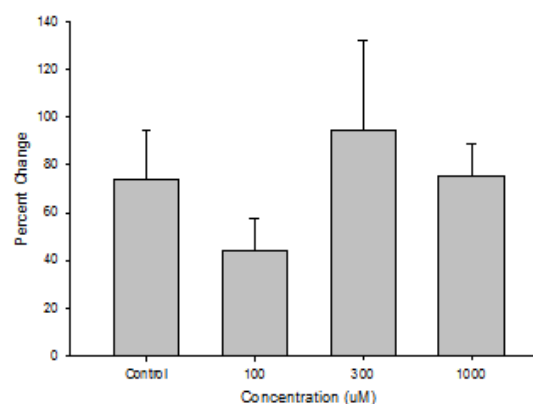
Compound Number: 53
 Cook Code: WYME-ST-N2Ph
 Promentis Code: Pro-092
 Chemical Formula: $C_{23}H_{28}N_2O_2S$
 Molecular Weight: 396.5
 Log P: 3.23
 Prodrug/Bioisostere: Prodrug
 Monomer/Dimer: Monomer



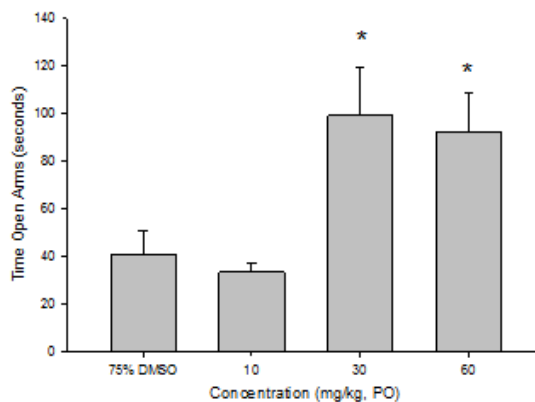
C^{14} Uptake



Glutamate Percent Change



Elevated Plus Maze



Compound Number: 60e

Cook Code: WYME-SS-NPh4N

Promentis Code: Pro-079

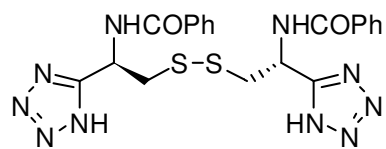
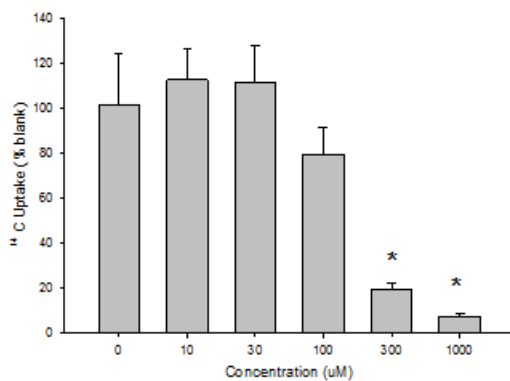
Chemical Formula: $C_{20}H_{20}N_{10}O_2S_2$

Molecular Weight: 496.57

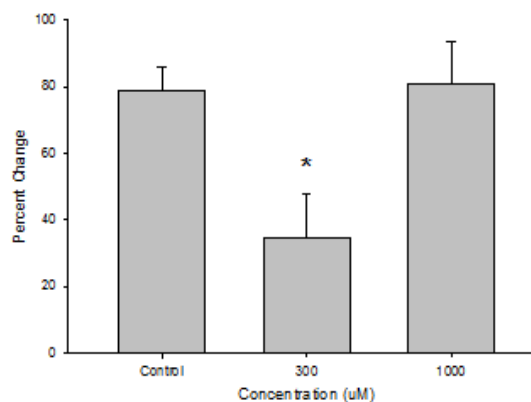
Log P: 3.09

Prodrug/Bioisostere: Bioisostere

Monomer/Dimer: Dimer

 C^{14} Uptake

Glutamate Percent Change



Compound Number: 76

Cook Code: WYME-ST-4NTMS

Promentis Code: Pro-069

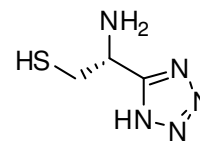
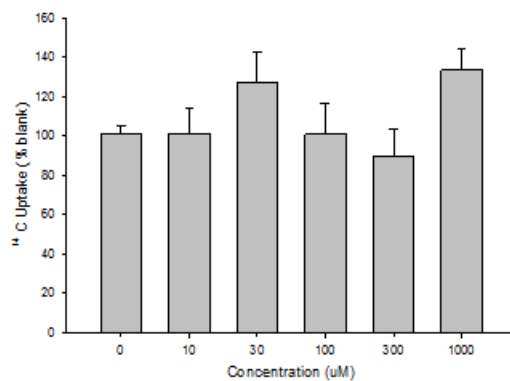
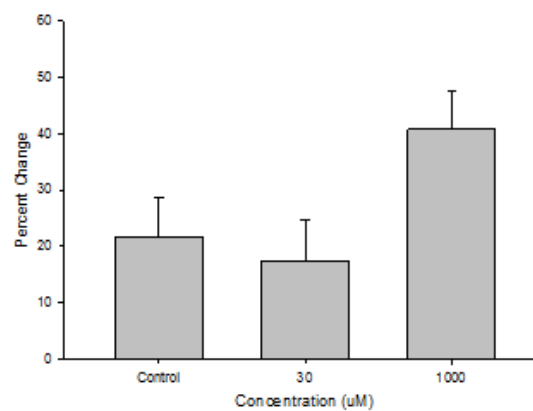
Chemical Formula: C₃H₇N₅S

Molecular Weight: 145.0

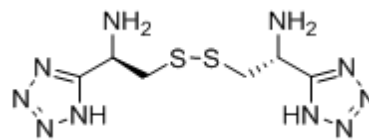
Log P: -0.52

Prodrug/Bioisostere: Bioisostere

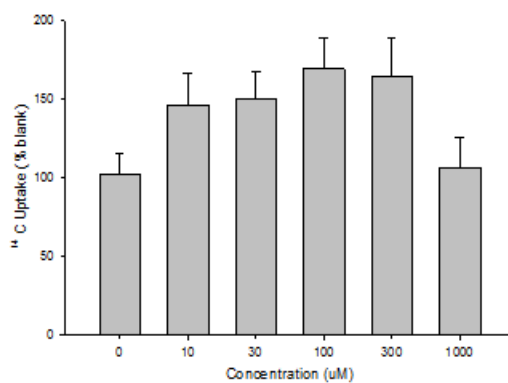
Monomer/Dimer: Monomer

**C¹⁴ Uptake****Glutamate Percent Change**

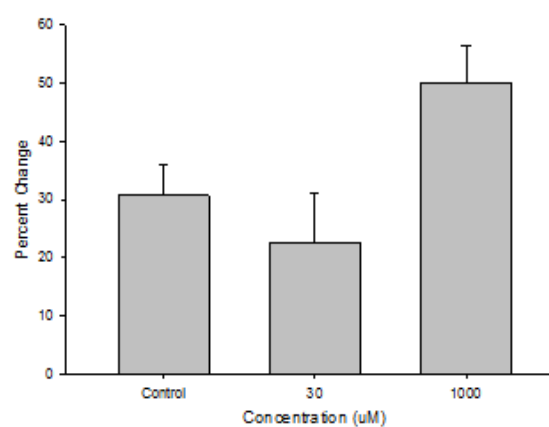
Compound Number: 77
Cook Code: WY-SS-4NTMS
Promentis Code: Pro-070
Chemical Formula: $C_6H_{12}N_{10}S_2$
Molecular Weight: 288.0
Log P: -0.57
Prodrug/Bioisostere: Bioisostere
Monomer/Dimer: Dimer



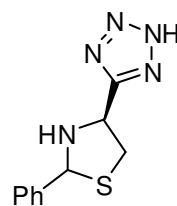
C^{14} Uptake



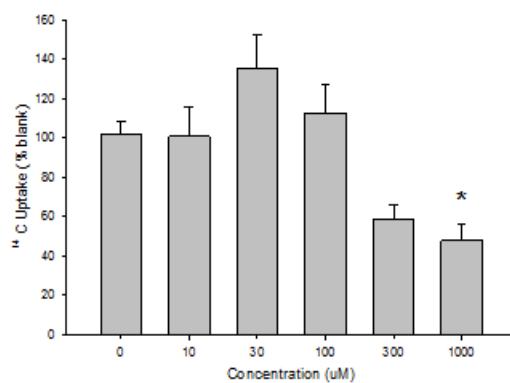
Glutamate Percent Change



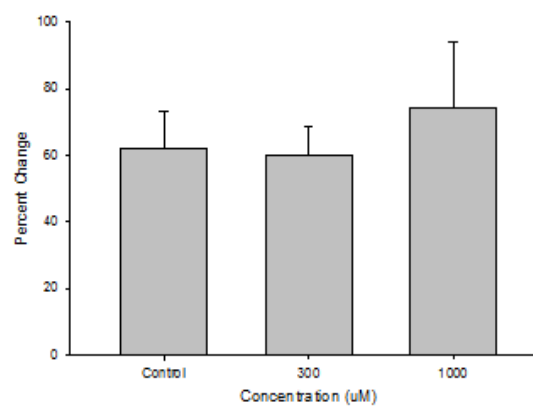
Compound Number: 78
Cook Code: WYME-NS-5PhN4
Promentis Code: Pro-083
Chemical Formula: C₁₀H₁₁N₅S
Molecular Weight: 233.0
Log P: 2.2
Prodrug/Bioisostere: Bioisostere
Monomer/Dimer: Monomer



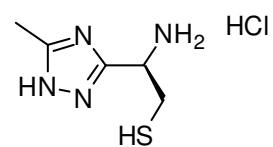
C¹⁴ Uptake



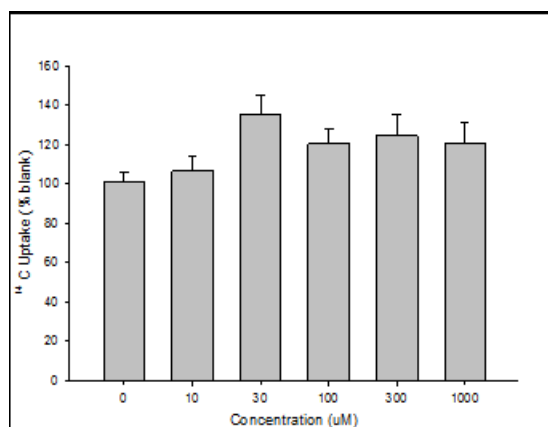
Glutamate Percent Change



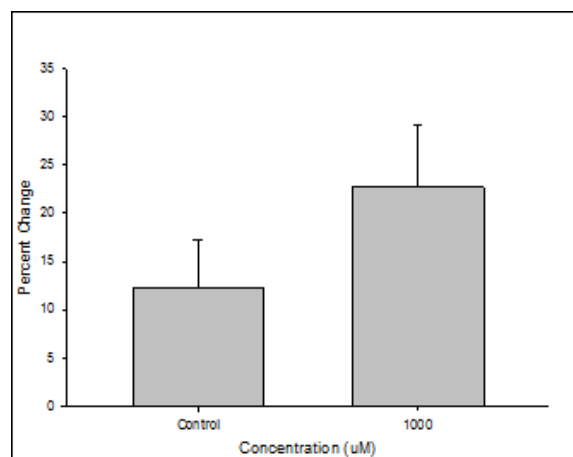
Compound Number: 79
Cook Code: MWL-273
Promentis Code: Pro-088
Chemical Formula: $C_5H_{11}ClN_4$
Molecular Weight: 194.69
Log P: 0.59
Prodrug/Bioisostere: Bioisostere
Monomer/Dimer: Monomer



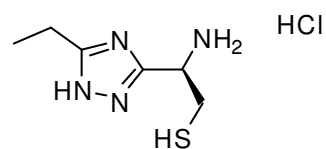
C^{14} Uptake



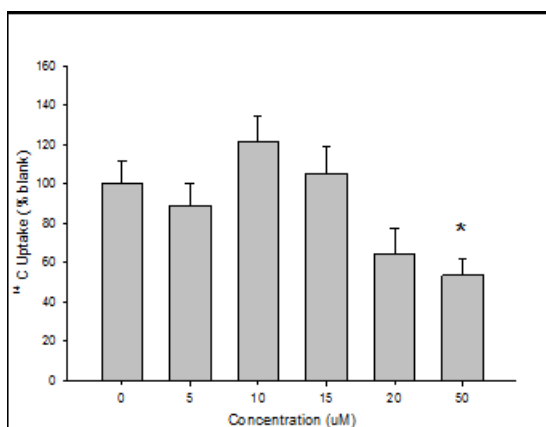
Glutamate Percent Change



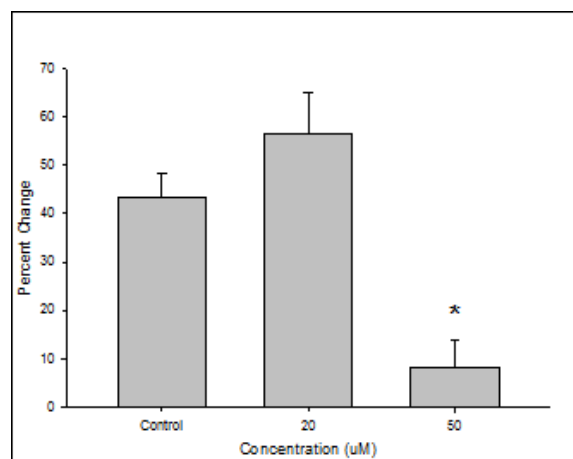
Compound Number: 80
Cook Code: MWL-283
Promentis Code: Pro-090
Chemical Formula: $C_6H_{13}ClN_4S$
Molecular Weight: 208.71
Log P: 1.16
Prodrug/Bioisostere: Bioisostere
Monomer/Dimer: Monomer



C^{14} Uptake



Glutamate Percent Change



Compound Number: 81

Cook Code: MWL-249

Promentis Code: Pro-078

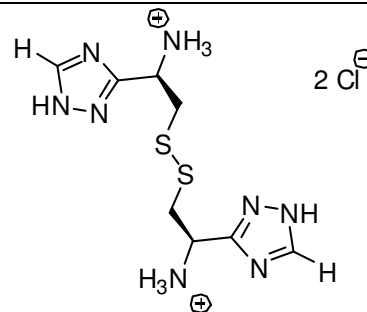
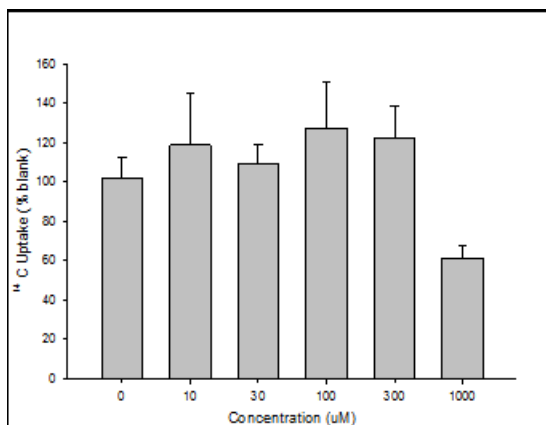
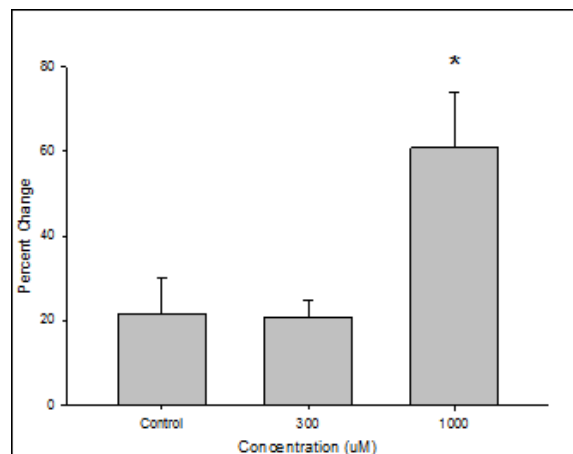
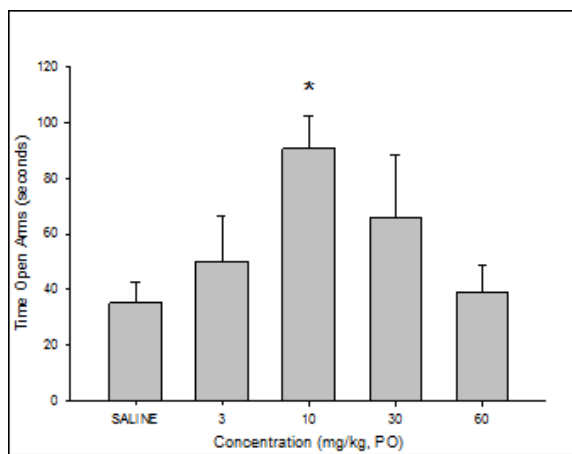
Chemical Formula: C₈H₁₆C₁₂N₈S₂

Molecular Weight: 359.3

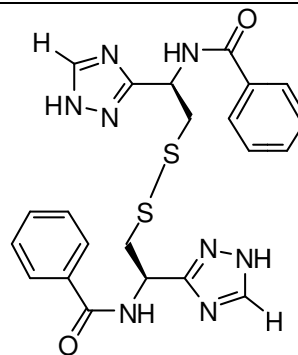
Log P: -1.32

Prodrug/Bioisostere: Bioisostere

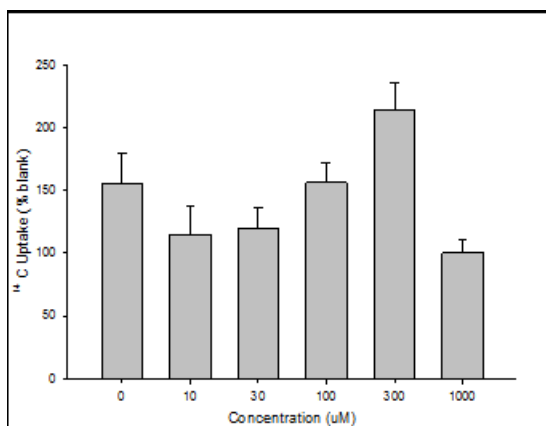
Monomer/Dimer: Dimer

**C¹⁴ Uptake****Glutamate Percent Change****Elevated Plus Maze**

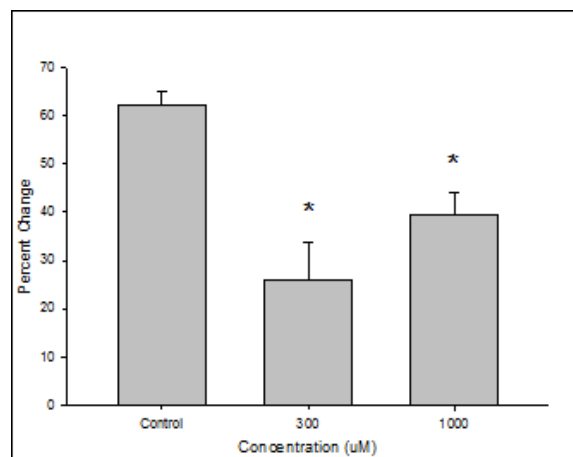
Compound Number: 82
Cook Code: MWL-299
Promentis Code: Pro-081
Chemical Formula: $C_{22}H_{22}N_8O_2S_2$
Molecular Weight: 494.59
Log P: 3.95
Prodrug/Bioisostere: Bioisostere
Monomer/Dimer: Dimer



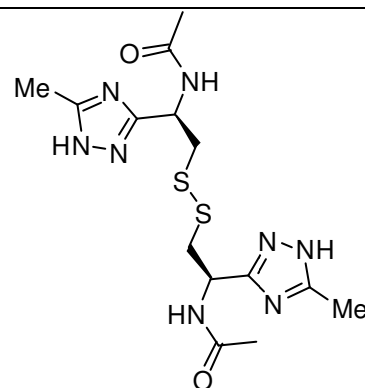
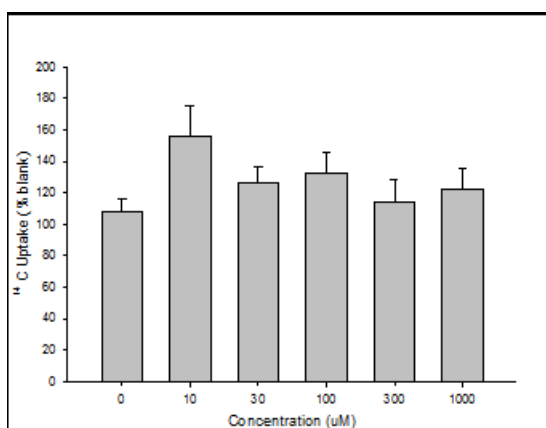
C^{14} Uptake



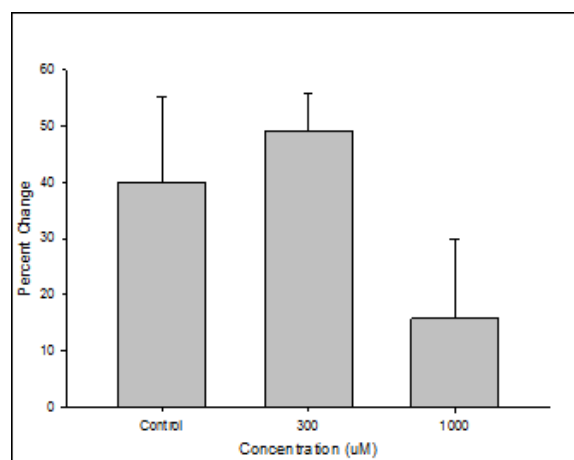
Glutamate Percent Change



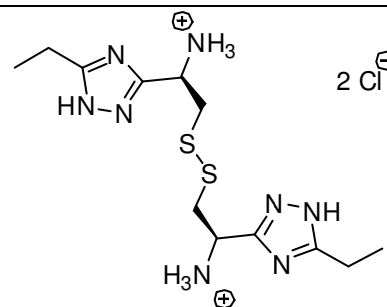
Compound Number: 83
Cook Code: MWL-258
Promentis Code: Pro-077
Chemical Formula: $C_{14}H_{22}N_8O_2S_2$
Molecular Weight: 398.51
Log P: 1.49
Prodrug/Bioisostere: Bioisostere
Monomer/Dimer: Dimer

 C^{14} Uptake

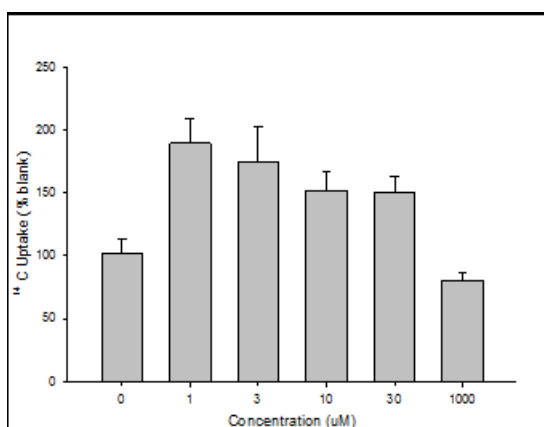
Glutamate Percent Change



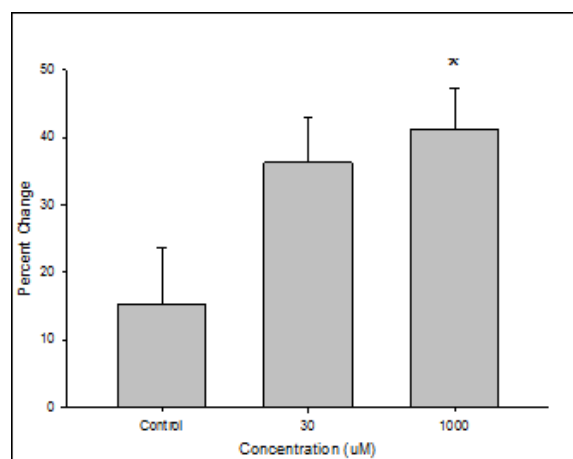
Compound Number: 84
 Cook Code: MWL-235
 Promentis Code: Pro-076
 Chemical Formula: $C_{12}H_{24}Cl_2N_8S_2$
 Molecular Weight: 415.41
 Log P: -2.21
 Prodrug/Bioisostere: Bioisostere
 Monomer/Dimer: Dimer



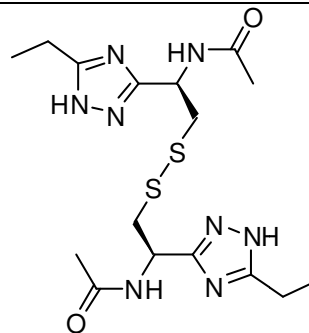
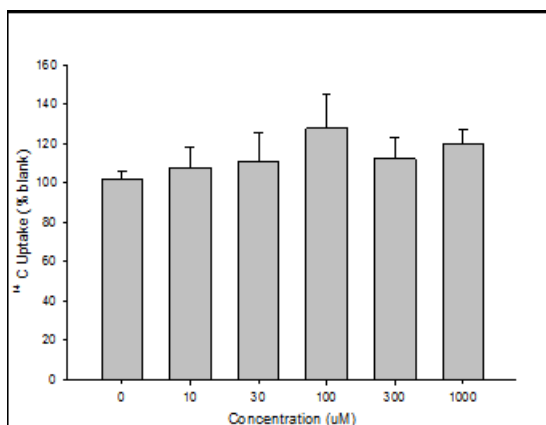
C^{14} Uptake



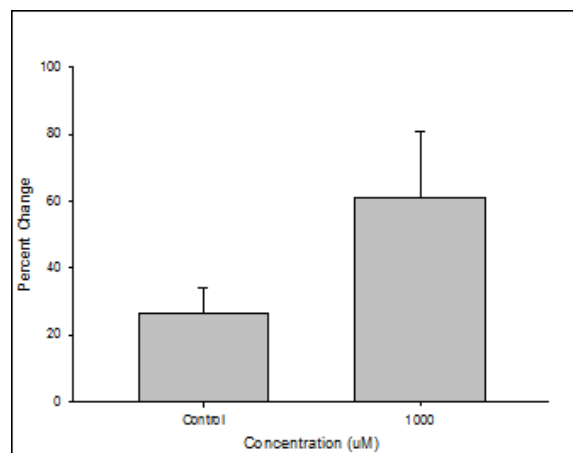
Glutamate Percent Change



Compound Number: 85
Cook Code: MWL-309
Promentis Code: Pro-085
Chemical Formula: $C_{16}H_{26}N_8O_2S_2$
Molecular Weight: 426.56
Log P: 2.64
Prodrug/Bioisostere: Bioisostere
Monomer/Dimer: Dimer

 C^{14} Uptake

Glutamate Percent Change



Compound Number: 86

Cook Code: MWL-284

Promentis Code: Pro-082

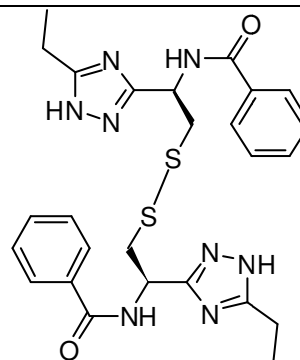
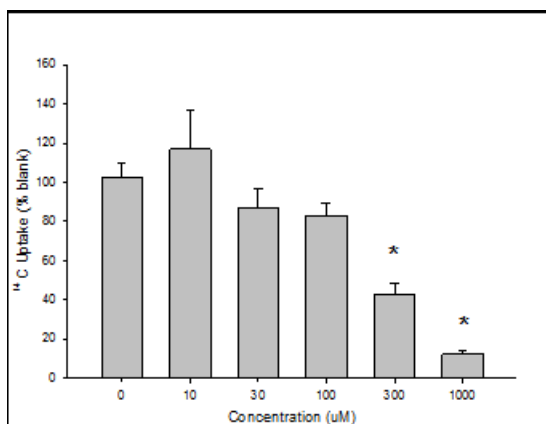
Chemical Formula: $C_{26}H_{30}N_8O_2S_2$

Molecular Weight: 550.7

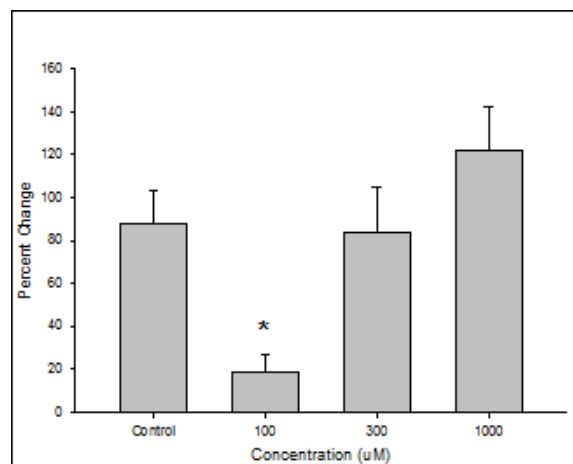
Log P: 6.44

Prodrug/Bioisostere: Bioisostere

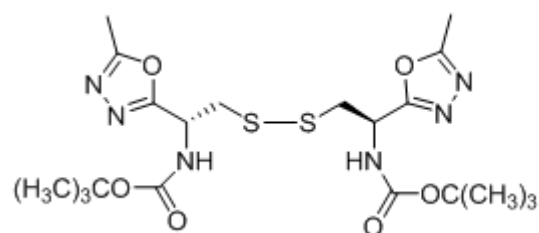
Monomer/Dimer: Dimer

 C^{14} Uptake

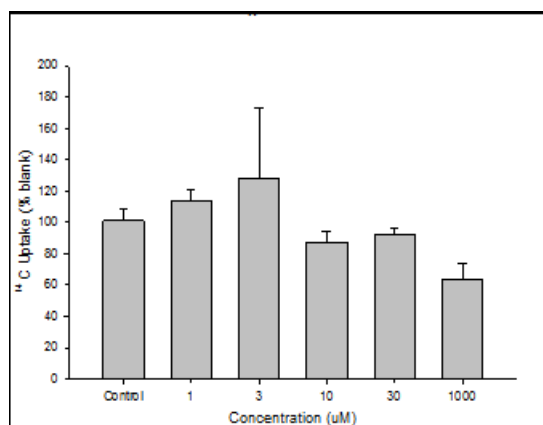
Glutamate Percent Change



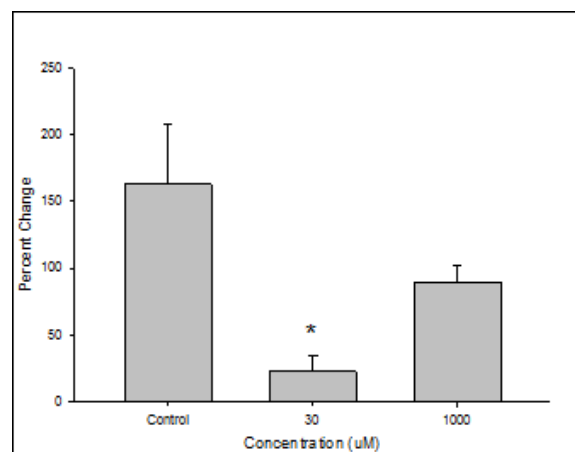
Compound Number: 87
Cook Code: WYME-SSI-AB
Promentis Code: Pro-038
Chemical Formula: $C_{20}H_{32}N_6O_6S_2$
Molecular Weight: 516.63
Log P: 4.56
Prodrug/Bioisostere: Bioisostere
Monomer/Dimer: Dimer



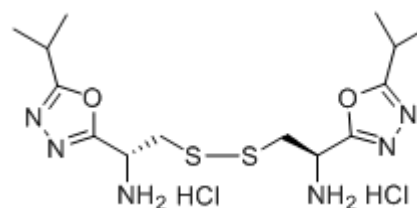
C^{14} Uptake



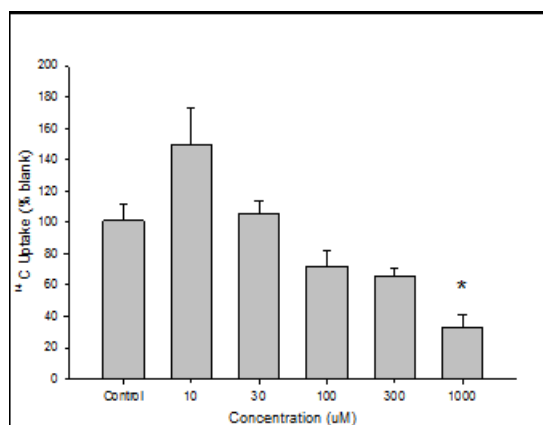
Glutamate Percent Change



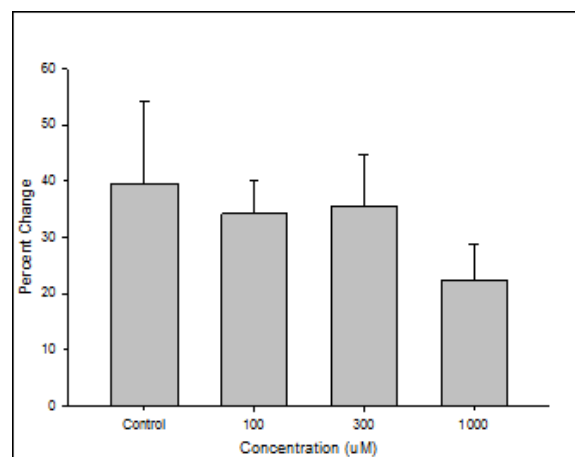
Compound Number: 88
Cook Code: WYME-SSI-P
Promentis Code: Pro-039
Chemical Formula: $C_{14}H_{26}C_{12}N_6O_2S_2$
Molecular Weight: 445.43
Log P: 3.89
Prodrug/Bioisostere: Bioisostere
Monomer/Dimer: Dimer



C^{14} Uptake



Glutamate Percent Change



Compound Number: 89

Cook Code: MWL-224

Promentis Code: Pro-073

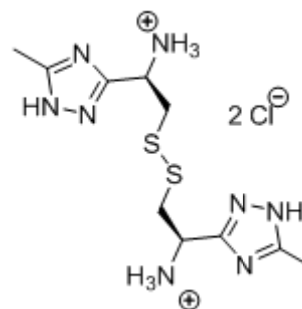
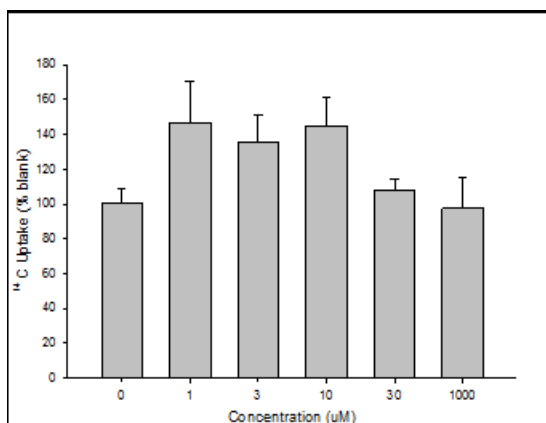
Chemical Formula: $C_{10}H_{20}Cl_2N_8S$

Molecular Weight: 387.36

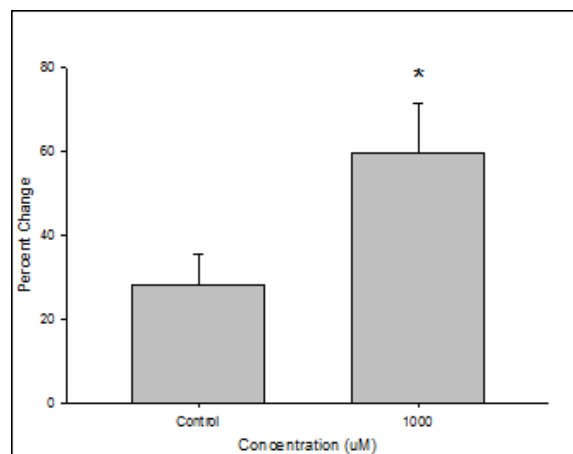
Log P: -3.12

Prodrug/Bioisostere: Bioisostere

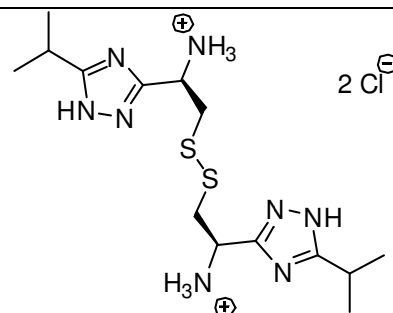
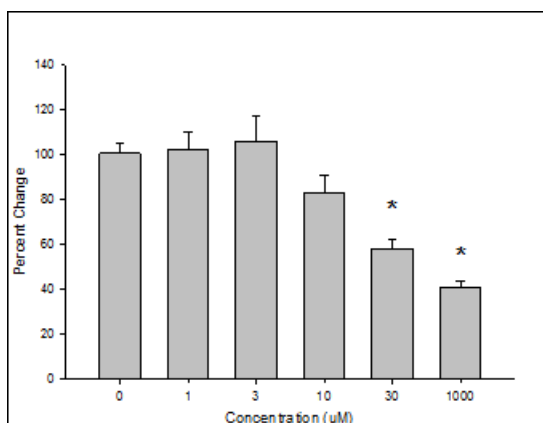
Monomer/Dimer: Dimer

 C^{14} Uptake

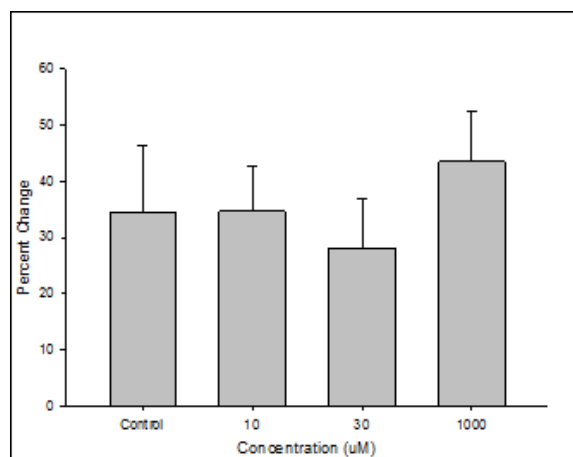
Glutamate Percent Change



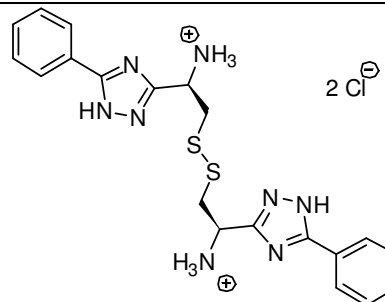
Compound Number: 90
Cook Code: MWL-236
Promentis Code: Pro-74
Chemical Formula: $C_{14}H_{28}Cl_2N_8S_2$
Molecular Weight: 443.46
Log P: -1.8
Prodrug/Bioisostere: Bioisostere
Monomer/Dimer: Dimer

 C^{14} Uptake

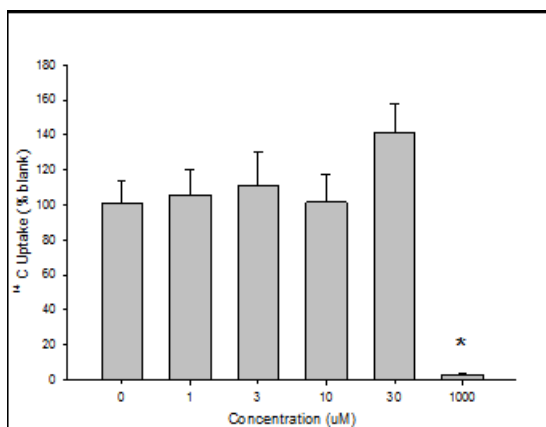
Glutamate Percent Change



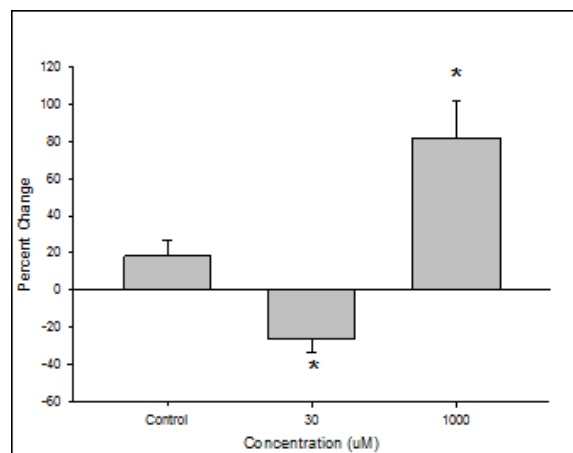
Compound Number: 91
Cook Code: MWL-220
Promentis Code: Pro-072
Chemical Formula: $C_{20}H_{24}C_{12}N_8S_2$
Molecular Weight: 511.49
Log P: -1.09
Prodrug/Bioisostere: Bioisostere
Monomer/Dimer: Dimer



C^{14} Uptake



Glutamate Percent Change



Compound Number: 92

Cook Code: WYME-SS-iPNPh

Promentis Code: Pro-075

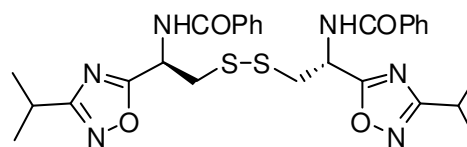
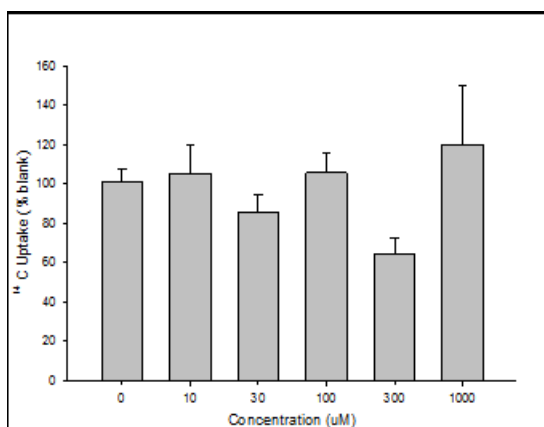
Chemical Formula: $C_{28}H_{32}N_6O_4S_2$

Molecular Weight: 580.72

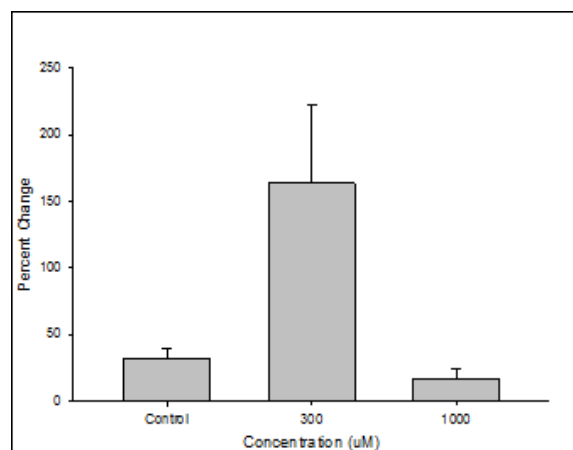
Log P: 7.55

Prodrug/Bioisostere: Bioisostere

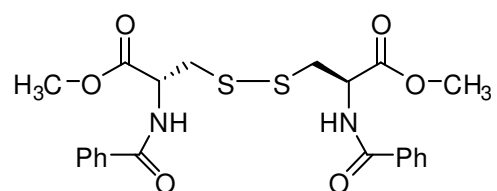
Monomer/Dimer: Dimer

 C^{14} Uptake

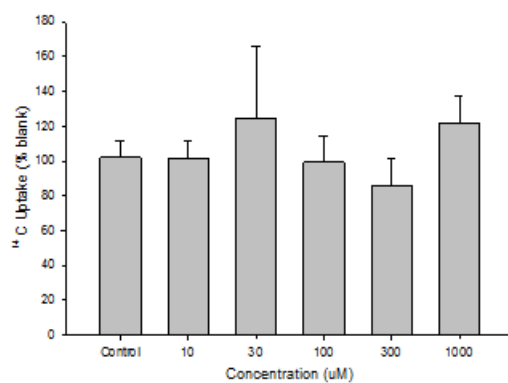
Glutamate Percent Change



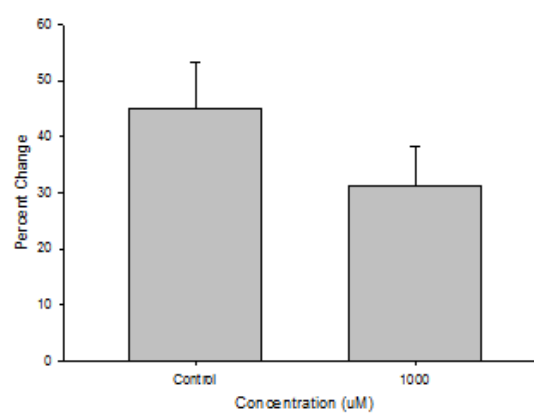
Compound Number: 109d
Cook Code: WYME-SS-BM
Promentis Code: Pro-034
Chemical Formula: $C_{22}H_{24}N_2O_6S_2$
Molecular Weight: 476.57
Log P: 2.8
Prodrug/Bioisostere: Prodrug
Monomer/Dimer: Dimer



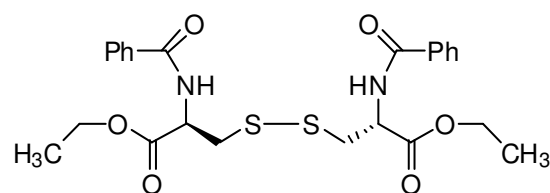
C^{14} Uptake



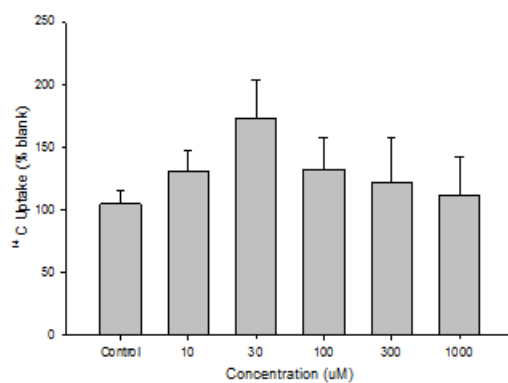
Glutamate Percent Change



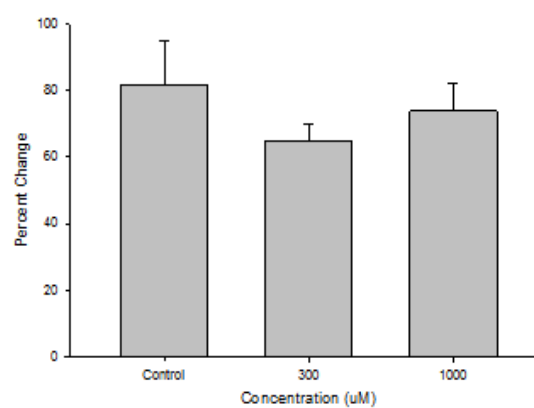
Compound Number: 109e
Cook Code: WYME-SS-BE
Promentis Code: Pro-033
Chemical Formula: $C_{24}H_{28}N_2O_6S_2$
Molecular Weight: 504.62
Log P: 3.48
Prodrug/Bioisostere: Prodrug
Monomer/Dimer: Dimer



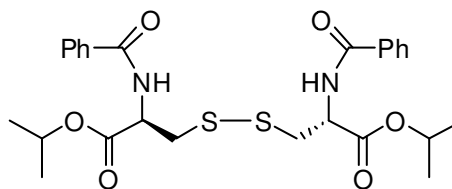
C^{14} Uptake



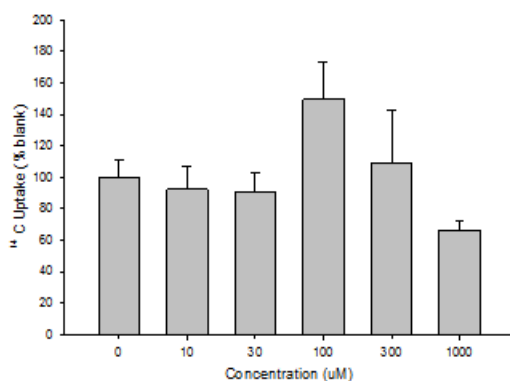
Glutamate Percent Change



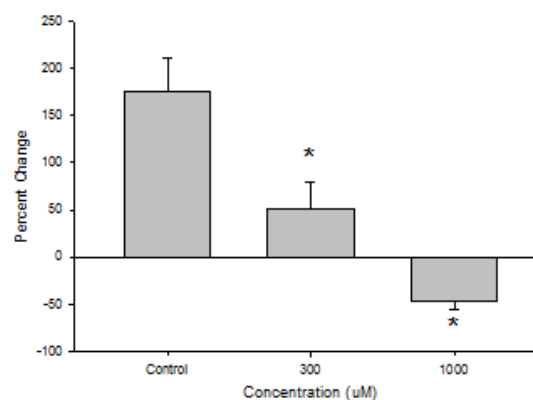
Compound Number: 109f
 Cook Code: WYME-SS-NPiPr
 Promentis Code: Pro-091
 Chemical Formula: $C_{26}H_{32}N_2O_6S_2$
 Molecular Weight: 532.67
 Log P: 4.11
 Prodrug/Bioisostere: Prodrug
 Monomer/Dimer: Monomer



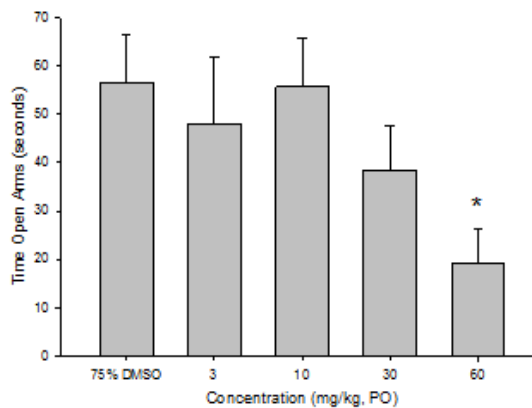
C^{14} Uptake



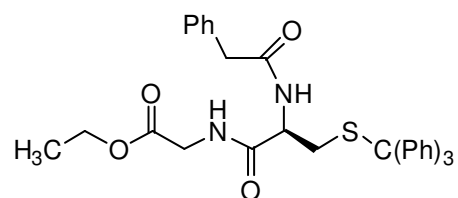
Glutamate Percent Change



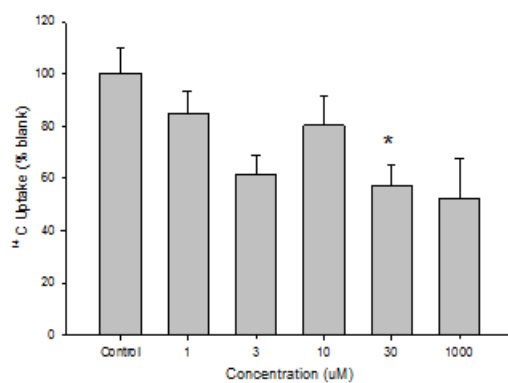
Elevated Plus Maze



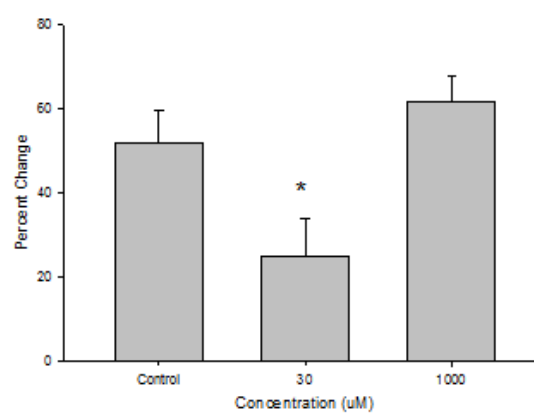
Compound Number: 112e
Cook Code: WYME-ST-C9
Promentis Code: Pro-050
Chemical Formula: $C_{34}H_{34}N_2O_4S$
Molecular Weight: 566.71
Log P: 5.62
Prodrug/Bioisostere: Prodrug
Monomer/Dimer: Monomer



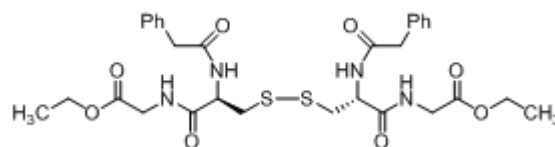
C^{14} Uptake



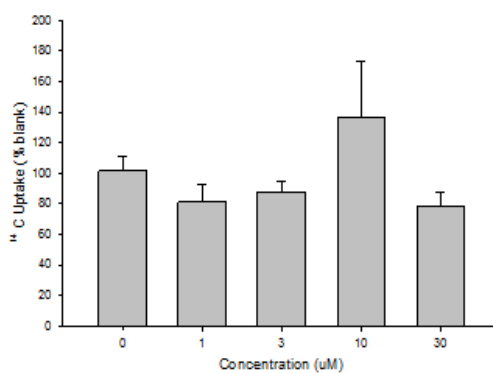
Glutamate Percent Change



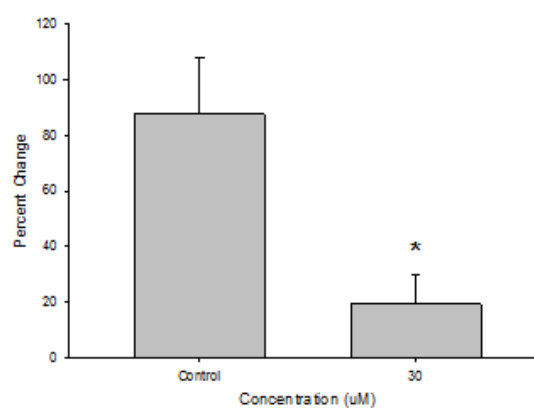
Compound Number: 113e
Cook Code: WYME-11g
Promentis Code: Pro-003
Chemical Formula: $C_{30}H_{38}N_4O_8S_2$
Molecular Weight: 646.77
Log P: 1.07
Prodrug/Bioisostere: Prodrug
Monomer/Dimer: Dimer



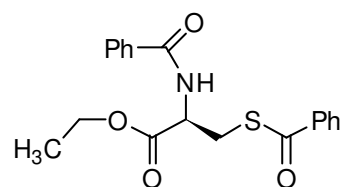
C^{14} Uptake



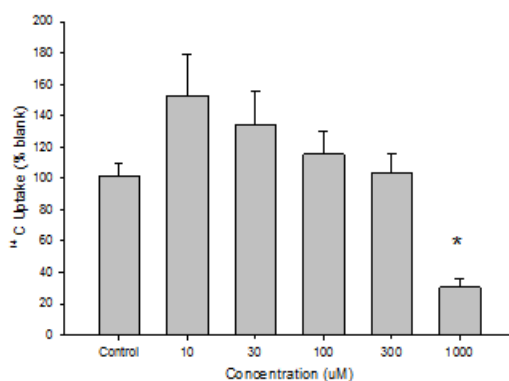
Glutamate Percent Change



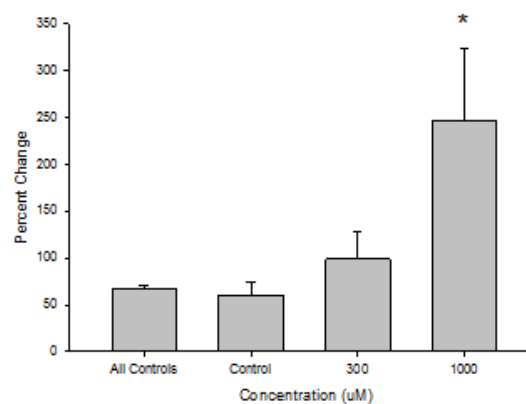
Compound Number: 115
 Cook Code: WYME-10e
 Promentis Code: Pro-001
 Chemical Formula: $C_{19}H_{19}NO_4S$
 Molecular Weight: 357.42
 Log P: 3.37
 Prodrug/Bioisostere: Prodrug
 Monomer/Dimer: Monomer



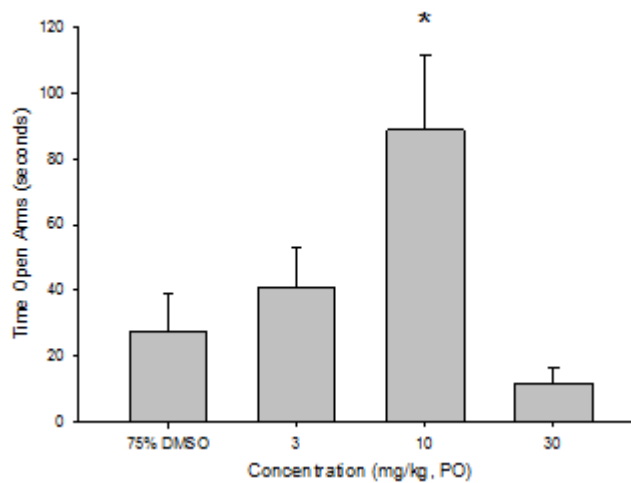
C^{14} Uptake



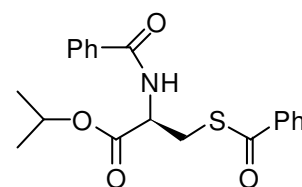
Glutamate Percent Change



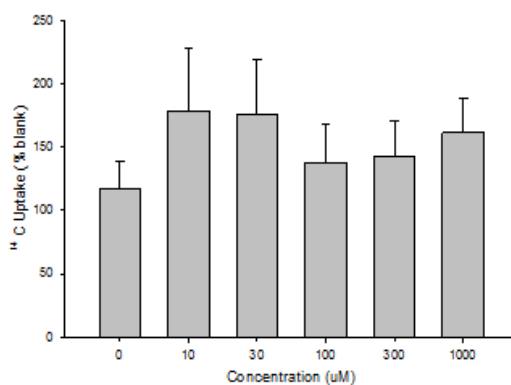
Elevated Plus Maze



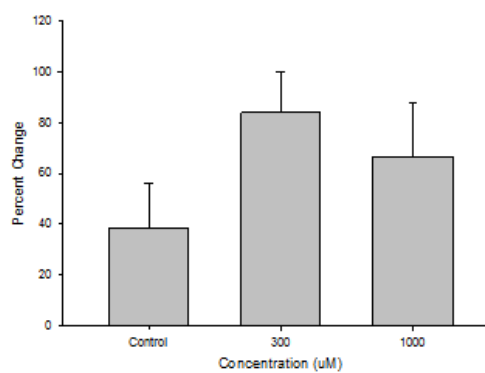
Compound Number: 116
 Cook Code: WYME-10f
 Promentis Code: Pro-002
 Chemical Formula: $C_{20}H_{21}NO_4S$
 Molecular Weight: 371.45
 Log P: 3.69
 Prodrug/Bioisostere: Prodrug
 Monomer/Dimer: Monomer



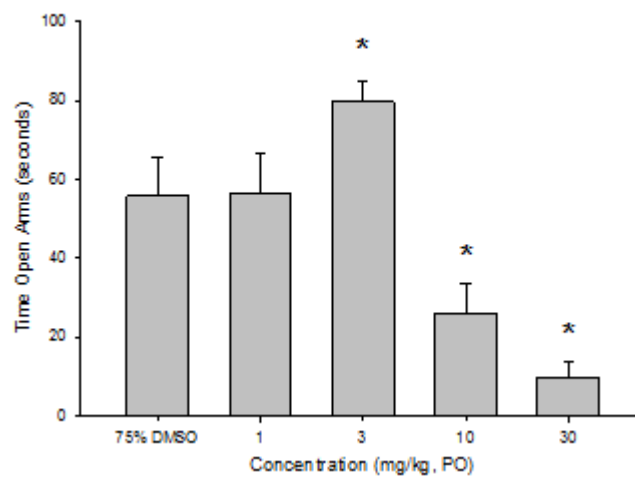
C^{14} Uptake



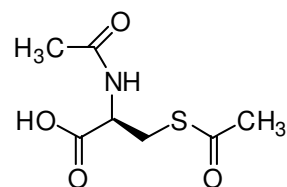
Glutamate Percent Change



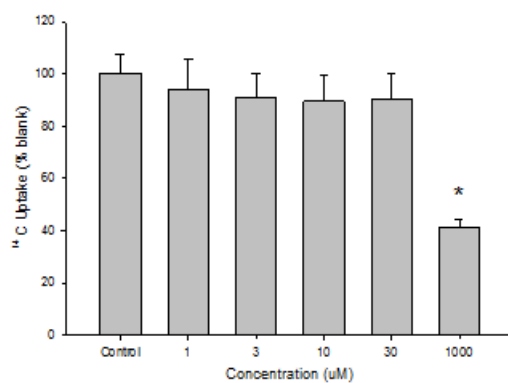
Elevated Plus Maze



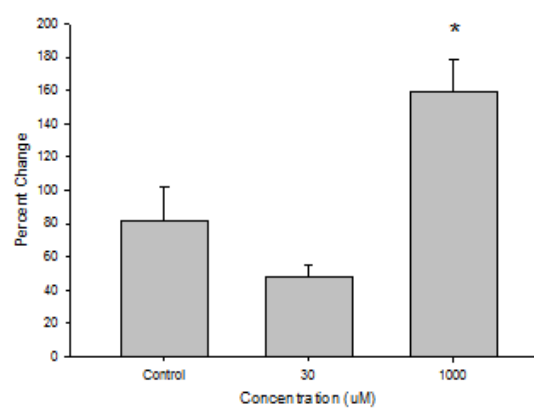
Compound Number: 117
Cook Code: WYME-diA
Promentis Code: Pro-008
Chemical Formula: $C_7H_{11}NO_4S$
Molecular Weight: 205.23
Log P: -1.02
Prodrug/Bioisostere: Prodrug
Monomer/Dimer: Monomer



C^{14} Uptake



Glutamate Percent Change



Compound Number: 118

Cook Code: WYME-SPh-CCO

Promentis Code: Pro-028

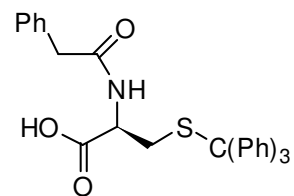
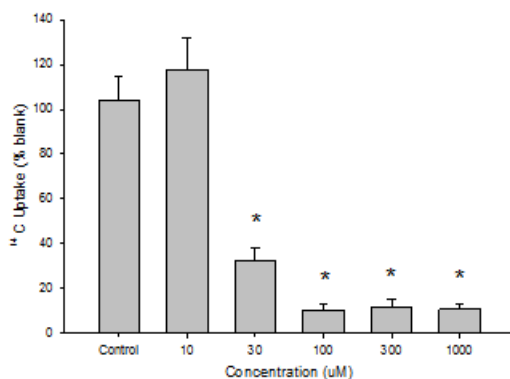
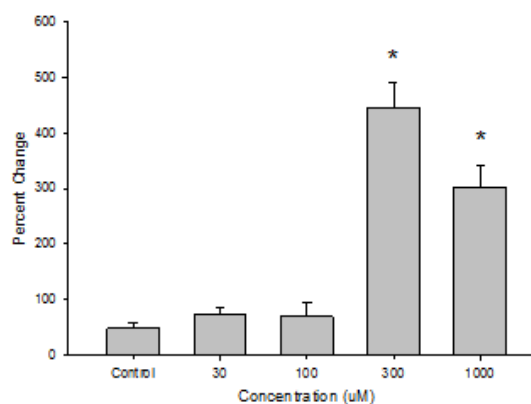
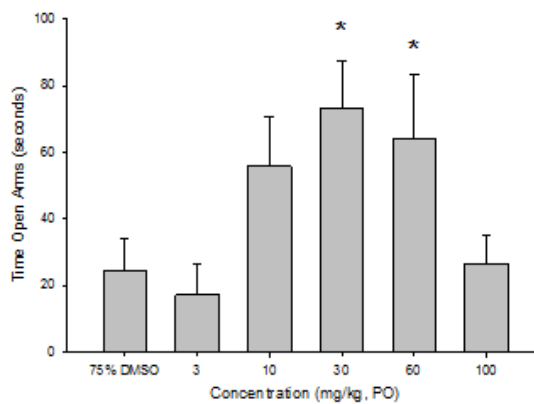
Chemical Formula: $C_{30}H_{27}NO_3S$

Molecular Weight: 481.61

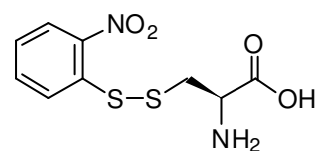
Log P: 6.17

Prodrug/Bioisostere: Prodrug

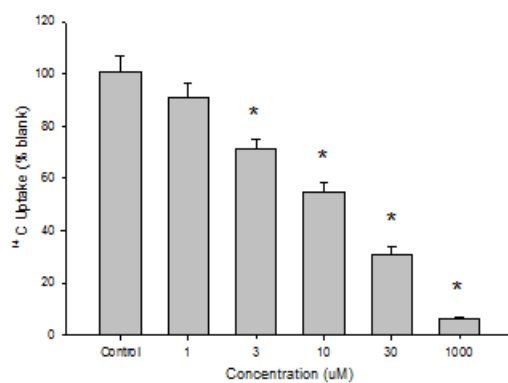
Monomer/Dimer: Monomer

 **C^{14} Uptake****Glutamate Percent Change****Elevated Plus Maze**

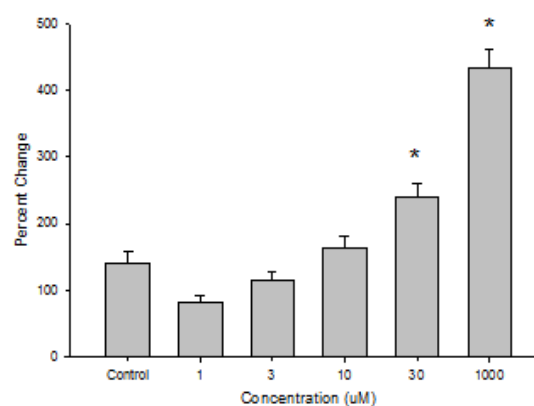
Compound Number: 119
Cook Code: WYME-SNPS
Promentis Code: Pro-026
Chemical Formula: $C_9H_{10}N_2O_4S_2$
Molecular Weight: 274.32
Log P: -1.03
Prodrug/Bioisostere: Prodrug
Monomer/Dimer: Monomer



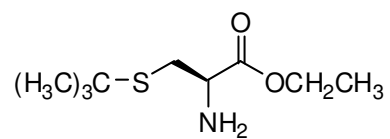
C^{14} Uptake



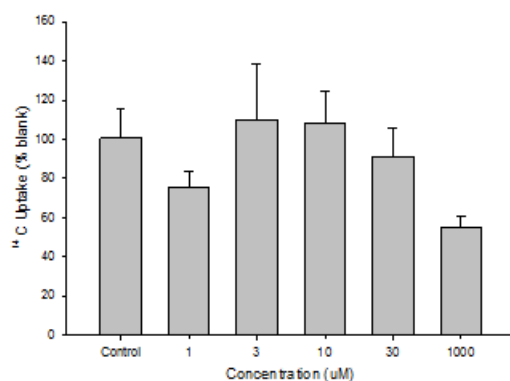
Glutamate Percent Change



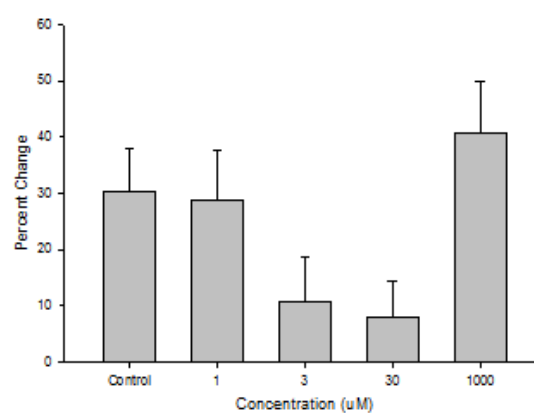
Compound Number: 120
Cook Code: WYME-SM-tBu
Promentis Code: Pro-025
Chemical Formula:
Molecular Weight: 205.32
Log P: 0.81
Prodrug/Bioisostere: Prodrug
Monomer/Dimer: Monomer

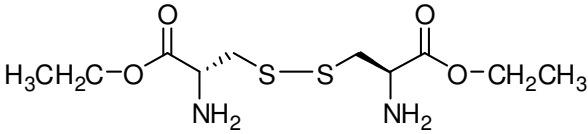
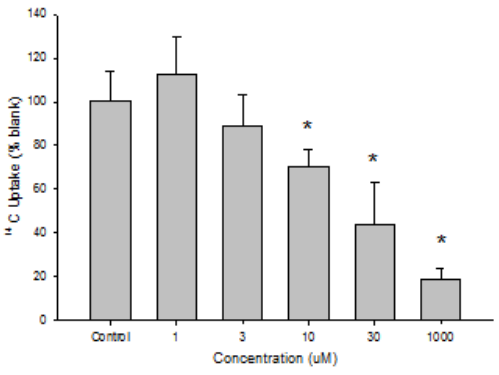
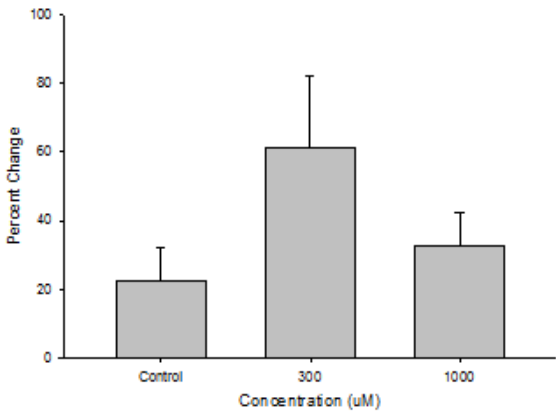


C^{14} Uptake

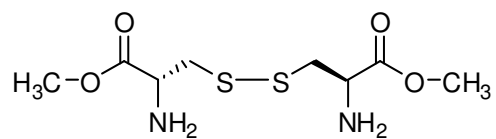


Glutamate Percent Change

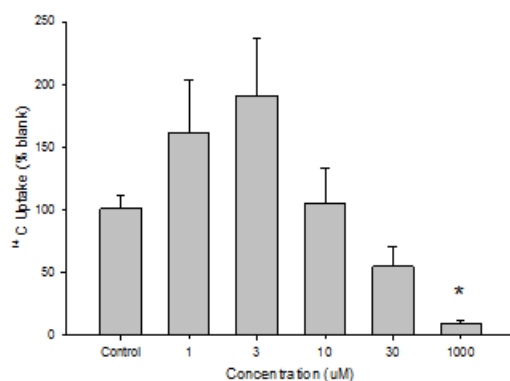


<p>Compound Number: 121 Cook Code: WYME-051707-SSE Promentis Code: Pro-036 Chemical Formula: $C_{10}H_{20}N_2O_4S_2$ Molecular Weight: 296.41 Log P: -0.18 Prodrug/Bioisostere: Prodrug Monomer/Dimer: Dimer</p>																							
<p>C^{14} Uptake</p>  <table border="1"><thead><tr><th>Concentration (uM)</th><th>C^{14} Uptake (% blank)</th></tr></thead><tbody><tr><td>Control</td><td>100</td></tr><tr><td>1</td><td>110</td></tr><tr><td>3</td><td>88</td></tr><tr><td>10</td><td>70*</td></tr><tr><td>30</td><td>45*</td></tr><tr><td>1000</td><td>20*</td></tr></tbody></table>	Concentration (uM)	C^{14} Uptake (% blank)	Control	100	1	110	3	88	10	70*	30	45*	1000	20*	<p>Glutamate Percent Change</p>  <table border="1"><thead><tr><th>Concentration (uM)</th><th>Percent Change</th></tr></thead><tbody><tr><td>Control</td><td>22</td></tr><tr><td>300</td><td>60</td></tr><tr><td>1000</td><td>32</td></tr></tbody></table>	Concentration (uM)	Percent Change	Control	22	300	60	1000	32
Concentration (uM)	C^{14} Uptake (% blank)																						
Control	100																						
1	110																						
3	88																						
10	70*																						
30	45*																						
1000	20*																						
Concentration (uM)	Percent Change																						
Control	22																						
300	60																						
1000	32																						

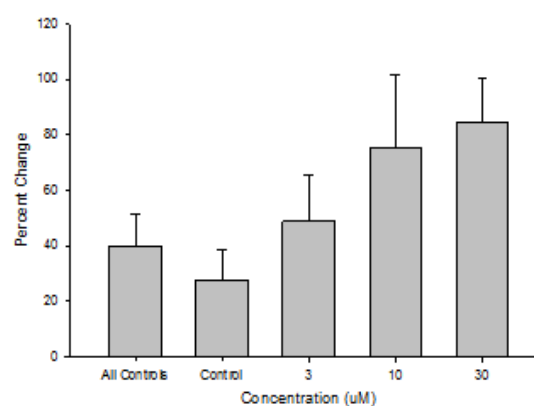
Compound Number: 122
Cook Code: WYME-060307-SSM
Promentis Code: Pro-037
Chemical Formula: $C_8H_{16}N_2O_4S_2$
Molecular Weight: 268.35
Log P: -0.86
Prodrug/Bioisostere: Prodrug
Monomer/Dimer: Dimer



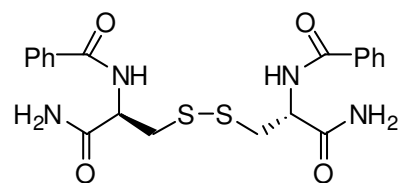
C^{14} Uptake



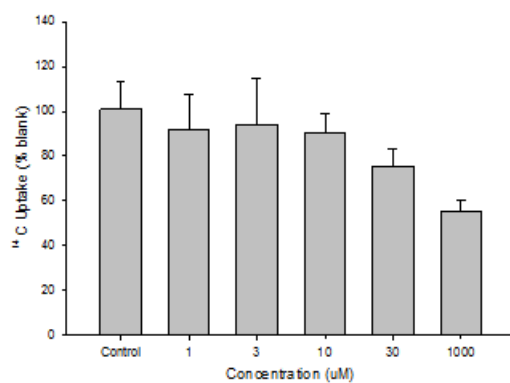
Glutamate Percent Change



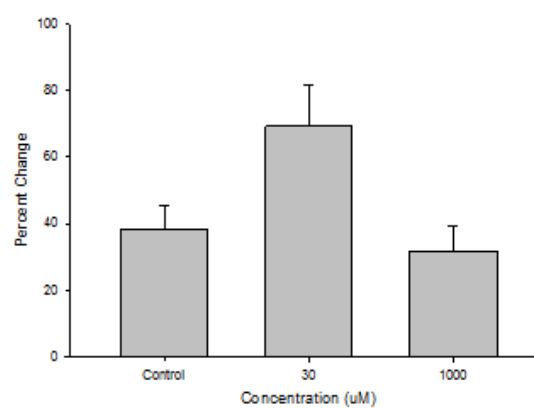
Compound Number: 123
Cook Code: WYME-SSNBam
Promentis Code: Pro-040
Chemical Formula: $C_{20}H_{22}N_4O_4S_2$
Molecular Weight: 446.55
Log P: 0.97
Prodrug/Bioisostere: Prodrug
Monomer/Dimer: Dimer



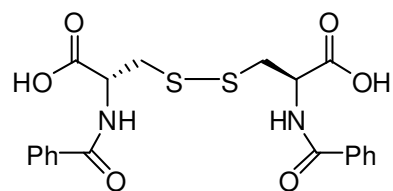
C^{14} Uptake



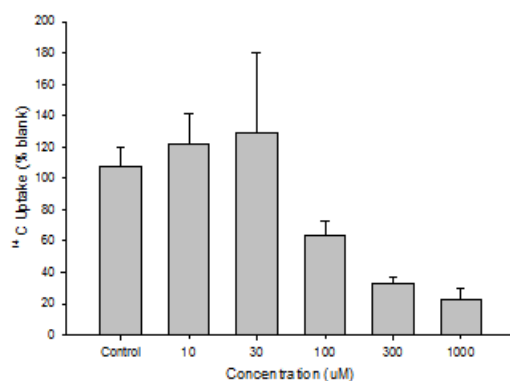
Glutamate Percent Change



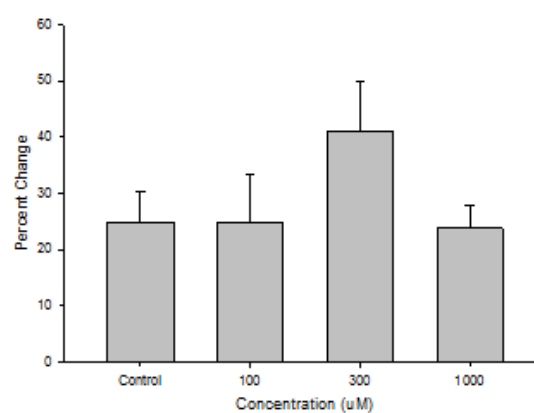
Compound Number: 124
Cook Code: ME-SBZ
Promentis Code: Pro-019
Chemical Formula: $C_{20}H_{20}N_2O_6S_2$
Molecular Weight: 448.51
Log P: 2.28
Prodrug/Bioisostere: Prodrug
Monomer/Dimer: Dimer



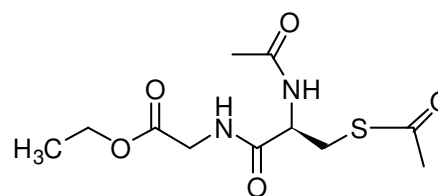
C^{14} Uptake



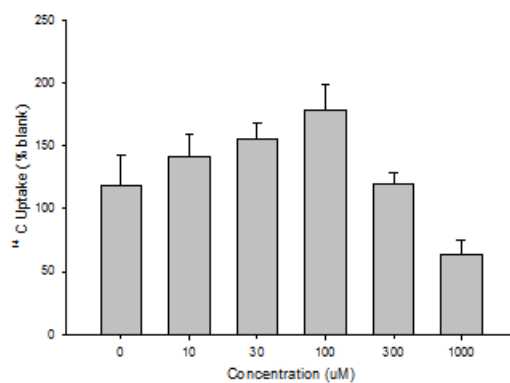
Glutamate Percent Change



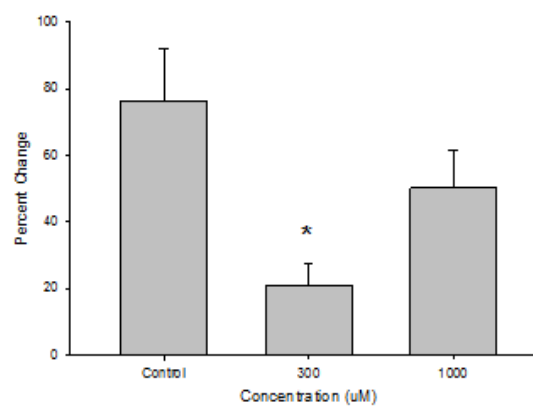
Compound Number: 125
Cook Code: WYME-diAcGly
Promentis Code: Pro-087
Chemical Formula: $C_{11}H_{18}N_2O_5S$
Molecular Weight: 290.3
Log P: -1.57
Prodrug/Bioisostere: Prodrug
Monomer/Dimer: Monomer



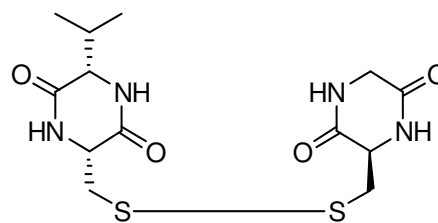
C^{14} Uptake



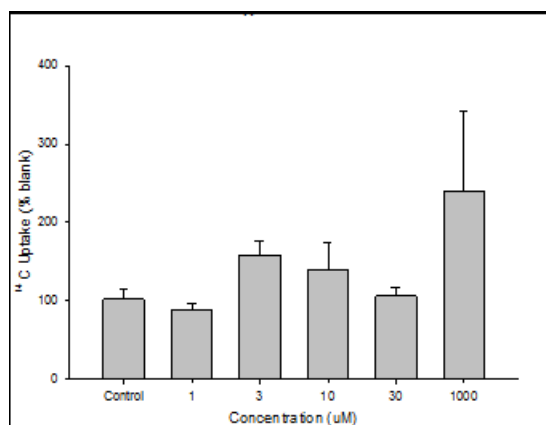
Glutamate Percent Change



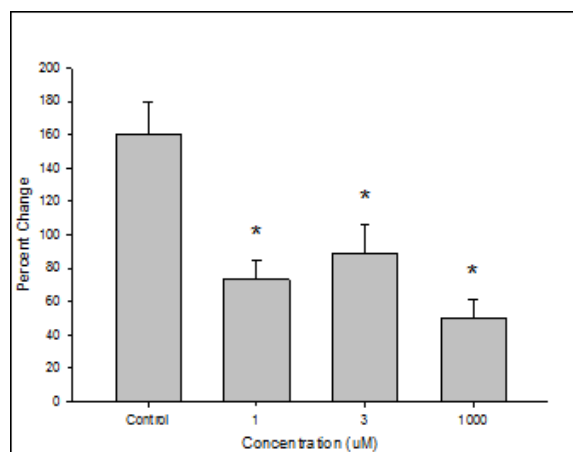
Compound Number: 131
Cook Code: WYME-ST-GV
Promentis Code: Pro-054
Chemical Formula: $C_{13}H_{20}N_4O_4S_2$
Molecular Weight: 360.45
Log P: -1.83
Prodrug/Bioisostere: Prodrug
Monomer/Dimer: Dimer



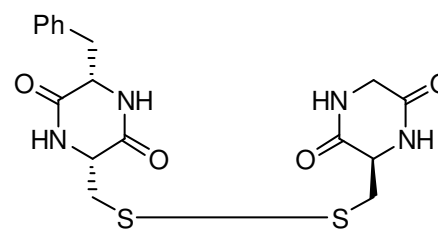
C^{14} Uptake



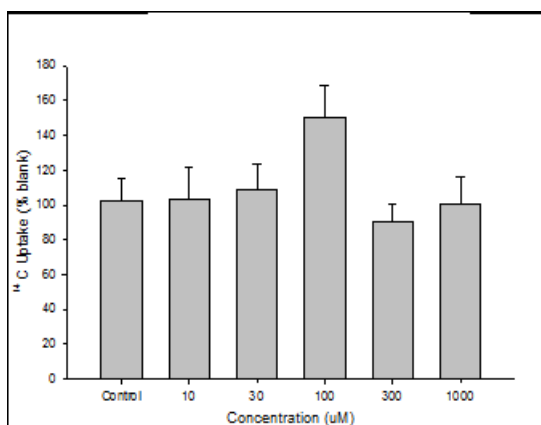
Glutamate Percent Change



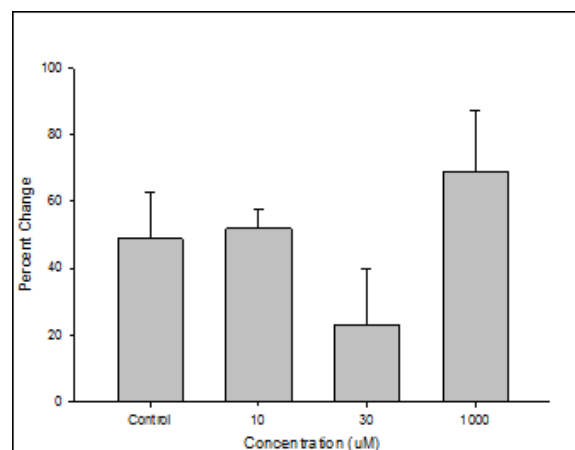
Compound Number: 132
Cook Code: WYME-ST-GP
Promentis Code: Pro-053
Chemical Formula: $C_{17}H_{20}N_4O_4S_2$
Molecular Weight: 408.5
Log P: -1.04
Prodrug/Bioisostere: Prodrug
Monomer/Dimer: Dimer

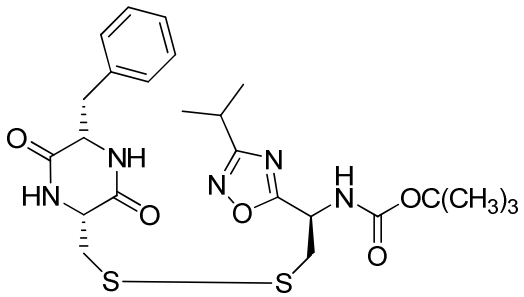


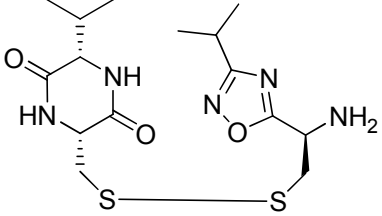
C^{14} Uptake

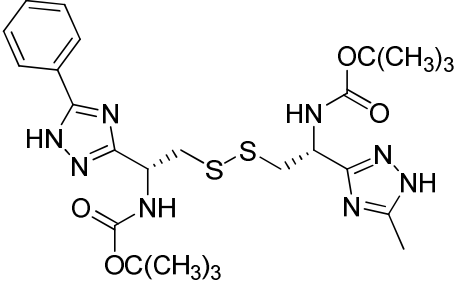


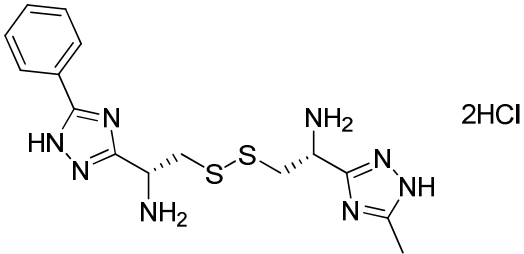
Glutamate Percent Change

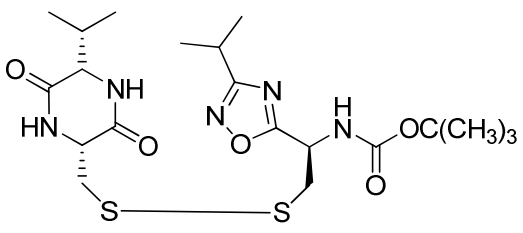


<p>Compound Number: 133 Cook Code: WYME-STPh-iPr Promentis Code: N/A Chemical Formula: $C_{24}H_{33}N_5O_5S_2$ Molecular Weight: 535.68 Log P: 3. Prodrug/Bioisostere: Both Monomer/Dimer: Dimer (Mixed)</p>	 <p>The chemical structure shows a dimeric molecule consisting of two glutamate-like units linked by a disulfide bridge (-S-S-). The left glutamate unit is substituted with a phenyl group at the C2 position. The right glutamate unit is substituted with an isopropyl group at the C2 position and a tert-butyl carbamate group (-NHCOOC(CH3)3) at the C1 position. The glutamate backbone includes a carboxamide group (-CONH-) and a secondary amine (-NH-).</p>
<p>C^{14} Uptake N/A</p>	<p>Glutamate Percent Change N/A</p>

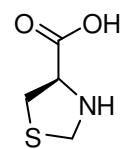
<p>Compound Number: 134 Cook Code: WYME-STVa-iPr-dBOC Promentis Code: N/A Chemical Formula: C₁₅H₂₅N₅O₃S₂ Molecular Weight: 387.52 Log P: 1.72 Prodrug/Bioisostere: Both Monomer/Dimer: Dimer (Mixed)</p>	
<p>C¹⁴ Uptake N/A</p>	<p>Glutamate Percent Change N/A</p>

<p>Compound Number: 135 Cook Code: VD-MD-01 Promentis Code: N/A Chemical Formula: $C_{25}H_{36}N_8O_4S_2$ Molecular Weight: 576.73 Log P: 5.8 Prodrug/Bioisostere: Bioisostere Monomer/Dimer: Dimer (Mixed)</p>	
<p>C^{14} Uptake N/A</p>	<p>Glutamate Percent Change N/A</p>

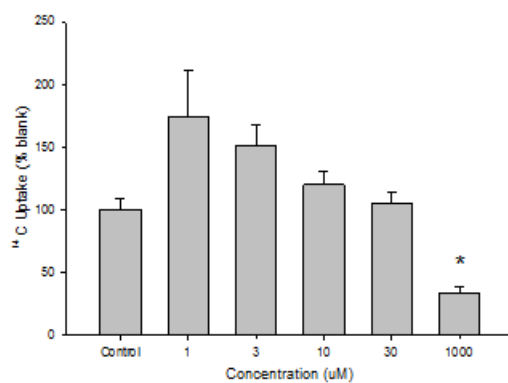
<p>Compound Number: 136 Cook Code: VR-MD-02 Promentis Code: N/A Chemical Formula: C₁₅H₂₂Cl₂N₈S₂ Molecular Weight: 448.08 Log P: 3.01 Prodrug/Bioisostere: Bioisostere Monomer/Dimer: Dimer (Mixed)</p>	 <p>2HCl</p>
<p>C¹⁴ Uptake N/A</p>	<p>Glutamate Percent Change N/A</p>

<p>Compound Number: 137 Cook Code: WYME-STVa-iPr Promentis Code: N/A Chemical Formula: $C_{20}H_{33}N_5O_5S_2$ Molecular Weight: 487.64 Log P: 3.11 Prodrug/Bioisostere: Bioisostere Monomer/Dimer: Dimer (Mixed)</p>	 <p>The chemical structure of Compound 137 is a dimeric molecule. It consists of two identical units linked by a disulfide bridge (-S-S-). Each unit features a central carbon atom bonded to a hydrogen atom (wedge), a tert-butyl amide group (-NH-C(=O)-OC(CH₃)₃), and a 1,2,4-oxadiazole ring. The oxadiazole ring is further substituted with an isopropyl group and a 2,6-piperidinedione ring. The piperidinedione ring has an isopropyl group attached to the nitrogen at the 2-position and a hydrogen atom at the 6-position.</p>
<p>C^{14} Uptake N/A</p>	<p>Glutamate Percent Change N/A</p>

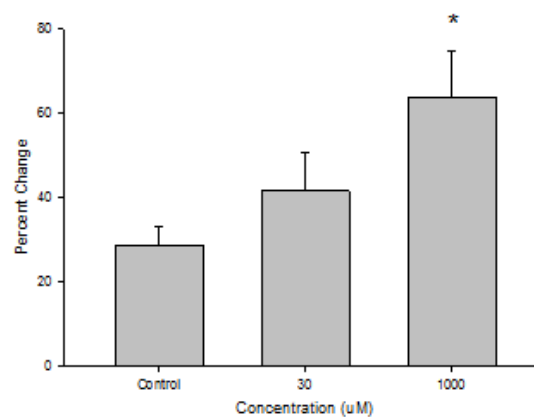
Compound Number: 138
Cook Code: WYME-051607-CS
Promentis Code: Pro-006
Chemical Formula: $C_4H_7NO_2S$
Molecular Weight: 113.17
Log P: 0.03
Prodrug/Bioisostere: Prodrug
Monomer/Dimer: Monomer



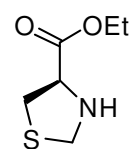
C^{14} Uptake



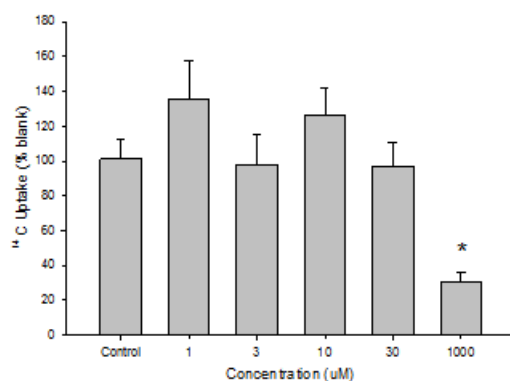
Glutamate Percent Change



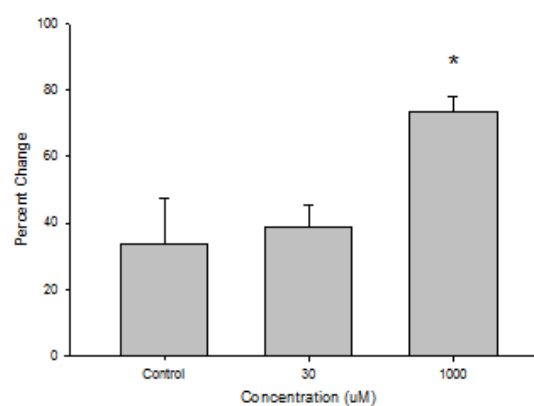
Compound Number: 139
Cook Code: WYME-051607-CSE
Promentis Code: Pro-007
Chemical Formula: $C_6H_{11}NO_2S$
Molecular Weight: 161.22
Log P: 0.63
Prodrug/Bioisostere: Prodrug
Monomer/Dimer: Monomer



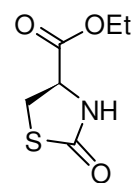
C^{14} Uptake



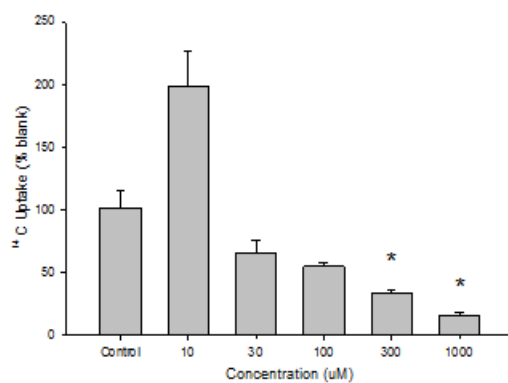
Glutamate Percent Change



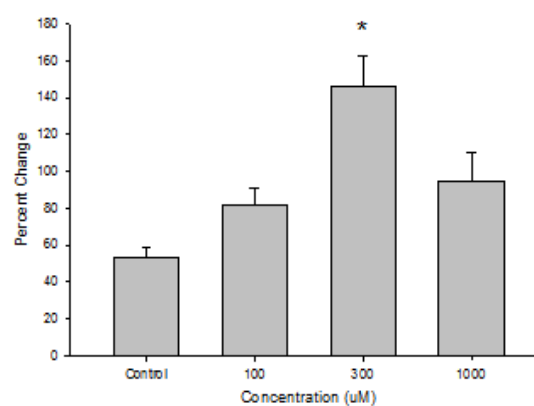
Compound Number: 140
Cook Code: WYME-051907-SEO
Promentis Code: Pro-022
Chemical Formula: $C_6H_9NO_3S$
Molecular Weight: 175.21
Log P: 0.21
Prodrug/Bioisostere: Prodrug
Monomer/Dimer: Monomer



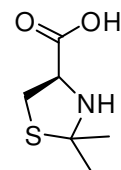
C^{14} Uptake



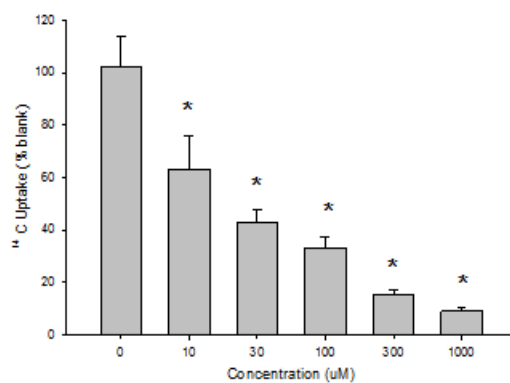
Glutamate Percent Change



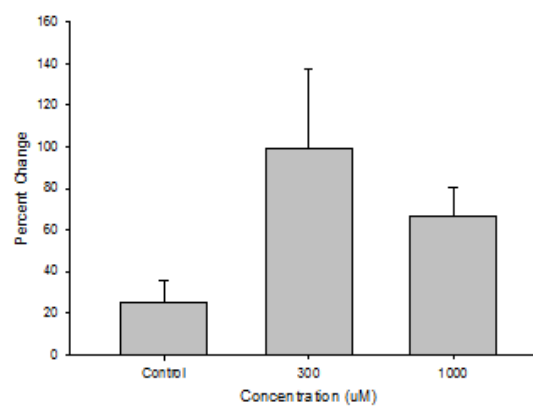
Compound Number: 141
Cook Code: WYME-SACE
Promentis Code: Pro-086
Chemical Formula: $C_6H_{11}NO_2S$
Molecular Weight: 161.2
Log P: 0.63
Prodrug/Bioisostere: Prodrug
Monomer/Dimer: Monomer



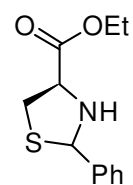
C^{14} Uptake



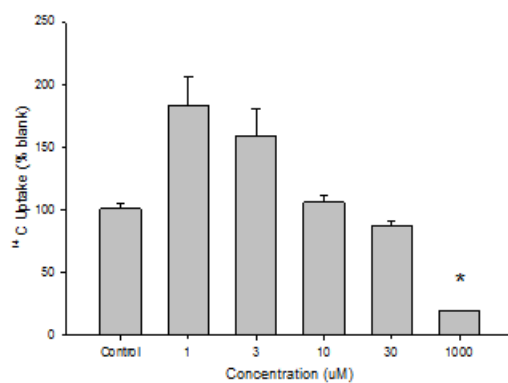
Glutamate Percent Change



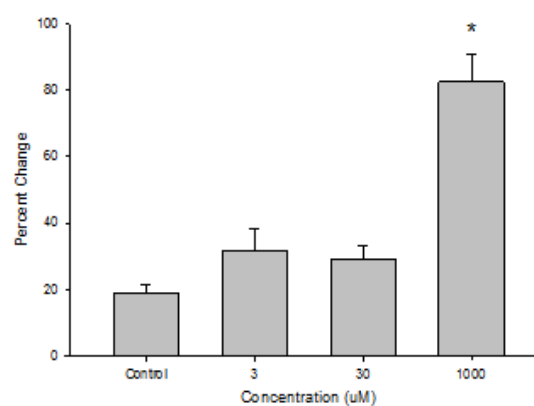
Compound Number: 142
Cook Code: WYME-052407-NSh
Promentis Code: Pro-010
Chemical Formula: $C_{12}H_{15}NO_2S$
Molecular Weight: 237.32
Log P: 2.53
Prodrug/Bioisostere: Prodrug
Monomer/Dimer: Monomer



C^{14} Uptake



Glutamate Percent Change



VIII. Conclusion.

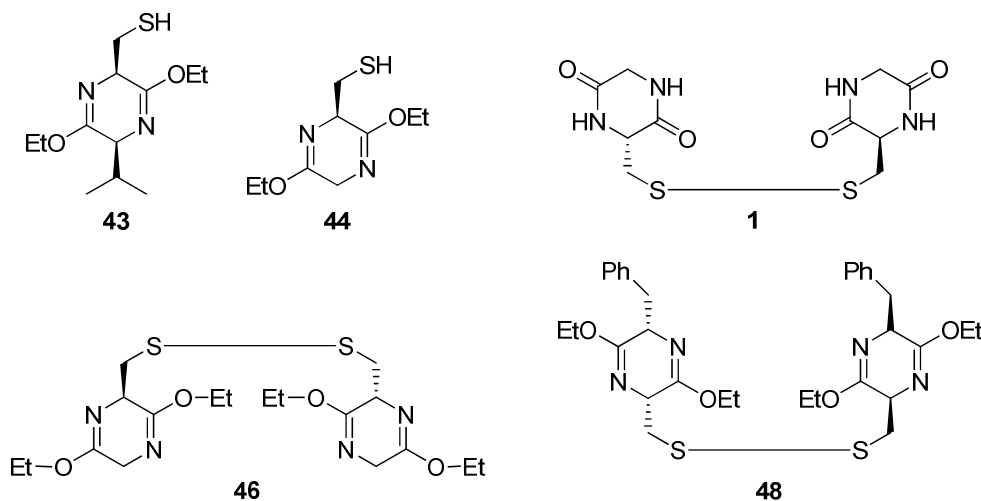
Schizophrenia is debilitating disorder that affects almost 1% of the world's population; pharmacotherapy expenditures for this disorder exceed \$10 billion dollars/year even though existing medications exhibit a poor safety/efficacy profile. It is estimated that 75% of patients discontinue drug treatment, in part due to poor safety/efficacy. Analysis of current data set demonstrate that cysteine prodrug NAC reverses the behavioral and neurochemical effects of PCP employed to model schizophrenia in rodents.

As a result, cysteine prodrugs represent a highly novel approach to treatment of schizophrenia. Indeed, these compounds may ultimately be more effective than existing medications because these drugs target the pathology underlying schizophrenia and reverse behaviors used to model negative symptoms and diminished cognition produced by PCP, which are behaviors and symptoms that are not treated with current first line medications. Specifically, therapeutic endpoints produced by cysteine prodrugs include increasing stimulation of group II metabotropic glutamate receptors and restoration of levels of glutathione. The latter effect has the potential to reverse several specific abnormalities that have been observed in schizophrenia including increased oxidative stress, decreased NMDA receptor function, altered gene expression, and abnormal cell proliferation / synaptic connectivity. Because cysteine prodrugs have several advantages relative to existing medications, it is possible that these compounds may rapidly gain a significant share of the \$10+ billion antipsychotic market.

Through the use of *in vivo* and *in vitro* screening methods, it has been shown that dialkylated diketopiperazine cystine prodrug monomers, especially compounds **43** and **44** (see **Figure 21**), demonstrates high promise as novel antipsychotic agents. Furthermore, the diketopiperazine cystine prodrug dimers, especially the lead compound **1** and dialkylated dimers **46** and **48** (see **Figure 21**), also has shown promise as novel antipsychotic agents by overcoming the detrimental effects of PCP-induced deficits in sensorimotor gating by restoring pre-pulse inhibition in multiple screenings.

Figure 21

Targets of Interest Based on Pre-Pulse Inhibition Screening Results

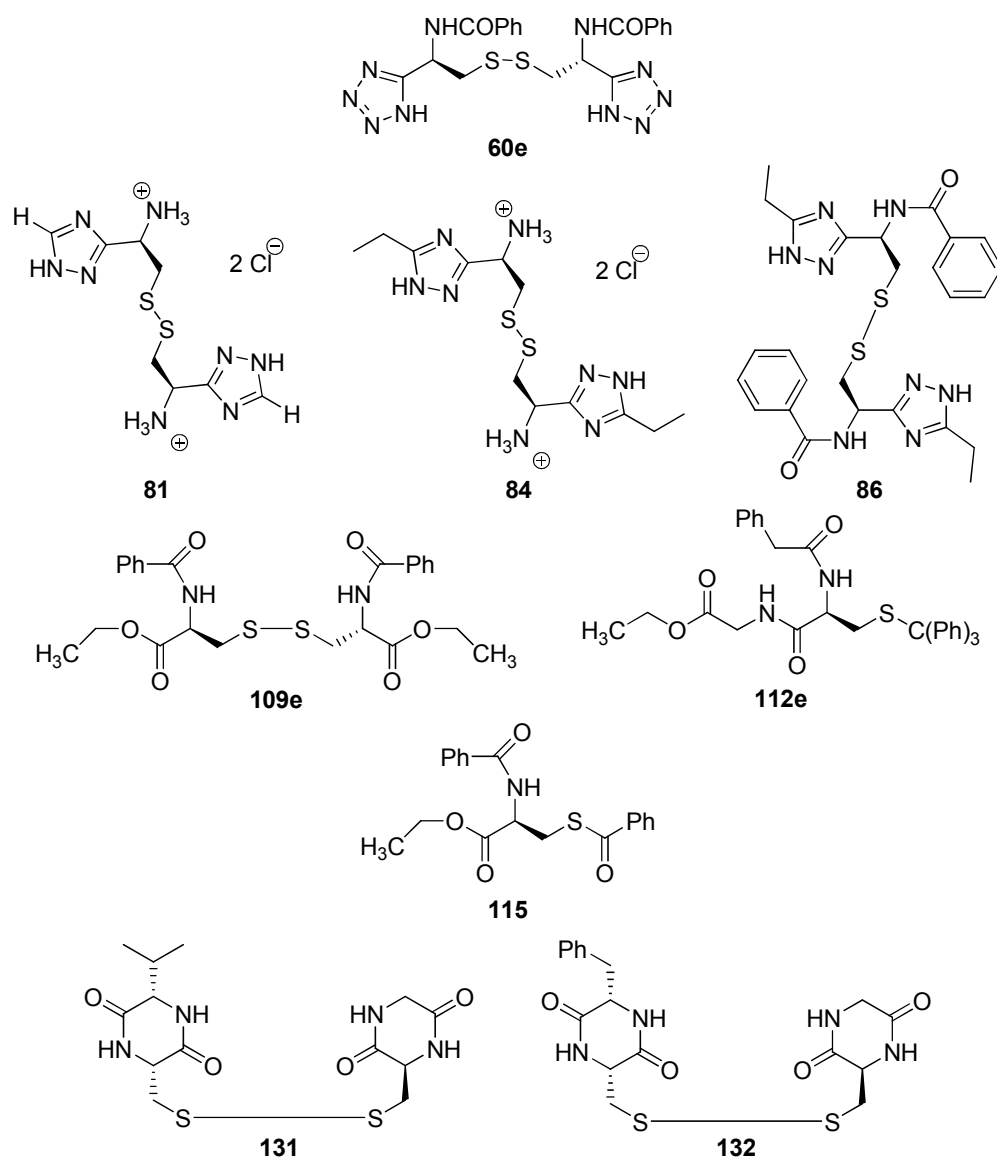


Bioisosteres, principally ligands **60e**, **81**, **84** and **86** (see **Figure 22**), of cysteine and cystine have shown vast improvements over N-Acetylcysteine by competing with C¹⁴ uptake and increasing glutamate levels by driving the cystine/glutamate antiporter. It has also been shown that simple modifications to the cysteine/cystine moiety, especially **109e**, **112e** and **115** (see **Figure 22**), also improved outcomes far greater than N-

acetylcysteine alone. Once the most effective ligands are determined by screening methods, the research would benefit by combining the two such ligands into an unsymmetrical disulfide (hetero dimer) in order to enhance their effects and help eliminate any disadvantages that we find. As an early example of this approach, ligands **131** and **132** (see **Figure 22**) have shown exciting results in recent screening methods.

Figure 22

Targets of Interest Based on C¹⁴ Uptake and
Glutamate Percent Change Screening Results

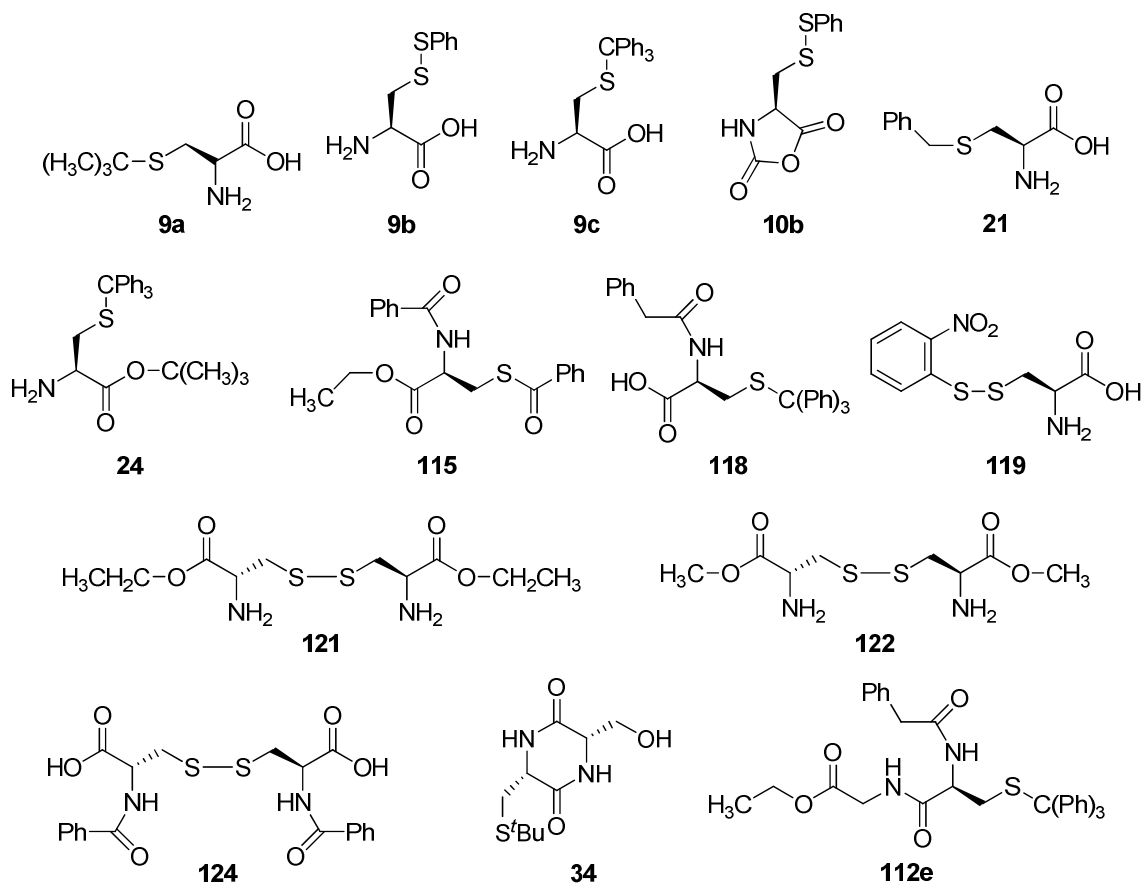


Upon further review of all target compounds and biological data a pattern becomes apparent and some general comments can be made about the structure activity relationships between the target compounds and observed biological data. Target compounds that are closely related to either cysteine and/or cystine by being either one or two biological metabolic steps from cysteine/cystine tend to be highly active, especially target compounds **9a**, **9b**, **9c**, **10b**, **21**, **24**, **115**, **118**, **119**, **121**, **122**, and **124** (see **Figure 23**).

This observation is reasonable because the human glial cells used in the *in vitro* testing have the ability to metabolize compounds. Therefore, target compounds closely related to cysteine and/or cystine will be metabolized quickly to their parent compounds cysteine/cystine. Since metabolism can take place in the *in vitro* cells, other compounds incorporated into the target compounds, such as glycine or serine, which can be liberated upon metabolism, consequently showed higher than average biological results, especially target compounds **34** and **112e** (see **Figure 23**). Glycine and serine are known modulators of the cystine/glutamate antiporter and increases the antiporter's sensitivity to cystine activity.

Figure 23

Targets of Interest that are Closely Related to Cysteine/Cystine

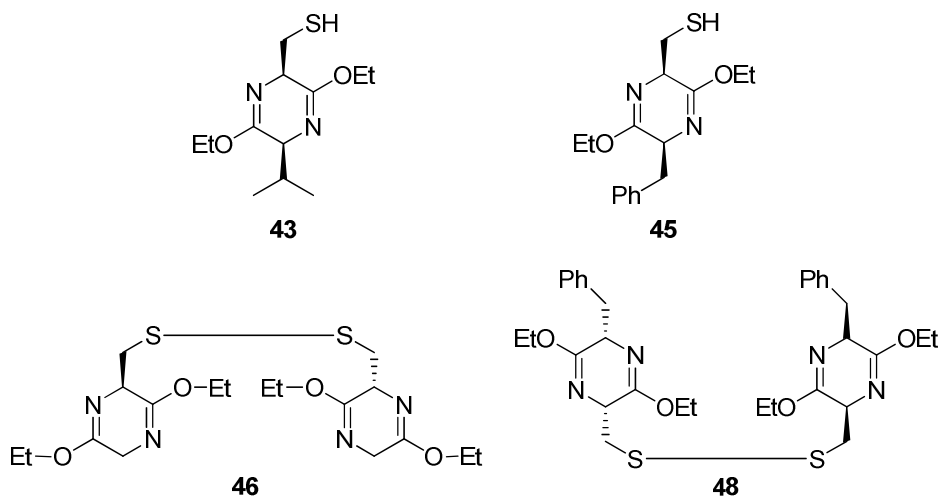


Dialkylated diketopiperazine target compounds, **43**, **45**, **46**, and **48** (see **Figure 24**), tend to exhibit higher than average biological results as compared to other diketopiperazine target compounds. This observation may well be explained by the ability of the human glial cell to rapidly metabolize the dialkylated diketopiperazine target compounds *in vitro* to their parent compounds cysteine/cystine. Dialkylated diketopiperazine compounds are more sensitive to hydrolysis and ring opening than their parent diketopiperazine. However, despite this trend, there were some dialkylated diketopiperazine target compounds that did not perform well *in vitro*, especially target

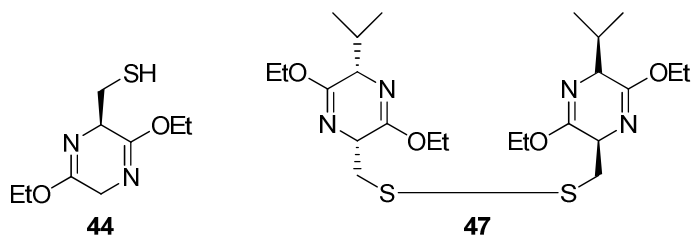
compounds **44** and **47** (see **Figure 24**). Diketopiperazine target compounds tended to have relatively lower than average biological activity. This may be due to the cells inability or slower metabolism of such target compounds.

Figure 24

Dialkylated Diketopiperazine Targets of Interest



Dialkylated Diketopiperazine Targets with Low Activity



Highly lipophilic substitutions, especially phenyl groups, on either the linear type (non-ring containing) or diketopiperazine type target compounds tended to show a higher than average biological response in vitro than other polar substituents as shown in the data for target compounds **21**, **43**, **45**, **48**, **50**, **51**, **112e**, **115**, **118**, and **124** (see **Figure**

25). Although increased lipophilicity tended to exhibit higher biological activity, it was also apparent that isopropyl groups, especially isopropyl esters, tended to have the least activity *in vitro*, as seen in the data for target compounds **88**, **90**, **92**, and **109f** (see **Figure 26**). This may be due to the cells inability or slower metabolism of such isopropyl substituted target compounds.

Figure 25

Highly Lipophilic Substituted Targets of Interest

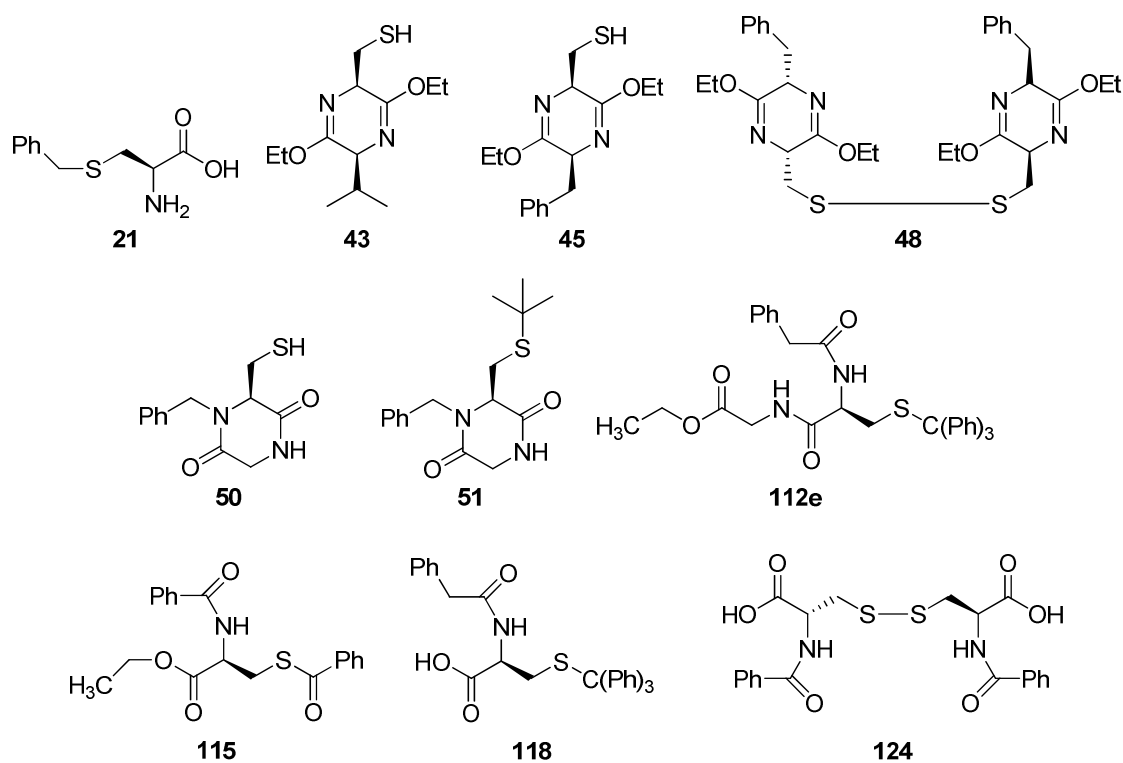
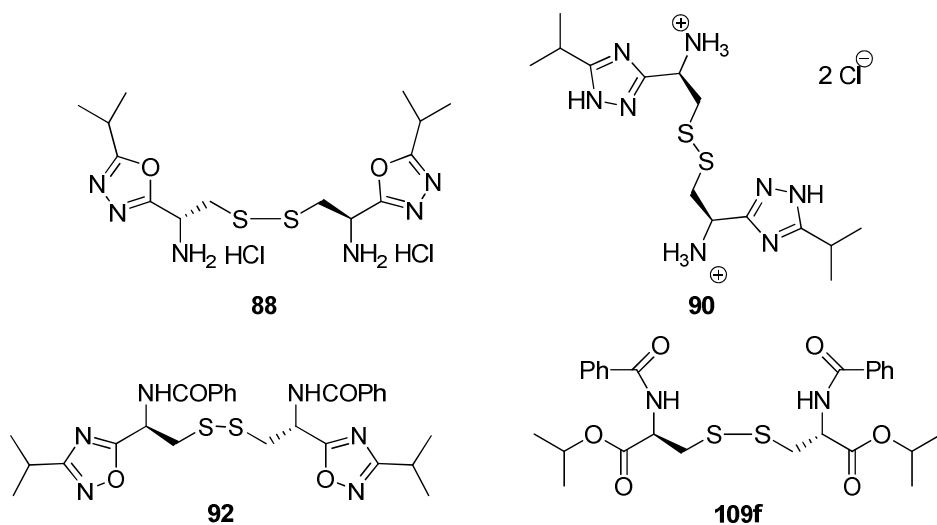


Figure 26

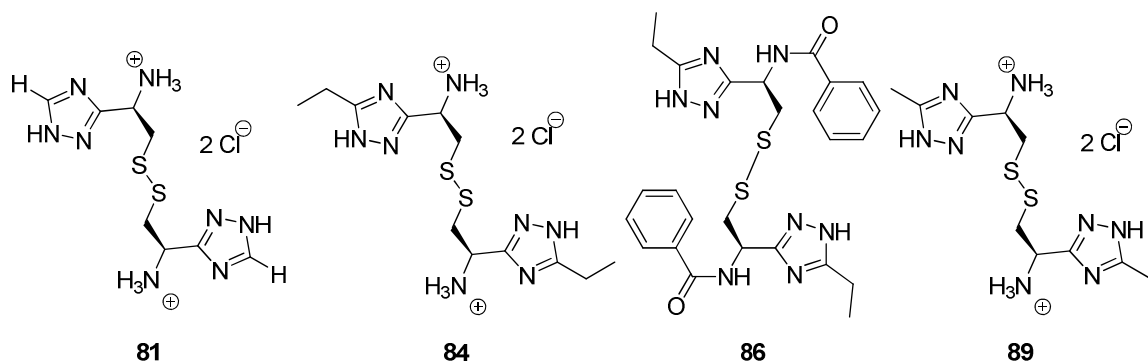
Highly Lipophilic Substituted Targets with Low Activity



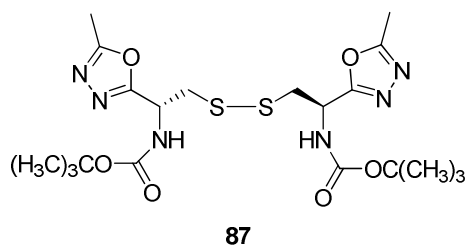
Bioisostere target compounds, especially 1,2,4-triazole bioisosteres, tend to exhibit higher than average biological activity as shown in the data for target compounds **81**, **84**, **86**, and **89** (see **Figure 27**). These results can be explained by the target compound's ability to drive the cystine/glutamate antiporter in its administered form in the *in vitro* human glial cell experiments. However, some bioisosteres such as oxadiazoles, especially 1,3,4-oxadiazole **87** (see **Figure 27**), tended to show lower than average biological results. The lack of required biological metabolism to produce an active compound is an important step forward in producing ligands to drive the cystine/glutamate antiporter and should be studied further.

Figure 27

Bioisostere Targets of Interest



Bioisostere Target with Low Activity



IX. Experimental Section.

Melting points were taken on a Thomas-Hoover melting point apparatus or an Electrothermal model IA8100 digital melting point apparatus and are uncorrected. Microanalyses were performed on a Perkin-Elmer 240C carbon, hydrogen, and nitrogen analyzer. All samples submitted for CHN analyses were first dried under high vacuum for a minimum of 6 h using a drying pistol with isopropyl alcohol as the solvent with phosphorus pentoxide in the drying bulb. Proton and carbon high resolution nuclear magnetic resonance spectra were obtained on a Bruker 300-MHz NMR spectrometer or a GE 500-MHz NMR spectrometer. The low resolution mass spectra (EI/CI) were obtained on a Hewlett-Packard 5985B gas chromatography-mass spectrometer, while high resolution mass spectra were recorded on a VG Autospec (Manchester, England) mass spectrometer. Infra-red spectra were recorded on a Nicolet MX-1 FT-IR or a Perkin Elmer 1600 Series FT-IR spectrometer. Analytical thin layer chromatography plates used were E. Merck Brinkmann UV-active silica gel (Kieselgel 60 F254) on plastic. Silica gel 60A, grade 60 for flash and gravity chromatography was purchased from E. M. Laboratories. Some high resolution mass spectra were carried out at the Centers for Mass Spectrometry, Texas A and M or the Chemistry Department of Kansas. The experimental data for some compounds have been published; see patent references 89, 90, 91, 92, 93, 94.

Preparation of 4-Methylbenzenesulfonyl Chloride.

Under a nitrogen atmosphere, N-chloro-succinimide (48.1 g, 0.36 mole) was slurried in CH_2Cl_2 (200 mL). While this solution was stirred at rt, 4-methylbenzenethiol (29.8 g, 0.24 mole) was added (2 g initial addition to start reflux and the remainder at a rate to maintain the reflux for approximately 10 min). The clear solution which resulted was then stirred at rt for 30 min. A small amount of precipitate which formed was removed by filtration. The filtrate, assumed to contain the theoretical quantity of 4-methylbenzenesulfonyl chloride (38.1 g, 0.24 mole), was used immediately and directly in the next step. Alternatively, 4-methylbenzene-sulfonyl chloride was isolated by evaporation to a solid *in vacuo* and used in the next step.

Representative Procedure for the Synthesis of the Bis-Dipiperazinedione (Symmetrical Dimers): Bis-[2,5-Piperazinedione, 3-(mercaptomethyl)-] (1).

The trityl protected diketopiperazine **27** (1.5 g, 3.73 mmol) was dissolved in a solution of CH_2Cl_2 (20 mL) and CH_3OH (40 mL) with stirring. Pyridine (1.2 mL, 15 mmol) was then added to the mixture which resulted and this was followed by addition of a solution of iodine (0.97 g, 3.8 mmol) in CH_3OH (5 mL). The mixture was allowed to stir for 1 h at rt. No precipitate had formed by this time; however, analysis by TLC (silica gel) indicated that the reaction was proceeding slowly by the appearance of a new spot under the starting material (UV light). A precipitate began to form within 2 h after

concentrating the solution to a volume of 10 mL and CH₃OH (30 mL) was added to result in a total volume of 40 mL. The solution was then stirred an additional 23 h and the precipitate which formed was removed by filtration. The solid was washed with cold CH₃OH and then decolorized by shaking with a solution of 10% aq sodium bisulfite (10 mL). The precipitate was filtered and dried to yield diketopiperazine dimer **1** as a white solid (680 mg, 57%). **1**: m.p. > 300 °C. ¹H NMR (300 MHz, DMSO-*d*₆) δ 3.11-3.21 (m, 2H), 3.70 (d, 1H, *J* = 0.96 Hz), 3.73 (d, 1H, *J* = 0.99 Hz), 4.11 (s, 1H), 8.17 (s, 1H), 8.19 (s, 1H); ¹³C NMR (75.5 MHz, DMSO-*d*₆): δ 44.0, 45.2, 54.8, 166.7, 167.1; HRMS *m/z* (M+H)⁺ calcd. 319.0535, found 319.0533.

(R)-2-Amino-3-(phenyldisulfanyl)propanoic acid (9b).

Powdered sodium bicarbonate (30 g, 0.36 mol) was added to a solution of L-cysteine hydrochloride monohydrate (47 g, 0.3 mol) in absolute EtOH (900 mL) was added at 0 °C in one portion. Phenylsulfenyl chloride (50 g, 0.345 mol) was then added dropwise with stirring to the mixture. After the complete addition of the sulfenyl chloride, the reaction mixture was allowed to stand at rt and the sodium chloride which was produced during the reaction was removed by filtration. After the mixture was brought to alkaline pH by the addition of pyridine (38 mL) into the filtrate, the fine precipitate which formed was allowed to stand for a couple of hours, then filtrated and washed well with EtOH and dried to provide the crude product as a white solid. After recrystallization from aq HCl solution (0.5 N, 4000 mL), the final ligand S-thiol-phenyl-L-cysteine (**9b**) was obtained (52 g) in 76% yield as colorless plates. **9b**: m.p. 192 °C

(decomp). ^1H NMR (300 MHz, $\text{CD}_3\text{CO}_2\text{D}$): δ 3.53-3.76 (m, 2H), 4.89 (t, 1H), 7.26-7.88 (m, 5H); ^{13}C NMR (75.5MHz, $\text{CD}_3\text{CO}_2\text{D}$): δ 35.5, 52.5, 127.6, 128.5, 129.1, 129.3, 133.5, 171.6. This material was employed directly in a later step.

2-Amino-3-tritylsulfanyl-propionic acid (*S*-Trityl-L-cysteine) (9c**).**

L-Cysteine hydrochloride (100 g, 0.634 mol) and trityl chloride (270 g, 0.969 mol) were allowed to stir in DMF (400 mL) for 2 days at rt. A 10% aq sodium acetate solution (3.5 L) was then added dropwise and the white precipitate which formed was filtered and washed with distilled water. Afterward the residue was stirred in acetone at 50 °C for 30 min, after which it was cooled to 0 °C and filtered. The precipitate which formed was washed with a small amount of acetone as well as diethyl ether and dried *in vacuo*. *S*-Trityl-L-cysteine **9c** (205 g, 89%) was obtained as a white powder. **9c**: m.p. 192 °C (decomp) ; ^1H NMR (300 MHz, $\text{DMSO}-d_6$) δ 2.45 (dd, 1H, $J = 9$ Hz, 12 Hz), 2.58 (dd, 1H, $J = 4.4$ Hz, 12 Hz), 2.91 (m, 1H), 7.22-7.36 (m, 15H); ^{13}C NMR (75.5 MHz, $\text{DMSO}-d_6$): δ 33.8, 53.7, 66.4, 127.1, 127.8, 128.1, 128.4, 129.5, 144.5, 168.4. This material was directly used in a later step without further purification.

(*R*)-4-(Phenyldisulfanyl)methyl-oxazolidine-2,5-dione (10b**).**

To a rapidly stirred (over-head stirrer) suspension of *S*-thiol-phenyl-L-cysteine **9b** (57.5 g, 0.25 mol) in THF (250 mL) was added solid triphosgene (26 g, 88 mmol) in one portion at 45-50 °C (before addition, remove the heating mantle). When the

temperature dropped to 45 °C, put the heating mantle back on and maintain the inside temperature around 45-50 °C until the solution becomes homogeneous. After the removal of the heating mantle, **the solution was purged with argon overnight into a NaOH bubbler to remove any residual phosgene.** The solvent was evaporated *in vacuo* and this provided anhydride **10b** (55 g) in 85% yield. **10b**: m.p. 217 °C (decomp) ; ¹H NMR (300 MHz, CDCl₃) δ 2.90-2.98 (m, 1H), 3.30 (d, 1H, *J* = 12 Hz), 4.68 (d, 1H, *J* = 9 Hz), 6.01 (s, 1H), 7.34-7.58 (m, 5 H); ¹³C NMR (75.5MHz, CD₃Cl₃): δ 39.4, 56.5, 128.3, 128.9, 129.5, 135.2, 150.8, 167.7. Due to the unstable nature of this anhydride it was stored in the refrigerator overnight under an atmosphere of argon and used immediately the next day without further purification.

4-Tritylsulfanylmethyl-oxazolidine-2,5-dione (10c).

This intermediate (**10c**) was prepared following the procedure for preparation of **10b** and obtained as a brown oil in 85% yield. **10c**: ¹H NMR (300 MHz, CDCl₃) δ 2.70-2.85 (m, 2H), 3.47-3.56 (m, 1H), 5.62 (s, 1H), 7.07-7.73 (m, 15H). This material was directly used in a later step without further purification.

Representative Procedure for Synthesis of Diketopiperazine Targets: 3-(mercaptomethyl)-2,5-Piperazinedione (12a**).**

a) A solution of the *N*-carboxy-anhydride **10b** (35.7 g, 0.14 mol) in THF (160 mL) was added dropwise to a vigorously stirred (overhead stirrer) mixture of glycine ethyl ester hydrochloride (28 g, 0.16 mol), freshly distilled triethylamine (20.4 g, ~ 28 mL, 0.20 mol) and dry chloroform (240 mL) at $-78\text{ }^{\circ}\text{C}$ in a three-neck flask (2 L). The reaction mixture was allowed to warm to $0\text{ }^{\circ}\text{C}$ over 8 h, and then was allowed to stir at rt for 12 h, after which the reaction solution was filtered to remove the triethylamine hydrochloride which precipitated. The filtrate was then concentrated under reduced pressure ($< 40\text{ }^{\circ}\text{C}$) and the crude dipeptide ester was used for the preparation of the diketopiperazine **12a** without further purification. ^1H NMR (300 MHz, CDCl_3): δ 1.29 (t, 3H), 1.93 (br, 2H), 2.74-2.82 (m, 1H), 3.40 (dd, 1H), 3.73 (dd, 1H), 4.03-4.19 (m, 2H), 4.19-4.26 (m, 2H), 7.34-7.58 (m, 5H). This material was used directly in the next step.

b) The crude dipeptide ester (37.6 g, 0.12 mol) was heated in refluxing toluene (1000 mL) for 12 h and then cooled to rt and kept at $0\text{ }^{\circ}\text{C}$ for 16 h. The bislactam **12a** which precipitated was isolated by vacuum filtration, washed with ether (3 x 150 mL), and dried under vacuum at $100\text{ }^{\circ}\text{C}$ to provide pure diketopiperazine **12a** (10.0 g) in 45% yield. The filtrate produced from washing the desired diketopiperazine was evaporated under vacuum and toluene (800 mL) was added to the residue. The toluene solution, which resulted, was heated at reflux for another 40 h (under argon) and then the above steps were repeated to collect another 5-8 grams of diketopiperazine **12a** (combined

yield, 73%). **12a**: m.p. 258 °C; ¹H NMR (300 MHz, DMSO-d₆): δ 3.09-3.26 (m, 2H), 3.68-3.88 (m, 2H), 4.10 (s, 1H), 8.17 (s, 1H), 8.19 (s, 1H); ¹³C NMR (500 MHz, DMSO-d₆): δ 43.5, 44.7, 54.3, 166.2, 166.6; EIMS (m/e, relative intensity) 160(M⁺, 12), 140(5), 126(72), 114(100), 97(20), 85(30). HRMS *m/z* C₅H₈N₂O₂S (M+H)⁺ calcd. 161.1942, found 161.1956.

(R)-3-(Phenyldisulfanyl)methyl-piperazine-2,5-dione (11b).

The solution which resulted from step b above, from compound **12a**, was cooled to 0 °C and kept at 0 °C for 12 h. The precipitate which resulted was filtered and provided phenyl-thiol analog **11b** in 30% yield. **11b**: ¹H NMR (300 MHz, DMSO-d₆): δ 3.09-3.21 (m, 2H), 3.65-3.82 (m, 2H), 4.10 (s, 1H), 7.11-7.55 (m, 5H), 8.18 (s, 1H), 8.20 (s, 1H); ¹³C NMR (75.5 MHz, DMSO-d₆): δ 43.5, 47.8, 54.2, 125.6, 127.7, 128.2, 129.5, 166.2, 166.6; EIMS (m/e, relative intensity) 268 (M⁺, 55), 250(35), 218(68), 159(66), 141(80), 126(70). HRMS *m/z* C₁₁H₁₂N₂O₂S₂ (M+H)⁺ calcd. 269.0340, found 269.0348.

(3R,6R)-3-Benzyl-6-(mercaptomethyl)piperazine-2,5-dione (12c).

This dione **12c** was prepared in 75% yield following the procedure for preparation of **12a** and obtained as a light yellow solid. **12c**: m.p. > 265 °C (decomp.) ; ¹H NMR (300 MHz, DMSO-d₆) δ 1.26 (d, *J* = 6.99 Hz, 1H), 3.05-3.49 (m, 2H), 3.66-3.89 (m, 3H), 4.10 (s, 1H), 7.13-7.31 (m, 5H), 8.23 (s, 1H), 8.28 (s, 1H); ¹³C NMR (75.5 MHz, CDCl₃) δ 19.0, 37.9, 44.7, 48.1, 51.2, 54.4, 126.5, 129.1, 129.4, 165.9, 166.5. EIMS (*m/e*, relative

intensity) 250 (M^+ , 10), 216(12), 160(5), 113(11), 91(100). HRMS m/z $C_{12}H_{14}N_2O_2S$ ($M+H$)⁺ calcd. 251.0776, found 251.0801.

(6R)-3-Isopropyl-6-(mercaptomethyl)piperazine-2,5-dione (12e).

This isopropyl analogue was prepared in 74% yield following the procedure for preparation of **12a** and gave dione as a white solid. **12e**: m.p. > 275 °C ; ¹H NMR (300 MHz, DMSO-*d*₆) δ 0.84 (dd, *J* = 7.14, 6.63 Hz, 3H), 0.94 (dd, *J* = 8.07, 6.9 Hz, 3H), 2.17-2.20 (m, 1H), 3.07-3.18 (m, 2H), 3.73 (s, 1H), 4.22 (s, 1H), 8.12 (s, 1H), 8.18s (s, 1H); ¹³C NMR (75.5 MHz, CDCl₃) δ 17.5, 18.8, 42.9, 53.9, 59.7, 166.7, 167.2; HRMS m/z $C_{10}H_{18}N_2O_2S_2$ ($M - H$)⁺ calcd 201.0698, found 201.0691.

(3R,8aR)-3-(Phenyldisulfanyl)methyl-hexahydropyrrolo[1,2-a]pyrazine-1,4-dione (25).

This phenyldisulfanyl analogue was prepared in 82% yield following the procedure for preparation of **11b** and gave dione **25** as a yellow solid. **25**: m.p. 120 °C ; ¹H NMR (300 MHz, CDCl₃) δ 1.66-2.02 (m, 1H), 2.03-2.11 (m, 2H), 2.36 (m, 1H), 2.80-2.89 (m, 1H), 3.54-3.62 (m, 3H), 4.07-4.10 (m, 1H), 4.39 (dd, *J* = 1.83, 1.77 Hz, 1H), 6.35 (s, 1H), 7.28-7.57 (m, 5H); ¹³C NMR (75.5 MHz, CDCl₃) δ 22.5, 28.2, 38.5, 45.4, 53.3, 59.1, 127.8, 128.6, 129.2, 135.6, 164.3, 169.0. HRMS m/z $C_{14}H_{16}N_2O_2S_2$ ($M+H$)⁺ calcd. 309.0653, found 309.0635.

3-Tritylsulfanylmethyl-piperazine-2,5-dione (27).

This trityl analogue was prepared following the similar procedure for preparation of **12a**. **27**: m.p. 225 – 227 °C. $[\alpha]_D^{26} = +7.8^\circ$ (c = 1.05, CHCl₃). ¹H NMR (300 MHz, CDCl₃) δ 2.73-2.91 (m, 2H), 3.12 (d, 1H, *J* = 12.3 Hz), 3.95 (s, 1H), 5.80 (s, 1H), 5.82 (s, 1H), 7.20-7.62 (m, 15H). ¹³C NMR (75.5 MHz, CDCl₃): δ 35.9, 44.8, 53.0, 126.9, 128.1, 129.4, 144.0, 166.6. HRMS *m/z* C₂₄H₂₂N₂O₂S (M+H)⁺ calcd. 402.1402, found 402.1398. This material was directly used in a later step without further purification.

(6R)-3-(tert-Butylthiomethyl)-6-(mercaptomethyl)piperazine-2,5-dione (32).

This dione was prepared in 70% yield following the procedure for preparation of **12a** and gave dione **32** as a yellow solid. **32**: m.p. > 280 °C (decomp.) ; ¹H NMR (300 MHz, DMSO-d₆) δ 1.25 (s, 9H), 2.88-2.92 (m, 1H), 3.03-3.10 (q, *J* = 7.5 Hz, 1H), 3.18-3.21 (m, 1H), 3.51 (d, *J* = 14.4 Hz, 1H), 4.14 (s, 2H), 8.13 (s, 1H), 8.24 (s, 1H); ¹³C NMR (75.5 MHz, CDCl₃) δ 31.1, 32.1, 43.2, 47.8, 54.1, 54.9, 166.3, 170.8; EIMS (*m/e*, relative intensity) 262 (M⁺, 30), 228(40), 206(45), 173(50), 160(70), 126(100); HRMS *m/z* C₁₀H₁₈N₂O₂S₂ (M + H)⁺ calcd 263.0482, found 263.0489.

(3S,6S)-3-Benzyl-6- (2R,5R)-5-benzyl-3,6-dioxopiperazin-2-yl-methyl-disulfanyl-methyl-piperazine-2,5-dione (36).

This benzyl analogue was prepared in 63% yield following the procedure for preparation of **1** employing starting material **29** and gave dione **36** as a yellow solid. **36**: m.p. > 280 °C (decomp.); ¹H NMR (300 MHz, CDCl₃) δ 1.29 (s, 9 H), 2.85-2.92 (m, 2 H), 3.10-3.13 (m, 2 H), 4.14 (s, 2 H), 8.12 (s, 2 H); ¹³C NMR (75.5 MHz, CDCl₃): δ 31.1, 32.1, 42.5, 43.2, 53.9, 54.1, 166.2, 166.3. HRMS *m/z* C₂₄H₂₂N₂O₂S (M+H)⁺ calcd. 403.1402, found 403.1415.

(3R,6S)-3-(tert-Butylthiomethyl)-6-((((2R,5S)-5-(tert-Butylthiomethyl)-3,6-dioxo-piperazin -2-yl)methyl) disulfanyl)methyl)piperazine-2,5-dione (37).

This *S-tert*-butyl dione dimer was prepared in 65% yield following the procedure for preparation of **1**, using *S*-trityl, *S'*-*tert*-butyl dione starting material **33** and gave dione **37** as a yellow solid. **37**: m.p. 278 °C ; ¹H NMR (300 MHz, CDCl₃) δ 1.29 (s, 9 H), 2.85-2.92 (m, 2 H), 3.10-3.13 (m, 2 H), 4.14 (s, 2 H), 8.12 (s, 2 H); ¹³C NMR (75.5 MHz, CDCl₃): δ 31.1, 32.1, 42.5, 43.2, 53.9, 54.1, 166.2, 166.3. HRMS *m/z* C₂₀H₃₄N₄O₄S₄ (M+H)⁺ calcd. 523.1463, found 523.1448.

(3R,3'R,6R,6'R)-6,6'-Disulfanediylbis(methylene)bis(3-isopropylpiperazine-2,5-dione) 38.

This dione (**38**) was prepared in 65% yield following the procedure for preparation of **1**, using S-trityl dione starting material **31** and obtained as a white solid (**38**): m.p. 270 °C ; ¹H NMR (300 MHz, CDCl₃) δ 0.86 (d, *J* = 6.75 Hz, 3 H), 0.96 (d, *J* = 7.05 Hz, 3 H), 2.17-2.21 (m, 1 H), 3.07-3.19 (m, 2 H), 3.72 (s, 1 H), 4.33 (s, 1 H), 8.11 (s, 1 H), 8.17 (s, 1 H); ¹³C NMR (75.5 MHz, CDCl₃): δ 17.5, 18.8, 31.4, 42.9, 53.9, 59.7, 166.7, 167.2; HRMS *m/z* (M+H)⁺ calcd. 403.1474, found 403.1479.

Representative Procedure for Synthesis of Dialkylated

Diketopiperazine: Preparation of Triethyloxonium tetrafluoroborate.⁷⁹

Note: Triethyloxonium tetra-fluoroborate is an expensive reagent; however, it is relatively easy to prepare even on large scale. A three-neck flask (500 mL), pressure equilibrating dropping funnel (125 mL) and a condenser were dried in an oven at 150 °C and assembled while hot under an atmosphere of argon. When the equipment had cooled to rt, ether [(100 mL) which had been previously dried over sodium benzophenone ketyl] and boron trifluoride diethyletherate (91 g, ~87 mL, 64 mmol) were combined [Note: On this scale the colorless BF₃ etherate was obtained from a freshly opened new bottle. If the reagent was slightly yellow or if the reaction was scaled down, the BF₃ etherate required vacuum distillation first].

The ethereal solution which resulted was heated to a gentle reflux after which dry epichlorohydrin (48.8 g, ~ 41 mL, 51.8 mmol) was added dropwise over 1 h. The mixture was heated at reflux for an additional 1 h and allowed to stand at rt (under argon) overnight. The ether was removed by applying a positive pressure of argon in one neck of the flask while forcing the ether out through a filter stick (fritted glass tube) inserted into another neck of the flask and into a collection flask. The slightly yellow solid which remained in the flask was rinsed twice in the same manner with anhydrous ether (3 x 50 mL) to provide a crystalline white solid. The solid was not weighed but directly used in the next step. The following sequence was based on the yield of this reaction process at the level of 80-85%.

(3,6-Diethoxy-2,5-dihydro-,pyrazin-2-yl)-methanethiol (44).

Dry CH₂Cl₂ (100 mL) was added to the flask (500 mL) which contained the freshly prepared triethyloxonium tetrafluoroborate (~42 g, 336 mmol) from the previous reaction (under argon). To this solution was added the dry diketopiperazine **12a** (5 g, 31.2 mmol) in portions with stirring (overhead stirrer). After 2 h the reaction mixture became homogenous. The solution was allowed to stir at rt under argon for 72 h after which the mixture was added *via* a cannula to an aq solution of NH₄OH (14%, 100 mL) mixed with ice (100 g). The organic layer was washed with a dilute aq solution of 0.1 N NaHCO₃ (2 x 50 mL) and brine (80 mL), after which it was dried (K₂CO₃). After filtration the solvent was removed under reduced pressure to provide the bis-ethoxy lactim ether **44** as a clear yellow liquid that was further purified by flash chromatography (EtOAc : hexane = 1:4) in 71% yield (4.8 g, 22 mmol). **44**: [α]_D²⁶ = +52.2 ° (c = 2.5, CHCl₃). ¹H NMR (300 MHz, CDCl₃) δ 1.32-1.36 (m, 6 H), 3.27-3.30 (m, 3 H), 4.08-4.22 (m, 6 H), 4.39 (s, 1H); ¹³C NMR (75.5 MHz, CDCl₃): δ 14.7, 46.3, 47.5, 56.1, 61.5, 61.6, 162.7, 163.6; HRMS *m/z* C₉H₁₆N₂O₂S (M+H)⁺ calcd. 217.2982, found 217.2990.

Bis[(3,6-Diethoxy-2,5-dihydro-pyrazin-2-yl)-methanethiol] (46).

To the bis-ethoxy lactim ether **44** (400 mg, 1.85 mmol) in dry EtOH (10 mL) was added a catalytic amount of I₂ (50 mg, 10 % mmol) at rt. The mixture was allowed to stir for 6~ 12 h under air until the analysis (TLC, silica gel) indicated the reaction was complete (new spot appeared under S.M. on the TLC plate). The organic solvent was

removed under reduced pressure. The mixture which resulted was dissolved into EtOAc (20 mL), washed with a saturated aq solution of sodium thiosulfate (5 ~ 10 mL) and dried (Na_2SO_4). The solvent was then removed under reduced pressure which provided the dimer **46**: ^1H NMR (300 MHz, CDCl_3) δ 1.32-1.36 (m, 6 H), 3.27-3.30 (m, 3 H), 4.08-4.22 (m, 6 H), 4.39 (s, 1H); ^{13}C NMR (75.5 MHz, CDCl_3): δ 14.7, 46.3, 47.5, 56.1, 61.5, 61.6, 162.7, 163.6; The NMR spectra was identical to its monomer except the S-H bond had disappeared. HRMS m/z $\text{C}_{18}\text{H}_{30}\text{N}_4\text{O}_4\text{S}_2$ (M+H) $^+$ calcd. 431.1787, found 431.1790.

1,2-Bis(2R,5R)-3,6-diethoxy-5-isopropyl-2,5-dihydropyrazin-2-yl-methyl-disulfane (47).

This disulfane (**47**) was prepared in 60% yield following the procedure for preparation of **46**, using starting material **43** and gave **47** as a colorless liquid. **47**: ^1H NMR (300 MHz, CDCl_3) δ 0.76-0.78 (m, 3 H), 1.06-1.09 (m, 3 H), 1.25-1.31 (m, 6 H), 2.18-2.23 (m, 1 H), 2.82-3.01 (m, 1 H), 3.21-3.45 (m, 1 H), 3.54-3.70 (m, 2 H), 4.07-4.33 (m, 4 H); ^{13}C NMR (75.5 MHz, CDCl_3): δ 14.2, 17.3, 31.1, 31.7, 45.2, 55.3, 60.5, 60.7, 161.0, 163.1; HRMS m/z $\text{C}_{24}\text{H}_{42}\text{N}_4\text{O}_4\text{S}_2$ (M+H) $^+$ calcd. 515.2726, found 515.2731.

1,2-Bis(2R,5R)-5-benzyl-3,6-diethoxy-2,5-dihydropyrazin-2-yl-methyl-disulfane (48).

The dimer (**48**) was prepared in 65% yield following the procedure for preparation of **46**, using starting material **45** and obtained (**48**) as a yellow liquid. **48**: ^1H NMR (300 MHz, CDCl_3) δ 1.26-1.35 (m, 6 H), 2.45-2.57 (m, 1 H), 3.05-3.22 (m, 2 H), 3.50-3.82 (m, 1H), 4.07-4.18 (m, 5 H), 4.32-4.38 (m, 1H), 7.06-7.28 (m, 5 H); ^{13}C NMR (75.5 MHz, CDCl_3): δ 14.3, 39.6, 42.9, 43.0, 54.9, 57.1, 60.7, 60.8, 126.2, 126.5, 127.8, 137.0, 162.2, 162.6; The NMR spectra was identical to its monomer except the S-H bond had disappeared. HRMS m/z $\text{C}_{32}\text{H}_{42}\text{N}_4\text{O}_4\text{S}_2$ (M+H) $^+$ calcd. 611.2681, found 611.2677.

(3R,6R)-6-Benzyl-5-ethoxy-3-(ethylthiomethyl)-1,6-dihydropyrazin-2(3H)-one (49).

This benzyl analogue (**49**) was prepared in 30% yield following the procedure for preparation of **44** using only 1 equiv of triethyloxonium tetrafluoroborate and starting material **12c**, in which **49** was obtained as a yellow solid. **49**: m.p. 118 °C ; ^1H NMR (300 MHz, CDCl_3) δ 1.19 (t, $J = 7.41$ Hz, 3 H), 1.30 (t, $J = 7.08$ Hz, 3 H), 2.37-2.45 (m, 3 H), 2.82-3.01 (m, 1 H), 2.95 (d, $J = 3.09$ Hz, 1 H), 3.03 (d, $J = 3.12$ Hz, 1 H), 3.23 (q, $J = 32.6, 5.1$ Hz, 2 H), 4.14-4.19 (m, 2 H), 4.46-4.47 (m, 1 H), 6.19 (s, 1 H), 7.17-7.29 (m, 5 H); ^{13}C NMR (75.5 MHz, CDCl_3): δ 14.1, 14.5, 25.7, 35.4, 39.8, 50.6, 60.0, 61.6, 126.5,

127.8, 130.2, 136.7, 157.8, 170.1; HRMS m/z $C_{16}H_{22}N_2O_2S$ (M+H)⁺ calcd. 305.1515, found 305.1522.

(R)-2-(tert-Butoxycarbonylamino)-3-(tritylthio)propanoic acid (54c).

Di-*tert*-butyldicarbonate (41 g, 187 mmol) was added to the solution of trt-cys-OH (22.68 g, 62.5 mmol) in dioxane (60 mL) and water (125 mL) at 45 °C, and the solution was adjusted with NaOH (4 M) until pH = 9.5. It was then allowed to stir at the same temperature overnight, after which, the water and dioxane were removed under reduced pressure. The residue was dissolved in water (150 mL) and extracted with EtOAc (2 x 100 mL). The aq layer was adjusted to pH = 2 with dilute aq HCl while in an ice bath and then the aq layer was extracted with EtOAc. The combined EtOAc layers were washed with water and dried over anhydrous magnesium sulfate. The removal of the solvent under vacuum yielded a yellow oil. The residue was then dissolved into ethyl ether and a 1:1 mixture of ethyl ether and hexane were carefully added while stirring to precipitate out the white solid in 60% yield. **54c**: ¹H NMR (300 MHz, CDCl₃): δ 1.46 (s, 9H), 2.69 (br, 2H), 4.21 (s, 1H), 4.97 (s, 1H), 7.20-7.44 (m, 15H), 10.2 (br, 1H); ¹³C NMR (75.5 MHz, CDCl₃): δ 28.1, 33.5, 52.4, 144.1, 155.4, 175.1. HRMS m/z $C_{27}H_{29}NO_4S$ (M+H)⁺ calcd. 464.1817, found 464.1815.

N, N' –Bis(*tert*-Butoxy)carbonylcystine (93).

A solution of di-*tert*-butyldicarbonate (41 g, 0.187 mol, 3 equiv) in dioxane (60 mL) was added at 0 °C to a solution of commercial L-cysteine (15 g, 0.06 mol) in aq NaOH (1 M; 125 mL). The reaction mixture which resulted was allowed to stir at 0 °C for 5 min and then at rt overnight. Half the volume of dioxane was removed under reduced pressure and the mixture which remained was extracted with EtOAc (3 x 50 mL). The combined aq phases were brought to pH = 1 with an aq solution of HCl (1 M) and extracted with EtOAc (3 x 50 mL). The combined organic layers were washed with brine, dried (anhydrous Na₂SO₄), filtered and concentrated under reduced pressure to afford protected cystine in 65% yield as white solid. **93**: m.p. 148 ~ 151 °C. ¹H NMR (DMSO-d₆): δ 1.46 (s, 9H), 2.84-2.92 (m, 1H), 3.07-3.13 (m, 1H), 7.19 (d, 1H, *J* = 9Hz), 12.8 (s, 1H); ¹³C NMR (75.5MHz, DMSO-d₆): δ 28.5, 53.0, 54.1, 78.6, 85.9, 155.7, 172.8. This material was employed directly in a later step.

(R)-*tert*-Butyl-1-(3-isopropyl-1,2,4-oxadiazol-5-yl)-2-(tritylthio) ethylcarbamate (94).

A solution of DCC (3.56 g, 17.28 mmol) in THF (20 mL) was added to a solution of trityl protected Boc-L-cysteine **54c**, (3.7 g, 8 mmol), isobutyl-imidoxine (1.75 g, 17.16 mmol), hydroxysuccinimide (19.7 g, 17.16 mmol) in THF (50 mL) at 0 °C over 15 min. The mixture was allowed to stir for 16 h while the temperature was allowed to warm to rt.

The mixture was then cooled to 0 °C and the precipitate which formed was removed by filtration. The filtrate was concentrated under vacuum and then dissolved into EtOAc (50 mL). The small amount of precipitate that formed was filtered off. The organic layer was washed with a dilute aq solution of 0.1 N NaHCO₃, brine, dried (anhydrous Na₂SO₄) and removed under reduced pressure to give the trityl protected Boc-L-cysteine acetamidoxime ester as white crystals. This material was taken up in toluene (200 mL) and the mixture which resulted was heated at reflux for 3 h; the water which formed was removed by a Dean-Stark trap. The solvent was removed under vacuum and the residue was purified by flash chromatography (hexane/EtOAc = 9:1) to form white crystals in 71% yield. **94** : ¹H NMR (300 MHz, CDCl₃): δ 1.15 (d, 6H, *J* = 3Hz), 1.44 (s, 9H), 2.67 (br, 1H), 3.03-3.07 (m, 1H), 4.18 (s, 1H), 5.03 (s, 1H), 7.23-7.46 (m, 15H), 8.76 (s, 1H); ¹³C NMR (75.5 MHz, CDCl₃): δ 19.6, 27.6, 28.1, 54.3, 67.1, 80.6, 126.7, 128.4, 129.4, 144.4, 155.3, 170.3, 177.6. HRMS *m/z* C₃₁H₃₅N₃O₃S (M+H)⁺ calcd. 530.2399, found 530.2387.

**General Procedure for the Cleavage of Disulfide Bonds on Bioisosteres:
Used for the Synthesis of Ligands 96, 98, 100 and 102.**

The bioisosteric disulfide (1 mmol) (**97**, **99**, **101** or **103**) was dissolved in 10 mL of EtOH and indium (1.1 mmol) was added in one portion with stirring. Then anhydrous NH₄Cl (2.2 mmol) was added to the suspension while stirring. The mixture which resulted was heated to reflux under argon for 4-6 hrs. After 4-6 hrs the solids were removed by filtration over a bed of celite. The solvent was removed under reduced

pressure until dryness. The residue was washed well with water to dissolve the inorganic salts. The mixture was filtered and dried to yield the product. The monomer (see below) can be purified by crystallization from dichloromethane (DCM) or EtOH. Yield 85-90%.

(R)-tert-Butyl-2-mercapto-1-(5-methyl-1H-1,2,4-triazol-3-yl) ethylcarbamate [R = CH₃] (96).

The carbamate (**96**) was prepared using the general procedure described above for the cleavage of disulfide bonds of bioisosteres starting with dimer **97** which was converted into monomer **96**: ¹H NMR (300 MHz, CDCl₃) δ 6.44 (d, 1H), 5.30 (s, 1H), 3.37 – 3.78 (m, 2H), 2.93 (s, 3H), 1.48 (s, 9H); ¹³C NMR (75 MHz, CDCl₃) δ 158.2, 155.8, 128.1, 127.8, 127.5, 81.0, 45.2, 28.3, 13.3 ppm. HRMS (ESI, M⁺+H, C₁₀H₁₉N₄O₂S) calc.: 259.1229, found: 259.1237 and (M⁺+Na, C₁₀H₁₈N₄O₂SNa) calcd. 281.1048, found 281.1056.

(R)-tert-Butyl-1-(5-ethyl-1H-1,2,4-triazol-3-yl)-2-mercapto ethylcarbamate [R = CH₂CH₃] (98).

The ethyl carbamate (**98**) was prepared using the general procedure described above for the cleavage of disulfide bonds of bioisosteres starting with dimer **99** which was converted into monomer **98**: ¹H NMR (300MHz, CDCl₃) δ 6.21(d,1H), 5.09(s, 1H),

2.94-3.54(m,2H), 2.79 – 2.87 (q, J=7.5, 2H), 1.45(s, 9H), 1.27-1.34(t, J=7.5,3H). HRMS (ESI, M⁺+H, C₁₁H₂₁N₄O₂S) calcd. 273.1385, found: 273.1392.

(R)-tert-Butyl-2-mercapto-1-(5-phenyl-1H-1,2,4-triazol-3-yl)ethylcarbamate [R = Ph] (100).

The phenyl analogue (**100**) was prepared using the general procedure described above for the cleavage of disulfide bonds of bioisosteres starting with dimer **101** which was converted into monomer **100**: ¹H NMR (300MHz, CDCl₃) δ 7.94-8.01(d,2H), 7.46(s,3H), 6.23(s,1H), 5.13(s,1H),2.95-3.64(m, 2H), 1.48(s,9H); HRMS (ESI, M⁺+H, C₁₅H₂₁N₄O₂S) calcd. 321.1385, found: 321.1391.

(R)-tert-Butyl-1-(5-isopropyl-1H-1,2,4-triazol-3-yl)-2-mercaptoethylcarbamate [R = CH(CH₃)₂] (102).

The isopropyl analogue (**102**) was prepared using the general procedure described above for the cleavage of disulfide bonds of bioisosteres starting with dimer **103** converted to **102**: ¹H NMR (300 MHz, CDCl₃) δ 6.44 (d, 1H), 5.16 (s, 1H), 2.81 – 3.66 (m, 3H), 1.48 (s, 9H), 1.37(s,6H); ¹³C NMR (75 MHz, CDCl₃) δ 159.3, 155.8, 142.1, 133.7, 81.1, 57.2, 39.8, 28.3, 21.5 ppm. HRMS (ESI, M⁺+H, C₁₂H₂₃N₄O₂S) calc.: 287.1542, found: 287.1547 and (M⁺+Na, C₁₂H₂₂N₄O₂SNa) calcd. 309.1361, found 309.1354.

***tert*-Butyl (1R,1'R)-2,2'-disulfanediybis(1-(3-isopropyl-1,2,4-oxadiazol-5-yl)ethane-2,1-diyl)dicarbamate (104).**

A solution of DCC (1.78 g, 8.64 mmol) in THF (10 mL) was added to a solution of Boc-L-cystine, previously prepared above, **93**, (1.8 g, 4 mmol), isobutyl-imidoxine (875 mg, 8.58 mmol), hydroxysuccimide (987 mg, 8.58 mmol) in THF (20 mL) was added at 0 °C over 15 min. The mixture which resulted was allowed to stir for 16 h while the temperature was allowed to warm to 20 °C. The mixture was then cooled to 0 °C and the precipitate which formed was removed by filtration. The filtrate was concentrated under vacuum and then dissolved into EtOAc (50 mL). The small amount of precipitate which formed was filtered off. The organic layer was washed with a dilute aq solution of 0.1 N sodium bicarbonate, brine, dried (anhydrous Na₂SO₄) and removed under reduced pressure to give Boc-L-cystine bis(acetamidoxime) ester as white crystals. This material was taken up in toluene (100 mL) and the mixture was heated at reflux for 3 h; the water which formed was removed by a Dean-Stark trap. The solvent was removed under vacuum and the residue was purified by flash chromatography (hexane/EtOAc = 9:1) to furnish white crystals in 73% yield as white solid. **104**: m.p. 130 ~ 131 °C. ¹H NMR (300 MHz, CDCl₃): δ 1.33 (d, 6H, *J* = 4.5 Hz), 1.46 (s, 9H), 3.03-3.13 (m, 1H), 3.25 (d, 2H, *J* = 3Hz), 5.32 (s, br, 1H), 5.51 (s, br, 1H); ¹³C NMR (75.5 MHz, CDCl₃): δ 20.2, 26.6, 28.2, 42.1, 47.8, 80.8, 154.6, 175.0, 176.8. HRMS *m/z* C₂₄N₄₀N₆O₆S₂ (M+H)⁺ calcd. 573.2451, found 573.2445.

***tert*-Butyl (1R,1'R)-2,2'-disulfanediylbis(1-(3-methyl-1,2,4-oxadiazol-5-yl)ethane-2,1-diyl)dicarbamate (105).**

The dicarbamate (**105**) was prepared in 50% yield following the above procedure for **104**, except the solvent was replaced with DMF to dissolve acetamidoxine. **105**: m.p. 138 ~ 140 °C. ¹H NMR (500 MHz, CDCl₃): δ 1.40 (s, 9H), 2.35 (s, 3H), 3.23 (s, 2H), 5.27 (s, 1H), 5.82 (s, 1H); ¹³C NMR (500 MHz, CDCl₃): δ 11.8, 28.5, 42.2, 48.0, 81.0, 155.2, 167.6, 176.7. HRMS *m/z* C₂₄H₄₀N₆O₆S₂ (M + H)⁺ calcd 517.1903, found 517.1912.

(1R,1'R)-2,2'-Disulfanediylbis(1-(3-methyl-1,2,4-oxadiazol-5-yl)ethanamine) (106a).

TFA (5 mL) was slowly added to a solution of acetamidoxine **105** (120 mg, 0.23 mmol) in DCM (5 mL) which had been cooled to 0 °C. The solution was allowed to gradually warmed to rt while stirring and then allowed to stir for 2 h until analysis by TLC (silica gel) indicated the starting material had disappeared. The solvent was removed under reduced pressure and the residue was dissolved in EtOAc (20 mL), washed with a saturated aq solution of sodium bicarbonate, brine and dried (anhydrous Na₂SO₄). The solvent was removed and ethyl ether (2 mL) was added into the oil which had formed. Ethyl ether saturated with anhydrous HCl gas was added at 0 °C until a white solid precipitated out. The solid was then collected by filtration and yielded the hydrochloride salt of **106a** in 92% yield. **106a**: ¹H NMR (300 MHz, CDCl₃): δ 2.40 (s,

3H), 3.07-3.16 (m, 1H), 3.26-3.34 (m, 1H), 4.55-4.59 (m, 1H); ^{13}C NMR (75.5 MHz, CDCl_3): δ 11.3, 43.9, 48.0, 167.1, 179.3. HRMS m/z $\text{C}_{10}\text{H}_{16}\text{N}_6\text{O}_2\text{S}_2$ ($\text{M} + \text{H}$) $^+$ calcd 317.0854, found 317.0850.

(1R,1'R)-2,2'-Disulfanediylbis(1-(3-isopropyl-1,2,4-oxadiazol-5-yl)ethanamine) (106b).

The oxadiazole (**106b**) was prepared in 89% yield following the procedure for preparation of **106a**. **106b**: ^1H NMR (300 MHz, CDCl_3): δ 1.34 (d, 6H, $J = 3\text{Hz}$), 2.8 (br, 2H), 3.08-3.15 (m, 1H), 3.26-3.34 (m, 2H), 4.70 (br, 1H); ^{13}C NMR (75.5 MHz, CDCl_3): δ 20.3, 28.0, 44.1, 48.2, 170.5, 179.6. HRMS m/z $\text{C}_{14}\text{H}_{24}\text{N}_6\text{O}_2\text{S}_2$ ($\text{M} + \text{H}$) $^+$ calcd. 373.1402, found 373.1418.

Phenyl acetyl-S-trityl-L-cysteine (108g).

A solution of phenylacetyl chloride (1.8 g, 12 mmol) in chloroform (20 mL) was added to a suspension of S-trityl-L-cysteine **9c** (4.4 g, 12 mmol) in chloroform (92 mL) containing triethylamine (2.7 g, 26.4 mmol) cooled in ice. The mixture which resulted was allowed to stir at 0–5 °C for 15 min. and then at rt for 24 hrs. Water was added (100 mL) and the pH was adjusted to 1.5 with a 5 N aq solution of HCl. The aq phase was removed and the organic phase was washed with a saturated aq solution of sodium chloride (100 mL), dried (anhydrous Na_2SO_4) and concentrated *in vacuo* to give a white crystalline solid (4.9 g) in 85% yield. **108g**: m.p. 60-62 °C ; $[\alpha]_{\text{D}} = +21.8^\circ$ (c 2,

CH₃OH); ¹H NMR (300 MHz, CDCl₃): δ 2.60-2.71 (m, 2 H), 3.5 (s, 1 H), 4.15-4.23 (m, 1 H), 5.92 (d, *J* = 6.48 Hz, 1 H), 7.21-7.33 (m, 20 H); ¹³C NMR (75.5 MHz, CDCl₃): δ 32.9, 43.1, 51.4, 67.8, 126.8, 127.2, 127.4, 127.8, 127.9, 128.4, 128.9, 129.1, 129.4, 144.1, 171.5, 172.5. This material was used directly in the next step.

N-Carbobenzoxy-S-trityl-L-cysteinylglycine ethyl ester (112e).

Phenyl acetyl-S-trityl-L-cysteine **108g** (4.8 g, 10 mmol) and N, N'-dicyclohexycarbodiimide (2.1 g, 10 mmol) were added to a solution of glycine ethyl ester hydrochloride (1.25 g, 9 mmol) in chloroform (50 mL) and triethylamine (1.25 mL). After the mixture was allowed to stir at rt for 12 h, this was followed by addition of a few drops of 50% aq acetic acid and the insoluble precipitate of dicyclohexylurea (1.7 g) which formed was removed by filtration. The filtrate was washed with dilute solutions of 0.1 N aq hydrochloric acid, 0.1 N potassium hydrogen carbonate and water, dried over anhydrous sodium sulfate and evaporated to dryness *in vacuo*. The residue was treated with EtOAc. Some undissolved material (dicyclohexylurea, 0.5 g) was filtered off and the filtrate was concentrated *in vacuo* to a small volume. Crystalline **112e** was filtered off in 85 % yield. **112e**: m.p. 152 °C; ¹H NMR (300 MHz, CDCl₃): δ 1.23-1.32 (m, 3 H), 2.57-2.62 (m, 2 H), 3.53 (s, 1 H), 3.87-3.91 (m, 2 H), 4.13 (d, *J* = 6.18 Hz, 1 H), 4.15-4.23 (m, 2 H), 5.91 (d, *J* = 7.41 Hz, 1 H), 6.55 (s, 1 H), 7.21-7.45 (m, 20 H); ¹³C NMR (75.5 MHz, CDCl₃): δ 14.0, 33.0, 41.3, 43.3, 51.9, 61.4, 67.0, 126.8, 127.3, 127.9, 128.9, 129.3, 129.5, 134.1, 144.3, 169.1, 169.9, 171.1. HRMS *m/z* C₃₄H₃₄N₂O₄S (M+H)⁺ calcd. 567.2239, found 567.2245.

Bis-[(R)-ethyl 2-(3-mercapto-2-(2-phenylacetamido)propanamido)acetate] (113e).

The dimer (**113e**) was prepared in 72% yield following the procedure employed for preparation of dimer **1** and obtained as a yellow solid. **113e**: m.p. 98 °C; ¹H NMR (300 MHz, CDCl₃): δ 1.27-1.31 (m, 1 H), 2.79-2.87 (m, 1 H), 3.00-3.07 (m, 1 H), 3.64 (s, 2 H), 3.68-3.76 (m, 1 H), 3.96-4.16 (m, 1 H), 4.04-4.23 (m, 2 H), 5.52-5.58 (m, 1 H), 6.56 (d, *J* = 9.15 Hz, 1 H), 7.25-7.35 (m, 5 H), 8.40-8.44 (s, 1 H); ¹³C NMR (75.5 MHz, CDCl₃): δ 14.1, 41.1, 43.1, 46.3, 53.0, 61.2, 127.2, 128.6, 129.5, 134.2, 169.1, 170.5, 171.5. HRMS *m/z* C₃₀H₃₈N₄O₈S₂ (M+H)⁺ calcd. 647.2131, found 647.2136.

N,S-Dibenzoyl-L-cysteine ethyl ester (115).

Benzoyl chloride (10 mL) was added to a solution of pure L-cysteine ethyl ester hydrochloride (7.5 g, 40 mmol) in pyridine (30 mL) precooled to 0 °C. After stirring for 1 h at rt, the mixture was poured onto ice. The precipitate which formed was collected by filtration and was recrystallized from CH₃OH in 88% yield (12 g). **115**: m.p. 81 °C ; ¹H NMR (300 MHz, CDCl₃): δ 1.41 (t, *J* = 6 Hz, 3 H), 3.40-3.48 (m, 1 H), 3.68-3.75 (m, 1 H), 4.15 (q, *J* = 7.11, 7.17 Hz, 2 H), 4.62-4.70 (m, 1 H), 7.48-7.57 (m, 5 H), 7.66-7.69 (m, 1 H), 7.84-7.93 (m, 4 H), 9.02 (d, *J* = 7.8 Hz, 1 H); ¹³C NMR (75.5 MHz, CDCl₃): δ 14.4, 29.9, 52.6, 61.4, 127.2, 127.7, 128.7, 129.5, 132.0, 133.8, 134.5, 136.4, 166.8, 170.5, 191.0; HRMS *m/z* C₁₉H₁₉NO₄S (M+H)⁺ calcd. 358.1113, found 358.1106.

(3S,6S)-3-Benzyl-6-(R)-3,6-dioxopiperazin-2-yl-methyl-disulfanyl-methyl-piperazine-2,5-dione (132).

The trityl protected diketopiperazine **27** (246 mg, 0.5 mmol) and diketopiperazine **28** (201 mg, 0.5 mmol) were dissolved in a solution of CH₂Cl₂ (5 mL) and CH₃OH (10 mL) with stirring. Pyridine (0.3 mL, 3.75 mmol) was then added to the mixture which resulted, followed by a solution of iodine (126 mg, 0.5 mmol) in CH₃OH (3 mL). The mixture was allowed to stir for 1 h at rt. No precipitate had formed by this time; however, analysis by TLC (silica gel) indicated that the reaction was proceeding slowly by the appearance of a new spot under the starting material (UV light). A precipitate began to form within 2 h after concentrating the solution to a volume of 2 mL. Methanol (5 mL) was added to result in a total volume of 7 mL. The solution was allowed to stir an additional 23 h and the precipitate was filtered off. The solid which formed was washed with cold CH₃OH. The precipitate was filtered off and dried to yield dimer **132** as a yellow solid (120 mg, 60%) in > 95% pure form. **132**: ¹H NMR (300 MHz, DMSO-*d*₆) δ 2.89-2.91 (m, 2 H), 3.09-3.21 (m, 3 H), 3.33-3.87 (m, 4 H), 4.11 (s, 1 H), 4.21 (s, 1 H), 7.13-7.36 (m, 5 H), 8.07 (s, 1 H), 8.32 (s, 2 H), 8.58 (s, 1 H); ¹³C NMR (75.5 MHz, DMSO-*d*₆) δ 42.3, 42.6, 43.1, 44.7, 53.3, 54.2, 54.3, 55.8, 127.2, 128.2, 130.6, 136.4, 165.9, 166.1, 166.5. HRMS *m/z* C₁₇H₂₀N₄O₄S₂ (M+H)⁺ calcd. 409.0926, found 409.0932.

***tert*-Butyl-(R)-2-(2R,5R)-5-benzyl-3,6-dioxopiperazin-2-yl-methyl-disulfanyl-1-(3-isopropyl-1,2,4-oxadiazol-5-yl)ethylcarbamate (133).**

The trityl protected diketopiperazine (**29**, 315 mg, 0.64 mmol) and bioisostere (**94**, 340 mg, 0.64 mmol) were dissolved in a solution of CH₂Cl₂ (5 mL) and CH₃OH (10 mL) with stirring. Pyridine (0.4 mL, 5.12 mmol) was then added to the mixture which resulted, followed by a solution of iodine (357 mg, 1.4 mmol) in CH₃OH (3 mL). The mixture which resulted was allowed to stir for 1 h at rt until analysis by TLC (silica gel) indicated that the reaction was proceeding slowly by the appearance of a new spot under the starting material (UV light). After allowing to stir for 2 h, the mixture was concentrated *in vacuo* to a volume of 2 mL and CH₃OH (5 mL) was added to result in a total volume of 7 mL. The solution was allowed to stir an additional 23 h and then washed with a saturated aq solution of sodium thiosulfate after which the solvent was removed under reduced pressure. The residue which resulted was dissolved in EtOAc (5 ~ 10 mL) and the precipitate which resulted was collected by filtration to yield the product as a white solid (or purified by preparative chromatography after washing with a low polar solvent)

133: ¹H NMR (300 NMR, DMSO-d₆) δ 1.04 (d, 6H, *J* = 3Hz), 1.38 (s, 9H), 2.68-3.15 (m, 6 H), 4.21 (s, 1H), 4.44-4.47 (m, 1H), 7.13-7.26 (m, 5 H), 8.13 (s, 1 H), 8.35 (s, 1 H), 10.7 (s, 1 H); ¹³C NMR (75.5 NMR, DMSO-*d*₆) δ 19.0, 28.5, 38.8, 43.2, 53.2, 55.1, 55.8, 78.8, 127.1, 128.5, 130.6, 136.4, 155.7, 166.0, 166.5, 171.8, 177.5. HRMS (ESI, M⁺+H, C₂₄H₃₃N₅O₅S₂) calcd. 536.2001, found: 536.2019.

General Procedure for the Dealkylation of the Boc Group by Chlorotrimethylsilane/Sodium Iodide: (3R,6S)-3-(R)-2-Amino-2-(3-isopropyl-1,2,4-oxadiazol-5-yl)ethyl-disulfanyl-methyl-6-isopropylpiperazine-2,5-dione (134).

These reactions were generally carried out on 1 mmol scale in a 10 mL flask which was flushed continuously with dry argon. Chlorotrimethylsilane (27 mg, 0.25 mmol) was added to a solution of the corresponding dimer **137** (0.25 mmol) and sodium iodide (37.5 mg, 0.25 mmol) in acetonitrile/dichloromethane (5 mL, 2:1) slowly with continuous stirring. The reaction mixture which resulted was allowed to stir at rt until the completion of the reaction indicated by analysis by TLC (silica gel). The solvent was removed under reduced pressure and the residue which resulted was dissolved in a mixed solvent (CH₂Cl₂/ CH₃OH = 9:1). The solution was washed with small amount of a saturated aq sodium thiosulfate solution, brine and dried (anhydrous Na₂SO₄). The products were further purified by plate chromatography on silica gel (preparative TLC) to yield pure amine in over 85% yield. **134**: ¹H NMR (300 NMR, DMSO-d₆) δ 0.86 (d, 3 H, *J* = 6.3 Hz), 0.96 (d, 3 H, *J* = 6.9 Hz), 1.23-1.30 (dd, 6 H), 2.20-2.25 (m, 1 H), 3.10-3.19 (m, 2 H), 3.28-3.30 (m, 2 H), 3.25-3.51 (m, 1 H), 3.51-3.57 (m, 1 H), 4.23 (s, 1 H), 5.09 (s, 1 H), 7.09-7.42 (m, 1 H), 8.13-8.22 (m, 1 H). HRMS *m/z* C₁₅H₂₅N₅O₃S₂ (M+H)⁺ calcd. 388.1399, found 388.1401.

General Procedure for the Synthesis of Mixed Dimers using the Benzotriazole Method: [*tert*-Butyl 1-mercapto-2-(5-phenyl-1H-1,2,4-triazol-3-yl)propan-2-ylcarbamate]-[(*R*)-*tert*-Butyl 2-mercapto-1-(5-methyl-1H-1,2,4-triazol-3-yl)ethylcarbamate]-disulfide (135).

Triazole monomer **100** (2 mmol) was added slowly under an inert atmosphere to a solution of benzotriazole (2 mmol) and chlorobenzotriazole (4 mmol) in dichloromethane (DCM) (15 mL) at -78°C with stirring. After stirring for 30 min, a solution of thiourea (6 mmol) in anhydrous THF (5 mL) was added and the mixture which resulted was allowed to stir for 30 min. The other triazole monomer **96** (2 mmol) in DCM was then added while the temperature was maintained at -78°C . The solution was allowed to stir for 18-20 hr, while the mixture slowly warmed to rt. The solvent was removed under reduced pressure and the residue was dissolved in DCM followed by washing with water (30 mL x 3 times). The organic layer was dried (anhydrous Na_2SO_4) and the solvent was then removed under reduced pressure. The dimer was purified by flash chromatography (yield 60-65%). (**VR-MD-01**) (**135**): $^1\text{H NMR}$ (300 MHz, CDCl_3) δ 8.33-8.51 (d, 2H), 7.34 (s, 3H), 5.30 (bs, 2H), 2.97 – 3.61 (m, 4H), 2.43 (s, 3H), 1.47 (s, 18H); HRMS (ESI, $\text{M}^+\text{+H}$, $\text{C}_{25}\text{H}_{37}\text{N}_8\text{O}_4\text{S}_2$) calcd. 577.2379, found: 577.2369 and ($\text{M}^+\text{+Na}$, $\text{C}_{25}\text{H}_{36}\text{N}_8\text{O}_4\text{S}_2\text{Na}$) calcd. 599.2199, found 599.2194.

General Procedure for Deprotection of the Boc group and Formation of the HCl Salt of Mixed-Dimers: (R)-2-(R)-2-Amino-2-(5-methyl-1H-1,2,4-triazol-3-yl)ethyl-disulfanyl-1-(5-phenyl-1H-1,2,4-triazol-3-yl)ethanamine dihydrochloride (136).

The BOC-protected mixed-dimer **135** (0.2 mmol) was dissolved in EtOH (5 mL) and a saturated solution of anhydrous HCl in EtOH (5 mL) was added. The mixture was allowed to stir for 2 h after which the solvent was removed under reduced pressure. The oily residue which formed was dissolved in distilled water (15 mL) and washed with DCM (3 x 10 mL) to remove organic impurities. The water was then removed under reduced pressure and the gummy residue was finally dried under high vacuum to obtain the solid hydrochloride salt (99% yield). (*VR-MD-02*) (**136**): ¹H NMR (300 MHz, CDCl₃) δ 7.74-7.76 (d, 2H), 7.47 (s, 3H), 4.88 (bs, 2H), 3.14 – 3.23 (m, 4H), 2.27 (s, 3H).

***tert*-Butyl (R)-1-(3-isopropyl-1,2,4-oxadiazol-5-yl)-2-(2R,5R)-5-isopropyl-3,6-dioxopiperazine-2-yl-methyl-disulfanyl-ethylcarbamate (137).**

The ethyl carbamate (**137**) was prepared following the procedure described above for **133** by using the starting materials, bioisostere **94** and diketopiperazine **31**. **137**.: ¹H NMR (300 NMR, DMSO-d₆) δ 0.96 (d, 3 H, *J* = 6.6 Hz), 1.07 (d, 3 H, *J* = 7.2 Hz), 1.34 (s, 3 H), 1.36 (s, 3 H), 1.48 (s, 9 H), 2.48-2.51 (m, 1 H), 2.84-2.92 (m, 1 H), 3.09-3.13 (m,

1 H), 3.28-3.30 (m, 2 H), 3.42-3.47 (dd, 1 H), 4.37 (s, 1 H), 5.38 (s, 1 H), 5.57 (s, 1 H), 6.58 (s, 1 H), 6.82 (s, 0.33 H), 6.96 (s, 0.66 H); ^{13}C NMR (75.5 NMR, DMSO- d_6) δ 18.8, 21.1, 26.8, 28.3, 31.4, 42.8, 47.9, 53.2, 60.3, 60.4, 81.1, 154.8, 166.8, 171.2, 175.2, 176.8. HRMS m/z $\text{C}_{20}\text{H}_{33}\text{N}_5\text{O}_5\text{S}_2$ (M+H) $^+$ calcd. 488.1923, found 488.1928.

X. References.

1. Hamon, J., Paraire, J., Velluz J., Anxiety States and Potentialized Barbiturates. *Ann Med Psychol.* (Paris): **110**, 403-407 (1952).
2. Jann, M.W., Grimsley, S.R., Gray, E.C., Chang, W.H., Pharmacokinetics and Pharmacodynamics of Clozapine. *Clin. Pharmacokinet.:* **24**,161-176 (1993).
3. Casey, D.E., The Relationship of Pharmacology to Side Effects. *J. Clin. Psychiatry:* 58 Suppl., **10**, 55-62 (1997).
4. Lieberman, J.A., Stroup, T.S., McEvoy, J.P., Swartz, M.S., Rosenheck, R.A., Perkins, D.O., Keefe, R.S., Davis, S.M., Davis, C.E., Lebowitz, B.D., Severe, J., Hsiao, J.K., Effectiveness of Antipsychotic Drugs in Patients with Chronic Schizophrenia. *N. Engl. J. Med.:* **353**, 1209-1223 (2005).
5. Luby, E.D., Cohen, B.D., Rosenbaum, G., Gottlieb, J.S., Kelley, R., Study of a New Schizophrenomimetic Drug. *AMA Arch. Neurol. Psychiatry:* **81**, 363-369 (1959).
6. Pearlson, G.D., Psychiatric and Medical Syndromes Associated with Phencyclidine (PCP) Abuse. *Johns Hopkins Med. J.:* **148**, 25-33 (1981).
7. Javitt, D.C., Zukin, S.R., Recent Advances in the Phencyclidine Model of Schizophrenia. *Am. J. Psychiatry:* **148**, 1301-1308 (1991).
8. Krystal, J., Karper, L., Seibyl, J., Freeman, G., Delany, R., Bremner, J., Heninger, G., Bowers, M., Charney, D., Effects of NMDA Receptor Antagonists: Implications for the Pathophysiology of Schizophrenia. *Arch. Gen. Psychiatry:* **59**,663-664 (2002).
9. Malhotra, A.K., Adler, C.M., Kennison, S.D., Elman, I., Pickar, D., Breier, A., Clozapine Blunts N-Methyl-Daspartate Antagonist-Induced Psychosis: A Study with Ketamine. *Biol, Psychiatry:* **42**, 664-668 (1997).
10. Lahti, A.C., Weiler, M.A., Tamara-Michaelidis, B.A., Parwani, A., Tamminga, C.A., Effects of Ketamine in Normal and Schizophrenic Volunteers. *Neuropsychopharmacology:* **25**, 455-467 (2001).
11. Verma, A., Moghaddam, B., NMDA Receptor Antagonists Impair Prefrontal Cortex Function as Assessed via Spatial Delayed Alternation Performance in Rats: Modulation by Dopamine. *J. Neurosci.:* **16**, 373-379 (1996).
12. Jentsch, J.D., Elsworth, J.D., Redmond, D.E., Jr., Roth, R.H., Phencyclidine Increases Forebrain Monoamine Metabolism in Rats and Monkeys: Modulation by the Isomers of HA966. *J. Neurosci.:* **17**, 1769-1775 (1997).

13. Moghaddam, B., Adams, B., Verma, A., Daly, D., Activation of Glutamatergic Neurotransmission by Ketamine: A Novel Step in the Pathway from NMDA Receptor Blockade to Dopaminergic and Cognitive Disruptions Associated with the Prefrontal Cortex. *J. Neurosci.*: **17**, 2921-2927 (1997).
14. Sies, H., Glutathione and its Role in Cellular Functions. *Free Radic. Biol. Med.*: **27**, 916-921 (1999).
15. Deegan, T.L., Nitz, T.J., Cebzanov, D., Pufko, D.E., Parallel Synthesis of 1,2,4-Oxadiazoles using CDI activation. *Bioorg. Med. Chem. Lett.*: **9**, 209-212 (1999).
16. Baker, D.A., Tran-Nguyen, T.L., Fuchs, R.A., Neisewander, J.L., Influence of Individual Differences and Chronic Fluoxetine Treatment on Cocaine-Seeking Behavior in Rats. *Psychopharmacology (Berl)*: **155**, 18-26 (2001).
17. Baker, D.A., McFarland, K., Lake, R.W., Shen, H., Tang, X.C., Toda, S., Kalivas, P.W., Neuroadaptations in Cystine-Glutamate Exchange Underlie Cocaine Relapse. *Nat. Neurosci.*: **6**, 743-749 (2003).
18. Jaffe, J.H., Cascella, N.G., Kumor, K.M., Sherer, M.A., Cocaine-Induced Cocaine Craving. *Psychopharmacol.*: **97**, 59-64 (1989).
19. Withers, N.W., Pulvirenti, L., Koob, G.F., Gillin, J.C., Cocaine Abuse and Dependence. *J. Clin. Psychopharmacol.*: **15**, 63-78 (1995).
20. Weiss, F., Ciccocioppo, R., Parsons, L.H., Katner, S., Liu, X., Zorrilla, E.P., Valdez G.R., Ben-Shahar, O., Angeletti, S., Richter, R.R., Compulsive Drug-Seeking Behavior and Relapse: Neuroadaptation, Stress, and Conditioning Factors. *Ann. N. Y. Acad. Sci.*: **937**, 1-26 (2001).
21. Satel, S.L., Southwick, S.M., Gawin, F.H., Clinical Features of Cocaine-Induced Paranoia. *Am. J. Psychiatry*: **148**, 495-498 (1991).
22. O'Brien, C.P., Childress, A.R., McLellan, A.T., Ehrman, R., A Learning Model of Addiction. *Res. Publ. Assoc. Res. Nerv. Ment. Dis.*: **70**, 157-177 (1992).
23. Childress, A.R., Mozley, P.D., McElgin, W., Fitzgerald, J., Reivich, M., O'Brien, C.P., Limbic Activation During Cue-Induced Cocaine Craving. *Am. J. Psychiatry*: **156**, 11-18 (1999).
24. Breier, A., Clozapine and Noradrenergic Function: Support for a Novel Hypothesis for Superior Efficacy. *J. Clin. Psychiatry*: **55**, Suppl. B, 122-125 (1994).

25. Volkow, N.D., Wang, G.J., Ma, Y., Fowler, J.S., Wong, C., Ding, Y.S., Hitzemann, R., Swanson, J.M., Kalivas, P., Activation of Orbital and Medial Prefrontal Cortex by Methylphenidate in Cocaine-Addicted Subjects but not in Controls: Relevance to Addiction. *J. Neurosci.*: **25**, 3932-3939 (2005).
26. Pierce, R.C., Bell, K., Duffy, P., Kalivas, P.W., Repeated Cocaine Augments Excitatory Amino Acid Transmission in the Nucleus Accumbens only in Rats having Developed Behavioral Sensitization. *J. Neurosci.*: **16**, 1550-1560 (1996).
27. Reid, M.S., Berger, S.P., Evidence for Sensitization of Cocaine-Induced Nucleus Accumbens Glutamate Release. *Neuroreport.*: **7**, 1325-1329 (1996).
28. Cornish, J.L., Kalivas, P.W., Glutamate Transmission in the Nucleus Accumbens Mediates Relapse in Cocaine Addiction. *J. Neurosci.*: **20**, RC89 (2000).
29. McFarland, K., Lapish, C.C., Kalivas, P.W., Prefrontal Glutamate Release into the Core of the Nucleus Accumbens Mediates Cocaine-Induced Reinstatement of Drug-Seeking Behavior. *J. Neurosci.*: **23**, 3531-3537 (2003).
30. McFarland, K., Davidge, S.B., Lapish, C.C., Kalivas, P.W., Limbic and Motor Circuitry Underlying Footshock-Induced Reinstatement of Cocaine-Seeking Behavior. *J. Neurosci.*: **24**, 1551-1560 (2004).
31. Volkow, N.D., Fowler, J.S., Addiction, a Disease of Compulsion and Drive: Involvement of the Orbitofrontal Cortex. *Cereb. Cortex.*: **10**, 318-325 (2000).
32. Baker, D.A., Xi, Z.X., Shen, H., Swanson, C.J., Kalivas, P.W., The Origin and Neuronal Function of in vivo Nonsynaptic Glutamate. *J. Neurosci.*: **22**, 9134-9141 (2002).
33. Xi, Z.X., Ramamoorthy, S., Baker, D.A., Shen, H., Samuvel, D.J., Kalivas, P.W., Modulation of Group II Metabotropic Glutamate Receptor Signaling by Chronic Cocaine. *J. Pharmacol. Exp. Ther.*: **303**, 608-615 (2002).
34. Bradford, H.F., Young, A.M., Crowder, J.M., Continuous Glutamate Leakage from Brain Cells is Balanced by Compensatory High-Affinity Reuptake Transport. *Neurosci. Lett.*: **81**, 296-302 (1987).
35. Miele, M., Boutelle, M.G., Fillenz, M., The Source of Physiologically Stimulated Glutamate Efflux from the Striatum of Conscious Rats. *J. Physiol.*: **497**, Part 3, 745-751 (1996).
36. Timmerman, W., Westerink, B.H., Brain Microdialysis of GABA and Glutamate: What Does it Signify? *Synapse*: **27**, 242-261 (1997).

37. Bannai, S., Induction of Cystine and Glutamate Transport Activity in Human Fibroblasts by Diethyl Maleate and other Electrophilic Agents. *J. Biol. Chem.*: **259**, 2435-2440 (1984).
38. Moran, M.M., McFarland, K., Melendez, R.I., Kalivas, P.W., Seamans, J.K., Cystine/Glutamate Exchange Regulates Metabotropic Glutamate Receptor Presynaptic Inhibition of Excitatory Transmission and Vulnerability to Cocaine Seeking. *J. Neurosci.*: **25**, 6389-6393 (2005).
39. Danbolt, N.C., Glutamate Uptake. *Prog. Neurobiol.*: **65**, 1-105 (2001).
40. Sato, H., Tamba, M., Ishii, T., Bannai, S., Cloning and Expression of a Plasma Membrane Cystine/Glutamate Exchange Transporter Composed of Two Distinct Proteins. *J. Biol. Chem.*: **274**, 11455-11458 (1999).
41. Bridges, C.C., Kekuda, R., Wang, H., Prasad, P.D., Mehta, P., Huang, W., Smith, S.B., Ganapathy, V., Structure, Function, and Regulation of Human Cystine/Glutamate Transporter in Retinal Pigment Epithelial Cells. *Invest. Ophthalmol. Vis. Sci.*: **42**, 47-54 (2001).
42. Cho, Y., Bannai, S., Uptake of Glutamate and Cysteine in C-6 Glioma Cells and in Cultured Astrocytes. *J. Neurochem.*: **55**, 2091-2097 (1990).
43. Murphy, T.H., Schnaar, R.L., Coyle, J.T., Immature Cortical Neurons are Uniquely Sensitive to Glutamate Toxicity by Inhibition of Cystine Uptake. *Faseb. J.*: **4**, 1624-1633 (1990).
44. Kim, J.Y., Kanai, Y., Chairoungdua, A., Cha, S.H., Matsuo, H., Kim, D.K., Inatomi, J., Sawa, H., Ida, Y., Endou, H., Low Cerebrospinal Fluid Glutamate in Schizophrenic Patients and a New Hypothesis on Schizophrenia. *Neurosci. Lett.*: **20**, 379-382 (2001).
45. Williamson, J.M., Meister, A., Stimulation of Hepatic Glutathione Formation by Administration of L-2-Oxothiazolidine-4-Carboxylate, a 5-Oxo-L-Proline Substrate. *Proc. Natl. Acad. Sci. U.S.A.*: **78**, 936-939 (1981).
46. Meister, A., Methods for the Selective Modification of Glutathione Metabolism and Study of Glutathione Transport. *Methods. Enzymol.*: **113**, 571-585 (1985).
47. Pileblad, E., Magnusson, T., Increase in Rat Brain Glutathione Following Intracerebroventricular Administration of Gamma-Glutamylcysteine. *Biochem. Pharmacol.*: **44**, 895-903 (1992).
48. Wade, L.A., Brady, H.M., Cysteine and Cystine Transport at the Blood-Brain Barrier. *J. Neurochem.* **37**:730-734 (1981).

49. Lu, S.C., Regulation of Hepatic Glutathione Synthesis: Current Concepts and Controversies. *Faseb. J.*: **13**, 1169-1183 (1999).
50. Do, K.Q., Trabesinger, A.H., Kirsten-Kruger, M., Lauer, C.J., Dydak, U., Hell, D., Holsboer, F., Boesiger, P., Cuenod, M., Schizophrenia: Glutathione Deficit in Cerebrospinal Fluid and Prefrontal Cortex in vivo. *Eur. J. Neurosci.*: **12**, 3721-3728 (2000).
51. Gupta, D.S., McCullumsmith, R.E., Beneyto, M., Haroutunian, V., Davis, K.L., Meador-Woodruff, J.H., Metabotropic Glutamate Receptor Protein Expression in the Prefrontal Cortex and Striatum in Schizophrenia. *Synapse*: **57**, 123-131 (2005).
52. Millar, A.B., Pavia, D., Agnew, J.E., Lopez-Vidriero, M.T., Lauque, D., Clarke, S.W., Effect of Oral N-Acetylcysteine on Mucus Clearance. *Br. J. Dis. Chest.*: **79**, 262-266 (1985).
53. Wang, T., Miller, K.W., Tu, Y.Y., Yang, C.S., Effects of Riboflavin Deficiency on Metabolism of Nitrosamines by Rat Liver Microsomes. *J. Natl. Cancer. Inst.*: **74**, 1291-1297 (1985).
54. De Benedetto, F., Aceto, A., Dragani, B., Spacone, A., Formisano, S., Pela, R., Donner, C.F., Sanguinetti, C.M., Long-Term Oral N-Acetylcysteine Reduces Exhaled Hydrogen Peroxide in Stable COPD. *Pulm. Pharmacol. Ther.*: **18**, 41-47 (2005).
55. Tomioka, H., Kuwata, Y., Imanaka, K., Hashimoto, K., Ohnishi, H., Tada, K., Sakamoto, H., Iwasaki, H., A Pilot Study of Aerosolized N-Acetylcysteine for Idiopathic Pulmonary Fibrosis. *Respirology*: **10**, 449-455 (2005).
56. Breithaupt, T.B., Vazquez, A., Baez, I., Eylar, E.H., The Suppression of T Cell Function and NF(kappa)B Expression by Serine Protease Inhibitors is Blocked by N-Acetylcysteine. *Cell Immunol.*: **173**, 124-130 (1996).
57. Omara, F.O., Blakley, B.R., Bernier, J., Fournier, M., Immunomodulatory and Protective Effects of N-Acetylcysteine in Mitogen-Activated Murine Splenocytes in vitro. *Toxicology*: **116**, 219-226 (1997).
58. De Rosa, S.C., Zaretsky, M.D., Dubs, J.G., Roederer, M., Anderson, M., Green, A., Mitra, D., Watanabe, N., Nakamura, H., Tjioe, I., Deresinski, S.C., Moore, W.A., Ela, S.W., Parks, D., Herzenberg, L.A., Herzenberg, L.A., N-Acetylcysteine Replenishes Glutathione in HIV Infection. *Eur. J. Clin. Invest.*: **30**, 915-929 (2000).
59. Spada, C., Treitinger, A., Reis, M., Masokawa, I.Y., Verdi, J.C., Luiz, M.C., Silveira, M.V., Michelon, C.M., Avila-Junior, S., Gil, D.O., Ostrowsky, S., The Effect of N-Acetylcysteine Supplementation Upon Viral Load, CD4, CD8, Total Lymphocyte Count and Hematocrit in Individuals Undergoing Antiretroviral Treatment. *Clin. Chem. Lab. Med.*: **40**, 452-455 (2002).

60. De Flora, S., Grassi, C., Carati, L., Attenuation of Influenza-Like Symptomatology and Improvement of Cell-Mediated Immunity with Long-Term N-Acetylcysteine Treatment. *Eur. Respir. J.:* **10**, 1535-1541 (1997).
61. Watt, G., Jongsakul, K., Ruangvirayuth, R., A Pilot Study of N-Acetylcysteine as Adjunctive Therapy for Severe Malaria. *Qjm.:* **95**, 285-290 (2002).
62. De Flora, S., Bennicelli, C., Camoirano, A., Serra, D., Romano, M., Rossi, G.A., Morelli, A., De Flora, A., In vivo Effects of N-Acetylcysteine on Glutathione Metabolism and on the Biotransformation of Carcinogenic and/or Mutagenic Compounds. *Carcinogenesis.:* **6**, 1735-1745 (1985).
63. De Flora, S., Rossi, G.A., De Flora, A., Metabolic, Desmutagenic and Anticarcinogenic Effects of N-Acetylcysteine. *Respiration:* **50**, Suppl. 1, 43-49 (1986).
64. Wilpart, M., Speder, A., Roberfroid, M., Anti-Initiation Activity of N-Acetylcysteine in Experimental Colonic Carcinogenesis. *Cancer Lett.:* **31**, 319-324 (1986).
65. Adair, J.C., Knoefel, J.E., Morgan, N., Controlled Trial of N-Acetylcysteine for Patients with Probable Alzheimer's Disease. *Neurology:* **57**, 1515-1517 (2001).
66. Gavish, D., Breslow, J.L., Lipoprotein(A) Reduction by N-Acetylcysteine. *Lancet:* **337**, 203-204 (1991).
67. Arstall, M.A., Yang, J., Stafford, I., Betts, W.H., Horowitz, J.D., N-Acetylcysteine in Combination with Nitroglycerin and Streptokinase for the Treatment of Evolving Acute Myocardial Infarction: Safety and Biochemical Effects. *Circulation:* **92**, 2855-2862 (1995).
68. Schneider, M.P., Delles, C., Schmidt, B.M., Oehmer, S., Schwarz, T.K., Schmieder, R.E., John S., Superoxide Scavenging Effects of N-Acetylcysteine and Vitamin C in Subjects with Essential Hypertension. *Am. J. Hypertens.:* **18**, 1111-1117 (2005).
69. Kleinveld, H.A., Demacker, P.N., Stalenhoef, A.F., Failure of N-Acetylcysteine to Reduce Low-Density Lipoprotein Oxidizability in Healthy Subjects. *Eur. J. Clin. Pharmacol.:* **43**, 639-642 (1992).
70. Borgstrom, L., Kagedal, B., Paulsen, O., Pharmacokinetics of N-Acetylcysteine in Man. *Eur. J. Clin. Pharmacol.:* **31**, 217-222 (1986).
71. Olsson, B., Johansson, M., Gabrielsson, J., Bolme P., Pharmacokinetics and Bioavailability of Reduced and Oxidized N-Acetylcysteine. *Eur. J. Clin. Pharmacol.:* **34**, 77-82 (1988).

72. De Caro, L., Ghizzi, A., Costa, R., Longo, A., Ventresca, G.P., Lodola, E., Pharmacokinetics and Bioavailability of Oral N-Acetylcysteine in Healthy Volunteers. *Arzneimittelforschung*: **39**, 382-386 (1989).
73. Mardikian, P.N., Larowe, S.D., Hedden, S., Kalivas, P.W., Malcolm, R.J., An Open-Label Trial of N-Acetylcysteine for the Treatment of Cocaine Dependence: A Pilot Study. *Prog. Neuropsychopharmacol. Biol. Psychiatry*: **12**, 154-187 (2006).
74. Abderhalden, E., Schwab, E., Compounds of the Type: Amino Acid-(2,5-diketopiperazine) and Their Behavior Toward Acid, Alkali and Enzymes. *Z. Physiol. Chem.*: **212**, 61-71 (1932).
75. Kawai, T., The Action of Erepsin on the Dipeptides Formed from Racemic Amino Acids. *Acta. Scholae. Medicinalis. Universitatiis. Imperialis. in Kioto.*: **11**, 131-135 (1928).
76. Greenstein, J.P., Multivalent Amino Acids and Peptides. VI. The Action of Proteolytic Enzymes on Certain Synthetic Substrates. *J. Biolog. Chem.*: **112**, 517-522 (1936).
77. Abderhalden, E., Weichert, K., Schumann, H., Haase, E., The Behavior of Diketopiperazines Toward Proteinases and Polypeptidases. *Fermentforschung*: **16**, 182-193 (1940).
78. Martins, M.B., Carvalho, I., Diketopiperazines: Biological Activity and Synthesis. *Tetrahedron*: **63**, 9923-9932 (2007).
79. Zhao, S., Liao, X., Wang, T., Flippen-Anderson, J., Cook, J.M., The Enantiospecific, Stereospecific Total Synthesis of the Ring-A Oxygenated Sarpagine Indole Alkaloids (+)-Majvinine, (+)-10-Methoxyaffinisine, and (+)-Na-Methylsarpagine, and Well as the Total Syntheses of the Alstonia Bisindole Alkaloid Macralstonidine. *J. Org. Chem.*: **68**, 6279-6295 (2003).
80. Pastuszak, J.J., Chimiak, A., tert-Butyl Group as Thiol Protection in Peptide Synthesis. *J. Org. Chem.*: **46**, 1868-1873 (1981).
81. Sakakibara, S., Tani, H., Synthesis of Polycysteine, *Bull. Chem Soc. (Japan)*: **29**, 85-88 (1956).
82. Zervas, L., Photaki, I., On Cysteine and Cystine Petides. I. New S-Protecting Groups for Cysteine. *J. Am. Chem. Soc.*: **84**, 3887-3897 (1962).
83. Biot, C., Bauer, H., Schirmer, R.H., 5-Substituted Tetrazoles as Bioisosteres of Carboxylic Acids. Bioisosterism and Mechanistic Studies on Glutathione Reductase Inhibitors as Antimalarials. *J. Med. Chem.*: **47**, 5972-5983 (2004).

84. Deegan, T.L., Nitz, T.J., Cebzanov, D., Pufko, D.E., Parallel Synthesis of 1,2,4-Oxadiazoles using CDI Activation. *Bioorg. Med. Chem. Lett.*: **9**, 209-212 (1999).
85. Kim, J.H., Park, J.H., Lee, H., Highly Efficient Novel Poly(p-phenylvinylene) Derivative with 1,3,4-Oxadiazole Pendant on a Vinylene Unit. *Chem. Mater.*: **15**, 3414-3416 (2003).
86. Katritzky, A., Qi, M., Feng, D., Zhang, G., Griffith, M., Watson, K., Synthesis of 1,2,4-Triazole-Functionalized Solid Support and Its Use in the Solid-Phase Synthesis of Trisubstituted 1,2,4-Triazoles. *Organic Letters*: **1**, 1189-1191 (1999).
87. Shiina, I., Kubota, M., Oshiumi, H., Hashizume, M., An Effective Use of Benzoic Anhydride and Its Derivatives for the Synthesis of Carboxylic Esters and Lactones: A Powerful and Convenient Mixed Anhydride Method Promoted by Basic Catalysts. *J. Org. Chem.*: **69**, 1822-1830 (2004).
88. Hunter, R., Caira, M., Stellenboom, N., Inexpensive, One-Pot Synthesis of Unsymmetrical Disulfides Using 1-Chlorobenzotriazole. *J. Org. Chem.*: **71**, 8268-8271 (2006).
89. Cook, J., Baker, D., Johnson, E.M., Yin, W., Cysteine and Cystine Prodrugs to Treat Schizophrenia and Drug Addiction. PCT/US 09/047099, filed April 16, 2009; WO 2009/137251A2, International Publication date, Nov. 12, 2009.
90. Cook, J., Baker, D., Johnson, E.M., Yin, W., Cysteine and Cystine Prodrugs to Treat Schizophrenia and Drug Addiction. Filed on 8/11/08. Application number 12189516. PCT WO 2009/100431 A1. Pub. Date: Aug. 13, 2009
91. Cook, J., Baker, D., Johnson, E.M., Yin, W., Cysteine and Cystine Prodrugs to Treat Schizophrenia and Drug Addiction. US Patent Issued No: US 7,829,709 B1, Nov. 9, 2010.
92. Cook, J., Baker, D., Johnson, E.M., Yin, W., Cysteine and Cystine Prodrugs to Treat Schizophrenia and Drug Cravings. US Utility Patent, Serial# 12/367,867, Filed Feb. 2, 2009, Issued May 8, 2012.
93. Cook, J., Baker, D., Johnson, E.M., Yin, W., Cysteine and Cystine Prodrugs to Treat Schizophrenia and Reduce Drug Cravings. US Patent, Divisional, Serial number 13/465,383; Filed May 7, 2012.
94. Cook, J., Baker, D., Johnson, E.M., Yin, W., Cysteine and Cystine Prodrugs to Treat Schizophrenia and Reduce Drug Cravings. Pub. No. US2012/0220596A1, Pub. Date: Aug. 30, 2012.

PART 2. DESIGN AND SYNTHESIS OF SUBTYPE SELECTIVE ESTER
BIOISOSTERES OF BZR LIGANDS FOR GABA_A / BENZODIAZEPINE
RECEPTORS TO ENHANCE METABOLIC STABILITY

by

Edward Merle Johnson II

I. Introduction.

1. General Background Information.

GABA_A/BzR chloride ion channels comprise the major inhibitory neurotransmitter system in the central nervous system (CNS). This central role carries with it a direct influence on many diseases of the CNS. Alterations in GABA_A function from controls are known to occur in many anxiety disorders¹⁻⁶; including panic disorder⁵, epilepsy,^{7a} hypersensitive behavior,^{7b} phobias⁶, schizophrenia⁸, alcoholism⁹, Angleman's syndrome,^{7b} and Rett's syndrome,¹⁰ as well as effects which lead to/or complicate drug abuse.¹¹ GABA receptors are divided into three main classes: (1) GABA_A receptors, which are members of the ligand-gated ion channel superfamily; (2) GABA_B receptors, which are members of the G-protein linked receptor superfamily; and (3) GABA_C receptors, also members of the ligand-gated ion channel superfamily, but their distribution is confined to the retina.¹² Benzodiazepine receptor ligands do not bind to GABA_B and GABA_C receptors, but only to an allosteric modulatory site on GABA_A receptors.¹³

The GABA_A /BzR chloride ion channel is a pentameric protein polymer mainly constructed from α , β , and γ subunits.¹³ A total of 21 subunits, 8 different types (6 α , 4 β , 4 γ , 1 δ , 1 π , 1 θ , 1 ϵ and 3 ρ) have been cloned and sequenced from the mammalian CNS.¹⁴ ¹⁶ The exact subunit composition of most GABA_A receptors is now known. All these polypeptides possess an approximate molecular mass of 50 kD and are structurally related. Each subunit consists of a large extracellular region, which contains several potential glycosylation sites and a characteristic "cys-loop" formed by a covalent bond

between two conserved cysteines. This extracellular region is also important because of its contribution to the agonist GABA and modulatory benzodiazepine binding sites. The protein then traverses the lipid bilayer four times and has a large intracellular loop located between transmembrane regions 3 and 4 (M3 and M4). This intracellular region contains possible phosphorylation sites necessary for regulation of the receptor. The homology within each subunit class is about 60 – 80 %, while the homology between subunit classes is about 30 – 40 %. Depicted in **Figure 1** is the proposed topology of a single GABA_A receptor subunit. The pentameric structure of a ligand-gated ion channel is shown in **Figure 2**.¹⁷⁻¹⁹

Figure 1. Proposed topology of a GABA_A receptor subunit. The extracellular domain begins with the N-terminus and M1-M4 represent the four transmembrane domains. Figure reprinted with permission.^{17, 19}

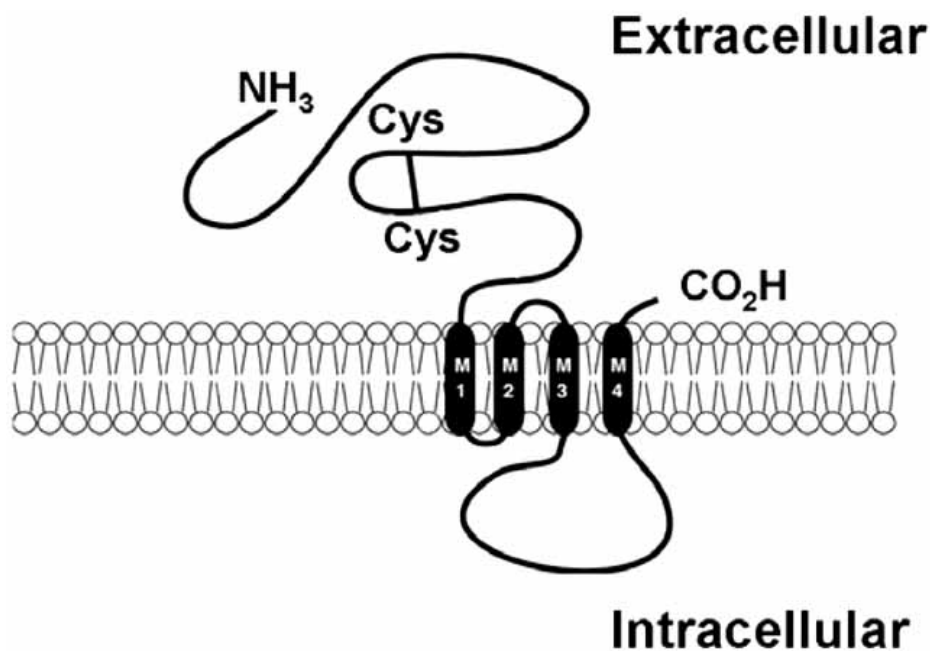
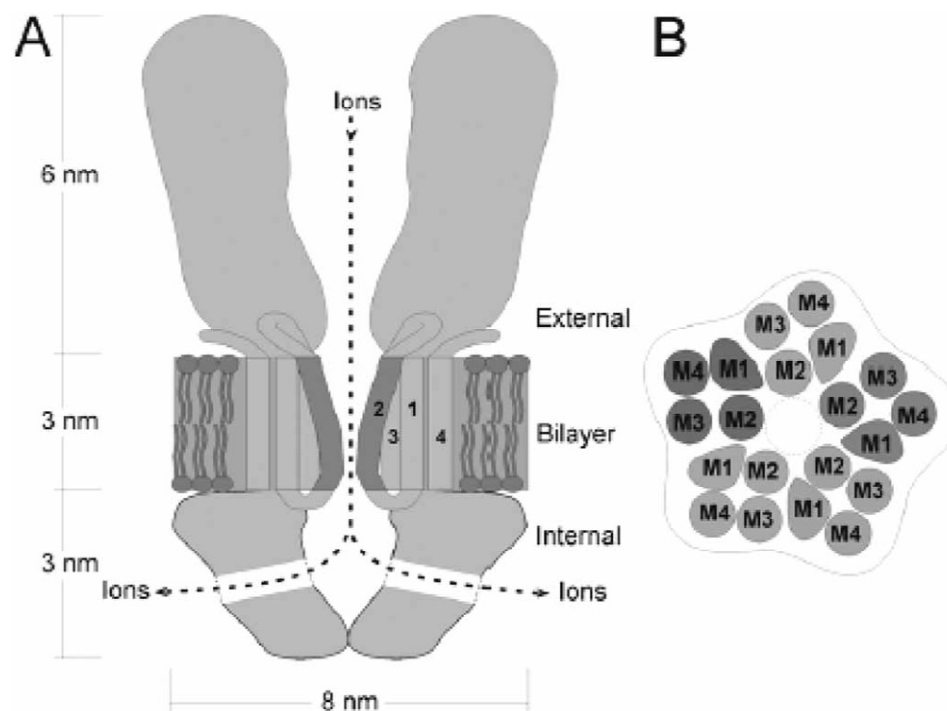
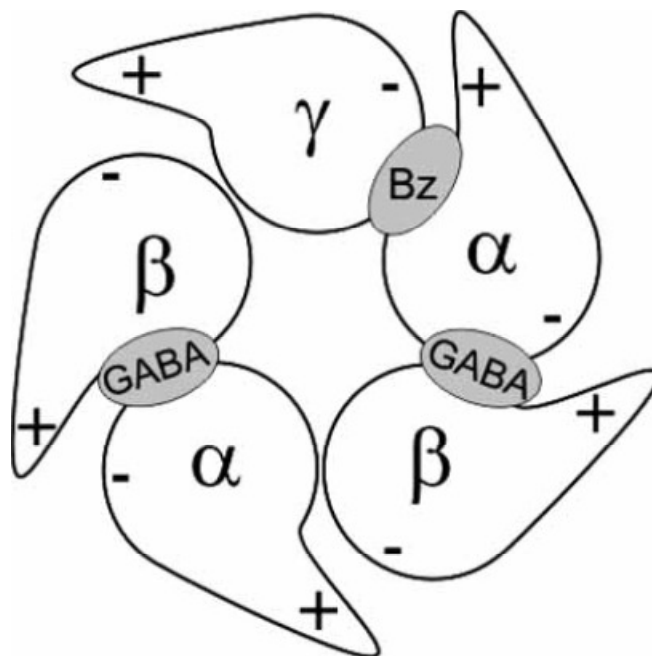


Figure 2. Longitudinal (A) and cross-sectional (B) schematic representations of a ligand-gated ion channel. The numbers 1-4 refer to the M1-M4 segments. The M2 segment contributes to the majority of the pore lining within the membrane lipid bilayer. Figure reprinted with permission.^{18, 22}



Studies by molecular cloning have shown that at least 3 types (2α , 2β and 1γ) of subunits are required to construct a fully functional recombinant GABA_A/BzR chloride channel which mimics the biological, electrophysiological and pharmacological properties of native GABA_A/BzR chloride channels.^{20, 21} It would be most desirable if each subtype only interacted with specific molecules [the α and β subunits are involved in the interaction with GABA, whereas the α and γ subunits are proposed to contain the binding site for benzodiazepines located between them (see **Figure 3**)].

Figure 3. Absolute subunit arrangement of the $\alpha 1\beta 2\gamma 2$ GABA_A receptor when viewed from the synaptic cleft. The GABA binding sites are located at the $\beta^+\alpha^-$ subunit interfaces and the Bz modulatory binding site is located at the $\alpha^+\gamma^-$ subunit interface. The part of the schematically drawn subunits marked by the + indicates loop C of the respective subunits.^{22, 23}



Before the cloning of the GABA_A receptor gene family, the benzodiazepine binding site was historically subdivided into two subtypes, BENZODIAZEPINE1 and BENZODIAZEPINE2, on the basis of radioligand binding studies on synaptosomal rat membranes.²⁴ The BENZODIAZEPINE1 subtype has been shown to be pharmacologically equivalent to a GABA_A receptor comprising the $\alpha 1$ subunit in combination with a β subunit and $\gamma 2$ subunit. This is the most abundant GABA_A receptor subtype and is believed to represent almost half of all GABA_A receptors in the brain, as stated.²⁵⁻²⁷

Subtype assemblies which contain an $\alpha 1$ subunit ($\alpha 1\beta 2/3\gamma 2$) are present in most areas of the brain and are thought to account for 40-50% of GABA_A receptors in the rat brain.²⁸ Subtype assemblies containing $\alpha 2$ and $\alpha 3$ subunits, respectively, are thought to account for about 25% and 17% of the GABA_A receptors in the rat brain, respectively. Subtype assemblies containing an $\alpha 5$ subunit ($\alpha 5\beta 3\gamma 2$) are expressed predominately in the hippocampus with some in the spinal cord and are thought to represent about 5% of GABA_A receptors in the rat brain.^{14, 29-35}

As indicated above, two other major populations are the $\alpha 2\beta_{(2/3)}\gamma 2$ and $\alpha 3\beta_{(2/3)}\gamma 2$ subtypes. Together these constitute approximately 35% of the total GABA_A receptor population.²⁸ Pharmacologically this combination appears to be equivalent to the BENZODIAZEPINE2 subtype as defined previously by radioligand binding on synaptosomal membranes, although the BENZODIAZEPINE2 subtype may also include certain $\alpha 5$ -containing subtype assemblies.²⁴ The exact physiological role of these subtypes has hitherto been unclear because no sufficiently selective agonists or antagonists were known.^{14, 36}

A characteristic property of all known GABA_A receptors is the presence of a number of modulatory sites, one of which is the benzodiazepine binding site.³⁶ The benzodiazepine binding site is the most explored of the GABA_A receptor modulatory sites. The 1, 4-benzodiazepines, which are employed to treat anxiety disorders as well as sleep disorders, exhibit anxiolytic, anticonvulsant, muscle relaxant/ataxic, sedative-hypnotic and amnestic effects.^{1-11, 37} In general, BDZs as a class offer many benefits as drug therapy.³⁸

For example, they are rapidly absorbed from the gastrointestinal tract and normally reach maximum blood concentrations within one to two hours of ingestion. They readily cross the blood-brain barrier, and are rapidly distributed within the brain. Electrophysiological changes attributed to certain BDZs can be detected as early as five minutes after intravenous injection.³⁹ At clinically relevant doses the BDZs do not induce significant liver microsomal enzymes that often can result in drug-drug interactions.⁴⁰

In general, benzodiazepines lack serious toxicity even when overdosed.^{41, 42} Unfortunately, BDZs produce many side effects such as drowsiness, somnolence, fatigue, ataxia, lethargy, sedation, muscle-relaxation, amnesia and tolerance to the anticonvulsant effects which limit their use as chronic anticonvulsant agents.^{41, 43-44} These side effects along with the issue of tolerance, which develops from the extended use of these agents both in animal models and patients, has been studied in detail.⁴¹⁻⁴⁷

The principal composition of GABA_A/BzR subtypes is defined as $\alpha 1\beta 3\gamma 2$, $\alpha 2\beta 3\gamma 2$, $\alpha 3\beta 3\gamma 2$, $\alpha 4\beta 3\gamma 2$, $\alpha 5\beta 3\gamma 2$, and $\alpha 6\beta 3\gamma 2$; however, in many cases the $\beta 3$ subunit has been replaced with a $\beta 2$ subunit with no loss in BzR binding or efficacy.^{16, 48-50} The distinct cellular and subcellular location of individual receptor subtypes suggests that they exhibit specific functions in the brain that can be selectively modulated by subtype specific drugs.⁵¹ A few ligands from the classes of the 1,4- benzodiazepines and the 3-substituted- β -carbolines have been shown to exhibit some $\alpha 1$, $\alpha 5$ or $\alpha 4/\alpha 6$ subtype selectivity and serve as lead compounds in many studies.⁵²⁻⁵⁵ The synthesis of new compounds which are capable of modulating responses produced by the above receptors

has been made possible by the development of an isoform model of the GABA_A/benzodiazepine receptor complex as well.^{14,36, 56, 57}

The ligands which interact at the GABA_A/BzR binding site comprise three types: positive allosteric modulators (agonists), negative allosteric modulators (inverse agonists) and antagonists, all of which can bind with high affinity.⁵⁸ Agonist binding to the receptor opens an intrinsic chloride ion channel, typically hyperpolarizing the cell membrane or at least opposing depolarization, thereby inhibiting neuronal transmission. Benzodiazepine BS ligands such as diazepam (Valium), chlordiazepoxide (Librium) and alprazolam (Xanax) are allosteric modulators, unable to induce channel openings themselves, but function to vary the frequency and not the channel opening times.^{59, 60} Positive allosteric modulators at the benzodiazepine binding site (agonists) increase this frequency, while negative allosteric modulators (inverse agonists) decrease the frequency. Currently, it is not clear whether benzodiazepine BS ligands allosterically modulate GABA affinity or channel gating. Recent studies⁶¹ support the view that high-affinity classical benzodiazepines modulate $\alpha 1\beta 2\gamma 2$ GABA_A receptors *via* allosteric coupling to channel gating.^{62, 63} Further studies are needed to determine whether the mechanism of modulation varies in different receptor subtypes.

The concept of receptor multiplicity has been extremely valuable in that different receptor subtypes reside within anatomically distinct regions of the brain and are responsible for different physiological and pathological processes (**Table 1**).^{51, 64-65}

These distinctions have thus become a motivation for the design of subtype selective ligands in order to elicit a single specific response.^{51, 66-73} Differences observed in the action of such drugs may be due to subtype-selective affinity and absolute and/or relative subtype-selective efficacy.⁷⁴ Development of ligands with selective efficacy at one or more receptor subtypes and/or ligands with selective binding affinity at one receptor subtype will result in a better understanding of which subtype mediates which neuronal response.⁷⁵

Table 1. Action of benzodiazepines at GABA_A $\alpha(1-6)\beta3\gamma2$ receptor subtypes.⁸⁷

Subtype	Associated Effect ^a
$\alpha1$	Sedation, anterograde amnesia, some anticonvulsant action, ataxia; in large part, addiction
$\alpha2$	Anxiolytic, hypnotic (EEG), anticonvulsant and some muscle relaxation (at higher doses)
$\alpha3$	Anxiolytic action, some muscle relaxation at higher doses
$\alpha4$	Diazepam-insensitive site
$\alpha5$	Cognition, temporal and spatial memory (maybe memory component of anxiety)
$\alpha6$	Diazepam-insensitive site

a) Updated at ISHC meeting Scotland, Glasgow, August, 2011.

Overall, the design, synthesis and biological evaluation of $\alpha x\beta3(\text{or } \beta2)\gamma2$ ($x=1-6$) subtype selective agents will provide the pharmacological tools necessary to determine which GABA_A/BzR subtype mediates which physiological response.⁷⁵ This will also provide entry into potential therapeutic agents to treat anxiety disorders, sleep disorders, epilepsy, enhance cognition in age-associated memory impairment in the absence of

deleterious side effects, as well as provide a potential new approach to treat drug addiction.^{14, 56, 76}

It is now believed that agents acting as benzodiazepine agonists at GABA_A/α₂, GABA_A/α₃, and/or GABA_A/α₅ receptors (schizophrenia) will possess desirable CNS properties. Ligands which are modulators of the benzodiazepine binding site of the GABA_A receptor by action as benzodiazepine agonists are referred to hereinafter as “GABA_A receptor agonists.” The GABA_A/α₁-selective (α₁β₂γ₂) agonists alpidem and zolpidem are clinically prescribed as hypnotic agents, suggesting that at least some of the sedation associated with known anxiolytic drugs which act at the BENZODIAZEPINE₁ binding site is mediated through GABA_A receptors containing the α₁β₂γ₂ subunit.

Accordingly, it is felt GABA_A/α₂, and GABA_A/α₃ receptor agonists rather than GABA_A/α₁ agonists will be effective in the treatment of anxiety or convulsant disorders with a reduced propensity to cause sedation.⁵⁷ Also, agents which are antagonists or inverse agonists at α₁ receptors might be employed to reverse sedation effected by α₁ agonists.⁷⁷

The GABA_A/BzR receptors which contain the α₅ subunit are of minor abundance (5%) in the whole brain, but are significantly expressed in the hippocampus, where they comprise 15-20% of the diazepam-sensitive GABA_A receptor population^{51, 56, 78} and are predominantly coassembled with β₃ and γ₂ subunits.^{32, 51} This has been confirmed by *in situ* hybridization and immunohistochemical studies which indicated that the hippocampus was relatively enriched in α₅ containing GABA_A receptors compared to

other brain areas.^{78,79} Interest in BzR/GABA_A α 5 subtypes has been stimulated recently by the report of Möhler et al.^{29, 80} on α 5 "knock in" mice. In brief, this group has provided strong evidence that hippocampal extrasynaptic α 5 GABA_A receptors play a critical role in associative learning and memory.^{29, 80}

In addition, an α 5 subtype selective inverse agonist was shown by Bailey et al.⁷⁶ to be important in the acquisition of fear conditioning and provided further evidence for the involvement of hippocampal GABA_A/benzodiazepine receptors in learning and anxiety.³⁰ A selective α 5 inverse agonist⁸¹ might have therapeutic utility as an agent to enhance cognition without the unwanted side effects associated with activity at other receptor subtypes.^{30,81-82} Most drugs currently used in the treatment of cognitive deficiency act through the cholinergic system and have moderate clinical efficacy. The GABA_A α 5 subtype selective inverse agonists may offer an alternative mechanism for the symptomatic treatment of memory impairment associated with Alzheimer's disease and related dementias.^{3,56,83-84} This has later been supported by the work of DeLorey et al. with α 5 selective inverse agonists,⁸² and antagonists as well as by Mckernan et al. and Atack et al.⁸⁵⁻⁸⁶ Recently, Savic et al have published several papers on PWZ-029, an α 5 subtype selective partial inverse agonist, which enhanced cognition in the passive avoidance paradigm (hippocampal-driven) in the Morris water maze and other paradigms.⁸⁷

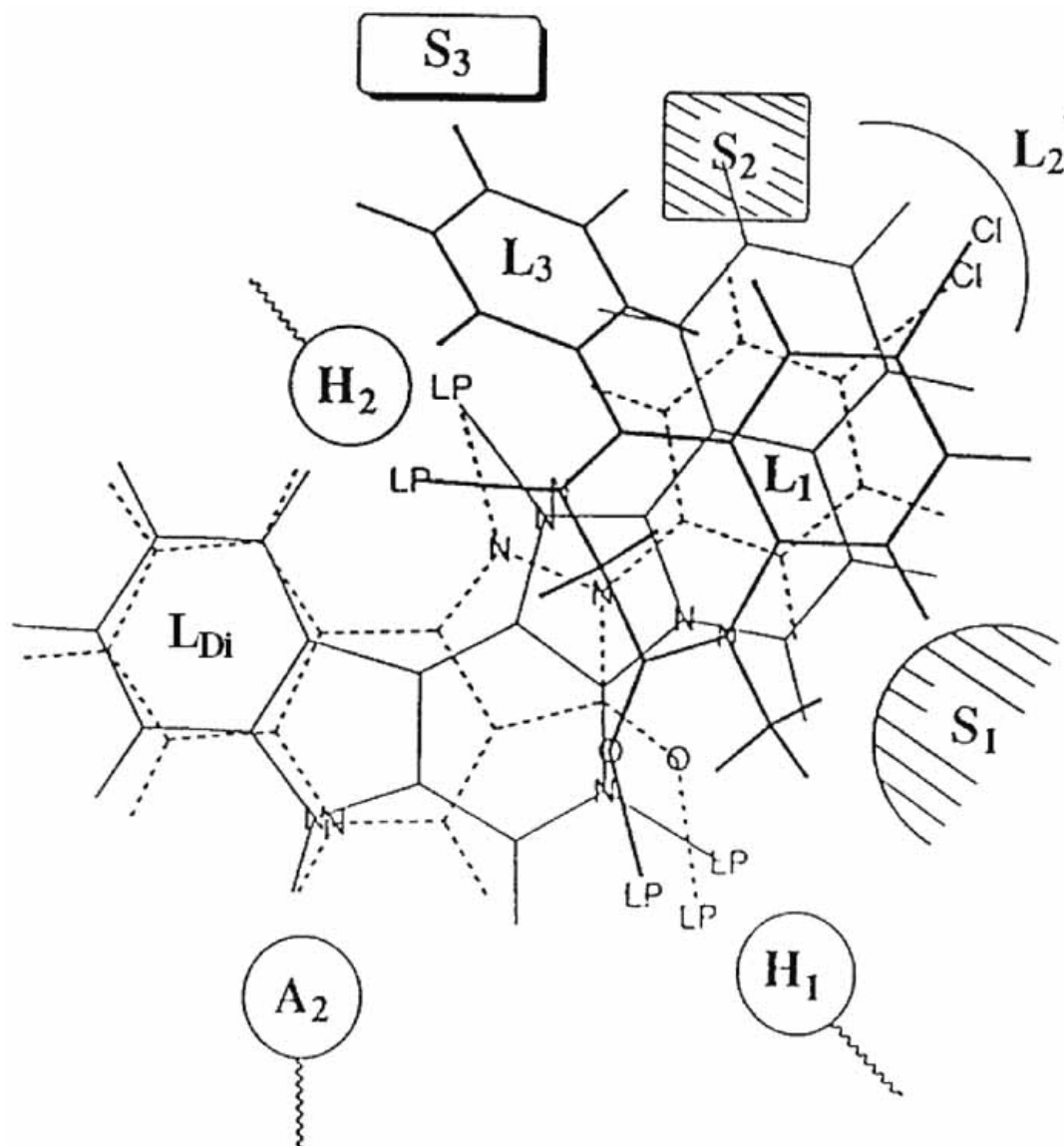
2. Molecular Modeling.

In recent years a unified pharmacophore/receptor model for agonists, antagonists and inverse agonists at the Bz BS was developed using the techniques of chemical synthesis, radioligand binding and receptor mapping.⁸⁸⁻⁸⁹ The overlap of these different modulators within the Bz BS has been supported by experimental data.⁹⁰⁻⁹² Using this ligand-based pharmacophore/receptor model and the $\alpha 1\beta 2\gamma 2$ GABA_A receptor models,^{23, 93} the experimental data of recent and past years have been evaluated and definite trends with regard to the orientation of the regions of the protein relative to the descriptors of the pharmacophore/receptor model have been identified and are presented in this work. The need to define such an orientation has been established,⁹⁴ since it permits inspection of ligand docking studies and the identification of possible roles specific residues may have within the benzodiazepine BS. These roles may then be explored in future studies involving covalent labeling, site-directed mutagenesis and structure-activity relationships, all of which contribute to the rational design of subtype specific modulators of the benzodiazepine BS of GABA_A receptors.

More than 166 agonists, antagonists and inverse agonists at the benzodiazepine BS,^{88, 89} which encompassed 15 structural families, were used for generating the unified pharmacophore/receptor model.⁸⁷ Although the relative affinities, efficacies and functional effects displayed by various ligands from the same structural class at the diazepam sensitive and diazepam insensitive benzodiazepine binding sites were taken into account, the approximate locations of descriptors (hydrogen bond donor sites,

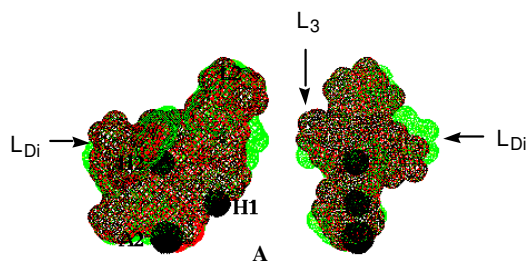
hydrogen bond acceptor sites, lipophilic regions, and regions of steric repulsion) were based primarily on *in vitro* binding affinities. Ligands from different structural classes were then superimposed on each other to satisfy the same descriptors, which resulted in the unified pharmacophore receptor model.²² Briefly, the pharmacophore/receptor model consists of two hydrogen bond donating descriptors (H_1 and H_2), one hydrogen bond acceptor descriptor (A_2) and one lipophilic descriptor (L_1). In addition to these descriptors, there are lipophilic regions of interaction (L_2 , L_3 and L_{Di}) as well as regions of negative steric repulsion (S_1 , S_2 and S_3). While occupation of L_2 and/or L_3 as well as interactions at H_1 , H_2 , and L_1 are important for positive allosteric modulation, inverse agonists only require interactions with the H_1 , L_1 , and A_2 descriptors of the pharmacophore/receptor model for potent activity *in vivo*.^{89, 95-98} The L_{Di} descriptor is a region of lipophilic interaction, for which the difference between the diazepam sensitive (DS) and the diazepam insensitive (DI) subtype pharmacophore receptor models is most pronounced. Depicted in **Figure 4** are the relative locations of the different descriptors and regions of the model.

Figure 4. Relative locations of the descriptors and regions of the unified pharmacophore/ receptor model. The pyrazolo[3,4-*c*]quinolin-3-one CGS-9896 (dotted line), a diazadiindole (thin line), and diazepam (thick line) aligned within the unified pharmacophore/receptor model for the Bz BS. H₁ and H₂ represent hydrogen bond donor sites within the Bz BS while A₂ represents a hydrogen bond acceptor site necessary for potent inverse agonist activity *in vivo*. L₁, L₂, L₃ and L_{Di} are four lipophilic regions and S₁, S₂, and S₃ are regions of negative steric repulsion. LP = lone pair of electrons on the ligands.

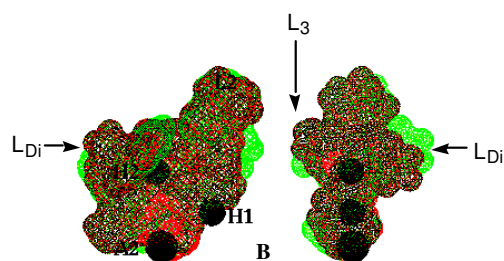


Moreover, pharmacophore/receptor models for 6 recombinant GABA_A/ BzR subtypes ($\alpha x\beta 3\gamma 2$, $x = 1-6$) have been established *via* an SAR ligand mapping approach (**Figure 5**).^{81, 83} This study was based on the affinities of 166 BzR ligands at 6 distinct ($\alpha 1-6\beta 3\gamma 2$) recombinant GABA_A/BzR receptor subtypes; the ligands were taken from at least twelve different structural families. Examination of the included volumes indicated that the shapes of binding pockets for $\alpha 1$, $\alpha 2$ and $\alpha 3$ subtypes are very similar to each other. Region L₂ for the $\alpha 5$ containing subtype appeared to be larger in size than the analogous region of the other receptor subtypes. Region L_{Di}, in contrast, appeared to be larger in the $\alpha 1$ subtype than in the other subtypes.^{34, 57, 85, 99-100} Moreover, region L₃ in the $\alpha 6$ subtype is either very small or nonexistent in this diazepam insensitive “DI” subtype as compared to the other subtypes (see **Figure 5** for details). Preliminary results for the $\alpha 4$ -containing receptor subtype (DI) indicated that region L₃ in the $\alpha 4$ subtype suffered a similar fate. With the aid of these models, several series of ligands have been prepared and evaluated pharmacologically to determine the extent of interactions at different anchor points individually and/or simultaneously in order to search for GABA_A/ benzodiazepine receptor subtype selective ligands.

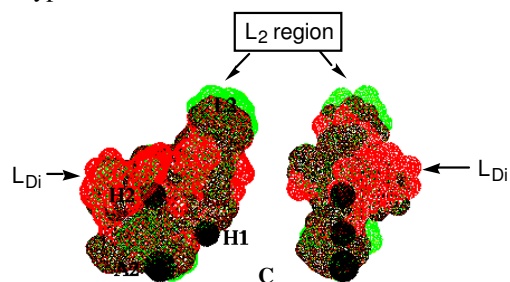
Figure 5. Orthogonal views of the overlap of the included volumes of the pharmacophore/receptor models for $\alpha 1\beta 3\gamma 2$ and the other five receptor subtypes ($\alpha 2\beta 3\gamma 2$, $\alpha 3\beta 3\gamma 2$, $\alpha 4\beta 3\gamma 2$, $\alpha 5\beta 3\gamma 2$, and $\alpha 6\beta 3\gamma 2$, respectively).



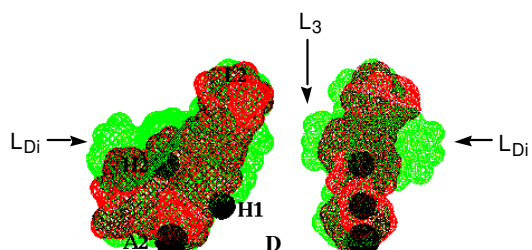
In grey is the included volume of the $\alpha 1$ subtype while depicted in black is the volume of the $\alpha 2$ subtype.



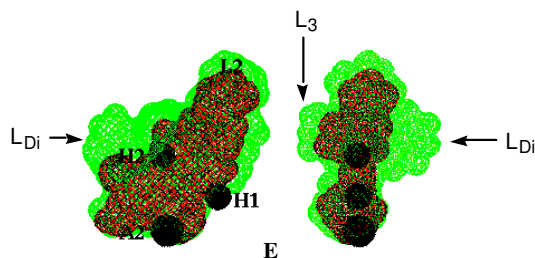
In grey is the included volume of the $\alpha 1$ subtype while depicted in black is the volume of the $\alpha 3$ subtype.



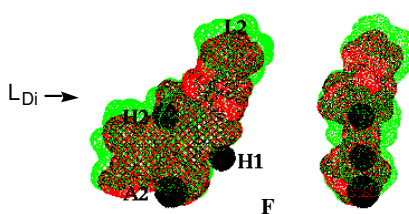
In grey is the included volume of the $\alpha 5$ subtype while depicted in black is the volume of the $\alpha 1$ subtype.



In grey is the included volume of the $\alpha 1$ subtype while depicted in black is the volume of the $\alpha 4$ subtype.



In grey is the included volume of the $\alpha 1$ subtype while depicted in black is the volume of the $\alpha 6$ subtype.



In grey is the included volume of the $\alpha 4$ subtype while depicted in black is the volume of the $\alpha 6$ subtype.

The pharmacophore models have been incorporated into a homology model of the $\alpha 1\beta 3\gamma 2$ subtype, the model for WYS8 ($\alpha 1\beta 3\gamma 2$) and recently expanded by Ernst and Sieghart in 2012.^{87a-d} The refined receptor binding model by Sieghart and Ernst is very

similar to that reported by Cook^{87a-d} and provides much of the insight into design of new ligands in this research.

3. Objectives of This Research.

One goal of this research was to design a quick and easy method to perfect the synthesis of benzodiazepines by allowing the reactions to be scaled up to multigram to kilogram size reactions, which has been accomplished. Another goal of this research was to reduce liver metabolism, increase bioavailability and increase duration of action of the imidazo benzodiazepines, Xe-II-053 and HZ-166, the former of which was in Phase I trials (BMS) as an anxiolytic several years ago. The commonly present ester moiety on most imidazo benzodiazepines is often responsible for the increase in liver metabolism, low bioavailability and decreased duration of action. The ester moiety is rapidly metabolized to the carboxylic acid by serum (rats, mice) and hepatic enzymes (humans); after which, the carboxylic acid metabolite undergoes further metabolism by hepatic enzymes, CYP-450's, to the acyl glucuronide, which in turn hinders passage through the blood-brain barrier and the metabolite form is rapidly excreted by the body. Replacement of the ester with a series of ester bioisosteres should provide ligands with much better pharmacokinetic properties and microsomal stability.

The term "bioisostere" refers to a compound which results from the exchange of an atom or of a group of atoms with another, broadly similar, atom or group of atoms. Such an exchange is termed a "bioisosteric replacement" and is useful to create a new

compound with similar biological properties to the parent compound but with much better pharmacokinetic properties. The bioisosteric replacement may be physicochemically or topologically based. Bioisosteric replacement generally enhances desired biological or physical properties of a compound without making significant changes in chemical structure. For example, the replacement of a hydrogen atom with a fluorine atom at a site of metabolic oxidation in a drug candidate may prevent such metabolism from taking place. Because the fluorine atom is similar in size to the hydrogen atom the overall topology of the molecule is not significantly affected, leaving the desired biological activity unaffected. However, with this retarded pathway for metabolism, the drug candidate may have a longer half-life. Another example is aromatic rings, a phenyl -C₆H₅ ring can often be replaced by a different aromatic ring such as thiophene or naphthalene which may improve efficacy or change binding specificity of a respective bioisostere.

Since $\alpha 1\beta 3\gamma 2$ GABA_Aergic subtypes are principally responsible for the sedative, ataxic and amnesic side effects of benzodiazepine receptor ligands as well as abuse potential,^{87a-d,101, 102} poor affinity and/or efficacy at these subtypes are a requirement here for ligands. Based on molecular modeling²² and the ability of BzR ligand PWZ-029 to enhance cognition,¹⁰²⁻¹⁰³ a series of new subtype selective ligands which had been previously designed and synthesized were converted into ester related bioisosteres. Furthermore, recently developed non-sedating anticonvulsants that target specific $\alpha 2$ or $\alpha 2/\alpha 3$ GABA_A receptor subtype(s) involved in mediation of the anticonvulsant action but not the sedative action^{3, 104} were also converted into ester related bioisosteres in order to

study the stability on liver microsomes. The selectivity for GABA_A receptor-subtypes may be achieved by selective efficacy.¹ Those ligands which are agonists with subtype selectivity for α 2- and α 3-GABA_A receptors that also have reduced agonistic and/or exhibit antagonistic activity at α 1-GABA_A receptors should provide ligands with analgesic, anxiolytic, and anticonvulsant properties, but with reduced sedative, ataxic and amnestic side effect, as well as little or no abuse liability.^{3, 104}

II. Results and Discussion.

1.1. An Improved Process for the Synthesis of 4H-Imidazo-[1,5-a]-[1,4]-Benzodiazepines.

Imidazo[1,5-a][1,4]benzodiazepines are well documented to exhibit potent activity at GABA_A/Bz receptors. This series belongs to one of the very few chemical families which have been extensively investigated for GABA_A/Bz receptor mediated activity.^{22, 105} Flumazenil (Ro 15-1788), an imidazo[1,5-a][1,4]benzodiazepine, was earlier shown to bind to central GABA_A receptors with little or no intrinsic agonist activity, but with the ability to block the activity of an agonist or inverse agonist at GABA_A/Bz receptors.¹⁰⁵ It is employed principally as an antidote to reverse the effects of exogenous benzodiazepines.¹⁰⁶ More recently ligands such as flumazenil have been shown to behave as weak inverse agonists or weak agonists depending on the biological paradigm employed. Many procedures have been reported, to date, to synthesize this

imidazo-type of structure.¹⁰⁷⁻¹⁰⁸ Most of them have been achieved in low yield through an iminophosphate/chloride intermediate.

As part of a program directed toward the development of clinically relevant imidazo[1,5-a][1,4]-benzodiazepines,^{22, 109} the construction of the imidazo-ring was considered a crucial step for the synthesis of gram quantities of imidazobenzodiazepine analogues. The previous process of using ethyl isocyanoacetate and iminophosphorochlorides/chlorides¹¹⁰⁻¹¹¹ was employed coupled with different solvents and bases, but the yields of these reactions were very low (15-30%). Since this step was highly convergent and at the very end of the synthetic route, it affected the overall economy of the route in a deleterious manner. It was, therefore, of interest to improve the annulation sequence for this series of CNS-active ligands.

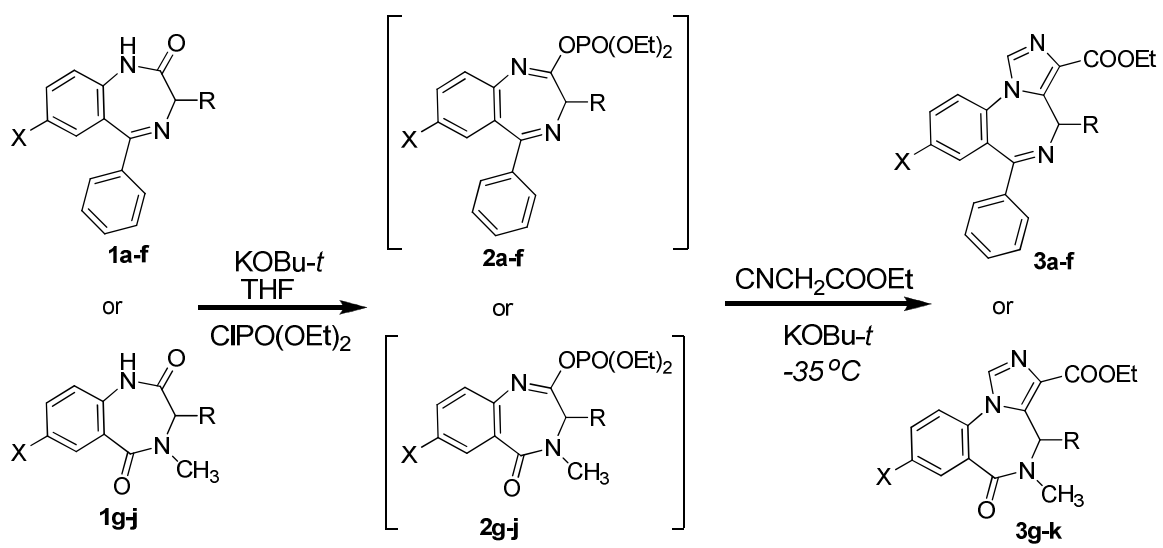
Certainly, a one-pot annulation process for the construction of imidazobenzodiazepines had been developed.¹¹⁰⁻¹¹¹ This procedure permitted the condensation of the less stable iminophosphates with ethyl isocyanoacetate under basic conditions without isolation of the less stable iminophosphates and the pre-formation of the carbanion of ethyl isocyanoacetate. For instance, Watjen et al.^{110a} had reported the formation of iminophosphates by using NaH or LDA in DMF, and then directly reacting this mixture with ethyl isocyanoacetate and potassium *tert*-butoxide to offer the imidazo molecules in 47% yield. Ian Fryer et al.^{110 b, c} had reported the use of potassium *tert*-butoxide as the base in both steps, and DMF as well as THF were chosen as solvents in

these cases; however, this process gave the ligands in only 44% yield. The latest report from Fryer's procedure gave the target imidazobenzo framework in only 30% yield.¹¹¹

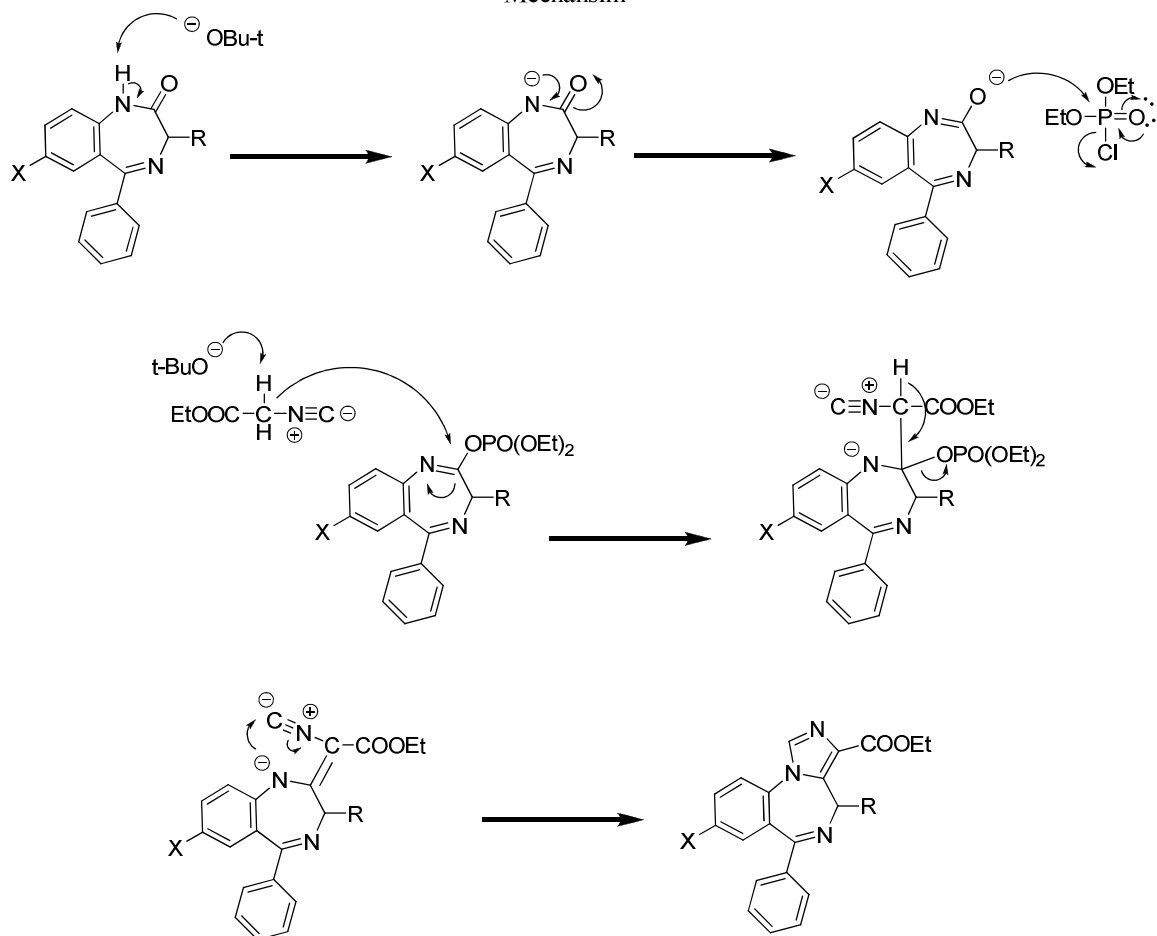
1.2. Scope and Limitations.

To improve the one-pot annulation reaction the procedure was modified and after many attempts it was found the ratio of the reagent combination and reaction temperature were critical for good yields on a consistent basis. As shown in **Scheme 1**, the initial amount of potassium *tert*-butoxide used to form the iminophosphates should be kept at 1.1 equivalents as compared to the amides (**1a-k**). The yield of the reaction was much lower if more potassium *tert*-butoxide (>1.1 equivalents) was employed. The amount of diethyl chlorophosphate (used as received) employed was only slightly higher (1.3 equivalents) than the potassium *tert*-butoxide to convert all the starting amide into the desired iminophosphates (**2a-k**). Importantly, the addition of ethyl isocyanoacetate, followed by the second addition of potassium *tert*-butoxide should be carried out at low temperature (-35°C is recommended). However, a temperature lower than -35°C (such as -78°C) was also acceptable in this procedure and the second addition of potassium *tert*-butoxide was kept at 1.1 equivalents. This procedure made the separation of the product much easier, which was critical for gram scale reactions. Most of the desired imidazobenzodiazepines were precipitated from diethyl ether after workup for no chromatography was needed.

Scheme 1



Mechanism



A variety of different amidobenzodiazepines (**1a-h**) were chosen as substrates for this study (See **Table 2**). The 5-phenyl-benzodiazepines (**1a-f**) and N-methyl-6-oxo-benzodiazepines (**1g-h**) readily condensed with ethyl isocyanoacetate to give the desired imidazobenzodiazepines (**3a-k**) in 70-89% yield in this improved process. The substituents in ring-A such as F, Cl and Br of **1a-h** did not affect the yield of the process. The chiral α -substituted amidobenzodiazepines (**1c-e**, and **1i**), which are more hindered than their unsubstituted parents (**1a-b** and **1f-1j**), also gave the imidazo analogues in 70-81% yield. In the case of optically active substrates (**1c-e**, and **1i**), this procedure provided the desired imidazo analogues without loss in optical activity. The *R* and *S* isomers have much different BzR/GABAergic receptor binding profiles.¹¹² All of these reactions can be scaled up with no difficulty. When this process was employed for reactions of *tert*-butyl isocyanoacetate, the corresponding imidazobenzodiazepine **3k** was obtained in 70% yield.

Table 2. Examples of imidazo-[1,5-a]-[1,4]-benzodiazepines obtained using the new procedure.¹¹³

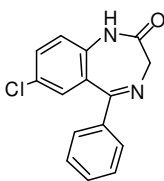
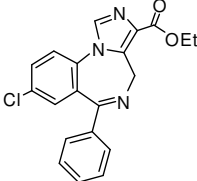
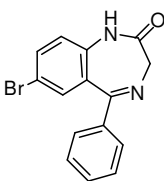
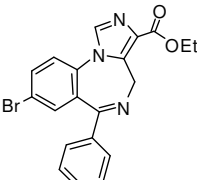
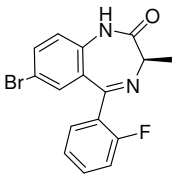
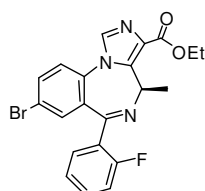
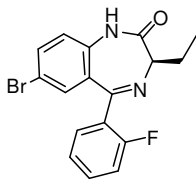
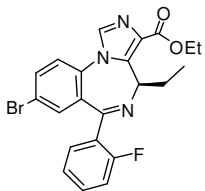
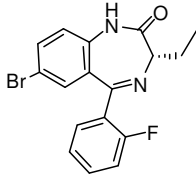
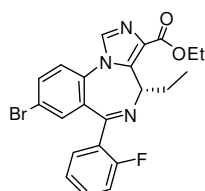
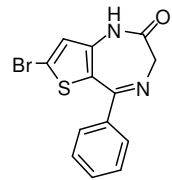
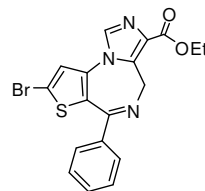
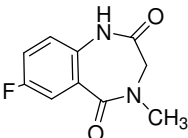
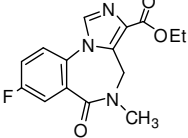
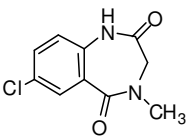
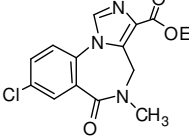
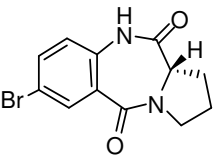
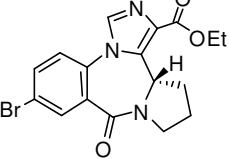
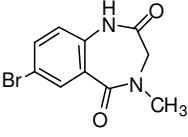
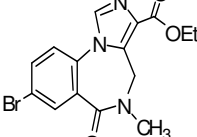
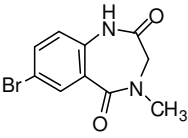
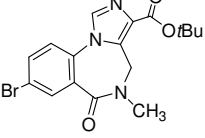
Starting material	Product	Yield(%)	Scale(g)
1a 	3a 	87	11
1b 	3b 	77	15
1c 	3c 	74	10
1d 	3d 	73	3.6
1e 	3e 	72	1
1f 	3f 	75	5

Table 2 (continued). Examples of imidazo-[1,5-a]-[1,4]-benzodiazepines obtained using the new procedure.¹¹³

Starting material	Product	Yield(%)	Scale(g)
1g 	3g 	75	2
1h 	3h 	89	15
1i 	3i 	81	15
1j 	3j 	72	15
1k 	3k 	70	20

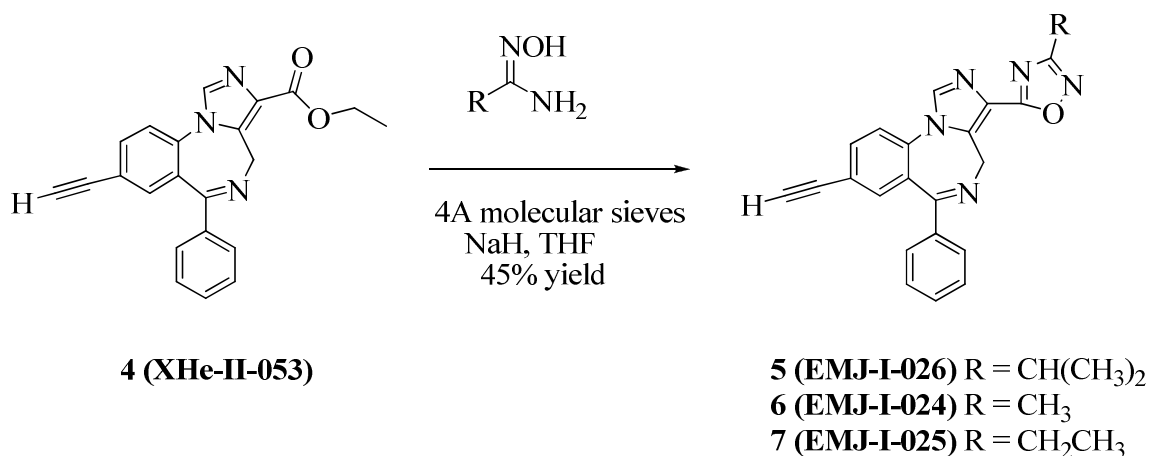
In summary, an efficient, practical, improved, one-pot annulation reaction for the construction of potent BzR active imidazobenzodiazepines was developed. A variety of substrates were successfully employed in this procedure. This one-pot process required neither the isolation of the unstable intermediates nor does it require the preformation of

the carbanion of the isocyanacetate. Moreover, potassium *tert*-butoxide is safer and easier-to-handle for scale-up, as compared to other bases such as NaH, LHMDS and LDA. In addition, no chromatography was required for this process.¹¹³

2. Synthesis of the Bioisosteric Imidazobenzodiazepine EMJ-I-026 (5) and Analogues for Lead Compounds.

The ethyl ester **4** (XHe-II-053), lead compound, was treated with sodium hydride and *N'*-hydroxyisobutyrylimidamide in the presence of dry THF and dried 4A^o molecular sieves to provide the isopropyl bioisostere **5** (EMJ-II-026) in 45% yield, as shown in **Scheme 2**. Other bioisosteric analogues, such as the methyl bioisostere **6** (EMJ-I-024) and ethyl bioisostere **7** (EMJ-I-025) was also synthesized using the same method.

Scheme 2



Binding affinity at α x β 3 γ 2 GABA_A/BzR subtypes for EMJ-I-026 (**5**)

α 1	α 2	α 3	α 4	α 5	α 6
5000	135	1027	ND	152	5000

Values are reported in nM. ND = Not Determined.

The C-3 substituted ligand EMJ-I-026 (**5**) is a classical bioisostere of the orally active, nonsedating, anxiolytic XHE-II-053 (**4**). Because this α 2/ α 3 Gabaergic receptor subtype selective ligand, XHE-II-053, was anxiolytic in rodents, dogs and primates with no sedative, amnestic, or ataxic side effects, it was decided to make C-3 ester analogues for SAR studies. Such alpha2/alpha3 Gabaergic receptor subtype selective ligands considered here would lack ester linkages and would be less sensitive to hydrolysis by esterases in animals or humans. The compound, EMJ-I-026, exhibited selective efficacy for the GABA_A/ α 2, GABA_A/ α 3, and/or GABA_A/ α 5 receptors relative to the GABA_A/ α 1 receptors (see **Figure 6**). This isopropyl bioisostere **5** desirably exhibited functional

selectivity at α_2 , α_3 and α_5 subtypes with very little efficacy at $\alpha_1\beta_2\gamma_2$ subtypes at 100 nM (physiologically relevant concentration). In mice (light/dark paradigm) it demonstrated anxiolytic activity with sedative activity due to decreased efficacy at $GABA_A/\alpha_1$ receptors when given i.p.

Gabaergic receptor subtype selective anxiolytics act preferably by selectively or preferentially activating (as agonists or partial agonists) the $GABA_A/\alpha_2$ receptors and/or $GABA_A/\alpha_3$ receptors as compared to the $GABA_A/\alpha_1$ receptors. A selective or preferential therapeutic agent will exhibit less binding affinity or less functional efficacy at $GABA_A/\alpha_1$ receptors, as compared to the $GABA_A/\alpha_2$ or $GABA_A/\alpha_3$ receptors. Alternatively, the agent might bind to $GABA_A/\alpha_1$, $GABA_A/\alpha_2$ and $GABA_A/\alpha_3$ receptors with a comparable affinity but exerts preferential efficacy of receptor activation at $GABA_A/\alpha_2$ and $GABA_A/\alpha_3$ receptors, as compared to the $GABA_A/\alpha_1$ receptors. In fact, in the case of XHe-II-053, this ligand had no efficacy at this $GABA_A/\alpha_1$ receptors subtype and was probably an antagonist at this subtype, a very desirable profile.

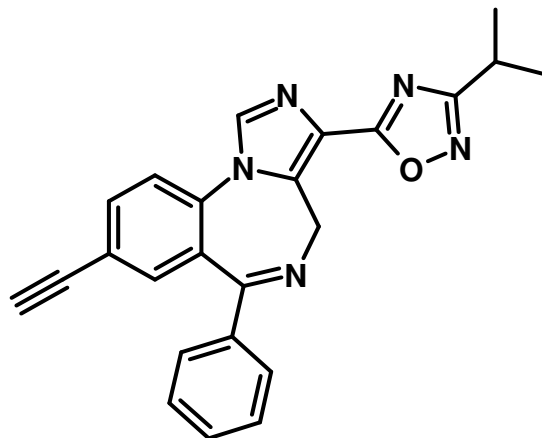
2.1. *In Vitro* Electrophysiological Studies on EMJ-I-026 (5) for Efficacy at BzR/GABAergic Subtypes.

The efficacy of EMJ-I-026 (5) on $GABA_A$ receptors was assessed (Ramerstorfer et al.)¹¹⁴ by two-electrode voltage clamp experiments in the cRNA injected *Xenopus* oocytes that functionally expressed several subtype combinations of $GABA_A$ receptors.¹¹⁴⁻¹¹⁸ Data from the electrophysiology indicated (in oocytes) at physiological

concentrations (100 nM, -7) that EMJ-I-026 (**5**) was an agonist at α_2 , α_3 , and α_5 subtypes, but was nearly silent at α_1 subtypes. This, as mentioned, was a very desirable profile. At higher concentrations of EMJ-I-026 (**5**; 1-10 μ M) this ligand was a potent agonist at α_2 , α_3 and α_5 subtypes with weak agonist efficacy at the less desirable α_1 subtypes. This ligand (EMJ-I-026 **5**) exhibited more than 10-fold selective efficacy for the GABA_A/ α_2 , GABA_A/ α_3 , and/or GABA_A/ α_5 receptors relative to the GABA_A/ α_1 receptors (refer to **Figure 6**). This compound also exhibited functional selectivity *in vivo*, for it demonstrated anxiolytic activity with no sedative/ ataxic effects due to decreased efficacy at GABA_A/ α_1 receptors. Because this agent was a nonsedating anxiolytic *in vivo* in rodents and the ester bioisostere should be more stable *in vivo*, this ligand is under study in a primate “conflict” model as an anxiolytic.

Figure 6. Oocyte Efficacy and *In Vitro* Receptor Binding Data of EMJ-I-026 (5). The $\log[M]$ at -7 is close to physiologically relevant concentrations of EMJ-I-026.

EMJ-I-026



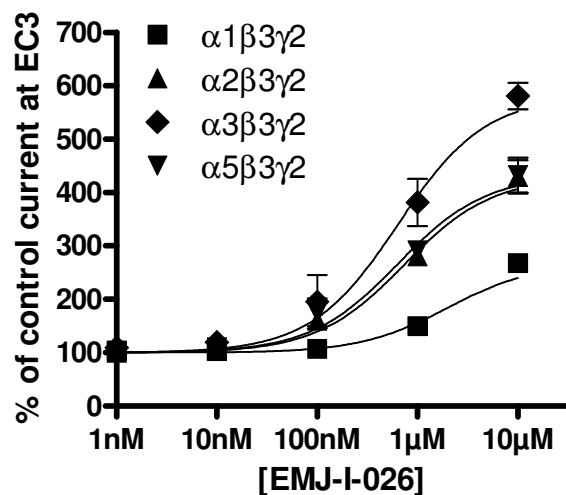
In vitro receptor binding data on HEK cells.

α_1	α_2	α_3	α_4	α_5	α_6
5000	135	1027	ND	152	5000

Values are reported in nM. ND = Not Determined.

Figure 6 is continued on the next page.

Figure 6. Continued.



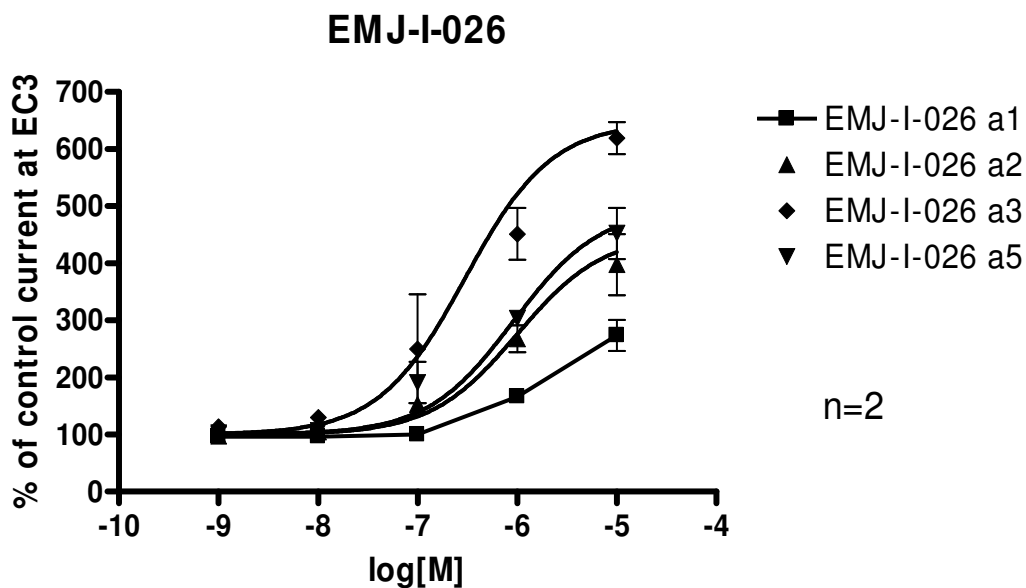
		$\alpha 1\beta 3\gamma 2$	$\alpha 2\beta 3\gamma 2$	$\alpha 3\beta 3\gamma 2$	$\alpha 5\beta 3\gamma 2$
EMJ-I-026	EC50 95%CI	>1.9µM	>0.7µM	>638nM	>633nM

Values are reported in µM, n = 3-4 oocytes.

	10nM	100nM	1µM	10µM
$\alpha 1$	103±4	107±4	150±10	268±13
$\alpha 2$	112±4	160±3	281±13	429±31
$\alpha 3$	119±8	195±5	381±45	581±25
$\alpha 5$	110±5	175±66	291±13	432±33

Figure 6 is continued on the next page.

Figure 6. Continued.

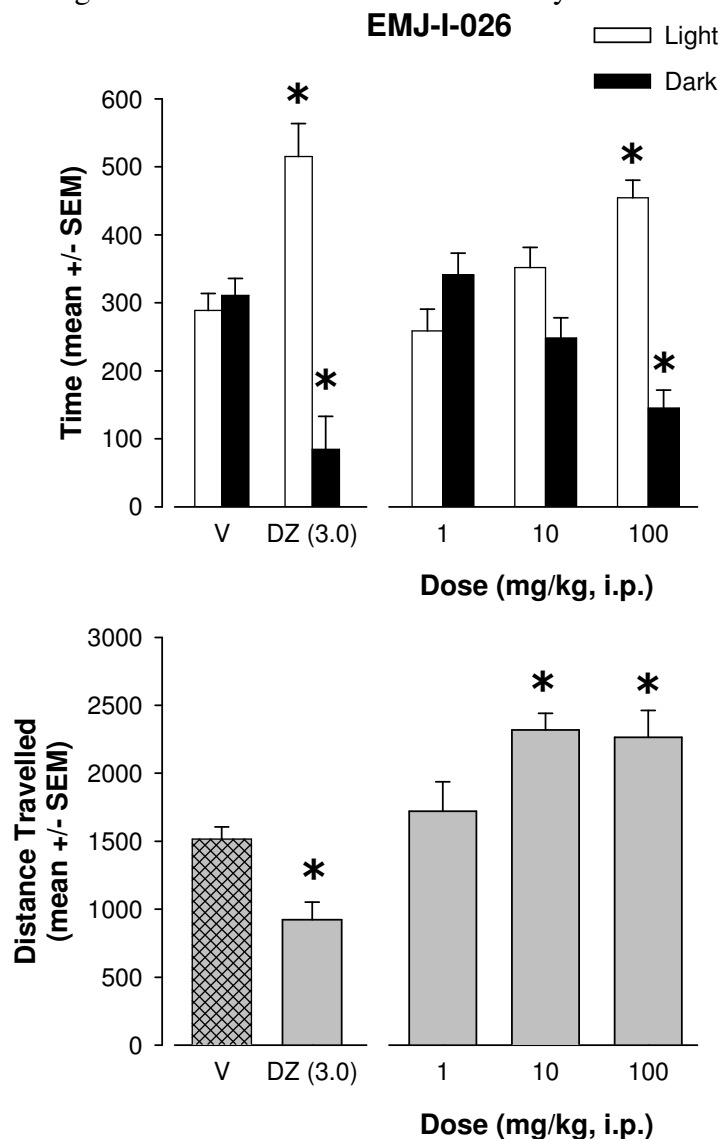


	EMJ-I-026 a1	EMJ-I-026 a2	EMJ-I-026 a3	EMJ-I-026 a5
BOTTOM	100.0	100.0	100.0	100.0
TOP	300.7	451.4	647.0	496.8
LOGEC50	-5.685	-6.000	-6.524	-6.037
HILLSLOPE	1.000	1.000	1.000	1.000
EC50	2.067e-006	1.000e-006	2.993e-007	9.175e-007

2.2. The Light/Dark and Locomotor Activity Assay on EMJ-I-026 (5).

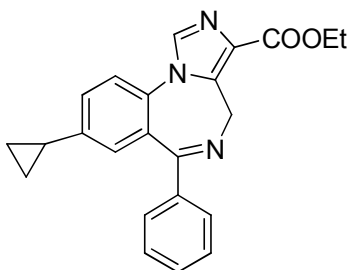
The light/dark assay was a test that was used to measure “anxiolytic-like behavior” in rodents. Increased time spent in the light area compared to vehicle indicated anti-anxiety effects. DZ represents the diazepam control. Diazepam was significantly anxiolytic as compared to vehicle, as expected. Doses (1, 10 and 100 mg/kg) of the EMJ-

I-026 (**22**) ligand showed significant anxiolytic activity at 10 and 100mg/kg. Locomotor activity was a measure of the animal's activity related to sedation, but not a direct measure of sedation; even though many laboratories use "suppression of locomotor activity" as a measure of sedation. DZ again represents the diazepam control. DZ significantly reduced locomotor activity over vehicle, i.e. an indicator of sedation, while EMJ-I-026 at doses of 10 and 100mg/kg significantly increased locomotor activity (refer to **Figure 7**). From this data, it was clear that EMJ-I-026 (**5**) did not decrease locomotor activity in rodents in this paradigm of J. Crawley executed in the laboratory of Rowlett et al. This data indicated in these mice, there appeared to be no effects from ataxia nor sedation. This indicated that EMJ-I-026 was a nonsedating anxiolytic and illustrated the ester function in these molecules can be replaced with a more stable ester bioisostere and still retain anxiolytic activity.

Figure 7. The Light/Dark Test and Locomotor Activity Test on EMJ-I-026 (**5**).

Based on the binding affinity of EMJ-I-026 (**5**) as well as its important anxi-selective activity (no sedation/ataxia), it was decided to prepare analogues of EMJ-I-026 (**5**). Based on the success of ligands EMJ-I-026 (**5**) and YT-III-231 (**8**), **Figure 8**, the ligands YT-III-40 (**9**) and YT-III-41 (**10**) were designed and synthesized (see below for their metabolic stability on microsomal enzymes).

Figure 8. Binding affinity at $\alpha\beta\gamma\delta$ GABA_A/BzR subtypes (values are reported in nM) for YT-III-231 (**8**).



8 YT-III-231

Screening No.	$\alpha 1$	$\alpha 2$	$\alpha 3$	$\alpha 4$	$\alpha 5$	$\alpha 6$
1	51.09	61.46	26.34	ND	9.124	ND
2	19.83	23.65	19.87	ND	1.105	ND

2.3. Acid/Base Stability Studies on EMJ-II-026 (5).

In order to test the stability of the bioisostere EMJ-II-026 (5) compared to the ethyl ester XHe-II-053 (4), both compounds were subjected to different extremes of pH values to simulate stomach and intestinal conditions for up to 60 hrs and analyzed by TLC for hydrolysis products. According to the information below in **Table 3**, it is clear that chemical hydrolysis of the ethyl ester XHe-II-053 (4) would take more time (> 48 hrs) to occur than the compound would normally be exposed to *in vivo*. However, with time, the ethyl ester XHe-II-053 (4) did begin to hydrolyze, which resulted, in formation of the carboxylic acid, whereas the bioisostere analogue EMJ-I-026 (5) was completely stable to both acidic and basic conditions for the 60 hrs.

Table 3. Acid/Base Stability Studies of XHe-II-053 (4) and EMJ-I-026 (5).

Compound	pH		1 hr		2 hr		5 hr		10 hr		24 hr		48 hr		60 hr
EMJ-I-026 5	2	A	N/A	A	N/A	A	N/A	A	N/A	A	N/A	A	N/A	A	N/A
	2	B	NR	B	NR	B	NRq	B	NR	B	NR	B	NR	B	NR
	10	A	N/A	A	N/A	A	N/A	A	N/A	A	N/A	A	N/A	A	N/A
	10	B	NR	B	NR	B	NR	B	NR	B	NR	B	NR	B	NR
XHe-II-053 4	2	A	NR	A	NR	A	NR	A	NR	A	NR	A	NR - small smearing of spot	A	NR - small smearing of spot
	2	B	NR	B	NR	B	NR	B	NR	B	NR	B	NR	B	NR
	10	A	NR	A	NR	A	NR	A	NR	A	NR	A	NR - small smearing of spot	A	NR - small smearing of spot
	10	B	NR	B	NR	B	NR	B	NR	B	NR	B	NR - small smearing of spot 95% 053 (RF=0.3) and 5% RF=0.2	B	NR - small smearing of spot 80% 053 (RF=0.3) and 20% RF=0.2
A = 2 mL of Buffer and 2 mg of compound								Common RF values for compounds							
B = 1 mL of Buffer and 1 mL of MeOH and 2 mg of compound								EMJ-I-026 = 0.8 XHe-II-053 = 0.3							
N/A = no spot because compound would not go into solution								Acid = Baseline to 0.2 smear							

2.4. *In Vitro* Metabolic Stability of XHe-II-053 (**4**) and EMJ-I-026 (**5**).

In humans XHe-II-053 (**4**) was largely transformed into the inactive metabolite XHe-II-053 Acid (**4**) via hepatic enzymes and then to a glucuronide, which resulted, in sub-optimal pharmacokinetics (BMS unpublished results). The synthesis of the related bioisostere EMJ-II-026 (**5**) was an effort to circumvent the metabolic liability of the compound on human liver microsomes versus the control anxiolytic **4**, in an effort to develop nonsedating anxiolytics with longer half lives in humans. Research with a CRO by Methridion (unpublished results) had already shown **4** and **5** were stable in human blood, brain and kidney.

A metabolic stability study of these compounds was undertaken at SRI International by Dr. Ng and coworkers as a collaborative project funded by National Institute of Mental Health (NIMH). In this study the test articles were incubated with pooled human liver microsomes which represented 150 human livers and the aliquots were analyzed at various time points using LC-MS/MS. The results from this study are shown in **Table 4**. Significant metabolic liability was observed at both 1 and 10 μ M for XHe-II-053 **4** (less than 14% remaining at 30 min). The corresponding carboxylic acid control of **4**, i.e. carboxylic acid **11**, **Figure 9**, was recovered unchanged during the test period. Additionally, all the compounds when incubated with heat-inactivated human liver microsomes underwent no significant change in the % remaining of any of the compounds, which indicates the ligands were all stable under the control incubation conditions. Analysis of these results indicated that the main site of metabolism on human

livers was due to the pendant ethyl ester moiety, which was not unexpected but designed earlier as a method of clearance (metabolic switching) to prevent buildup of the drug *in vivo* (patients).

Figure 9. Carboxylic Acid of XHe-II-053

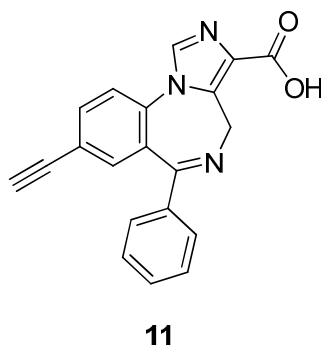


Table 4: *In Vitro* Metabolic Stability of Compounds 4, 5 and 11 Using Human Liver Microsomes by SRI International

Test Article	Time, min	Mean % Remaining vs T = 0 min ^a	
		1 μ M ^b	10 μ M ^b
4	15	41.4	47.6
	30	11.2	13.9
	60	1.5	1.7
4 with HI ^c microsomes	60	107.4	101.8
5	15	100.0	109.2
	30	109.7	108.0
	60	90.8	96.6
5 with HI ^c microsomes	60	137.5	118.9
11	15	107.6	95.3
	30	110.4	94.8
	60	110.7	94.8
11 with HI ^c microsomes	60	105.8	97.2

^a % remaining at T =0 is 100%

^b Samples were assayed in duplicates

^c HI = Heat Inactivated, for control purposes

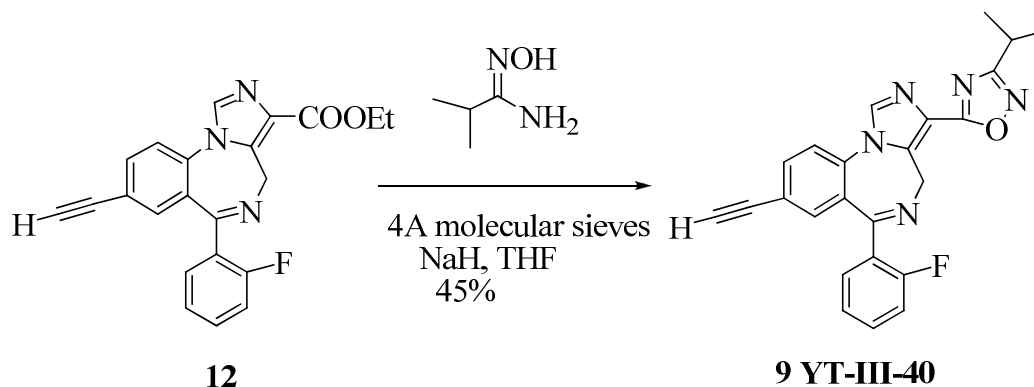
Based on these findings it was decided to design and synthesize novel analogues with bioisosteric replacement of the labile ethyl ester moiety analogues to that of the lead analogue XHe-II-053 (**4**). Previously, in the case of GABA_A modulators in the benzodiazepine series of compounds, it had been demonstrated that replacement of the ethyl ester at the 3-position by a 1,2,4-oxadiazole moiety resulted in higher intrinsic efficacy at benzodiazepine receptors as compared to the corresponding ethyl esters.^{110a} Substituted 1,2,4-oxadiazoles are also metabolically stable and slightly less lipophilic than the corresponding ester derivatives,^{110d} hence compound **5** had been synthesized. Substituted 1,2,4-oxadiazole analogue **5** (EMJ-I-026) was significantly stable as compared to **4** (XHe-II-053), as expected, based on medicinal chemistry precedents.

2.5. Synthesis of YT-III-40 (**9**).

In the design of the following ligands the goal was to choose ligands with good $\alpha 2/\alpha 3$ Gabaergic receptor subtype selectivity or efficacy as the lead to synthesize ligands that lack ester linkages and are thus relatively insensitive to hydrolysis by esterases *in vivo*. It was known the 2' substituent (-F) should increase affinity at BzR BS and the replacement of the ester, if compatible, should render this ligand a long-lived $\alpha 2/\alpha 3$ selective agonist.

The ethyl ester **12**, was treated with sodium hydride and N'-hydroxyisobutyrylimidamide in the presence of dry THF and dry 4A^o molecular sieves to provide the isopropyl bioisostere **9** (YT-III-40) in 45% yield, as shown in **Scheme 3**.

Scheme 3



Binding affinity at $\alpha\beta\gamma\delta$ GABA_A/BzR subtypes.

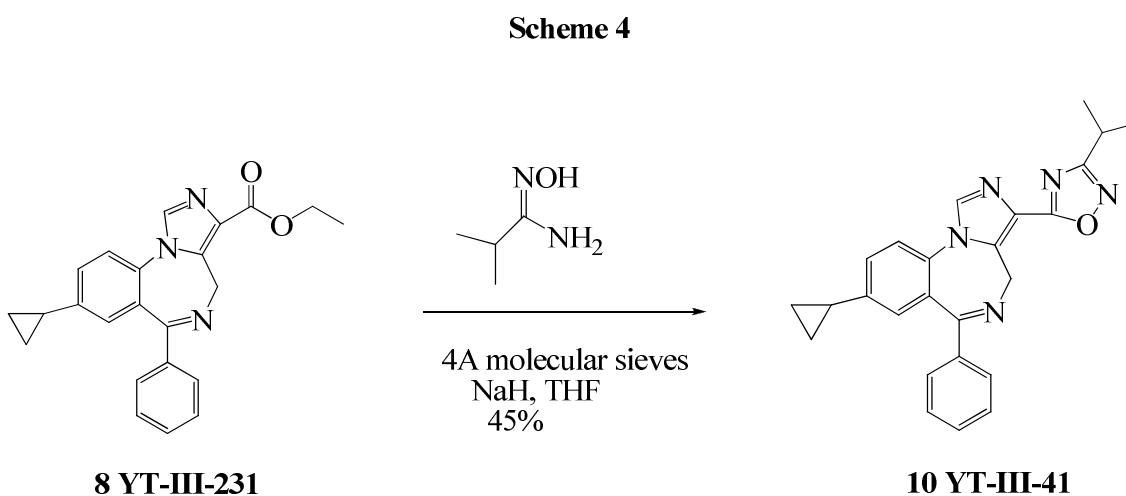
$\alpha 1$	$\alpha 2$	$\alpha 3$	$\alpha 4$	$\alpha 5$	$\alpha 6$
1454	2576	3543	ND	112.6	ND

Values are reported in nM. ND = Not Determined.

Unfortunately, this molecule, it was felt, was too large to fit in the receptor binding pocket of $\alpha 2/\alpha 3$ subtypes. However, a second explanation as regards the lack of affinity of **9** may stem from a screen at UNC done by the rapid screening technique which may have resulted in erroneous results, this is being investigated. The laboratory at UNC was having trouble transfecting the $\alpha 2$ and $\alpha 3$ related HEK cells for receptor binding hence the results at $\alpha 2$ and $\alpha 3$ subtypes maybe completely wrong. At the same time the transfection of the $\alpha 1$ and $\alpha 5$ related HEK cells were going well so the data at $\alpha 1$ and $\alpha 5$ subtypes is reliable.

2.6. Synthesis of YT-III-41(10).

The ligand **10** was a hybrid of EMJ-I-026 (**5**) and YT-III-231 (**8**). This synthesis was aimed at the design of a ligand which had both $\alpha 2/\alpha 3$ and $\alpha 5$ subtype selectivity while avoiding activity at $\alpha 1$ subtypes, as well as resistant to esterase hydrolysis. The ethyl ester **8** (YT-III-231) was treated with sodium hydride and *N*'-hydroxyisobutyrylimidamide in the presence of dry THF and dry 4A° molecular sieves to provide the isopropyl bioisostere **10** (YT-III-41) in 45% yield, as shown in **Scheme 4**.



Binding affinity at $\alpha\beta\gamma 2$ GABA_A/BzR subtypes.

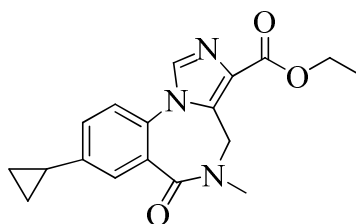
$\alpha 1$	$\alpha 2$	$\alpha 3$	$\alpha 4$	$\alpha 5$	$\alpha 6$
3052	745.7	510.8	ND	416.8	ND

Values are reported in nM. ND = Not Determined.

This molecule may be too large to fit in the binding pocket, however, again this molecule was analyzed by the rapid screening technique which may not be accurate. As mentioned before, this is being reinvestigated and rescreened as well because the $\alpha 2$ and $\alpha 3$ subtypes were not expressed correctly at UNC.

2.7. Synthesis of YT-III-42 (14).

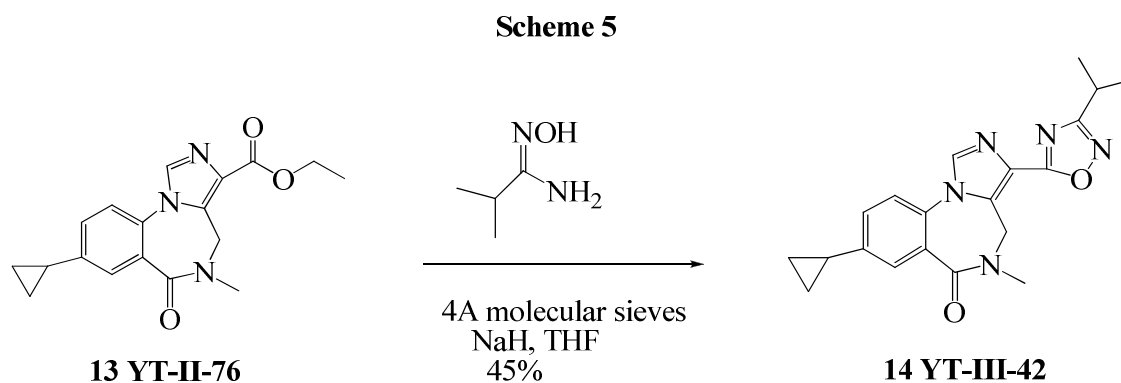
Because the initial studies on YT-II-76 (**13**; 2370 fold $\alpha 5$ over $\alpha 1$, **Figure 10**) demonstrated potent subtype selectivity at $\alpha 5$ subtypes, it was decided to convert this cyclopropyl substituted imidazobenzodiazepine into an ester bioisostere to retard ester metabolism (hydrolysis). The ethyl ester **13** (YT-II-76), prepared earlier, was treated with sodium hydride and N'-hydroxyisobutyrylimidamide in the presence of dry THF and dry 4A^o molecular sieves to provide the isopropyl bioisostere **14** (YT-III-42) in 45% yield, as shown in **Scheme 5**, analogues to previous chemistry.

Figure 10. Binding affinity at $\alpha\beta\gamma\delta$ GABA_A/BzR subtypes for YT-II-76 (**13**).**13 YT-II-76**

Screening No.	$\alpha 1$	$\alpha 2$	$\alpha 3$	$\alpha 4$	$\alpha 5$	$\alpha 6$
1	95.34	2.797	0.056	ND	0.04	ND
2	101.1	1.897	5.816	ND	11.99	ND
3*	6.71	29.28	81.82	ND	7.72	ND

* This run was carried out by the rapid screening technique and may not be accurate because of the lack of reliability at the $\alpha 2$ and $\alpha 3$ subtypes.

Values are reported in nM. ND = Not Determined.



Binding affinity at $\alpha\beta\gamma\delta$ GABA_A/BzR subtypes.

Screening No.	$\alpha 1$	$\alpha 2^*$	$\alpha 3^*$	$\alpha 4$	$\alpha 5$	$\alpha 6$
1	382.9	16.83	44.04	ND	9.77	ND
2	154.1	532.9	529	ND	143.7	ND

* These run was carried out by the rapid screening technique and may not be accurate because of the lack of reliability at the $\alpha 2$ and $\alpha 3$ subtypes.

Values are reported in nM. ND = Not Determined.

From the initial data on ligand **14** (YT-II-42), it was 40 fold more selective for $\alpha 5$ subtypes over $\alpha 1$ subtypes and certainly more selective at $\alpha 2$ and $\alpha 3$ subtypes as compared to $\alpha 1$ subtypes. This was a very good binding profile. The second set of data was determined by the rapid screening technique and may be flawed, as previously stated. More data will have to be obtained on this ligand *in vitro* to determine its real potential. The efficacy on oocytes at $\alpha 1$, $\alpha 2$, $\alpha 3$ and $\alpha 5$ ion channels must be obtained on HEK cells before proceeding further.

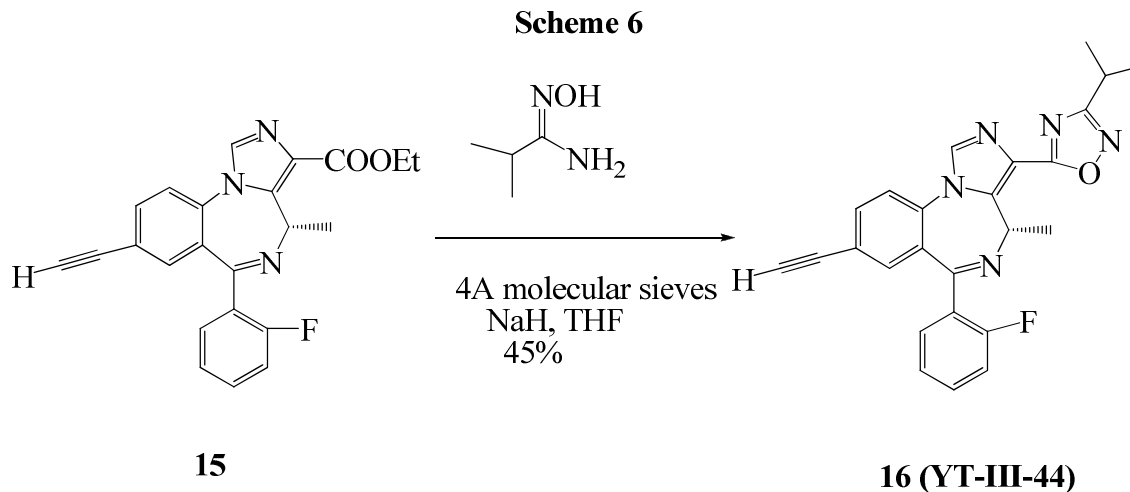
2.8. Synthesis of YT-III-44 (16).

Recently, Sieghart et al. have demonstrated the chiral imidazobenzodiazepine (SH-053-2'-F-S-CH₃) **15** binds with selective efficacy at α_2 , α_3 and α_5 subtypes with very little efficacy at α_1 subtypes at physiologically relevant concentrations (100 nM). Moreover, its R-enantiomer (SH-053-2'-F-R-CH₃) bound potently only at α_5 subtypes and had a different biological profile.¹¹⁴ Moreover, Fischer and Rowlett have demonstrated in the conflict model in rhesus monkeys that SH-053-2'-F-S-CH₃ was a non-sedating anxiolytic, while the R-isomer was largely inactive. For this reason, it was decided to alter the esterase labile ester function in **15** to the more stable isopropyl bioisostere in **16** (YT-III-44). This was to potentiate the duration of action of these ligands *in vivo*, as described in previous cases. The R-enantiomer of 8-phenyl substituted imidazobenzodiazepines exhibits subtype selective α_5 agonist properties and could be used by Savic et al. to study amnesia and the effect of α_5 agonists on cognition. It was also active in PPI (Baker et al. unpublished results) and the MAM model in rodents of schizophrenia, hence both S and R isomers are important for potential leads for treatment of schizophrenia (resets gating in CNS).

It was known the S-enantiomers of 3-substituted 1,4-benzodiazepines were more active than the R-isomers.^{119, 120} This has been supported by the published work on the framework constrained 4,5-disubstituted pyrroloimidazobenzodiazepines; the S-enantiomers were much more potent *in vitro* than the R-isomers.¹²¹ As mentioned above in the previous work, the pharmacophoric descriptors H₁, H₂ and A₂ in the pharmacophore/receptor models of the 6 major BzR have been shown to be very

similar.¹²¹ Consequently, it was felt, the major differences in the topology of these subtypes may stem from asymmetry/or lack thereof in the lipophilic pockets designated L₁, L₂, L₃ and L_{Di}.^{57, 121-123} The optically active ligands were designed to enhance/probe these differences. According to computer modeling, the S-enantiomers of these agents fit the computer model very well, while the phenyl ring of the R-isomer protruded out of the pharmacophore included volume of the α 1, α 2 and α 3 subtypes, which interacted negatively with the receptor protein.^{122, 123} The R-isomer did fit the α 5 subtype to a somewhat better degree. The R-isomer, therefore, may be less active or inactive based on modeling. Based on the previous work of Shengming Huang and Savic¹¹⁴ it was expected that the (S)-4-methyl ligands would provide better subtype selective affinity and efficacy at α 2, α 3 and/or α 5 subtypes while the (R)-4 enantiomers would interact only with α 5 β 2 γ 2 receptor subtypes important in schizophrenia.

The 2'-F,(S)-CH₃ substituted ester **15** was treated with sodium hydride and N'-hydroxyisobutyrylimidamide in the presence of dry THF and molecular sieves to provide the isopropyl bioisostere **16** (YT-III-44) in 45% yield, as shown in **Scheme 6**.



Binding affinity at $\alpha\beta\gamma 2$ GABA_A/BzR subtypes.

$\alpha 1$	$\alpha 2$	$\alpha 3$	$\alpha 4$	$\alpha 5$	$\alpha 6$
37.83	9717*	373.9*	ND	24.04	ND

* These runs were carried out by the rapid screening technique and may not be accurate because of the lack of reliability at the $\alpha 2$ and $\alpha 3$ subtypes at UNC.

Values are reported in nM. ND = Not Determined.

It is clear that YT-III-44 (**16**) binds to BzR subtypes but it binds more potently to $\alpha 1$ and $\alpha 5$ subtypes in contradiction to the expected affinities. Because this was determined by the rapid screening mechanism which may be invalid, efforts are underway to rescreen this ligand in a more classical sense. Because the ester bioisosteres YT-III-40 (**9**), YT-III-41 (**10**), YT-III-42 (**14**), and YT-III-44 (**16**) did not bind as potently to BzR as desired, a number of other analogues were designed with groups known to withstand ester hydrolysis in other cases. For this approach the lead ligand to be modified was chosen from the $\alpha 2/\alpha 3$ subtype selective ligands already shown to be non-sedating anxiolytics *in vivo*.¹¹⁴ This work is being carried out by new students in Milwaukee.

III. Conclusion.

In this study it was clear that the improved method for synthesizing benzodiazepines was successful. This was based on the number and quantities of numerous compounds synthesized utilizing the improved method. Although the efficacy of XHe-II-053 (**4**) was decreased in Phase I because of the metabolism of the C-3 ester to the acid, the bioisostere EMJ-I-026 (**5**) has been shown to exhibit non-sedating anxiolytic activity in mice as well as a binding/oocyte profile *in vitro* consistent with a non-sedating anxiolytic. Based on this success seven bioisosteric analogues were designed in order to circumvent any potential metabolic liability in humans of the previously described ligand. In fact, the bioisosteric analogues were much more stable in human liver microsomes than XHe-II-053 (**4**) again indicating these bioisosteres are potential nonsedating anxiolytics as well as useful for treatment of anxiety disorders in human populations.

Gratifyingly, ligand **5** was clearly an efficacious α_3 Bz/GABAergic receptor subtype selective ligand at pharmacologically relevant doses (approximately 100 nM) and, presumably, provides an agent to study physiologically processes mediated by α_3 subtypes including anxiety, and on addition was much more stable in human liver microsomes. In this regard α_3 subtype selective ligand oxadiazole **5** (EMJ-I-026) has been evaluated in the light dark paradigm and clearly was a nonsedating anxiolytic in mice, wherein this ligand was anxiolytic with no sedative properties, *in vivo*, as compared to diazepam. This study indicated that the ester function in these molecules can be replaced with a metabolically more stable ester bioisostere and the ligand still retains

anxiolytic activity. The in depth study of these ligands in animal models and other receptor systems are underway and will be reported in due course, especially since the $\alpha 2$ and $\alpha 3$ receptor binding data at UNC was not reliable at this time due to problems in transfection of the $\alpha 2$ and $\alpha 3$ HEK cells (B. Roth, private communication).

IV. Screening Methods.

1. Computer Modeling Methods.

The core structures of the ligands were taken from available X-ray crystallographic coordinates or generated using the SYBYL fragment library.^{22, 124} The structures which resulted were energy minimized using MM2 (molecular mechanics program 2) or MMFF (Merck molecular force field), and the subsequent Monte Carlo conformational searches were carried out on MacroModel 6.0 on a Silicon Graphics Personal Iris 4D/35 workstation or a Silicon Graphics Octane SI 2P 175 R10000 workstation, respectively. The low energy conformations were then fully optimized *via* molecular orbital calculations at the 3-21G basis set with torsional angles fixed. The structures which resulted were further calibrated with 6-31G* single point calculations at an “SCF=TIGHT” convergence criteria *via* Gaussian 92¹²⁵ on a Silicon Graphics Indigo R4400 workstation, or Gaussian 94¹²⁶ on a Silicon Graphics Octane SI2P175R10000 workstation.³⁴

2. Competition Binding Assays (With Dr. Majumder and Dr. Roth).

Competition binding assays were performed in a total volume of 0.5 mL at 4 °C for 1 hour using [3H]flunitrazepam as the radiolabel. For these binding assays, 20-50 mg of membrane protein harvested with hypotonic buffer (50 mM Tris-acetate, pH 7.4 at 4°C) was incubated with the radiolabel as previously described (Choudhary et al., 1992). Nonspecific binding was defined as radioactivity bound in the presence of 100 µM diazepam and represented less than 20% of total binding. Membranes were harvested with a Brandel cell harvester followed by three ice-cold washes onto polyethyleneimine-pretreated (0.3%) Whatman GF/C filters. Filters were dried overnight and then soaked in Ecoscint, a liquid scintillation cocktail (National Diagnostics; Atlanta, GA). Bound radioactivity was quantified by liquid scintillation counting. Membrane protein concentrations were determined using an assay kit from Bio-Rad (Hercules, CA) with bovine serum albumin as the standard.

3. Preparation of Cloned mRNA (with Dr. R. Furtmüller, Dr.

Ramerstorfer and Dr. W. Sieghart).¹¹⁴⁻¹¹⁷

The cloning of GABA_A receptor subunits α 1, β 3 and γ 2 into pCDM8 expression vectors (Invitrogen, CA) has been described elsewhere.^{22, 115-118, 127} GABA_A receptor subunit α 4 was cloned in an analogous way. The cDNAs for subunits α 2, α 3 and α 5 were gifts from P. Malherbe and were subcloned into a pCI-vector. The cDNA for the α 6 subunit was a gift from P. Seeburg and was subcloned into the vector pGEM-3Z

(Promega). After linearizing the cDNA vectors with appropriate restriction endonucleases, capped transcripts were produced using the mMessage mMachine T7 transcription kit (Ambion, TX). The capped transcripts were polyadenylated using yeast poly (A) polymerase (USB, OH) and were diluted and stored in diethylpyrocarbonate-treated water at -70°C .¹¹⁵⁻¹¹⁸

4. Functional Expression of GABA_A Receptors (with Dr. R. Furtmüller, Dr. Ramerstorfer and Dr. W. Sieghart).^{114,115}

The methods used for isolating, culturing, injecting and defolliculating the oocytes were identical with those described by E. Sigel.^{128, 129} Mature female *Xenopus laevis* (Nasco, WI) were anaesthetized in a bath of ice-cold 0.17 % Tricain (ethyl-m-aminobenzoate, Sigma, MO) before decapitation and removal of the frog ovary. Stage 5 to 6 oocytes with the follicle cell layer around them were singled out of the ovary using a platinum wire loop. Oocytes were stored and incubated at 18°C in modified Barths medium [MB, containing 88 mM NaCl, 10 mM HEPES-NaOH (pH 7.4), 2.4 mM NaHCO₃, 1 mM KCl, 0.82 mM MgSO₄, 0.41mM CaCl₂, 0.34 mM Ca(NO₃)₂] that was supplemented with 100 Units/mL penicillin and 100 µg/mL streptomycin. Oocytes with follicle cell layers still around them were injected with 50 nL of an aq solution of the cRNA. This solution contained the transcripts for the different alpha subunits and the beta 3 subunit at a concentration of 0.0065 ng/nL as well as the transcript for the gamma 2 subunit at 0.032 ng/nL. After injection of the cRNA, oocytes were incubated for at least 36 h before the enveloping follicle cell layers were removed.

To this end, oocytes were incubated for 20 minutes at 37 °C in MB that contained 1 mg/mL collagenase type IA and 0.1 mg/mL trypsin inhibitor I-S (both Sigma). This was followed by osmotic shrinkage of the oocytes in doubly concentrated MB medium supplied with 4 mM Na-EGTA. Finally, the oocytes were transferred to a culture dish containing MB and were gently pushed away from the follicle cell layer which stuck to the surface of the dish. After removal of the follicle cell layer, oocytes were allowed to recover for at least 4 h before being used in electrophysiological experiments.^{114,115}

5. Electrophysiological Experiments (with Dr. R. Furtmüller, Dr Ramerstorfer and Dr. W. Sieghart) .^{114,115}

For electrophysiological recordings, oocytes were placed on a nylon-grid in a bath of *Xenopus* Ringer solution [XR, containing 90 mM NaCl, 5 mM HEPES NaOH (pH 7.4), 1 mM MgCl₂, 1 mM KCl and 1 mM CaCl₂]. The oocytes were constantly washed by a flow of 6 mL/min XR which could be switched to XR containing GABA and/or drugs. Drugs were diluted into XR from DMSO solutions which resulted in a final concentration of 0.1 % DMSO perfusing the oocytes. Drugs were preapplied for 30 seconds before the addition of GABA, which was coapplied with the drugs until a peak response was observed. Between two applications, oocytes were washed in XR for up to 15 minutes to ensure full recovery from desensitization. For current measurements the oocytes were impaled with two microelectrodes (2–3 mΩ) which were filled with 2 mM KCl.

All recordings were performed at room temperature (rt) at a holding potential of –60 mV using a Warner OC-725C two-electrode voltage clamp (Warner Instruments, Hamden, CT).^{91, 92} Data were digitized, recorded and measured using a Digidata 1322A data acquisition system (Axon Instruments, Union City, CA). Results of concentration response experiments were fitted using GraphPad Prism 3.00 (GraphPad Software, San Diego, CA). The equation used for fitting concentration response curves was $Y = \text{Bottom} + (\text{Top} - \text{Bottom}) / (1 + 10^{((\text{LogEC50} - X) * \text{HillSlope}))}$; X represents the logarithm of concentration, Y represents the response; Y starts at Bottom and goes to Top with a sigmoid shape. This is identical to the "four parameter logistic equation."¹¹⁴

V. Experimental Section.

Melting points were taken on a Thomas-Hoover melting point apparatus or an Electrothermal model IA8100 digital melting point apparatus and are uncorrected. Microanalyses were performed on a Perkin-Elmer 240C carbon, hydrogen, and nitrogen analyzer. All samples submitted for CHN analyses were first dried under high vacuum for a minimum of 6 h using a drying pistol with isopropyl alcohol as the solvent with phosphorus pentoxide in the drying bulb. Proton and carbon high resolution nuclear magnetic resonance spectra were obtained on a Bruker 300-MHz NMR spectrometer or a GE 500-MHz NMR spectrometer. The low resolution mass spectra (EI/CI) were obtained on a Hewlett-Packard 5985B gas chromatography-mass spectrometer, while high resolution mass spectra were recorded on a VG Autospec (Manchester, England) mass spectrometer. Infra-red spectra were recorded on a Nicolet MX-1 FT-IR or a Perkin Elmer 1600 Series FT-IR spectrometer. Analytical thin layer chromatography plates used were E. Merck Brinkmann UV-active silica gel (Kieselgel 60 F254) on plastic. Silica gel 60A, grade 60 for flash and gravity chromatography was purchased from E. M. Laboratories.

7-Chloro-4-methyl-3,4-dihydro-1H-benzo-[e]-[1,4]-diazepine-2,5-dione (1h).

A mixture of 5-chloroisatoic anhydride (20.0 g, 101 mmol) and sarcosine (9.02 g, 101 mmol) in DMSO (160 mL) was heated at 150 °C for 5 hr, cooled to rt and poured into ice water (750 mL) to furnish a light brown precipitate. This solid was collected by filtration, washed with water (3 × 200mL) and dried. The benzodiazepine **1h** (19g, 84.0% yield) was obtained as a light brown solid. This material was used directly in a later step. The spectral data were identical to the published values.¹³⁰

General Procedure for the Synthesis of Imidazo-[1,5-a]-[1,4]-Benzodiazepines.

Potassium *t*-butoxide (t-BuOK; 1.1 mmol) was added to a solution of the amidobenzodiazepine **1(a-j)** (1.0 mmol) in anhydrous THF (20 mL) at 0 °C and this was allowed to stir for 20 min. The reaction mixture, which resulted, was cooled to -35 °C and diethylchlorophosphate (1.3 mmol) was added slowly. After stirring this mixture at 0 °C for 30 min, the mixture was cooled to -78 °C and ethyl isocynoacetate (1.1 mmol) was added and this followed by addition of t-BuOK (1.1 mmol). The second addition can be run at -35 °C instead of -78 °C with the same result. After allowing the reaction mixture to stir at rt for 4 h, the reaction was quenched with a saturated solution of aq NaHCO₃ (30 mL) and extracted with EtOAc (3x 50 mL). The combined organic layers were dried (Na₂SO₄), concentrated and the product was precipitated from ether to give

most of the imidazobenzodiazepine. The mother liquor was purified by flash chromatography on silica gel (gradient elution, 40%-60% EtOAc in hexane) to afford additional imidazobenzodiazepine (yields 70-89%; see **Table 2**).

Large Scale Procedure for the Synthesis of Imidazo-[1,5-a]-[1,4]-Benzodiazepine (3j).

Potassium *t*-butoxide (t-BuOK; 6.88g, 61.33 mmol) was added to a solution of **1j** (15g, 55.76 mmol) in anhydrous THF (1500 mL) at 0 °C over 20 min. The reaction mixture was then cooled to -35 °C and diethylchlorophosphate (10.42ml, 72.49 mmol) was added slowly. After stirring this mixture at 0 °C for 30 min, the mixture was cooled to -78 °C (or -35 °C) and ethyl isocyanoacetate (6.70ml, 61.33 mmol) was added. This was followed by addition of t-BuOK (6.88g, 61.33 mmol). After stirring at rt for 4 h, the reaction mixture was quenched with a saturated solution of aq NaHCO₃ (500 mL) and extracted with EtOAc (3x 1000 mL).

The combined organic layers were dried (Na₂SO₄) and concentrated *in vacuo* to give a solid residue. This solid residue was triturated with ether (250 mL) and the product **3j** was precipitated as an off-white solid. The mother liquor was further purified by flash chromatography on silica gel (gradient elution, 40%-60% EtOAc in hexane) to afford additional imidazobenzodiazepine **3j** with an overall yield of 72% (14.61g).

Ethyl-8-Chloro-6-Phenyl-4*H*-Imidazo-[1,5-*a*]-[1,4]-Benzodiazepine-3-Carboxylate (3a).

This material was prepared under conditions analogous to the synthesis of **3j**.

3a: Mp: 180-182 °C; ¹H NMR (300 MHz, CDCl₃) δ 7.93 (s, 1 H), 7.68 (dd, 1H, *J*= 2.3, 2.3 Hz), 7.58 (s, 1H), 7.55-7.37 (m, 6 H), 6.06 (d, 1H, *J*=12.3Hz), 4.70 (m, 2H), 4.15 (d, 1H, *J*=14Hz), 1.46 (t, *J*=7.12Hz, 3 H); HRMS for C₂₀H₁₆ClN₃O₂: (M+1) 366.1007. Found (relative intensity, %): 366.1000 (M+1, 100); 368.0902 (M+3, 32).

Ethyl-8-Bromo-6-Phenyl-4*H*-Imidazo-[1,5-*a*]-[1,4]-Benzodiazepine-3-Carboxylate (3b).

This material was prepared under conditions analogous to the synthesis of **3j**.

3b: White solid; Mp: 175-178 °C; ¹H NMR (300 MHz, CDCl₃) δ 7.95 (s, 1 H), 7.82 (dd, 1H, *J*= 2.2, 8.6Hz), 7.60 (d, 1H, *J*=2.2Hz), 7.53-7.40 (m, 6 H), 6.08 (d, 1H, *J*=12.3Hz), 4.49-4.38 (m, 2H), 4.09 (d, 1H, *J*=12.1Hz), 1.44 (t, 3 H, *J*=7.1Hz); EIMS *m/e* (relative intensity, %) 411 (M+1, 34), 410 (M⁺, 8), 409 (34), 365 (61), 337 (100), 335 (100), 285 (21), 232 (17). Anal. Calcd. for C₂₀H₁₆BrN₃O₂: C, 58.55; H, 3.93; N, 10.24. Found: C, 58.30; H, 3.91; N, 9.94.

(R)-Ethyl-8-Bromo-4-Methyl-6-(2'-Fluorophenyl)-4H-Imidazo-[1,5-a]-[1,4]-Benzodiazepine-3-Carboxylate (3c).

This material was prepared under conditions analogous to the synthesis of **3j**.

3c: White solid; Mp: 261-262 °C; $[\alpha]_D^{25}$ -10.9 (c, 0.54, EtOAc); $^1\text{H NMR}$ (300 MHz, CDCl_3) δ 7.92 (s, 1 H), 7.72 (dd, 1H, $J = 1.5, 8.2\text{Hz}$), 7.60 (t, 1H, $J = 6.9\text{Hz}$), 7.48 (d, 1H, $J = 8.5\text{Hz}$), 7.49-7.42 (m, 2H), 7.29-7.23 (m, 1H), 7.05 (t, 1H, $J = 9.3\text{Hz}$), 6.71 (q, 1H, $J = 7.3\text{Hz}$), 4.41 (m, 2H), 1.42 (t, 3 H, $J = 7.1\text{Hz}$), 1.29 (d, 3H, $J = 7.2\text{Hz}$). EIMS m/e (relative intensity, %) 442 (M^+ , 5), 443 ($\text{M}+2$, 5), 428 (7), 381 (58), 355 (100). Anal. Calcd. for $\text{C}_{21}\text{H}_{17}\text{BrFN}_3\text{O}_2$: C, 57.03; H, 3.87; N, 9.50. Found: C, 57.13; H, 3.89; N, 9.51.

(R)-Ethyl-8-Bromo-4-Ethyl-6-(2'-Fluorophenyl)-4H-Imidazo-[1,5-a]-[1,4]-Benzodiazepine-3-Carboxylate (3d).

This material was prepared under conditions analogous to the synthesis of **3j**.

3d: White solid; Mp: 253-254°C; $^1\text{H NMR}$ (300 MHz, CDCl_3): δ 7.93 (s, 1H), 7.72 (dd, 1H, $J = 8.1\text{Hz}$), 7.59 (t, 1H, $J = 7.5\text{Hz}$), 7.48-7.42 (m, 2H), 7.28-7.23 (m, 1H), 7.06 (t, 1H, $J = 9.3\text{Hz}$), 6.51 (q, 1H, $J = 7.8\text{Hz}$), 4.43 (m, 2 H), 1.76-1.52 (m, 3H), 1.43 (t, 3H, $J = 7.2\text{ Hz}$), 0.96 (t, 3H, $J = 7.2\text{Hz}$). HRMS Calcd. for $\text{C}_{22}\text{H}_{19}\text{BrFN}_3\text{O}_2$: 456.0723; Found: 456.0709.

(S)-Ethyl-8-Bromo-4-Ethyl-6-(2'-Fluorophenyl)-4H-Imidazo-[1,5-a]-[1,4]-Benzodiazepine-3-Carboxylate (3e).

This material was prepared under conditions analogous to the synthesis of **3j**.

3e: White solid; Mp: 254-255 °C; ¹H NMR (300 MHz, CDCl₃): δ 7.92 (s, 1H), 7.72 (dd, 1H, *J*=7.2Hz), 7.59 (t, 1H, *J*=6.9Hz), 7.48-7.41 (m, 2H), 7.28-7.23 (m, 1H), 7.06 (t, 1H, *J*=9.3Hz), 6.51 (m, 1H), 4.45-4.37 (m, 2H), 1.75-1.54 (m, 3H), 1.42 (t, 3H, *J*=6.9Hz), 0.94 (t, 3H, *J*=7.2Hz). HRMS Calcd. for C₂₂H₁₉BrFN₃O₂: 456.0723 (M+1); Found (relative intensity): 456.0703 (M+1, 100); 458.0648 (M+3, 99.8).

Ethyl-8-Bromo-6-Phenyl-4H-Imidazo-[1,5-a]-Thieno-[2,3-f]-[1,4]-Diazepine-3-Carboxylate (3f).

This material was prepared under conditions analogous to the synthesis of **3j**.

3f: White solid; Mp: 180-182 °C; ¹H NMR (300 MHz, CDCl₃) δ 8.33 (s, 1 H), 8.02 (s, 1 H), 7.63-7.35 (m, 5 H), 5.31 (s, 2 H), 4.34-4.27 (q, 2 H, *J*=7.1Hz), 1.32 (t, 3 H, *J*=7.1Hz). HRMS for C₁₈H₁₄BrN₃O₂S: 416.0068 (M+1). Found (relative intensity, %): 416.0049 (M+1, 100); 418.0018 (M+3, 100).

Ethyl-8-Fluoro-5,6-Dihydro-5-Methyl-6-Oxo-4H-Imidazo-[1,5-a]-[1,4]-Benzodiazepine-3-Carboxylate (3g).

This material was prepared under conditions analogous to the synthesis of **3j**.

3g: Off-white solid; Mp: 200-202 °C; ¹H NMR (300 MHz, CDCl₃) δ 7.88 (s, 1H), 7.81-7.78 (m, 1H), 7.74-7.36 (m, 2H), 5.25 (br s, 1H), 4.44 (q, 2 H, *J*=7.3Hz), 4.38 (br s, 1H), 3.27 (s, 3H), 1.47 (t, 3H, *J*=7.3Hz). HRMS for C₁₅H₁₄FN₃O₃: (M+1) 304.1097. Found: 304.1091. The spectral data for **3g** were identical to the published values.^{109,110}

Ethyl-8-Chloro-5,6-Dihydro-5-Methyl-6-Oxo-4H-Imidazo-[1,5- α]-[1,4]-Benzodiazepine-3-Carboxylate (3h).¹

The tBuOK (9.0g, 80mmol) was added to a solution of **1h** (15g, 67mmol) in THF (1000mL) at 0°C. After the solution was allowed to stir at 0°C for 20 min, the reaction mixture was cooled to -35°C and diethyl chlorophosphate (15 g, 87 mmol) was added slowly. After stirring at 0°C for 30 min, the reaction mixture was cooled to -78°C and ethyl isocynoacetate (8.3g, 73 mmol) was added and this was followed by addition of tBuOK (8.2 g, 73mmol). The reaction solution was stirred at rt for 4h, after which the reaction was quenched with a saturated aq solution of NaHCO₃ and extracted with ethyl acetate. The combined organic layers were dried (Na₂SO₄) and concentrated under reduced pressure. The residue was purified by flash chromatography on silica gel (ethyl acetate) and then crystallized from ethyl acetate to give white crystals **3h** (19g, 89%

yield). **3h**: mp 192-193 °C; ¹H NMR (300 MHz, CDCl₃) δ 8.1 (d, *J* = 2.4 Hz, 1H), 7.90 (s, 1H), 7.62 (dd, *J* = 8.6, 2.5 Hz, 1H), 7.40 (d, *J* = 8.6 Hz, 1H), 5.23 (br s, 1H), 4.46 (q, *J* = 7.12 Hz, 2H), 4.13 (br s, 1H), 3.27 (s, 3H), 1.47 (t, *J* = 7.12 Hz, 3H); C₁₅H₁₄ClN₃O₂, MS (EI) *m/e* (rel. intensity) 319 (M⁺, 100). This material was used directly in a later step.

(S)-Ethyl-7-Bromo-11,12,13,13a-Tetrahydro-9-Oxo-9H-Imidazo-[1,5-a]-Pyrrolo-[2,1-d]-[1,4]-Benzodiazepine-1-Carboxylate (3i).

This material was prepared under conditions analogous to the synthesis of **3j**. **3i**: White solid; Mp: 249 °C; [α]_D²⁵ +45 (c, 1, CHCl₃); ¹H NMR (300 MHz, CDCl₃) δ 8.23 (s, 1H), 7.82 (s, 1H), 7.75 (d, 1H, *J*=7.5Hz), 7.26 (d, 1H, *J*=10.0Hz), 4.72 (d, 1H, *J*=6.0Hz), 4.38 (q, 2H, *J*=7.5Hz), 3.75 (m, 1H), 3.56-3.48 (m, 2H), 2.27-2.14 (m, 3H), 1.41 (t, 3H, *J*=7.5Hz). EIMS *m/e* (relative intensity, %) 390 (M⁺, 10), 345 (60), 316 (100), 314 (98), 154 (24). Anal. Calcd. for C₁₇H₁₆BrN₃O₃: C, 52.32; H, 4.13; N, 10.77. Found: C, 52.70; H, 4.48; N, 10.64. HRMS for C₁₇H₁₆BrN₃O₃: 389.0375. Found (relative intensity, %): 389.0373 (M+1, 100); 391.0258 (M+3, 98.8).

Ethyl-8-Bromo-5,6-Dihydro-5-Methyl-6-Oxo-4H-Imidazo-[1,5-a]-[1,4]-Benzodiazepine-3-Carboxylate (3j).

This material was prepared under conditions as described earlier for large scale procedure for the synthesis of Imidazo-1[1,5-a]-1[1,4]-Benzodiazepine. **3j**: Off-white solid; Mp: 192-193 °C; ¹H NMR (300 MHz, CDCl₃) δ 8.23 (s, 1H), 7.79 (s, 1H), 7.77 (d, 1H, *J*=2.3Hz), 7.35 (d, 1H, *J*=6.4Hz), 5.17 (br s, 1H), 4.43 (m, 3H), 3.28 (s, 3H), 1.45 (t, 3H, *J*=7.1Hz). C₁₅H₁₄BrN₃O₃, EIMS m/e (relative intensity, %) 364 (M⁺, 100); 366 (M+2, 99).

***tert*-Butyl-8-Bromo-5,6-Dihydro-5-Methyl-6-Oxo-4H-Imidazo-[1,5-a]-[1,4]-Benzodiazepine-3-Carboxylate (3k).**

This material was prepared under conditions analogous to the synthesis of **3j**. **3k**: Mp: 180-183 °C, ¹H NMR (300 MHz, DMSO-*d*₆) δ 8.33 (s, 1H), 7.92 (s, 1H), 7.69 (dd, 1H), 7.03 (dd, 1H), 4.71 (br, 1H), 4.12 (br, 1H), 3.10 (s, 3H), 1.56 (s, 9H). C₁₇H₁₈BrN₃O₃, EIMS m/e (relative intensity, %) 394 (M⁺, 100), 396 (M+2, 98).

5-(8-Ethynyl-6-Phenyl-4H-Benzo-[f]-Imidazo-[1,5-a]-[1,4]-Diazepine)-3-Isopropyl-1,2,4-Oxadiazole (5, EMJ-I-026).

Isopropyl amido oxime (95 mg, 0.931 mmol) was added to a stirred suspension of dry powdered 4 Å molecular sieves (100 mg) in anhydrous THF (30 mL) under argon. After the mixture was stirred at rt for 10 min, NaH (37 mg of 60% in mineral oil, 0.931 mmol) was added to the mixture. After the mixture was stirred for a further 30 min, a solution of the forgoing ester **4** (XHeII-053, 165 mg, 0.465 mmol) in THF (30 mL) was added. The mixture which resulted was heated to reflux for 8 hr. It was cooled to rt, after which acetic acid (56 mg, 0.931 mmol) was added. After the solution was allowed to stir for 10 min, the mixture was filtered through celite. The filtrate was diluted with CH₂Cl₂ (75 mL) and washed with water, brine and dried (K₂CO₃). Evaporation of the solvent under reduced pressure afforded a pale yellow solid, which was purified by flash column chromatography (silica gel, EtOAc/hexane, 2:3) to furnish **5** as a white solid (EMJ-I-026, 82 mg, 0.209 mmol, 45%). **5**: mp 190°C; IR (KBr) ν 3291, 3057, 2972, 1613, 1574, 1494, 1466, 1303, 1264, 939, 832, 781, 734, 699, 666 cm⁻¹. ¹H NMR (300 MHz, CDCl₃) δ 8.07 (s, 1H), 7.81-7.79 (dd, 1H), 7.64-7.61 (m, 2H), 7.53-7.37 (m, 5H), 6.14 (d, 1H, J=13.1Hz), 4.19 (d, 1H, J=12.8Hz), 3.20 (s, 1H), 3.24-3.15 (m, 1H), 1.44-1.41 (d, 6H, J=6.93Hz); MS (EI) m/e (relative intensity) 393(100); Anal. Calcd. for C₂₄H₁₉N₅O: C, 73.27; H, 4.87; N, 17.80. Anal. Calcd. for C₂₄H₁₉N₅O•0.37 CH₂Cl₂: C, 68.89; H, 4.68; N, 16.48. Found: C, 68.94; H, 4.59; N, 16.32 (CHN sample was transferred to a vial for drying with CH₂Cl₂ which may explain the contaminant).

5-(8-Ethynyl-6-(2-Fluorophenyl)-4H-Benzo-[f]-Imidazo-[1,5-a]-[1,4]-Diazepine-3-yl)-3-Isopropyl-1,2,4-Oxadiazole (9, YT-III-40).

Isopropyl amido oxime (0.55g, 5.4 mmol) was added to a stirred suspension of dry powdered 4 Å molecular sieves (250 mg) in anhydrous THF (30 mL) under argon. After the mixture was stirred at rt for 10 min, NaH (60% solid in mineral oil, 0.147 g, 4.0 mmol) was added to the mixture. After the mixture was stirred for a further 30 min, a solution of the forgoing ester **12** (1g, 2.68 mmol) in THF (30 mL) was added. The mixture which resulted was heated to reflux for 8 hr. It was then cooled to rt, after which acetic acid (0.3g, 5.36 mmol) was added. After the solution was allowed to stir for 10 min, the mixture was filtered through celite. The filtrate was diluted with CH₂Cl₂ (100 mL) and washed with water, brine and dried (K₂CO₃). Evaporation of the solvent under reduced pressure afforded a pale yellow solid, which was purified by flash column chromatography (silica gel, EtOAc/hexane, 2:3) to furnish **9** as a white solid (YT-III-40, 0.5g, 1.2 mmol, 45%). **9**: mp 160-165°C; IR (neat) ν 3194, 2961, 2924, 2854, 1631, 1610, 1495, 1450, 1414, 1394, 1367, 1342, 1312, 1259, 1221, 1071, 1011, 940, 903, 862, 793, 767, 754, 697, 671 cm⁻¹; ¹H NMR (300MHz, CDCl₃) δ 8.09 (s, 1H), 7.80 (dd, 1H, *J*=1.78, 1.78Hz), 7.69 (m, 3H), 7.51 (m, 2H), 7.07 (m, 1H), 6.26 (brs, 1H), 4.40 (brs, 1H), 3.24 (m, 2H), 1.43 (d, 6H, *J*=6.93Hz); MS (EI) *m/e*(relative intensity) 411 (M⁺, 43), 383 (98), 325 (100), 299 (74), 178 (74), 57 (57); HRMS(ESI) Calcd. for C₂₄H₁₈FN₅O (M+H)⁺ 412.1644, found: 412.1628.

5-(8-Cyclopropyl-6-Phenyl-4H-Benzo-[f]-Imidazo-[1,5-a]-[1,4]-Diazepine-3-yl)-3-Isopropyl-1,2,4-Oxadiazole (10, YT-III-41).

Isopropyl amido oxime (0.33g, 3.2 mmol) was added to a stirred suspension of powdered 4 Å molecular sieves (200 mg) in anhydrous THF (20 mL) under argon. After the mixture was stirred at rt for 10 min, NaH (60% solid in mineral oil, 0.089 g, 2.4 mmol) was added to the mixture. After the mixture was stirred for a further 30 min, a solution of the forgoing ester **8** (YT-III-231, 0.6g, 1.6 mmol) in THF (20 mL) was added. The mixture which resulted was brought to reflux for 8 hr. It was then cooled to rt, after which acetic acid (0.2g, 3.2 mmol) was added. After the solution was allowed to stir for 10 min, the mixture was filtered through celite. The filtrate was diluted with CH₂Cl₂ (60 mL) and washed with water, brine and dried (K₂CO₃). Evaporation of the solvent under reduced pressure afforded a pale yellow solid, which was purified by flash column chromatography (silica gel, EtOAc/hexane, 2:3) to furnish **10** as a white solid (YT-III-41, 0.3g, 0.7 mmol, 45%). **10**: mp 100-103°C; IR (neat) ν 2970, 2931, 1614, 1576, 1502, 1465, 1446, 1420, 1389, 1365, 1339, 1303, 1266, 1216, 1177, 1125, 1097, 1056, 1010, 978, 940, 903, 819, 781, 770, 746, 699, 666 cm⁻¹; ¹H NMR (300 MHz, CDCl₃) δ 8.02 (s, 1H), 7.53 (m,7H), 7.13 (d, 1H, *J*=1.91Hz), 6.08 (d, 1H, *J*=12.6Hz), 4.05 (d, 1H, *J*=12.7Hz), 3.25 (m,1H), 1.98 (m, 1H), 1.42 (d, 6H, *J*=6.95Hz), 1.06 (m, 2H), 0.71 (m,2H); MS (EI) *m/e* (relative intensity) 409 (M⁺, 42), 381 (76), 324 (100), 297 (48), 193 (48), 115 (59), 77 (50), 55 (52). HRMS (ESI) calcd. for C₂₅H₂₃N₅O (M+H)⁺ 410.1981, found 410.1977; Anal. Calcd. for C₂₅H₂₃N₅O•0.2EtOAc: C, 72.46; H, 5.82; N, 16.31. Found: C, 72.53; H, 5.92; N, 16.26.

8-Cyclopropyl-3-(3-Isopropyl-1,2,4-Oxadiazole-5-yl)-5-Methyl- 4H-Benzo-[f]-Imidazo-[1,5-a]-[1,4]-Diazepine-6(5H)-one (14, YT-III-42).

Isopropyl amido oxime (0.37g, 3.6 mmol) was added to a stirred suspension of dry powdered 4 Å molecular sieves (200 mg) in anhydrous THF (20 mL) under argon. After the mixture was allowed to stir at rt 10 min, NaH (60% solid in mineral oil, 0.1 g, 2.7 mmol) was added to the mixture. After the mixture was allowed to stir for a further 30 min, a solution of the forgoing ester **13** (YT-III-76, 0.6g, 1.8 mmol) in THF (20 mL) was added. The mixture which resulted was brought to reflux for 8 hr. It was then cooled to rt, after which acetic acid (0.2g, 3.6 mmol) was added. After the solution was allowed to stir for 10 min, the mixture was filtered through celite. The filtrate was diluted with CH₂Cl₂ (60 mL) and then washed with water, brine and dried (K₂CO₃). Evaporation of the solvent under reduced pressure afforded a pale yellow solid, which was purified by flash column chromatography (silica gel, EtOAc/hexane, 2:3) to furnish **14** as a white solid (YT-III-42, 0.3g, 0.8 mmol, 45%). **14**: mp 170-175°C; ¹H NMR (300 MHz, CDCl₃) δ 7.87 (s, 1H), 7.75 (s, 1H), 7.53 (d, *J*=4.47Hz, 1H), 7.32 (s, 1H), 5.27 (brs, 1H), 4.50 (brs, 1H), 3.26 (m, 4H), 2.04 (m, 1H), 1.42 (d, 6H, *J*=6.95Hz), 1.11 (m, 2H), 0.82 (m, 2H); MS (EI) *m/e*(relative intensity) 364 (M⁺, 27), 335 (38), 322 (78), 277 (71), 251 (96), 237 (55), 223 (33), 182 (25), 115 (100), 55 (28). HRMS (ESI) calcd. for C₂₀H₂₁N₅O₂ (M+H)⁺ 364.1774, found 364.1781; Anal. Calcd. for Anal. C₂₀H₂₁N₅O₂: C, 66.10; H, 5.82; O, 8.81. Calcd. for C₂₀H₂₁N₅O₂•0.7 EtOAc : C, 63.27; H, 5.92; N, 17.18. Found: C, 63.39; H, 6.08; N, 17.03 (CHN sample was transferred to a vial for drying with ethyl acetate which may explain the contaminant).

**(S)-5-(8-Ethynyl-6-(2-Fluorophenyl)-4-Methyl-4H-Benzo-[f]-Imidazo-[1,5-a]-[1,4]-Diazepine-3-yl)-3-Isopropyl-1,2,4-Oxadiazole
(16, YT-III-44).**

Isopropyl amido oxime (0.53g, 5 mmol) was added to a stirred suspension of powdered 4 Å molecular sieves (250 mg) in anhydrous THF (30 mL) under argon. After the mixture was allowed to stir at rt for 10 min, NaH (60% solid in mineral oil, 0.14 g, 3.9 mmol) was added to the mixture. After the mixture was allowed to stir for a further 30 min, a solution of the forgoing ester **15** (1g, 2.6 mmol) in THF (30 mL) was added. The mixture which resulted was allowed to heat to reflux for 8 hr. It was then cooled to rt, after which acetic acid (0.3g, 5.2 mmol) was added. After the solution was allowed to stir for 10 min, the mixture was filtered through celite. The filtrate was diluted with CH₂Cl₂ (100 mL) and washed with water, brine and dried (K₂CO₃). Evaporation of the solvent under reduced pressure afforded a pale yellow solid, which was purified by flash column chromatography (silica gel, EtOAc/hexane, 2:3) to furnish **16** as a white solid (YT-III-44, 0.5g, 1.2 mmol, 45%). **16**: mp190-193°C; ¹H NMR (300 MHz, CDCl₃) δ 8.34 (s, 1H), 7.83 (d, 1H), 7.81 (d, 1H), 7.79 (d, 1H), 7.5 (m, 1H), 7.36 (dd, 1H), 7.29 (m, 1H), 6.89 (s, 1H), 4.59 (q, *J*=11.52 Hz, 1H), 4.05 (s, 1H), 3.18 (m, *J*=29.73 Hz, 1H), 1.56 (d, *J*=33.02 Hz, 3H) 1.2 (d, *J*=30.5 Hz, 6H); HRMS (ESI) calcd. for C₂₅H₂₀FN₅O (M+H)⁺ 426.1730, found 426.1719.

VI. References.

1. Atack, J.R., Anxiolytic Compounds Acting at the GABA_A Receptor Benzodiazepine Binding Site, *CNS Neur. Dis.*, **2**, 213-232 (2003).
2. Greenberg, P.E., Sisitsky, T., Kessler, R.C., Finkelstein, S.N., Berndt, E.R., Davidson, J.R.T., Ballenger, J.C. and Fyer, A.J., The Economic Burden of Anxiety Disorders in the 1990s, *J. Clin. Psychiatry.*, **60**, 427-435 (1999).
3. Möhler, H., Fritschy, J.M., Crestani, F., Hensch, T. and Rudolph, U., Specific GABA_A Circuits in Brain Development and Therapy, *Biochem. Pharmacol.*, **68**, 1685-1690 (2004).
4. Basile, A.S., Lippa, A.S. and Skolnick, P., Anxiolytic Anxiolytics: Can Less Be More?, *Eur. J. Pharmacol.*, **500**, 441-451 (2004).
5. (a) Goddard, A., Mason, G., Rothman, D., Behar, K., Petroff, O. and Krystal, J., Family Psychopathology and Magnitude of Reductions in Occipital Cortex GABA Levels in Panic Disorder, *Neuropsychopharm.*, **29**, 639-40 (2004). (b) Shekhar, A., Keim, S., Simon, J. and McBride, W., Dorsomedial Hypothalamic GABA Dysfunction Produces Physiological Arousal Following Sodium Lactate Infusions, *Pharmacol. Biochem. Behav.*, **55**, 249-256 (1996). (c) Charney, D.S., Heninger, G.R., Price, L. and Breier, A., Major Depression and Panic Disorder: Diagnostic and Neurobiological Relationships, *Psychopharmacol. Bulletin.*, **22**, 503-511 (1986). (d) Kash, S., Tecot, L., Hodge, C. and Baekkeskov, S., An Increased Anxiety and Altered Responses to Anxiolytics in Mice Deficient in the 65-kDa Isoform of Glutamic Acid Decarboxylase, *Proc. Natl. Acad. Sci.*, **96**, 1698-1703 (1999). (e) Stork, D., Ji, F.-Y., Kaneko, K., Stork, S., Yoshinobu, Y., Moriya, T., Shibata, S. and Obata, K., Postnatal Development of a GABA Deficit and Disturbance of Neuronal Functions in Mice Lacking GAD65, *Brain Res.*, **865**, 45-58 (2000).
6. (a) Crestani, F., Matthias, L., Baer, K., Essrich, C., Benke, D., Laurent, J., Belzung, C., Fritschy, J.-M., Lüschen, B. and Möhler, H., Decreased GABA_A-Receptor Clustering Results in Enhanced Anxiety and a Bias for Threat Cues, *Nature (Neuroscience)*, **2**, 833 - 839 (1999). (b) McNaughton, N., A Gene Promotes Anxiety in Mice-and Also in Scientists, *Nature (Medicine)*, **5**, 1131-1132 (1999). (c) Kuikka, J., Pitkänen, A., Lepola, U., Partanen, K., Vainio, P., Bergström, K., Wieler, H., Kaiser, K., Mittlebach, L., Koponen, H., Leinonen, E. and Riekkinen, P., Abnormal Regional Benzodiazepine Receptor Uptake in the Prefrontal Cortex in Patients with Panic Disorder, *Nuc. Med. Commun.* **16**, 273-280 (1995). (d) Moroz, G., Rosenbaum, J., Efficacy, Safety and Gradual Discontinuation of Clonazepam in Panic Disorder: A Placebo-controlled, Multicenter Study Using Optimized Dosages, *J. Clin. Psychiatry.*, **60**, 604-611 (1999). (e) Crowe R., Wang, Z., Noyes Jr., R., Albrecht, B., Darlison, M., Bailey, M., Johnson, K. and Zoëga, T., Candidate Gene Study of Eight GABA_A Receptor Subunits in Panic Disorder, *Am. J. Psychiatry.*, **154**, 1096-1100 (1997).
7. (a) Banejee, P.K., Tillakaratne, N., Brailowsky, S., Olsen, R.W., Tobin, A. and Snead, O.C., Alterations in GABA_A Receptor $\alpha 1$ and $\alpha 4$ Subunit mRNA Levels in Thalamic Relay Nuclei Following Absence-Like Seizures in Rats, *Exp. Neurology.*, **154**, 213-223 (1998).

- (b) Karle, J., Woldbye, D., Elster, L., Diemer, N., Bolwig, T., Olsen, R. and Nielsen, M., Antisense Oligonucleotide to GABA_A Receptor γ 2 Subunit Induces Limbic Status Epilepticus, *J. Neurosci. Res.*, **54**, 863-869 (1998). (c) Homanics, G., Delorey, T., Firestone, L., Quinlan, J., Handforth, A., Harrison, N.L., Krasowski, M., Rick, C., Korpi, E., Makela, R., Brilliant, M., Hagiwara, N., Ferguson, C., Snyder, K. and Olsen, R.W., Mice Devoid of γ -Aminobutyrate Type A Receptor β 3 Subunit Have Epilepsy, Cleft Palate and Hypersensitive Behavior, *Proc. Natl. Acad. Sci. U.S.A. (Neurobiology)*, **94**, 4143-4148 (1997). (d) DeLorey, T., Handforth, A., Anagnostaras, S., Homanics, G.E., Minassian, B., Asatourian, A., Fanselow, M., Delgado- Escueta, A., Ellison, G.D. and Olsen, R. W., Mice Lacking the β 3 Subunit of the GABA_A Receptor Have the Epilepsy Phenotype and Many of the Behavioral Characteristics of Angelman Syndrome, *J. Neurosci.*, **18**, 8505-8514 (1998).
8. Benes, F., Wickramasinghe, R., Vincent, S., Khan, Y. and Todtenkopf, M., Uncoupling of GABA_A and Benzodiazepine Receptor Activity in the Hippocampal Formation of Schizophrenic Brain, *Brain Res.*, **755**, 121-129 (1997).
 9. (a) Mahmoudi, M., Kang, M.-H., Tillakaratne, N., Tobin, A. and Olsen, R., Chronic Intermittent Ethanol Treatment in Rats Increases GABA_A Receptor α 4 Subunit Expression: Possible Relevance to Alcohol Dependence, *J. Neurochem.*, **68**, 2485-2492 (1997). (b) Cadete-Leite, A., Brandão, F., Andrade, L., Ribeiro-DaSilva, A. and Paula-Barbosa, M., The GABAergic System of the Dentate Gyrus after Withdrawal from Chronic Alcohol Consumption: Effects of Intracerebral Grafting and Putative Neuroprotective Agents, *Alcohol and Alcoholism.*, **32**, 471-484 (1997).
 10. Blue, M., Sakkubai, N. and Johnston, M., Altered Development of Glutamate and GABA Receptors in the Basal Ganglia of Girls with Rhetts Syndrome, *Exp. Neurology.*, **156**, 345-352 (1999).
 11. (a) Leshner, A., Drug Abuse and Mental Disorders: Comorbidity is Reality, *NIDA Notes.* **14**, 3-4 (1999). (b) Goeders, N., Irby, B.D., Shuster, C. and Guerin, G., Tolerance and Sensitization to the Behavioral Effects of Cocaine in Rats: Relationship to Benzodiazepine Receptors, *Pharm. Biochem. Behav.*, **57**, 43-56 (1997). (c) Kushner, S., Dewey, S. and Kornetsky, C., The Irreversible γ -Aminobutyric Acid (GABA) Transaminase Inhibitor γ -Vinyl-GABA Blocks Cocaine Self-Administration in Rats, *J. Pharmacol. Exp. Ther.*, **290**, 797-802 (1999). (d) Gerasimov, M., Ashby Jr., C., Gardner, E., Mills, M., Brodie, J. and Dewey, S., Gamma-Vinyl GABA Inhibits Methamphetamine, Heroin or Ethanol-induced Increases in Nucleus Accumbens Dopamine, *Synapse.*, **34**, 11-19 (1999).
 12. Sigel, E., Baur, R., Trube, G., Möhler, H. and Malherbe, P., The Effect of Subunit Composition of Rat Brain GABA_A Receptors on Channel Function. *Neuron.* **5**, 703-711 (1990).
 13. Nayeem, N., Green, T. P., Martin, I. L. and Barnard, E. A., Quaternary Structure of the Native GABA_A Receptor Determined by Electron Microscopic Image Analysis. *J.Neurochem.* **62** (2), 815-18 (1994).

14. Cook, J. M., Zhou, H., Huang, S., Sarma, P. V. V. S. and Zhang, C. Patent Title: Preparation of Benzodiazepines, in Particular 1,4-Benzodiazepines, as Anxiolytic and Anticonvulsant Agents with Reduced Sedative and Ataxic Effects. Applied Patent Number 2006003995, Application: US 20050630, Accession Number An 2006:11549, US Patent 7119196 (2006).
15. Malherbe, P., Sigel, E., Baur, R., Persohn, E., Richards, J. G., Möhler, H., Functional Characteristics and Sites of Gene Expression of the $\alpha 1, \beta 1, \gamma 2$ -Isoform of the Rat GABA_A Receptor. *J. Neurosci.*, **10**, (7), 2330-7 (1990).
16. Davies, P. A., Hanna, M. C., Hales, T. G. and Kirkness, E. F., Insensitivity to Anaesthetic Agents Conferred by a Class of GABA_A Receptor Subunit. *Nature*. **385** (6619), 820-823 (1997).
17. Burt, D. R., Kamatchi, G. L., GABA_A Receptor Subtypes: From Pharmacology to Molecular Biology, *FASEB J.* **5** (14), 2916-2923 (1991).
18. Keramidas, A., Moorhouse, A., Schofield, P. C. and Barry, P., Ligand-Gated Ion Channels: Mechanisms Underlying Ion Selectivity, *Prog. Biophys. Mol. Biol.* **86**, 161-204 (2004).
19. Ernst M., Bruckner, S., Boresch, S., Sieghart, W., Comparative Models of GABA(A) Receptor Extracellular and Transmembrane Domains: Important Insights in Pharmacology and Function, *Mol Pharmacol.* **68** (5), 1291-300 (2005).
20. Tretter, V., Ehya, N., Fuchs, K., Sieghart, W., Stoichiometry and Assembly of a Recombinant GABA_A Receptor Subtype. *J. Neurosci.* **17** (8), 2728-2737 (1997).
21. Huang, Q., Zhang, W., Liu, R., McKernan, R. M. and Cook, J. M., Benzo-Fused Benzodiazepines Employed as Topological Probes for the Study of Benzodiazepine Receptor Subtypes. *Med. Chem. Res.* **6** (6), 384-391 (1996).
22. Clayton, T., Chen, J.L., Ernst, M., Richter, L., Cromer, B.A., Morton, H.N., Kaczorowski, C.C., Helmstetter, F.J., Furtmuller, R., Ecker, G., Parker, M.W., Sieghart, W. and Cook, J.M., Analysis of the Benzodiazepine Binding Site on γ -Aminobutyric Acid (A) Receptors: Correlation of Experimental Data with Pharmacophore and Comparative Models. *Curr. Med. Chem.* **14**, (26), 2755-2775 (2007).
23. Ernst, M., Brauchart, D., Boresch, S., and Sieghart, W., Comparative Modeling of GABA_A Receptors: Limits, Insights, Future Developments, *Neuroscience*. **119**, 933-943 (2003).
24. Dennis, T., Dubois, A., Benavides, J. and Scatton, B., Distribution of Central Omega 1 (Benzodiazepine1) and Omega 2 (Benzodiazepine2) Receptor Subtypes in the Monkey and Human Brain. An Autoradiographic Study with [3H]Flunitrazepam and the Omega 1 Selective Ligand [3H]Zolpidem. *J. Pharmacol. Exp. Thera.* **247** (1), 309-22 (1988).

25. Schoch, P., Richards, J.G., Haring, P., Takacs, B., Stahli, C., Staehelin, T., Haefely, W., and Möhler, H., Co-localization of GABA Receptors and Benzodiazepine Receptors in the Brain Shown by Monoclonal Antibodies. *Nature* **314** (6007), 168-71 (1985).
26. Caruncho, H. J., Puia, G., Möhler, H. and Costa, E., The Density and Distribution of Six GABA(A) Receptor Subunits in Primary Cultures of Rat Cerebellar Granule Cells. *Neurosci. (Oxford)*, **67** (3), 583-93 (1995).
27. Bohlhalter, S., Weinmann, O., Möhler, H. and Fritschy, J. M., Laminar Compartmentalization of GABA(A)-Receptor Subtypes in the Spinal Cord: an Immunohistochemical Study. *J. Neurosci.* **16** (1), 283-97 (1996).
28. Fritschy, J. M., Möhler, H., GABA(A)-Receptor Heterogeneity in the Adult Rat Brain: Differential Regional and Cellular Distribution of Seven Major Subunits. *J. Comp. Neurol.* **359** (1), 154-94 (1995).
29. Collinson, N., Kuenzi, F. M., Jarolimek, W., Maubach, K. A., Cothliff, R., Sur, C., Smith, A., Otu, F. M., Howell, O., Atack, J. R., McKernan, R. M., Seabrook, G. R., Dawson, G. R., Whiting, P. J. and Rosahl, T. W., Enhanced Learning and Memory and Altered GABAergic Synaptic Transmission in Mice Lacking the Alpha 5 Subunit of the GABA_A Receptor. *J. Neurosci.* **22** (13), 5572-5580 (2002).
30. Bailey, D. J., Tetzlaff, J. E., Cook, J. M., He, X. H. and Helmstetter, F. J., Effects of Hippocampal Injections of a Novel Ligand Selective for the $\alpha 5 \beta 2 \gamma 2$ Subunits of the GABA/Benzodiazepine Receptor on Pavlovian Conditioning. *Neurobiol. Learn. Mem.* **78** (1), 1-10 (2002).
31. Zimprich, F., Zezula, J., Sieghart, W. and Lassmann, H., Immunohistochemical Localization of the $\alpha 1$, $\alpha 2$ and $\alpha 3$ Subunit of the GABA_A Receptor in the Rat Brain. *Neurosci. Lett.* **127** (1), 125-8 (1991).
32. McKernan, R. M., Cox, P., Gillard, N. P. and Whiting, P., Differential Expression of GABA(A) Receptor Alpha-Subunits in Rat Brain During Development. *FEBS Lett.* **286** (1-2), 44-6 (1991).
33. Buchstaller, A., Fuchs, K., Sieghart, W., Identification of Alpha 1-, Alpha 2- and Alpha 3-Subunit Isoforms of the GABA_A-Benzodiazepine Receptor in the Rat Brain. *Neurosci. Lett.* **129** (2), 237-41 (1991).
34. He, X., Huang, Q., Ma, C., Yu, S., McKernan, R. and Cook, J. M., Pharmacophore/Receptor Models for GABA/BzR $\alpha 2 \beta 3 \gamma 2$, $\alpha 3 \beta 3 \gamma 2$ and $\alpha 4 \beta 3 \gamma 2$ Recombinant Subtypes. Included Volume Analysis and Comparison to $\alpha 1 \beta 3 \gamma 2$, $\alpha 5 \beta 3 \gamma 2$ and $\alpha 6 \beta 3 \gamma 2$ subtypes. *Drug Des. and Discov.* **17**, 131-171 (2000).

35. June, H. L., Harvey, S. C., Foster, K. L., McKay, P. F., Cummings, R., Garcia, M., Mason, D., Grey, C., McCane, S., Williams, L. S., Johnson, T. B., He, X. H., Rock, S. and Cook, J. M., GABA_A Receptors Containing $\alpha 5$ Subunits in the CA1 and CA3 Hippocampal Fields Regulate Ethanol-Motivated Behaviors: An Extended Ethanol Reward Circuitry. *J. Neurosci.* **21** (6), 2166-2177 (2001).
36. (a) McKernan, R. M., Quirk, K., Prince, R., Cox, P. A., Gillard, N. P., Ragan, C. I. and Whiting, P., GABA_A Receptor Subtypes Immunopurified from Rat Brain with Alpha Subunit-Specific Antibodies Have Unique Pharmacological Properties. *Neuron.* **7** (4), 667-76, (1991). (b) Sieghart, W., Ramerstorfer, J., Sarto-Jackson, I., Varagic, Z., Ernst, M., A Novel GABA_A Receptor Pharmacology: Drugs Interacting with the $\alpha^+ \beta^-$ interface. *British J Pharm.* **166** (2), 476-485 (2012).
37. (a) Tulinsky, J., Gammil, R.B., The Chemistry and Pharmacology of GABA_B Ligands, *Curr. Med. Chem.*, **1**, 226-253 (1994). (b) Haefely, W.E., The GABA_A-Benzodiazepine Receptor: Biology and Pharmacology, in *Handbook of Anxiety*, **3**, *The Neurology of Anxiety*, Burrows, G. D., Roth, M. and Noyes, Jr. R., (eds.), Elsevier, **3**, 165-188 (1990). (c) Krosgaad-Larsen, P., GABA Agonists and CNS Receptors, in *Advances in CNS Drug-Receptor Interactions*, **1**, Cannon, J. G (ed.), JAI Press, London, 23-35 (1991). (d) For other earlier references to the anxiolytic, anticonvulsant, muscle-relaxant/ataxic, and sedative-hypnotic effects of the 1,4-benzodiazepines see Enna, S. L, Karbon, E.W., *Benzodiazepines/GABA Receptors and Chloride Channels: Structure and Functional Properties*, Olson, R. W., Venter, J. C. and Liss, A R., (eds.), Wiley Interscience, New York, 46-59 (1986) and references cited therein. (e) Skolnick, P., Paul, S.M., *ISI Atlas of Science, Pharmacology*, **2**, 19-22 (1988) and references to key contributors [Barker, Beer, Barnard, Stephenson, Seeburg, Braestrup, Costa, Johnston, Karobath, Möhler, Haefely, Olsen, Sieghart, Squires, Tallman, Ticku, and Yamamura] cited therein. (f) Greenblatt, D.J., Shader, R.I., *Benzodiazepines in Clinical Practice*, Wiley, J. and Sons, New York, (1974). (g) Delorey, T., Olsen, R.W., γ -Aminobutyric Acid_A Receptor Structure and Function, *J. Biol. Chem.* **267**, 16747-16750 (1992) and references cited therein. (h) Olsen, R.W., Venter, C.J., *Benzodiazepine/GABA Receptors and Chloride Channels: Structure and Functional Properties*, Liss, A R., New York. E. Costa and A. Guidotti, Molecular Mechanisms in the Receptor Action of Benzodiazepines, *Ann. Rev. Pharmacol. Toxicol.* **19**, 531-545 (1979). (i) Klepner, C., Lippa, A., Benson, D., Sano, M. and Beer, B., Resolution of Two Biochemically and Pharmacologically Distinct Benzodiazepine Receptors, *Pharmacol. Biochem. Behav.* **11**, 457-462 (1979). (j) Lippa, A.S., Meyerson, L. R., Beer, B., Molecular Substrates of Anxiety: Clues from the Heterogeneity of Benzodiazepine Receptors, *Life Sci.* **31**, 1409-1494 (1982). (k) Skolnick, P., Is Receptor Heterogeneity Relevant to the Anxiolytic Actions of Benzodiazepine Receptor Ligands in *New Concepts in Anxiety*, **4**, Briley, M. and Files, S., (eds.), Macmillan Press, London, 199-202 (1991). (l) Skolnick, P., Wong, G., Drug Receptor Interactions in Anxiety, *Imidazopyridines in Anxiety Disorders: A Novel Experimental and Therapeutic Approach*, B. Zivkovic et al. (eds.), Raven Press, New York, 23 -32 (1993). (m) Williams, M.J., Anxiolytic Anxiolytics, *J. Med. Chem.* **26**, 619-628 (1983). (n) Taken from "Panic Disorder Found to Increase Risk of Suicide, *ADAMHA News*, **XVI** (2), March-April (1990). (o) Benzodiazepines differ from each other primarily in their half-lives. Librium, Valium and Dalmane, for example, have extremely long half-lives and can remain in the body as long

- as four days after the last dose has been taken. For this reason they are contraindicated in the elderly, because of impaired metabolism, the elderly can have exaggerated responses to any medication and are particularly susceptible to the sedative effects of these drugs. One physician stated that hip fractures in the elderly could be reduced dramatically if doctors stopped prescribing Librium, Valium and Dalmane. He hypothesized that many elderly victims of hip fracture are still sedated from the previous day's drug usage. Taken from B. Kratz, Ed. of DMDA News (The Depressive and Manic-Depressive Association of Greater Milwaukee) September Issue, p. 3 (1990). (p) Hauser J., Rudolph, U., Keist, R., Mohler, H., Feldon, J. and Yee, B., Hippocampal $\alpha 5$ Subunit-containing GABA(A) Receptors Modulate the Expression of Prepulse Inhibition, *Mol. Psychiatry*. **10**, 201-207 (2005). (q) Swerdlow, N., Geyer, M., Bratt, D., Neural Circuit Regulation of Prepulse Inhibition of Startle in the Rat: Current Knowledge and Future Challenges, *Psychopharmacol.* **156**, 194-215 (2001). (r) Gilman, N., Rosen, P., Early, J., Cook, C., Todaro, L., Atropisomers of 1,4-Benzodiazepines. Synthesis and Resolution of a Diazepam-Related 1,4-Benzodiazepine, *J. Am. Chem. Soc.*, **112**, 3969-3978 (1990). (s) Carlier, P., Zhao, H., DeGuzman, J., Lam P.C.-H., Enantioselective Synthesis of Quaternary 1,4-Benzodiazepine-2-one Scaffolds *via* Memory of Chirality, *J. Am. Chem. Soc.* **125**, 11482-11483 (2003). (t) Lam, P.C.-H., Carlier, P., Experimental and Computational Studies of Ring Inversion of 1,4-Benzodiazepin-2-ones: Implications for Memory Chirality Transformations, *J. Org. Chem.* **70**, 1530-1538 (2005). (u) Cook, J.M., Zhou, T., Huang, S., Sarma, P.V.V.S., and Zhang, C., Stereospecific Anxiolytic and Anticonvulsant Agents with Reduced Muscle-relaxant, Sedative-hypnotic and Ataxic Effects, Patent published on 1/12/2006 (WO2006/004945A1). (v) Yin, W., Sarma, P.V.V.S., Ma, J. Han, D., Chen, J. and Cook, J. M. Synthesis of Bivalent Ligands of β -Carboline-3-Carboxylates *via* a Palladium-catalyzed Homocoupling Process, *Tetrahedron Letters*. **46**, 6363-6368 (2005). (w) Rowlett, J., Cook, J.M., Duke, A., Platt, D. Selective Antagonism of GABA(A) Receptor Subtypes. An *In Vivo* Approach to Exploring the Therapeutic and Side Effects of Benzodiazepine-Type Drugs, *CNS Spectra*. **10**, 40-48 (2005).
38. Gorman, J. M. Benzodiazepines: Taking the Good with the Bad and the Ugly. *CNS Spectrums*. **10**, 14-15 (2005).
 39. GaRattini, S., Mussini, E., Marcucci, F. and Guaitani, A., Metabolic Studies on Benzodiazepines in Various Animal Species. In *The Benzodiazepines*, GaRattini, S., Mussini, E. and Randall, L. O., (eds.), Raven Press.: New York, 75-97 (1973).
 40. Stevenson, I. H., Browning, M., Crooks, J., O'Malley, K. Changes in Human Drug Metabolism after Long-Term Exposure to Hypnotics. *Br. Med. J.* **4**, 322-324 (1972).
 41. Rogawski, M. A. Principles of Antiepileptic Drug Action. In *Antiepileptic Drugs*, 5th ed., Levy, R. H., Mattson, R. H., Meldrum, B. S., Perucca, E., (eds.), Lippincott Williams and Wilkins.: Philadelphia, 3-22 (2002).
 42. Hillestad, L., Hansen, T., Melsom, H. Diazepam Metabolism in Normal Man. II. Serum Concentration and Clinical Effect after Oral Administration and Cumulation. *Clin. Pharmacol. Ther.* **16**, 485-489 (1974).

43. Macdonald, R. L., Benzodiazepines Mechanisms of Action. In *Antiepileptic Drugs*, 5th ed., Levy, R. H., Mattson, R. H., Meldrum, B. S., Perucca, E., (eds.), Lippincott Williams and Wilkins.: Philadelphia, 179-186 (2002).
44. Killam, E. K., Suria, A., Benzodiazepines. In *Antiepileptic Drugs: Mechanisms of Action*, Glaser, G. H., Penry, J. K., Woodbury, D. M., (eds.), Advances in Neurology. **27**, Raven Press.: New York, 597-615 (1980).
45. De Sarro, G., Gambardella, A., De Sarro, A., Benzodiazepines in Pathology of Epilepsy. In *Benzodiazepine*, Biggio, G., (eds.), Springer-Verlag.: Milan, 259-279, (2000).
46. Shorvon, S. D. The Use of Clobazam, Midazolam, and Nitrazepam in Epilepsy. *Epilepsia*. **39**, S15-S23 (1998).
47. Söderpalm, B., Eriksson, E., Engel, J. A., Anticonflict and Rotarod Impairing Effects of Alprazolam and Diazepam in Rat After Acute and Subchronic Administration. *Prog. Neuropsychopharmacol. Biol. Psych.* **13**, 269-283 (1989).
48. Barnard, E. A., Skolnick, P., Olsen, R. W., Möhler, H., Sieghart, W., Biggio, G., Braestrup, C., Bateson, A. N. and Langer, S. Z., International Union of Pharmacology. XV. Subtypes of γ -Aminobutyric Acid (A) Receptors: Classification on the Basis of Subunit Structure and Receptor Function. *Pharmacol. Rev.* **50** (2), 291-313 (1998).
49. Verdoorn, T. A., Draguhn, A., Ymer, S., Seeburg, P. H., Sakmann, B., Functional Properties of Recombinant Rat GABA_A Receptors Depend Upon Subunit Composition. *Neuron*. **4** (6), 919-28 (1990).
50. Benavides, J., Peny, B., Ruano, D., Vitorica, J. and Scatton, B., Comparative Autoradiographic Distribution of Central (Benzodiazepine) Modulatory Site Subtypes with high, Intermediate and Low Affinity for Zolpidem and Alpidem. *Brain Res.* **604** (1-2), 240-50 (1993).
51. Sieghart, W., Sperk, G., Subunit Composition Distribution and Function of GABA_A Receptor Subtypes, *Curr. Topics in Med.Chem.* **2**, 795-816 (2002).
52. Sieghart, W., Benzodiazepines, Benzodiazepine Receptors, and Endogeneous Ligands. *Medical Psychiatry*. **21**, (Handbook of Depression and Anxiety (2nd Edition)), 415-442 (2003).
53. Cox, E. D., Hagen, T. J., McKernan, R. M. and Cook, J. M., Bz1 Receptor Subtype Specific Ligands, Synthesis and Biological Properties of BCCT, a Bz1 Receptor Subtype Specific Antagonist. *Med. Chem. Res.* **5** (9), 710-18 (1995).
54. Allen, M. S., Hagen, T. J., Trudell, M. L., Coddington, P. W., Skolnick, P. and Cook, J. M., Synthesis of Novel 3-Substituted β -Carbolines as Benzodiazepine Receptor

- Ligands: Probing the Benzodiazepine Receptor Pharmacophore. *J. Med. Chem.* **31** (9), 1854-61 (1988).
55. Hagen, T. J., Guzman, F., Schultz, C., Cook, J. M., Skolnick, P. and Shannon, H. E., Synthesis of 3,6-Disubstituted β -Carbolines which Possess either Benzodiazepine Antagonist or Agonist Activity. *Heterocycles*. **24** (10), 2845-55 (1986).
 56. Cook, J. M., Huang, Q., He, X., Li, X., Yu, J., Han, D., Lelas, S. and McElroy, J. F. Preparation of Benzodiazepines, in Particular 1,4-Benzodiazepines, as Anxiolytic and Anticonvulsant Agents with Reduced Sedative and Ataxic Effects. *PCT Int. Appl.* (2003), 125 pp. CODEN: PIXXD2 WO 2003082832 A2 20031009 CAN 139:323542 AN 2003:796671 CAPLUS (2003).
 57. Huang, Q., He, X., Ma, C., Liu, R., Yu, S., Dayer, C. A., Wenger, G. R., McKernan R. and Cook, J. M., Pharmacophore/Receptor Models for GABA_A/BzR Subtypes ($\alpha 1\beta 3\gamma 2$, $\alpha 5\alpha 3\gamma 2$, and $\alpha 6\beta 3\gamma 2$) via a Comprehensive Ligand-Mapping Approach, *J. Med. Chem.* **43** (1), 71-95 (2000).
 58. Sigel, E., Dodd, R. H., Novel Positive Allosteric Modulators of GABA_A Receptors, *Drugs of the Future*. **26** (12), 1191-1197 (2001).
 59. Study, R., Diazepam and (--)Pentobarbital: Fluctuation Analysis Reveals Different Mechanisms for Potentiation of γ -Aminobutyric Acid Responses in Cultured Central Neurons, *Proc. Natl. Acad. Sci. USA*. **78**, 7180-7184 (1981).
 60. Rogers, C., Twyman, R. E., MacDonald, R. L. Benzodiazepine and β -carboline Regulation of Single GABA_A Receptor Channels of Mouse Spinal Neurones in Culture, *J. Physiol. (London)*. **475**, 69-82 (1994).
 61. Kash, T. L., Jenkins, A., Kelley, J. C., Trudell, J. and Harrison, N. L. Coupling of Agonist Binding to Channel Gating in the GABA_A Receptor, *Nature*. **421**, 272-275 (2003).
 62. Rüsçh, D., Forman, S. A., Classic Benzodiazepines Modulate the Open-Close Equilibrium in $\alpha 1\beta 2\gamma 2$ L [γ]-Aminobutyric Acid Type (A) Receptors, *Anesthesiology*. **102**, 783-792 (2005).
 63. Baur, R., Sigel, E., Benzodiazepines Affect Channel Opening of GABA_A Receptors Induced by Either Agonist Binding Site, *Mol. Pharmacol.* **67**, 1005-1008 (2005).
 64. Doble, A., Martin, I. L., Multiple Benzodiazepine Receptors: No Reason for Anxiety, *Trends Pharmacol. Sci.* **13**, 76-81 (1992).
 65. Harvey, S. C., Foster, K. L., McKay, P. F., Carrol, M. R., Seyoum, R., Woods J. E., Grey, C., Jones, C. M., McCane, S., Cummings, R. et al., The GABA_A Receptor $\alpha 1$

- Subtype in the Ventral Pallidum Regulates Alcohol-Seeking Behaviours. *J. Neurosci.* **22** (9), 3765-75 (2002).
66. Lelas, S., Rohrbach, K., Glick, S. D., Zeller, K., Bourin, C., Sieracki, K., Bertekap, R., Chen, J., Cook, C. M., Helmstetter, F. J., Li, X. H., Westphal, R., Lindner, M., Tertshnikova, S., Cook, J., McElroy, J. F., *Manuscript in preparation*.
 67. Cook, J.M, He, X., Ma, C., Yu, S. and June, H., Search for Selective Ligands for GABA_A/BzR Subtypes and Their Role in Alteration of Alcohol Dependence, 219th National ACS Meeting, San Francisco, CA, March 26-30, 2000, abst. MEDI-101.
 68. Liu, R. Y., Hu, R. J., Zhang, P. W., Skolnick, P. and Cook, J. M., Synthesis and Pharmacological Properties of Novel 8-Substituted Imidazobenzodiazepines: High-Affinity, Selective Probes for α 5-Containing GABA_A Receptors. *J. Med. Chem.* **39**, 1928-1934 (1996).
 69. Griebel, G., Perrault, G., Simiand, J., Cohen, C., Granger, P., Decobert, M., Francon, D., Avenet, P., Depoortere, H., Tan, S., Oblin, A., Schoemaker, H., Evanno, Y., Sevrin, M., George, P. and Scatton, B., SL651498: An Anxiolytic Compound with Functional Selectivity for 2- and 3-Containing γ -Aminobutyric Acid (A; GABA_A) Receptors, *J. Pharmacol. Exp. Ther.* **298**, 753-768 (2001).
 70. Minier, F., Sigel, E., Positioning of the α -Subunit Isoforms Confers a Functional Signature to γ -Aminobutyric Acid Type (A) Receptors, *Proc. Natl. Acad. Sci. USA.* **101**, 7769-7774 (2004).
 71. Wafford, K.A., Macaulay, A.J., Fradley, R., O'Meara, G.F., Reynolds, D.S. and Rosahl, T.W., Differentiating the Role of γ -Aminobutyric Acid Type (A; GABA_A) Receptor Subtypes. *Biochem. Soc. Trans.* **32**, 553-556 (2004).
 72. Casula, M.A., Bromidge, F.A., Pillai, G.V., Wingrove, P.B., Martin, K., Maubach, K., Seabrook, G.R., Whiting, P.J., Hadingham, K.L. Identification of Amino Acid Residues Responsible for the 5 Subunit Binding Selectivity of L-655,708, a Benzodiazepine Binding Site Ligand at the GABA_A Receptor, *J. Neurochem.* **77**, 445-451 (2001).
 73. Wafford, K.A., Whiting, P.J., Kemp, J.A. Differences in Affinity and Efficacy of Benzodiazepine Receptor Ligands at Recombinant γ -Aminobutyric Acid (A) Receptor Subtypes, *Mol. Pharmacol.* **43**, 240-244 (1993).
 74. Atack, J.R., The Benzodiazepine Binding Site of GABA_A Receptors as a Target for the Development of Novel Anxiolytics, *Expert Opin. Invest. Drugs.* **14**, 601-618 (2005).

75. Li, X. Y., Ma, C. R., He, X. H., Yu, J. M., Han, D. M., Zhang, C. C., Atack, J. R. and Cook, J. M., Studies in Search of Diazepam-Insensitive Subtype Selective Agents for GABA_A/Bz Receptors. *Med. Chem. Res.* **11** (9), 504-537 (2002).
76. Sarter, M., Taking Stock of Cognition Enhancers. *Trends Pharmacol. Sci.* **12** (12), 456-461 (1991).
77. De Almeida Rosa, M. M., Rowlett J. K., Cook, J.M., Yin, W. and Miczek Klaus, A., GABA_A/α1 Receptor Agonists and Antagonists: Effects on Species Typical and Heightened Aggressive Behavior After Alcohol Self-Administration in Mice, *Psychopharmacol.* **172** (3), 255-63 (2004).
78. Sieghart, W. Structure and Pharmacology of γ-Aminobutyric Acid (A) Receptor Subtypes, *Pharm. Rev.* **47**, 181-234, (1995).
79. Pirker, S., Schwarzer, C., Wieselthaler, A., Sieghart, W. and Sperk, G., GABA_A Receptors: Immunocytochemical Distribution of 13 Subunits in the Adult Rat Brain. *Neuroscience.* **101**, 815-850 (2000).
80. Crestani, F., Keist, R., J.-M., F., Benke, D., Vogt, K., Prut, L., Bluthmann, H., Mohler, H. and Rudolph, U., Trace Fear Conditioning Involves Hippocampal α5 GABA_A Receptors. *Neurobiology.* **99**, 8980-8985 (2002).
81. Sternfeld, F., Carling, R. W., Jelley, R. A., Ladduwahetty, T., Merchant, K. J., Moore, K. W., Reeve, A. J., Street, L. J., O'Connor, D., Sohal, B., Atack, J. R., Cook, S., Seabrook, G., Wafford, K., Collinson, F. D. T. N., Dawson, G. R., Castro, J. L. and MacLeod, A. M., Selective, Orally Active γ-Aminobutyric Acid (A) α5 Receptor Inverse Agonists as Cognition Enhancers. *J Med Chem.* **47**, 2176-2179 (2004).
82. DeLorey, T., Lin, R., McBrad, B., He, X., Cook, J. M., Lamah, J. and Loew, G., Influence of Benzodiazepine Binding Site Ligands on Fear-Conditioned Contextual Memory, *Eur J Pharmacol.* **426**, 45-54 (2001).
83. Möhler, H., Crestaini, F., Rudolph, U., GABA_A-Receptor Subtypes: A New Pharmacology. *Current Opinion in Pharmacology.* **1**, 22-25 (2001).
84. Möhler, H., Crestaini, F., *The 12th Neuropharmacology Conference, GABA_A Receptors in Cellular and Network Excitability.* Sheraton World Resort, Orlando, FL, Oct 31-Nov 2 (2002).
85. Zhang, C. and Cook, J.M., Study of Pharmacophore/Receptor Models for GABA_A/BzR Subtypes. Abst. 238, 37th National Organic Chemistry Symposium, Montana State University, Bozeman, MT, June 10-14 (2001).

86. Sur, C., Quirk, K., Dewar, D., Atack, J. R. and McKernan, R., Rat and Human Hippocampal $\alpha 5$ Subunit-Containing γ -Aminobutyric Acid (A) Receptors Have $\alpha 5\beta 3\gamma 2$ Pharmacological Characteristics. *Mol Pharmacol.* **54**, 928-933 (1998).
87. (a) Cook, J.M., June, H., Weerts, E., Van Linn, M.L., Platt, D., DeLorey, T., Savic, M., Clayton, T. Serendipity Rediscovered – An Oxymoron or Rational Drug Design: Studies on Subtype Selective BzR/GABAergic Ligands. Abstracts of Papers, 234th ACS National Meeting, Boston, MA, United States, Aug. 19-23, (2007). (b) Savic, M., Milic, M., Divljakovic, J., Rallapalli, S., Van Linn, M., Timic, T., Cook, J.M., The Role of $\alpha 1$ and $\alpha 5$ subunit-containing GABA_A Receptors in Motor Impairment Induced by Benzodiazepines in Rats. *Behav. Pharma.* **23** (2) 191-197 (2012). (c) Savic, M., Clayton, T., Furtmuller, R., Gavrilovic, I., Samarzic, J., Savic, S., Huck, S., Sieghart, W., Cook, J.M. PWZ-029, A Compound with Moderate Inverse Agonist Functional Selectivity at GABA_A Receptors Containing $\alpha 5$ Subunits, Improves Passive, but not Active, Avoidance Learning in Rats. *Brain Res.* **1208**, 150-159 (2008). (d) Srdan, J., Divljakovic, J., Van Linn, M., Varagic, Z., Brajkovic, G., Milinkovic, M., Yin, W., Timic, T., Sieghart, W., Cook, J.M., Savic, M. Benzodiazepine-Induced Spatial Learning Deficits in Rats are Regulated by the Degree of Modulation of $\alpha 1$ GABA_A Receptors. *Nuropsychopharmacol.* (2012).
88. Zhang, W., Diaz-Arauzo, H., Allen, M.S., Koehler, K.F. and Cook, J.M., Chemical and Computer Assisted Development of the Inclusive Pharmacophore of Benzodiazepine Receptors, *Studies in Medicinal Chemistry*, M.I. Choudhary, Editor. Harwood Academic Publishers: 303 (1996).
89. Zhang, W., Koehler, K. F., Zhang, P. and Cook, J.M., Development of a Comprehensive Pharmacophore Model for the Benzodiazepine Receptor. *Drug Des. Discov.* **12**, 193-248 (1995).
90. Sigel, E., Schaerer, M.T., Buhr, A. and Baur, R. The Benzodiazepine Binding Pocket of Recombinant 122 -Aminobutyric Acid (A) Receptors: Relative Orientation of Ligands and Amino Acid Side Chains, *Mol. Pharmacol.* **54**, 1097-1105 (1998).
91. Dunn, S.M.J., Davies, M., Muntoni, A.L. and Lambert, J.J., Mutagenesis of the Rat 1 Subunit of the γ -Aminobutyric Acid A Receptor Reveals the Importance of Residue 101 in Determining the Allosteric Effects of Benzodiazepine Site Ligands, *Mol. Pharmacol.* **56**, 768-774 (1999).
92. Davies, M., Bateson, A.N., Dunn, S.M.J., Structural Requirements for Ligand Interactions at the Benzodiazepine Recognition Site of the GABA_A Receptor, *J. Neurochem.* **70**, 2188-2194 (1998).
93. Cromer, B., Morton, C., Parker, M.W., Anxiety over GABA_A Receptor Structure Relieved by AChBP, *Trends Biochem. Sci.* **27**, 280-287 (2002).

94. Sigel, E., Mapping of the Benzodiazepine Recognition Site on GABA_A Receptors, *Curr. Top. Med. Chem.* **2**, 833-840 (2002).
95. Allen, M. S., Tan, Y. C., Trudell, M. L., Narayanan, K., Schindler, L., Martin, M. J., Schultz, C. A., Hagen, T. J., Koehler, K. F., Coddington, P., Skolnick, P. and Cook, J. Synthetic and Computer-Assisted Analyses of the Pharmacophore for the Benzodiazepine Receptor Inverse Agonist Site *J. Med. Chem.* **33**, 2343-2357 (1990).
96. Zhang, P.W., Zhang, W.J., Liu, R.Y., Harris, B., Skolnick, P. and Cook, J.M., Synthesis of Novel Imidazobenzodiazepines as Probes of the Pharmacophore for "Diazepam-Insensitive" GABA_A Receptors *J. Med. Chem.* **38**, 1679-1688 (1995).
97. Allen, M.S., Laloggia, A.J., Dorn, L.J., Martin, M.J., Constantino, G., Hagen, T.J., Koehler, K.F., Skolnick, P. and Cook, J.M., Predictive Binding of β -carboline Inverse Agonists and Antagonists via the CoMFA/GOLPE Approach, *J. Med. Chem.* **35**, 4001-4010 (1992).
98. Wong, G., Koehler, K.F., Skolnick, P., Gu, Z.Q., Ananthan, S., Schönholzer, P., Hunkeler, W., Zhang, W.J. and Cook, J.M. Synthetic and Computer-Assisted Analysis of the Structural Requirements for Selective, High-Affinity Ligand Binding to Diazepam-Insensitive Benzodiazepine Receptors, *J. Med. Chem.* **36**, 1820-1830 (1993).
99. Huang, Q., He, X., Yu, S., Ma, C., Cook, J.M. Study of Pharmacophore/Receptor Models for Benzodiazepine Receptor Subtypes via Preparation of Rigidly Substituted Pyrazoloquinolinones. presented at the 216th ACS National Meeting, Boston, MA, August 223-227 (1998).
100. Huang, Q., Cox, E.D., Gan, T., Ma, C., Bennett, D.W., McKernan, R.M. and Cook, J.M., Studies of Molecular Pharmacophore/Receptor Models for GABA_A/Benzodiazepine Receptor Subtypes: Binding Affinities of Substituted β -Carboline Ligands for α x β 3 γ 2(x=1-3, 5, 6) Subtypes and Quantitative Structure-Activity Relationship Studies via Comparative Molecular Field Analysis. *Drug Des. Discov.* **16**, 55-76 (1999).
101. Platt, D.M., Rowlett, J.K., Speakman, R.D., Cook, J. and Ma, C.R., Selective Antagonism of the Ataxic Effects of Zolpidem and Triazolam by the GABA_A/ α 1-Preferring Antagonist β -CCt in Squirrel Monkeys. *Psychopharmacology.* **164**, (2), 151-159 (2002).
102. Savic, M.M., Clayton, T., Furtmueller, R., Gavrilovic, I., Samardzic, J., Savic, S., Huck, S., Sieghart, W. and Cook, J. M., PWZ-029, a Compound with Moderate Inverse Agonist Functional Selectivity at GABA_A Receptors Containing α 5 Subunits, Improves Passive, But Not Active, Avoidance Learning in Rats. *Brain Res.* **1208** (1), 150-159 (2008).

103. Harris, D.L., Clayton, T., Cook, J.M., Peyman, S., Halliwell, R. F., Furmueller, R., Huck, S., Sieghart, W. and Delorey, T. M., Selective Influence on Contextual Memory: Physicochemical Properties Associated with Selectivity of Benzodiazepine Ligands at GABA_A Receptors containing the $\alpha 5$ Subunit. *J. Med. Chem.* **51** (13), 3788-3803 (2008).
104. Sieghart, W., Ernst, M., Heterogeneity of GABA_A Receptors: Revived Interest in the Development of Subtype-Selective Drugs. *Curr. Med. Chem.: Cent. Nerv. Sys. Agents.* **5**, 217-242 (2005).
105. Polc, P., Laurent, J.P., Scherchlicht, R. and Haefely, W., Electrophysiological Studies on the Specific Benzodiazepine Antagonist Ro 15-1788, *Naunyn Schmiedebergs Arch. Pharmacol.* **316** (4), 317-25 (1981).
106. Hoffman, E.J. and Warren, E.W., Flumazenil, a Benzodiazepine Antagonist. *Clinical Pharmacy*, **12**, 641-56, (1993).
107. F. Hoffmann-La Roche, & Co. A.-G., Switz. Diazepine Derivatives. Neth. Appl. 7803585, 1978, *Chem. Abstr.* 90:152254g (1978).
108. Rogers-Evans, M., Spurr, P., Hennig, M., The Isolation and Use of a Benzodiazepine Iminochloride for the Efficient Construction of Flumazenil, and references cited therein, *Tetrahedron Lett.* **44**, 2425 (2003).
109. (a) Cook, J.M., Han, D., Clayton, T., GABAergic Agents to Treat Memory Deficits, Provisional patent filed June 30, 2005. Published in 2006. Patent No. PCT/US 2006018721; US Patent No. 7,595,395; (2009). (b) Li, X., Yu, J., Atack, J. R., Cook, J.M., Development of Selective Ligands for Benzodiazepine Receptor Subtypes by Manipulating the Substituents at Positions 3- and 7- of Optically Active BzR Ligands, *Med. Chem. Res.* **13**, 259-81 (2004). (c) Codding, P. W., Roszak, A. W., Szaradzinska, M. B. , and Cook, J. M. Structure-Activity Relationships in Antagonists and Inverse Agonist Ligands for the Benzodiazepine Receptor, *Can. J. Chem.*, **73**, 449-512 (1995). (d) Zhang, P. W., Liu, R., McKernan, R.M., Wafford, K. and Cook, J.M., Studies of Novel Imidazobenzodiazepine Ligands at GABA_A/BzR Subtypes: Effect of C(3) Substituents on Receptor Site Selectivity. *Med. Chem. Res.* **5**, 487-95 (1995).
110. (a) Watjen, F., Baker, R., Engelstoff, M., Herbert, R., MacLeod, A., Knight, A., Merchant, K., Moseley, J. and Saunders, J., Novel Benzodiazepine Receptor Partial Agonists: Oxadiazolyimidazobenzodiazepines, *J. Med. Chem.* **32** (10), 2282-91 (1989). (b) Ian Fryer, R., Walser, A., Eur. Pat. Appl. EP 135770, 1985, *Chem. Abstr.* 103:160545 (1985), (c) Ian Fryer, R., Gu, Z- Q., Wang, C.G., Synthesis of Novel, Substituted 4H-Imidazo-[1,5-a][1,4]-Benzodiazepines, *J. Heterocyclic Chem.* **28** (7), 1661 (1991). (d) Bostrom, J., Hogner, A., Llinas, A., Wellner, E., Plowright, A.T., Oxadiazoles in Medicinal Chemistry. *J. Med. Chem.*; **55**, 1817-1830 (2012).

111. Anzini, M., Braile, C., Valenti, S., Cappelli, A., Vomero, S., Marinelli, L., Limongelli, V., Novellino, E., Betti, L., Giannaccini, G., Lucacchini, A., Ghelardini, C., Norcini, M., Makovec, F., Giorgi, G. and Ian Fryer, R., Ethyl 8-Fluoro-6-(3-Nitrophenyl)-4H-Imidazo-[1,5-a][1,4]-Benzodiazepine-3-Carboxylate as Novel, Highly Potent, and Safe Antianxiety Agent, *J. of Med. Chem.* 51 (15), 4730–4743 (2008).
112. Rivas, F.M., Stables, J.P., Murphree, L.M., Edwarker, R.V., Edwanker, C.R., Huang, S., Jain, H.D., Zhou, H., Majumder, S., Sanker, S., Roth, B.L., Ramerstorfer, J., Furtmüller, R., Sieghart, W. and Cook, J.M., Antiseizure Activity of Novel γ -Aminobutyric Acid (A) Receptor Subtype-Selective Benzodiazepine Analogues in Mice and Rat Models, *J. Med. Chem.*, **52** (7), 1795-98 (2009).
113. Yang, J., Teng, Y., Ara, S., Rallapalli, S., and Cook, J.M., An Improved Process for the Synthesis of 4H-Imidazo-[1, 5- a] [1, 4]-Benzodiazepines, *Synthesis*, **06**, 1036-40 (2009).
114. Savić, M.M., Huang, S., Furtmuller, R., Clayton, T., Huck, S., Obradović, D.I., Ugrešić, N.D., Sieghart, W., Bokonjić, D.R. and Cook, J.M., Are GABA(A) Receptors Containing $\alpha 5$ Subunits Contributing to the Sedative Properties of Benzodiazepine Site Agonists? *Neuropsychopharmacol.* 1-8 (2007).
115. Li, X., Cao, H., Zhang, C., Furtmueller, R., Fuchs, K., Huck, S., Sieghart, W., Deschamps, J. and Cook J.M., Synthesis, in vitro Affinity, and Efficacy of a Bis-8-Ethynyl-4H-Imidazo[1,5a]- [1,4]Benzodiazepine Analogue, the First Bivalent $\alpha 5$ Subtype Selective BzR/GABA(A) Antagonist. *J. Med. Chem.* **46** (26), 5567-70 (2003).
116. El Hadri, A., Abouabdellah, A., Thomet, U., Baur, R., Furtmuller, R., Sigel, E., Sieghart, W. and Dodd Robert, H., N-Substituted-Amino-3,3-Dipropyl-2(3H)-Furanones: New Positive Allosteric Modulators of the GABA(A) Receptor Sharing Electrophysiological Properties with the Anticonvulsant Loreclezole. *J. Med. Chem.* **45**, (13), 2824-31 (2002).
117. Sieghart, W., Pharmacology of Benzodiazepine Receptors: an update. *JPN.* 19, (1), 24-9 (1994).
118. Schreibmayer, W., Lester, H.A., Dascal, N., Voltage clamping of *Xenopus Laevis* Oocytes Utilizing Agarose-Cushion Electrodes. *Pflugers Arch.: European Journal of physiology.* **426** (5), 453-458 (1994).
119. Haefely, W., Kyburz, E., Gerecke, M. and Möhler, H., Recent Advances in the Molecular Pharmacology of Benzodiazepine Receptors and in the Structure-Activity Relationships of Their Agonists and Antagonists, *Adv. Drug Res.* Academic Press: New York, 165-322 (1985).

120. Borea, P.A., Gilli, G., Bertolasi, V. and Ferretti, V., Stereochemical Features Controlling Binding and Intrinsic Activity Properties of Benzodiazepine-Receptor Ligands, *Mol. Pharmacol.* **31** (4), 334-344 (1987).
121. Huang, S., Terry, C., Dai, M., Edwankar, R., Sawant, C. and Cook, J.M., Synthesis of Optically Active Subtype Selective BzR Ligands, *Abstracts of Papers, 232nd ACS National Meeting*, MEDI-502. San Francisco, CA, United States, Sept. 10-14 (2006).
122. He, X., Yu, S., Ma, C., Huang, Q., McKernan, R. and Cook, J.M., Study of Pharmacophore/Receptor Models for GABA(A)/BzR Subtypes via QSAR Analysis of Symmetrically Substituted Pyrazoloquinolinones. *Book of Abstracts, 217th ACS National Meeting*, MEDI-095, Anaheim, Calif., March 21-25 (1999).
123. He, X. H., Zhang, C. C., Cook, J.M., Model of the BzR Binding Site: Correlation of Data from Site-Directed Mutagenesis and the pharmacophore/receptor model. *Med. Chem.Res.* **10** (5), 269-308 (2001).
124. Mohamadi, F., Richards, N. G. J., Guida, W. C., Liskamp, R., Lipton, M., Caufield, C., Chang, G., Hendrickson, T. and Still, W.C., MacroModel - An Integrated Software System for Modeling Organic and Bioorganic Molecules Using Molecular Mechanics, *J. Comput. Chem.* **11** (4), 440-67 (1990).
125. Gaussian 92, G., Inc., Carnegie Office Park, Bldg. 6, Pittsburgh, PA 15106, Gaussian 92 ed.
126. Gaussian94, G., Inc., Carnegie Office Park, Bldg. 6, Pittsburgh, PA 15106, Gaussian 94 ed.
127. Fuchs, K., Zezula, J., Slany, A. and Sieghart, W., Endogenous [3H] Flunitrazepam Binding in Human Embryonic Kidney Cell Line 293, *Eur. J. Pharmacol.* **289** (1), 87-95, (1995).
128. Sigel, E., Baur, R., Allosteric Modulation by Benzodiazepine Receptor Ligands of the GABA(A) Receptor channel expressed in *Xenopus* Oocytes. *J. Neurosci.* **8** (1), 289-95, (1988).
129. Sigel, E., Minier, F., The *Xenopus* Oocyte: System for the Study of Functional Expression and Modulation of Proteins, *Molecular Nutrition & Food Research.* **49** (3), 228-234, (2005).
130. Gu, Z.Q., Wong, G., Dominguez, C., de Costa, B.R., Rice, K.C. and Skolnick, P., Synthesis and Evaluation of Imidazo-[1,5-a][1,4]-Benzodiazepine Esters with High Affinities and Selectivities at "Diazepam-Insensitive" Benzodiazepine Receptors, *J. Med. Chem.* **36**, 1001-1006, (1993).

CURRICULUM VITA

Title of Dissertation:

Part1. Design and Synthesis of Cysteine / Cystine Prodrugs and Bioisosteres including Symmetrical and Unsymmetrical Disulfides Designed to Increase Cystine Levels in the CNS in Order to Drive the Cystine / Glutamate Antiporter: A Novel Treatment for Schizophrenia and Drug Addiction.

Part 2. Design and Synthesis of Subtype Selective Ester Bioisosteres of BZR Ligands for GABA_A / Benzodiazepine Receptors to Enhance Metabolic Stability.

Full Name: Edward Merle Johnson II

Place and Date of Birth: Beckley, West Virginia, USA. 08/17/1979

Colleges and Universities:

University of Wisconsin-Milwaukee 8/2003 - 12/2012, Ph.D.

West Virginia University, School of Pharmacy 8/1997 - 5/2003, Pharm.D.

Professional Licenses:

West Virginia Board of Pharmacy – Registered Pharmacist; License # RP0006564

Wisconsin Board of Pharmacy – Registered Pharmacist; License # 14019 – 040

Membership in Learned or Honored Societies:

Phi Lambda Sigma Pharmacy Leadership Society
January 2002 – Present

Rho Chi Pharmacy Fraternity
Chapter President 2001 – 2002, April 2001 – Present

West Virginia University School of Pharmacy Accreditation Committee
August 2002 – May 2003

Academic Review Committee for West Virginia University School of Pharmacy
April 2001 – May 2003

Training Certificates:

ACLS – Advanced Cardiovascular Life Support - Sponsored by the Orthopaedic Hospital of Wisconsin, Glendale, WI, 53212, October 2012.

BLS – Basic Life Support – Sponsored by the Orthopaedic Hospital of Wisconsin, Glendale, WI, 53212, August 2012.

PSW Immunization Delivery for Pharmacists – June 2011

CME Online Pain Management Course, sponsored by West Virginia Academy of Family Physicians, Glade Springs Resort, Daniels, West Virginia. February 14, 2003.

Statewide Healthcare Provider Training for Tobacco Cessation, sponsored by West Virginia Chapter, American Academy of Family Physicians and West Virginia State Medical Association, Glade Springs Resort, Daniels, West Virginia. February 14, 2003.

Patents:

1. Cook, J., Baker, D., **Johnson, E.M.**, Yin, W., Cysteine and Cystine Prodrugs to Treat Schizophrenia and Reduce Drug Cravings. Serial NO/13/465383 US, Filed on March 7, 2012, Pending.
2. Cook, J., Baker, D., **Johnson, E.M.**, Yin, W., Cysteine And Cystine Bioisosteres To Treat Schizophrenia And Reduce Drug Cravings. Serial NO/2721433 Canada, Filed on October 13, 2010, Pending.
3. Cook, J., Baker, D., **Johnson, E.M.**, Yin, W., Cysteine Prodrugs to Treat Schizophrenia and Drug Addiction. Serial NO/12/897353 US, Filed on October 4, 2010, Pending.

4. Cook, J., Baker, D., **Johnson, E.M.**, Yin, W., Cysteine and Cystine Bioisosteres to Treat Schizophrenia and Reduce Drug Cravings. Serial NO/9743238.9 US, Filed on September 16, 2010, Pending.
5. Cook, J., Baker, D., **Johnson, E.M.**, Yin, W., Cysteine and Cystine Prodrugs to Treat Schizophrenia and Reduce Drug Cravings. Serial NO/2010-546090 Japan, Filed on August 6, 2010, Pending.
6. Cook, J., Baker, D., **Johnson, E.M.**, Yin, W., Cysteine And Cystine Bioisosteres To Treat Schizophrenia And Reduce Drug Cravings. Serial NO/09707256.5 EPC, Filed on June 9, 2010, Pending.
7. Cook, J., Baker, D., **Johnson, E.M.**, Yin, W., Cysteine and Cystine Bioisosteres To Treat Schizophrenia and Reduce Drug Cravings. Serial NO/12/425063 US, Filed on April 16, 2009, Pending.
8. Cook, J., Baker, D., **Johnson, E.M.**, Yin, W., Cysteine and Cystine Prodrugs to Treat Schizophrenia and Reduce Drug Cravings. Patent NO/8173809B2, Serial NO/12/367867 US, Filed on February 2, 2009, Issued on March 8, 2012.
9. Cook, J., Baker, D., **Johnson, E.M.**, Yin, W., Cysteine Prodrugs to Treat Schizophrenia and Drug Addiction. Patent NO/7829709, Serial NO/12/189516 US, Filed on August 11, 2008, Issued on November 9, 2010.

Publications:

1. Namjoshi, O., Wang, Z., Rallapalli, S., **Johnson, E. M.**, Johnson, Y.T., Ramerstorger, J., Sieghart, W., Roth, B., Rowlett, J.K., Cook, J. M. Development of Alpha2/Alpha3 Subtype Selective GABAA-Benzodiazepine Receptor Agonists: Design, Synthesis and In Vitro and In Vivo Evaluation of Metabolically Stable Bioisosteric Analogs. *BioOrg. Med. Chem.* in press (2012).
2. Fischera, B.D., Licataa, S.C., Edwankarb, R.V., Wangb, Z.J., Huangb, S., Heb, X., Yub, J., Zhoub, H., **Johnson, E.M.**, Cook, J.M., Furtmüllerc, R., Ramerstorferc, J., Sieghartc, W., Rothd, B.L., Majumderd, S., Rowletta, J.K., Anxiolytic-like effects of 8-acetylene imidazobenzodiazepines in a rhesus monkey conflict procedure. *Neuropharmacology*. **59** (7-8), 612-618 (2010).
3. Western, E.C., Daft, J.R., **Johnson, E.M.**, Gannett, P.M., and Shaughnessy, K.H. Efficient One-Step Suzuki Arylation of Unprotected Halonucleosides using Water-Soluble Palladium Catalysts. *J. Org. Chem.* **68** (17), 6767-74 (2003).

4. **Johnson, E.M.**, Lucas, K. Zelnorm® (tegaserod maleate). *New Drug Update*, **9** (2), 6-8 (2003).
5. Greiner, E., Prisinzano, T., **Johnson, E.M.**, Dersch, C.M., Marcus, J., Partilla, J.S., Rothman, R.B., Jacobson, A.E., Rice, K.C. Structure-Activity Relationship Studies of Highly Selective Inhibitors of the Dopamine Transporter: N-Benzyl Piperidine Analogues of 1-[2-[Bis(4-fluorophenyl)methoxy]ethyl]-4-(3phenylpropyl)piperazine (GBR 12909): High Affinity Ligands for the Dopamine Transporter. *J. Med. Chem.* **45**, 4371-74 (2002).
6. Gannett, P.M. **Johnson, E.M.**, Grimmes, M., Myers, A., Deavers, III, R.E., and Tracy, T.S. Synthesis of Deuterated 4,4'-diaminodiphenylsulfone (Dapsone) and Analogs. *J. Labeled Comp. and RadioPharm.* **46**, 107-114 (2002).
7. Gannett, P.M., Darian, E., Powell, J.H., **Johnson, E.M.**, Ramsey, C.M., Dalal, S.N., and Budil, D.E. Probing Triplex Formation by EPR Spectroscopy and Spin Labeled Oligonucleotides. *Nucleic Acids Research.* **30** (23), 5328-37(2002).
8. Gannett, P.M., Powell, J.H., **Johnson, E.M.**, Darian, E., Dalal, N., Norton, M.L., Budil, D.E. Solid Phase DNA Annealing Characterization by EPR Spectroscopy, *Tet. Letters.* **43** (11), 1931-33 (2002).
9. Gennett, P.M., Darian, E., Powell, J.H., and **Johnson, E.M.** A Short Procedure for Synthesis of 4-ethynyl-2,2,6,6-tetramethyl-3,4-dehydro-piperidine-1-oxyl Nitroxide. *Synthetic Comm.* **31** (14), 49-53 (2001).
10. Powell, J.H., **Johnson, E.M.**, and Gannett, P.M. Improvement of a Critical Intermediate Step in the Synthesis of a Nitroxide-Based Spin-Labeled Deoxythymidine Analog. *Molecules.* **5**, 1289-95 (2000).

Presentations:

1. Johnson, Y.T., **Johnson, E.M.**, and Cook, J.M. Synthesis of Selective Bivalent Ligands for GABAA/ Benzodiazepine Receptors. Annual Awards Day, UW - Milwaukee, Spring (2008).